Repair and genetic consequences of DNA double strand breaks during animal development

Bennie Lemmens

Cover design: Bennie Lemmens and Ana Agostinho
Layout: Gildeprint
Printing: Gildeprint

ISBN: 9789461088192

Repair and genetic consequences of DNA double strand breaks during animal development

Proefschrift

ter verkrijging van de graad van Doctor aan de Universiteit Leiden,
op gezag van Rector Magnificus prof. mr. C.J.J.M. Stolker,
volgens besluit van het College voor Promoties
te verdedigen op dinsdag 9 december 2014
klokke 11:15

door

Bennie Benjamin Lodewijk Gerardus Lemmens

geboren te Casteren
in 1984

Promotiecommissie

Promotor:	Prof. dr. M. Tijsterman	
Overige leden:	Dr. H. Vrieling	
	Prof. dr. H.C. Korswagen	Hubrecht Institute Utrecht
	Prof. dr. H. te Riele	Netherlands Cancer Institute Amsterdam

Table of contents

1

DNA double-strand break repair in *Caenorhabditis elegans*

Lemmens BB, Tijsterman M

Adapted from Lemmens *et al.*
Chromosoma 2011 Feb;120(1):1-21

1

Abstract

Faithful repair of DNA double-strand breaks (DSBs) is vital for animal development, as inappropriate repair can cause gross chromosomal alterations that result in cellular dysfunction, ultimately leading to cancer, or cell death. Correct processing of DSBs is not only essential for maintaining genomic integrity, but is also required in developmental programs, such as gametogenesis, in which DSBs are deliberately generated. Accordingly, DSB repair deficiencies are associated with various developmental disorders including cancer predisposition and infertility. To avoid this threat, cells are equipped with an elaborate and evolutionarily well-conserved network of DSB repair pathways. In recent years, *Caenorhabditis elegans* has become a successful model system in which to study DSB repair, leading to important insights in this process during animal development. This review will discuss the major contributions and recent progress in the *C. elegans* field to elucidate the complex networks involved in DSB repair, the impact of which extends well beyond the nematode phylum.

Introduction

DNA double-strand breaks and development

Genomes are constantly attacked by DNA damaging agents, such as endogenous cellular metabolites, exogenous genotoxins, and radiation. Moreover, genomes are continuously challenged by mutagenic processes, such as transposition and imperfect replication. All of these sources of DNA damage generate a vast amount of DNA lesions, among which single-strand DNA lesions (SSLs) are the most common. It is estimated that, in normal human cells, approximately 1% of endogenous SSLs are converted into roughly 50 DNA double-strand breaks (DSBs) per cell per cell cycle (Vilenchik and Knudson 2006), which pose a serious threat to all proliferating cells. DSBs are the most toxic forms of DNA damage, as a single DSB has the potential to activate cell cycle arrest and can be lethal to a cell if left unrepaired (Bennett et al. 1993). Improper repair of DSBs can also lead to large deletions and gross chromosomal rearrangements, which ultimately result in cellular dysfunction. However, some cells deliberately inflict DSBs to induce genetic variation, as seen in budding yeast during mating-type switching, in lymphocytes during V(D)J recombination, and in sexually reproducing organisms during meiosis. In fact, during meiosis, DSB repair products establish transient physical links between chromosomes that are essential for proper chromosome segregation. Although mutations can be beneficial on an evolutionary scale, faithful repair of all types of lesions is vital to ensure genomic stability and is therefore fundamental to the fitness of a cell and the reproductive success of a species. As a result, multiple DSB repair pathways have evolved to handle this inevitable and constant threat.

The DSB repair network

In human cells, most DSBs are repaired via a conserved pathway called non-homologous end joining (NHEJ), which is an error-prone pathway that readily joins broken DNA ends together independent of sequence context (Fig. 1; Lieber 2010). In addition, mutagenic repair pathways called single-strand annealing (SSA) and micro-homology-mediated end joining (MMEJ) use long (30–400 bp) or short (5–15 bp) sequences of homology flanking the DSB to anneal and re-ligate the DSB ends, respectively (McVey and Lee 2008; Sugawara et al. 2000). DSBs can also be repaired via homologous recombination (HR), a high-fidelity repair route that uses an undamaged homologous DNA template from a sister chromatid or homologous chromosome to restore the sequence information lost at the break site (Fig. 1; Li and Heyer 2008). These DSB repair pathways form a complex network to safeguard genome integrity, operating in both competitive and collaborative manners, depending on the repair context, stage of the cell cycle, and state of the broken DNA. In the last 30 years, many genes involved in these DSB repair pathways have been identified and many of them have been implicated in severe disorders (*i.e.*, cancer predisposition syndromes and premature aging) (Hoeijmakers 2009; Fig. 2).

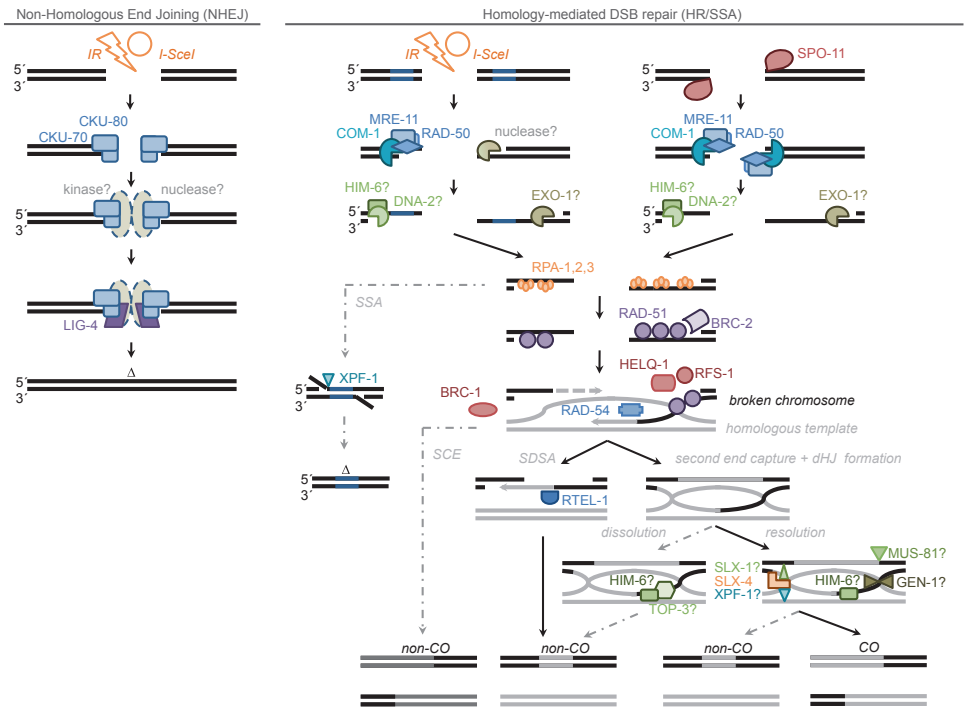

Fig. 1 Schematic overview of DSB repair pathways in C. elegans. See text for details. SSA single-strand annealing, SCE sister chromatid exchange, SDSA synthesis-dependent strand annealing

Caenorhabditis elegans as a DSB repair model

In 1974, Sydney Brenner launched a new animal model: a small transparent nematode called *C. elegans*, which proved to be very convenient to study developmental processes, including cell death and differentiation (Brenner 1974; Hoffenberg 2003; Horvitz 2003; Sulston 2003). Soon after the entire *C. elegans* genome was sequenced in 1998, its potential to contribute to our understanding of DSB repair was appreciated, as this model organism has allowed in-depth analysis of known DSB repair genes (e.g., Adamo et al. 2008; Alpi et al. 2003; Chin and Villeneuve 2001; Zalevsky et al. 1999), but has also permitted efficient forward genetic screens (Kelly et al. 2000; Winand et al. 1998) as well as high-throughput reverse genetic screens (Pothof et al. 2003; van Haaften et al. 2006) to identify novel DSB response factors. For some of these novel genes, a role in DSB repair has recently been demonstrated for their cognate human ortholog (Smeenk et al. 2010; Polo et al. 2010; H. van Attikum personal communication).

Because DSBs can be repaired via distinct pathways, each consisting of numerous factors, mutations in individual DSB repair genes can have very different consequences. For example, some DSB repair defects result in frequent gross chromosomal aberrations (leading to developmental retardation or even embryonic death), while others only induce a minor shift towards efficient but error-prone repair modes (ultimately driving the accumulation of mutations and resulting in associated diseases such as cancer; Fig. 2). In worms, both erroneous DSB repair and chromosomal instability often result in developmental abnormalities, altered chromosome morphology, and/or DNA damage sensitivity, all of which are phenotypes that can be readily detected without the need of complex techniques (Fig. 2). Furthermore, elevated chromosomal instability in the germline often manifests as increased X chromosome non-disjunction, which in *C. elegans* results in an overrepresentation of males (X0) in the otherwise hermaphrodite (XX)-dominated population (Fig. 2). This so-called high-incidence-of-males (Him) phenotype has proved to be a convenient readout and has revealed several DSB repair factors that are crucial to proper meiotic progression (Kelly et al. 2000; Tang et al. 2010). Unique features such as an invariant cell lineage, the linear array of meiotic stages along the hermaphrodite gonad, and easy knockdown via systemic RNAi make this multicellular animal a suitable model in which to study DSB repair in the context of somatic as well as germline tissues (Figs. 2 and 3)

In addition to many repair pathways, the damage response to DSBs also encompasses an elaborate signaling network that regulates cell cycle checkpoint arrest and/or apoptosis. In recent years, comprehensive overviews have been published on the latter two aspects of the DNA damage response in *C. elegans* (O'Neil and Rose 2006; Gartner et al. 2008). Here, we will discuss the major contributions and recent progress in the *C. elegans* field to elucidate the complex networks involved in DSB repair. In the first part, we will discuss the regulation and repair of (programmed) DSBs in the worm germline, and in the second part, we will focus on DSB repair in somatic cells.

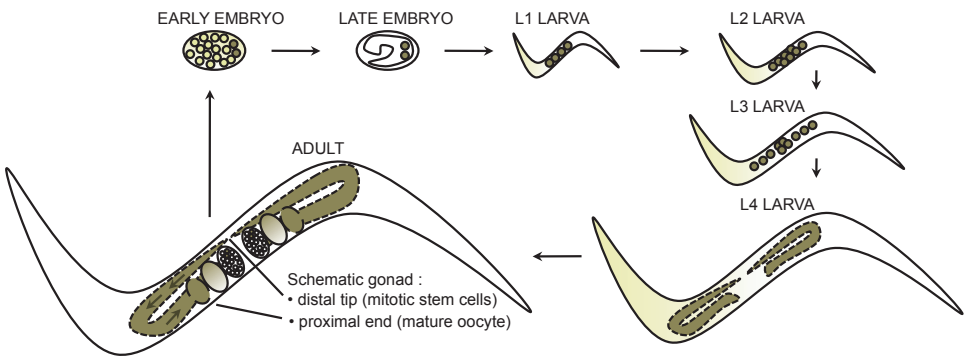

	MEIOSIS	MITOSIS (CYCLING)	MITOSIS (NON-CYCLING)	REF
GERMLINE	HR	HR	HR	Clejan et al. 2006
SOMA	-	HR	NHEJ	Clejan et al. 2006
SOMA	-	HR + SSA + NHEJ		Pontier et al. 2009

Fig. 2 Consequences of faulty DSB repair in C. elegans and humans. DSB repair defects result in the accumulation of DSBs, which ultimately will result in genetic defects. Depending on the cell type in which the genetic defects occur (germline or soma), distinct developmental abnormalities become apparent. In the C. elegans field, these phenotypes are often used as readouts for specific forms of genomic instability, allowing researchers to delineate developmental consequences of known DSB repair defects, and also to screen for novel DSB repair factors. Often-used genomic instability readouts are: embryonic viability, frequency of X0 males, nuclear morphology of diakinesis/intestinal nuclei (insets), occurrence of vulval defects, and transgenic reporter readouts. Notably, the genetic defects underlying these phenotypes are strongly associated with severe diseases in humans, including DSB repair deficiency disorders

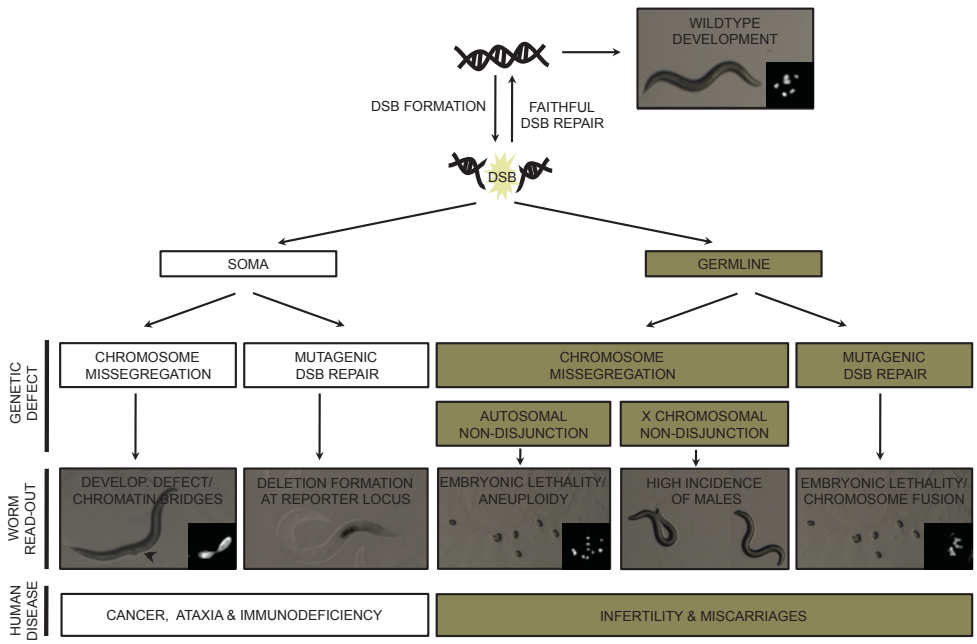

Fig. 3 Visualization of DSB repair in the adult germline. Represen- tative image of a dissected DAPI-stained wild-type C.elegans germline. The convenient spatio-temporal organization of meiotic prophase, paralleled by dynamic changes in chromosome organization (upper panel), allow in-depth analysis of chromosomal stability during gametogenesis, including HR-mediated DSB repair events typified by RAD-51 recruitment (lower panel)

DSB repair during meiosis

Meiosis and the worm germline

Perhaps the most important biological process that involves the deliberate generation and repair of DSBs is the specialized cell division program of meiosis. In brief, meiosis enables diploid germ cells to produce haploid gametes. The primary function of meiosis is to reduce the chromosome complement by half, which is achieved by having a single round of DNA replication followed by two subsequent rounds of chromosome segregation (named meiosis I and meiosis II). In *C. elegans*, mitotically proliferating germ cell nuclei reside at the distal end of the gonadal syncitium, in the so-called “mitotic zone”. As these nuclei move to the proximal end of the germline, they progress through different meiotic stages (Figs. 3 and 5). First, nuclei enter a “transition zone”, where meiosis I begins and maternal and paternal versions of each chromosome (homologous chromosomes) pair and align. Around this time, several DSBs are introduced by a highly conserved topoisomerase-like endonuclease called SPO-11, and HR is initiated to repair the SPO-11-induced DSBs (Dernburg et al. 1998; Keeney and Neale 2006). As the nuclei enter the “pachytene zone”, a proteinaceous structure known as the

synaptonemal complex (SC) is assembled to temporarily keep the homologous chromosomes in close proximity to each other, a process called synapsis. Meanwhile, a specific set of HR events between the homologous chromosomes result in repair products known as crossovers (COs). These COs (together with sister chromatid cohesion) generate the transient physical links, called chiasmata, that physically connect the homologous chromosomes and allow the homologs to separate adequately during the first meiotic division. During the "diplotene stage", the chromosomes desynapse, but remain condensed and are held together by the chiasmata. At the "diakinesis stage", the pairs of homologous chromosomes can be easily identified in the maturing oocyte as six discrete bivalents (Fig. 3). As soon as the oocyte is fertilized in the spermatheca, meiotic spindles are formed and the homologous chromosomes are separated during anaphase I. After one set of chromosomes has been excluded (a process called polar body extrusion), meiosis II starts and the other chromosomes align at the spindle equator. In anaphase II, the sister chromatids are separated and again one set is excluded. As meiosis completes, six chromosomes remain and form the oocyte pronucleus, which together with the sperm-derived pronucleus contains all the genetic information necessary for the development of a new individual.

The chiasmata are crucial for the homologs to correctly orient toward opposite spindle poles during anaphase I. Therefore, the induction and resolution of chiasmata is critical for faithful chromosome segregation, as is illustrated by the fact that worms that are unable to introduce meiotic DSBs (e.g., *spo-11* mutants) produce hardly any viable offspring, due to excessive aneuploidy (Dernburg et al. 1998), whereas worms that cannot repair the SPO-11-induced DSBs (e.g., HR defective *rad-51* mutants) produce no viable progeny at all (Alpi et al. 2003). In addition to their essential role in chromosome dynamics, meiotic DSBs are also the sites of genetic exchange between the broken chromosome and its repair template, either the sister chromatid or homologous chromosome. In the case of the latter, CO-mediated DSB repair leads to the exchange of large sections between the paternal and maternal chromosome. Therefore, the choice between non-CO or CO-mediated DSB repair has a significant impact on the genetic variation within a species. Meiotic DSB repair needs thus to be accurate in order to safeguard genomic stability, but also needs to allow genetic changes that can result in evolutionary benefits.

Synapsis and meiotic DSB repair

The repair of SPO-11-induced DSBs is a complex multistep process that is accompanied by dynamic changes in chromosome architecture. HR is the principal mode of meiotic DSB repair in *C. elegans* (Clejan et al. 2006; Martin et al. 2005) and requires a homologous template: either the sister chromatid (always resulting in non-CO) or the homologous chromosome (resulting in either non-CO or CO). Because chromosome structure affects the availability of these substrates, several protein complexes involved in meiotic chromosome organization

have been shown to affect DSB repair outcome. Mutation of SC genes hampers the ability of homologous chromosomes to stay in close juxtaposition at the moment when the meiotic DSBs are repaired, and accordingly, these mutations lead to a severe reduction in CO recombination (Colaiacovo et al. 2003; Couteau et al. 2004; Garcia-Muse and Boulton 2007; Goodyer et al. 2008; Smolikov et al. 2007; Zetka et al. 1999). However, synapsis mutants generally have no defects in SPO-11-mediated DSB induction, and the majority of DSBs are ultimately repaired. For instance, synapsis does not occur in *syp-2* mutants, but RAD-51 foci (as markers for DSB repair intermediates) disappear late in meiotic prophase, implying that meiotic DSBs are repaired eventually, likely via error-free HR using the sister chromatid as a template (Colaiacovo et al. 2003). Instead of six bivalents, *syp-2* mutants have 12 intact univalents at diakinesis, indicative of a lack of CO formation and chiasmata establishment (Colaiacovo et al. 2003). Indeed, when inter-sister HR is inhibited in such a synapsis defective background (either via *brc-1* mutation, *rad-51*, or *rec-8* RNAi), faithful meiotic DSB repair is impaired, leading to severe chromosomal fragmentation (Adamo et al. 2008; Colaiacovo et al. 2003; Smolikov et al. 2007). Although the majority of SC factors likely affect meiotic DSB repair indirectly, by controlling repair template availability, some structural components of the SC seem to affect meiotic DSB repair in a more direct fashion. For example, the axial SC components HTP-1 and HIM-3 have been shown to prevent inter-sister HR and are therefore crucial for the inter-homolog bias during meiotic recombination and subsequent CO formation in early prophase (Couteau et al. 2004; Martinez-Perez and Villeneuve 2005).

Whereas homologous chromosomes are temporarily held together via the SC, sister chromatids are held together by cohesin complexes. Meiosis-specific cohesin components have been implicated in meiotic DSB repair efficacy (Pasierbek et al. 2001). Recently, Severson and colleagues have studied the consequences of a complete absence of sister chromatid cohesion (SCC) on genome integrity. They showed that mutation of the general cohesin component SMC-1 or simultaneous depletion of meiotic cohesin subunits REC-8, COH-3, and COH-4 results in discrete chromosomal fragments in diakinesis nuclei (Severson et al. 2009). Lack of SCC eradicates the availability of all DNA templates needed for HR, blocking both inter-sister and inter-homolog HR. Interestingly, direct inactivation of HR (via *rad-51*, *brc-2*, or *rad-54* mutation) does not lead to persistent DSBs and fragmented chromosomes, but instead provokes inaccurate DSB repair, resulting in irregular chromatin aggregates at diakinesis (Martin et al. 2005; Ward et al. 2010). Chromosome aggregation in *rad-51* and *brc-2* mutants has been shown to (partially) depend on canonical NHEJ factors, which are apparently able to act on meiotic DSBs under these conditions (Martin et al. 2005). These diakinesis phenotypes clearly contrast those observed in SSC deficient germlines, in which the DSBs seem to persist and undergo no repair at all (Adamo et al. 2008; Svendsen et al. 2009). A question that follows from these observations is: why do defects in HR allow other repair pathways, such as NHEJ, to take over, while the unavailability of a proper HR template does not?

Synapsis and meiotic DSB formation

In yeast, plants, and mammals, meiotic DSBs are not only important for CO/chiasmata formation; they are also required for the processes of SC formation and synapsis itself (Zickler 2006). Such a link between DSB formation and chromosome organization was thought to be absent in worms and flies, as synapsis can occur normally in *spo-11* mutants in these model species (Dernburg et al. 1998). However, more nuances to this view was provided recently by Smolikov and colleagues, who identified *cra-1* as a regulator of SC assembly and showed that, in the absence of *cra-1*, HR-mediated repair of meiotic DSBs was needed for the proper recruitment and polymerization of SC components (Smolikov et al. 2008). Another possible link between DSB formation and synapsis came from investigating a unique meiotic axis component called HTP-3, which was shown to have a dual role during meiosis, being required for synapsis as well as meiotic DSB formation (Goodyer et al. 2008). HTP-3 interacts with HIM-3, one of the above-mentioned SC components controlling synapsis and sister chromatid exchange (SCE). Interestingly, HTP-3 also formed a complex with two members of the so-called Mre11-Rad50-Nbs1 (MRN) complex. The MRN complex is required for Spo11-mediated DSB formation in yeast and is implicated in several DSB repair pathways (Johzuka and Ogawa 1995; Rupnik et al. 2010). In line with a role in DSB formation, both *htp-3* and MRN-deficient worms resemble *spo-11* mutants, as their germlines lack RAD-51 foci in early pachytene and typically show 12 intact univalents at diakinesis. Furthermore, similar to *spo-11* mutation, both *htp-3* and MRN mutations can rescue the DSB-dependent chromosomal aggregation observed in RAD-51 depleted germlines (Chin and Villeneuve 2001; Goodyer et al. 2008; Hayashi et al. 2007). However, artificially induced DSBs can rescue CO formation in *spo-11* mutants, but not in *htp-3* mutants, revealing an additional role for HTP-3 downstream of meiotic DSB formation. Recently, HTP-3 has been shown to be critical for the chromosomal association of HIM-3 as well as several other SC components and the cohesion factor REC-8, making it a crucial factor for meiotic chromosome axis organization and a prerequisite for proper meiotic DSB induction and subsequent CO formation (Goodyer et al. 2008; Severson et al. 2009).

Chromosome structure and meiotic DSB formation

In recent years, additional factors altering chromosome structure have been shown to coordinate meiotic DSB formation. The Villeneuve lab identified HIM-17, a chromatin-associated protein that is essential for meiotic DSB induction, but in contrast to HTP-3, is dispensable for synapsis. *him-17* mutants resemble *spo-11* mutants by showing no RAD-51 foci in early pachytene and no chiasmata at diakinesis (Reddy and Villeneuve 2004). Both phenotypes can be restored by artificially induced DSBs, confirming a specific role for HIM-17 in DSB induction. Intriguingly, *him-17* mutant germlines also displayed altered patterns of histone H3 methylation, which could suggest that chromatin modification contributes to the competence for initiation of meiotic recombination.

Recently, the Meyer lab discovered an additional link between chromosome structure and meiotic DSB induction. They revealed a novel role for condensin complexes in controlling chromosome structure and meiotic DSB formation. Using elegant tools, including a terminal deoxynucleotidyl transferase mediated dUTP nick-end-labeling (TUNEL) assay that enabled them to label 3′ ends of meiotic DSBs, they demonstrated that CO number and CO distribution are controlled on a chromosome-wide basis at the level of DSB formation by a condensin complex (Mets and Meyer 2009). Specifically, lack of the condensin subunit *DPY-28* led to a remarkable expansion of the axis of meiotic chromosomes, which was paralleled by an elevated number of DSBs and altered CO distribution (Mets and Meyer 2009; Tsai et al. 2008), suggesting that specific condensins limit DSB formation by controlling chromosome organization. Reinforcing this view, *dpy-28* mutations partially restored DSB formation in *him-17* mutants (Tsai et al. 2008). Vice versa, the restored DSB formation in *dpy-28; him-17* double mutants argues for the hypothesis that HIM-17 promotes meiotic DSB formation by influencing chromatin structure.

Meiotic DSB induction and CO formation

Using the TUNEL assay and mutants that trapped RAD-51 (a marker for HR intermediates) at the break sites, Mets and Meyer assessed the number of DSBs inflicted during normal meiosis (Mets and Meyer 2009). Their data suggests that meiotic nuclei encounter approximately 10–12 DSBs in *C. elegans*, which is surprisingly low, considering that each of the six chromosome pairs needs at least one DSB to be able to form the obligate CO/chiasmata. This finding implies the existence of a surveillance mechanism that ensures that at least one half of the DSBs are repaired via a CO intermediate. Moreover, these COs should be distributed over the genome such that every homolog pair has at least one CO and that the COs do not occur in close proximity to each other (phenomena referred to as “CO homeostasis” and “CO interference“, respectively). The degree of interference and the number of COs per meiosis vary between organisms. In *C. elegans*, CO interference is absolute, such that each chromosome pair undergoes only a single CO (Hillers and Villeneuve 2003; Wood 1988). CO interference is also reported in budding yeast, which has 16 chromosomes and 150–200 DSBs per meiosis (Buhler et al. 2007). Similar to the nematode, one half of the DSBs are converted into COs, in this case, resulting in approximately five crossovers per homolog pair (Mortimer et al. 1992). In contrast, CO interference is not observed in fission yeast, which has only three chromosomes and a relatively large number of COs, reaching up to 44 COs per meiosis (Munz 1994).

How meiotic DSB formation and CO distribution are regulated on a molecular level and how these processes are entangled with the dynamic changes in meiotic chromosome architecture are still poorly understood, but based on the progress made in recent years, *C. elegans* research will likely contribute significantly to our understanding of these vital processes during meiosis.

Meiotic DSB formation and early DSB processing

Once Spo11 has catalyzed DSB formation, it remains covalently attached to the 5′ termini of the broken DNA (Keeney et al. 1997; Keeney and Kleckner 1995). To allow HR to occur, this protein–DNA complex must be removed. In yeast, Spo11-bound oligonucleotides are removed by the MRN complex (consisting of Rad50, Xrs2/Nbs1, and the nuclease Mre11) and another associated nuclease known as Sae2 (Keeney and Kleckner 1995; McKee and Kleckner 1997; Milman et al. 2009; Ogawa et al. 1995; Prinz et al. 1997; Fig. 1). Yeast Sae2 deletion mutants allow DSB formation, but are completely defective in Spo11 removal (McKee and Kleckner 1997). This function of Sae2 seems to be conserved in *C. elegans*, as nematodes lacking the Sae2 homolog *com-1* also are able to induce meiotic DSBs; yet, these lesions seem to persist and undergo improper repair, resulting in chromatin aggregates at the diakinesis stage (Penkner et al. 2007). Additionally, *com-1* mutants fail to recruit the crucial HR factor RAD-51 to SPO-11-induced DSBs, implying a defect in the early processing of SPO-11-bound DSBs. Importantly, these mutants did show many RAD-51 foci upon γ-irradiation (IR), revealing a specific dependency for COM-1 only at meiotic DSBs (Penkner et al. 2007).

In yeast, the MRN complex is needed for Spo11-mediated DSB formation as well as subsequent DSB end-processing, making it difficult to study these individual (but interdependent) functions of the MRN complex. In yeast, this problem is solved by the identification of separation-of-function alleles of MRN complex components. For example, so-called Mre11-1 and Rad50S mutants allow meiotic DSB formation but are defective in Spo11 removal (McKee and Kleckner 1997; Ogawa et al. 1995). To date, no such mutations have been identified in *C. elegans*. Nevertheless, both functions of the MRN complex are likely to be conserved: first, germlines that are deficient in *mre-11* or *rad-50* typically show 12 univalents at diakinesis due to the lack of chiasmata, in line with the role of the MRN complex in meiotic DSB formation (Chin and Villeneuve 2001; Hayashi et al. 2007). Notably, RAD-51 foci are not detected in pachytene nuclei, as expected in the absence of meiotic DSBs. Second, *mre-11* mutant nuclei, but not wild-type nuclei, display chromosomal fragmentation upon IR, confirming a defect in DSB end-processing in the absence of the MRN complex (Chin and Villeneuve 2001). Similar to *com-1* mutants, both *rad-50* and *mre-11* mutants can recruit RAD-51 to IR-induced breaks, suggesting that other redundant nucleases exist that can process IR-induced substrates but are unable to act on SPO-11-induced DSBs (Fig. 1). Intriguingly, Hayashi and coworkers discovered that the level of redundancy between these nucleases depends not only on substrate specificity but also on meiotic stage (Hayashi et al. 2007). By carefully analyzing *rad-50* mutant germlines, they showed that the dynamics and regulation of RAD-51 loading at IR-induced DSBs changes during meiotic prophase progression. Specifically, these authors discovered a distinct meiotic DSB repair mode, acting from the onset of meiotic prophase until the mid-pachytene/late pachytene transition, which was characterized by dependence on *rad-50* for rapid accumulation of RAD-51 and by the

competence for converting IR-induced DSBs into COs (Hayashi et al. 2007). Recently, a study in yeast revealed that Sae2 phosphorylation by cyclin-dependent kinase 1 (Cdk1) is required for Spo11 removal and subsequent DSB processing, providing a mechanism for coordinating DSB repair during meiotic prophase (Manfrini et al. 2010). The critical Cdk-1 phosphorylation motif is evolutionarily conserved, being present in yeast Sae2 and *C. elegans COM-1*, as well as the human homolog CtIP (Penkner et al. 2007); however, whether such a phosphorylation event also controls early DSB processing during meiotic prophase in these higher eukaryotes still awaits confirmation.

Homology exposure and DNA end resection

A crucial step in HR is the exposure of sequence information surrounding the DSB in order to search for a homologous template and restore the break. This is achieved by a process called DNA end resection, which involves 5′–3′ DNA degradation to create long 3′ single-stranded DNA (ssDNA) tails. These ssDNA tails are initially coated with replication protein A (RPA), which is then replaced by Rad51, the crucial mediator for homologous strand invasion. The observation that DNA end resection can still occur in yeast Sae2 null and Mre11 nuclease-dead mutants (Clerici et al. 2005; Llorente and Symington 2004) has led to a search for redundant activities that can process DSB ends.

One of the strongest candidates for DNA end resection during meiosis is Exo1, as it has 5′–3′ exonuclease activity as well as 5′ flap endonuclease activity *in vitro*, is highly expressed during meiosis, and is known to affect CO recombination (Lee et al. 1999; Tran et al. 2004). In yeast, Exo1 overexpression suppresses DNA repair defects in mutant cells lacking the MRN complex (Lewis et al. 2002). On the other hand, DNA end resection can still occur in Mre11; Exo1 double mutants (Moreau et al. 2001), which is suggestive of further redundancy in this pathway. In 2008, this third pathway was identified and, surprisingly, involved a RecQ helicase (Sgs1) together with an endonuclease (Dna2). In the current model, Sgs1 unwinds both strands at either end of the DSB, and Dna2 (or Exo1) cuts off the exposed 5′ strand, rapidly creating long 3′ ssDNA tails. Several laboratories have established that Sgs1/Dna2 and Exo1 act in parallel pathways to control long-range end resection in mitotic as well as meiotic cells (Fig. 1; Gravel et al. 2008; Huertas 2010; Manfrini et al. 2010; Mimitou and Symington 2008; Zhu et al. 2008). Although Mre11, Rad50, Exo1, Dna2, and RecQ helicases are highly conserved in *C. elegans*, little is known about end resection in this model organism. For example, the contribution of the MRN complex to DNA end resection is still unclear since the null mutants are defective in meiotic DSB formation and separation-of-function alleles for *mre-11* or *rad-50* are still lacking. Also, worms lacking only *exo-1* show no obvious meiotic defects (B. Lemmens unpublished data), which is in line with the high degree of redundancy and the mild defects in DNA end resection observed in yeast Exo1 single mutants (Manfrini et al. 2010).

While Sgs1 is the sole RecQ helicase in yeast, *C. elegans* has four RecQ helicases and humans have as many as five members of this family. In mammalian cells, EXO1 functions in parallel with the RecQ helicase BLM to promote DNA end resection, DSB signaling, and resistance to DSB-inducing agents (Gravel et al. 2008; Nimonkar et al. 2008). In the worm, deletion of the BLM ortholog *him-6* results in radiation sensitivity, increased chromosomal non-disjunction, and shortened lifespan, underscoring the crucial role of this conserved RecQ helicase in genome maintenance (Grabowski et al. 2005; Wicky et al. 2004). Similar to Sgs1 and BLM (Klein and Symington 2009), *him-6* has a non-redundant role in one of the final steps of HR, as will be discussed later in this review. Its dual role in the HR process together with the high degree of redundancy in early DSB processing has masked the potential role of *him-6* in DNA end resection. Similarly, eukaryotic counterparts of the nuclease Dna2 (including the worm homolog DNA-2) have been implicated in many DNA metabolic processes, complicating interpretation of its DNA repair functions (Budd et al. 2005; Huertas 2010; Kang et al. 2010; Lee et al. 2003). Nevertheless, the *C. elegans* model system may provide new insights into DNA end resection, as it has been shown to be a useful tool with which to study redundant activities during meiotic DSB repair (Barber et al. 2008; Ward et al. 2010), and unbiased synthetic lethal screens can be employed. Importantly, the genetic interactions between the above-mentioned end resection factors are likely to be conserved, as we recently have observed strong synergystic effects on genome instability upon combined loss of *exo-1* and either *dna-2* or *him-6* (B. Lemmens unpublished data). Although technically challenging, it will be interesting to test whether EXO-1 and HIM-6/DNA-2 are responsible for the residual DNA end resection activity observed in the absence of MRE-11/COM-1. Moreover, the molecular basis for the different DSB repair modes during meiotic prophase progression is still elusive, but could well be regulated via posttranslational modification of the implicated nucleases/helicases (as seen for yeast Sae2 and Exo1 proteins; Bolderson et al. 2010; Huertas et al. 2008) and/or via their differential expression throughout the worm germline.

Homologous template search and DNA strand invasion

Subsequent to DNA end resection, the 3′ ssDNA tails are protected by RPA, which is subsequently replaced by RAD-51 to form a nucleoprotein filament that is able to seek a homologous DNA molecule. In the current model, the invading 3′ end of the broken chromosome binds to the complementary donor strand (either from the sister chromatid or homologous chromosome) and primes DNA synthesis to regenerate the sequence information lost at the break site (Fig. 1). In the case of synthesis-dependent strand annealing (SDSA), the elongated invading strand is then displaced and annealed to the complementary ssDNA tail on the other side of the DSB. The remaining single-strand gaps are filled and finally the nicks are ligated, resulting in non-CO products only (Fig. 1). During strand invasion, the second DSB end can also be captured by the displacement strand of the donor duplex (D-loop) and

can be used to prime another round of DNA synthesis covering the initial DSB. This DSB repair mode ultimately generates a double Holliday Junction (dHJ) intermediate, which can be resolved by endonucleolytic cleavage to form either CO or non-CO products (Fig. 1).

In order to create the COs needed for successful meiosis, the RAD-51-coated DSB end must invade the homologous chromosome. Therefore, the homologous chromosome must be recognized and positioned close to the broken chromosome. How this is established is still largely unknown, but early homolog recognition and pairing events coincide with marked changes in nuclear morphology. In the nematode, these events involve special regions on each chromosome known as pairing centers (Phillips et al. 2009). During *C. elegans* meiosis, initial homolog pairing takes place in the “transition zone”, when the polarized redistribution of chromosomes gives rise to the characteristically crescent-shaped DNA (Fig. 3). In 2009, two studies provided some molecular insights into this process by linking homology search to cytoskeletal forces and posttranslational modification of the nuclear envelope protein SUN-1 (Penkner et al. 2009; Sato et al. 2009). Penkner and coworkers showed that SUN-1 is phosphorylated at its N-terminus and forms rapidly moving aggregates at putative homolog attachment sites in the “transition zone”. Similar SUN-1 aggregates were observed after the induction of ectopic DSBs by IR. Importantly, mutation of these N-terminal SUN-1 phosphorylation sites has elicited severe defects in homolog pairing and subsequent CO formation, ultimately resulting in chromosome univalency at diakinesis. How and whether such protein complexes in the nuclear envelope (together with SC proteins) also affect RAD-51-mediated strand invasion in a more direct fashion is still unclear.

One factor that is known to directly control RAD-51-mediated strand invasion in human cells is the well-conserved breast cancer susceptibility gene BRCA2 (Venkitaraman 2001). Human BRCA2 binds RAD51 via a so-called BRC motif, and this interaction is known to stimulate RAD51 multimerization, nucleofilament formation, and HR reactions both *in vitro* and *in vivo* (Chen et al. 1998; Davies et al. 2001; Moynahan et al. 2001; Yuan et al. 1999). In order to study the role of BRCA2 during meiotic DSB repair, the Boulton laboratory has investigated the germline functions of the worm homolog BRC-2. BRC-2 is crucial for proper recruitment of RAD-51 to both endogenous and exogenous DSBs in the germline (Martin et al. 2005). In vitro follow-up studies were performed to acquire more mechanistic insights and revealed that recombinant BRC-2, like human BRCA2, stimulates RAD-51-mediated D-loop formation and controls nucleoprotein filament stability (Petalcorin et al. 2007; Petalcorin et al. 2006). In keeping with a role in strand invasion, germlines that are deficient in *brc-2* allow RPA recruitment; however, they show abnormal chromosome aggregates due to faulty repair of meiotic DSBs. Interestingly, formation of these chromosomal aggregations depends on LIG-4, a crucial NHEJ factor (Martin et al. 2005). By itself, NHEJ-mediated repair of meiotic breaks can be toxic because it never results in COs, which are required for proper chromosome segregation. Illegitimate HR events can also be detrimental, as they can lead to gross

chromosomal rearrangements and tumorigenesis in mammals (Honma et al. 1997; Luo et al. 2000). Therefore, the activities of NHEJ and HR must be tightly controlled during meiotic prophase.

DNA strand invasion and CO formation

One of the best-characterized antagonists of HR is the budding yeast helicase Srs2; however, sequence conservation suggests that an obvious homolog is lacking in higher eukaryotes. In 2008, Barber and colleagues reported the identification of a functional Srs2 analog in *C. elegans*, named *rtel-1* (Barber et al. 2008). Although *in vitro* studies have revealed differences between the biochemical activities of RTEL1 and Srs2, both proteins counteract HR by dismantling DNA strand invasion intermediates. Similar to Srs2 mutants, worms deficient in *rtel-1* show hyperrecombination, lethality upon deletion of the RecQ helicase Sgs1/*him-6*, and sensitivity to DNA damaging agents. Importantly, human cells depleted of the ortholog RTEL1 exhibit similar hyperrecombination and DNA damage sensitivity phenotypes.

Recently, Youds and coworkers elaborated on the role of RTEL-1 during *C. elegans* meiosis and reported a crucial role for RTEL-1 in CO control (Youds et al. 2010). Specifically, RTEL-1 prevents excess meiotic COs, most likely by promoting meiotic SDSA (Fig. 1). *Rtel-1* mutants show an average of two COs per chromosome pair (instead of only one), which totals up to 12 COs per nucleus, implicating a role for RTEL-1 in CO interference. Based on the data from the Meyer lab, this would mean that all meiotic DSBs are converted into COs in the absence of RTEL-1 (Mets and Meyer 2009). These observations also suggest that, in wild-type worms, virtually all meiotic DSBs are repaired via the homologous chromosome, one half through SDSA and the other half via a CO intermediate. Yet, a minor fraction of meiotic DSB may escape repair via the homologous chromosome. In that case, the nearby sister chromatid could be used to faithfully restore the damage, as will be discussed later in this review.

Similar to *rtel-1* mutation, loss of the condensin DPY-28 also results in additional COs. However, in *dpy-28* mutants, this phenomenon is assigned to elevated numbers of meiotic DSBs, rather than altered DSB repair (Mets and Meyer 2009). If RTEL-1 and DPY-28 controlled CO formation via different mechanisms, one would expect to find an additive effect on CO recombination when these deficiencies are combined. Indeed, *rtel-1*; *dpy-28/+* double mutants have more COs than either single mutant (*rtel-1* or *dpy-28/+*), resulting in many triple or occasionally even quadruple COs, which implies that RTEL-1 also inhibits CO formation at these extra-meiotic DSBs. Still, many of the extra DSBs observed in *dpy-28* single mutants are repaired via a CO intermediate (despite the presence of RTEL-1), which suggests the existence of a counteracting mechanism that promotes CO formation. Conceivably, such a mechanism may involve the aforementioned SC components HIM-3 and HTP-1, which are known to restrain inter-sister HR and therefore promote CO formation (Couteau et al. 2004; Martinez-Perez and Villeneuve 2005).

Recently, two additional factors, *rfs-1* and *helq-1*, have been implicated in the post-invasion steps of HR and, as predicted, interact genetically with *rtel-1* (Ward et al. 2010). The RAD-51 paralog RFS-1 and the helicase HELQ-1 promote postsynaptic RAD-51 filament disassembly during *C. elegans* meiosis. Here again, redundant mechanisms have evolved to ensure proper meiotic DSB repair, as only the combined deficiency of both *rfs-1* and *helq-1* results in the persistence of RAD-51 foci, severe chromosomal aberrations, and, consequently, unviable progeny. Based on *in vitro* studies, RFS-1 and HELQ-1 both bind RAD-51 and work in complementary but mechanistically different pathways to promote RAD-51 removal from dsDNA. Interestingly, the phenotypes of the *helq-1; rfs-1* double mutants are very similar to those observed in *C. elegans rad-54* mutants (Mets and Meyer 2009). In *Saccharomyces cerevisiae*, Rad54 mutants are defective in HR and also exhibit retarded removal of Rad51 (Shinohara et al. 2000; Solinger and Heyer 2001). Yeast Rad54 is a motor protein that translocates along dsDNA and performs several important functions in HR, including the stimulation of Rad51-mediated strand exchange, extension of heteroduplexes, and chromatin remodeling (Mazin et al. 2010). Rad54 may well have identical roles in *C. elegans* because, virtually all SPO-11-induced DSBs persist and retain RAD-51 proteins in *rad-54* mutant germlines, causing these worms to be completely infertile (Mets and Meyer 2009).

As portrayed above, homology search and subsequent strand invasion steps are intriguing but complex processes and involve many factors that often have multiple roles in genome maintenance. Moreover, several backup mechanisms appear to exist to guarantee faithful HR-mediated repair of meiotic DSBs. Many of the aforementioned meiotic DSB repair factors have only recently been discovered or characterized in detail, and many questions follow from these studies, such as how do all these seemingly redundant factors interact genetically, how is their activity regulated, and what determines repair template choice?

Holliday junction resolution

One of the final intermediates in HR is the so-called dHJ intermediate, which consists of two complex four-way DNA joints known as Holliday junctions (HJs); (Figs. 1 and 4). These HJs tie the chromosomes to each other and must eventually be resolved to complete meiosis (and other forms of HR-mediated DSB repair). In 1991, two research groups jointly discovered an enzyme in *Escherichia coli* capable of resolving these HJs (Connolly et al. 1991; Sharples and Lloyd 1991). This discovery evoked a challenging search for eukaryotic equivalents of this bacterial HJ resolvase—a mission that was surprisingly difficult and took almost 20 years to accomplish (see West 2009 for an excellent historical overview). The bacterial RuvC enzyme is able to symmetrically cleave HJs *in vitro* and generates products that can be religated without further processing. For decades, this activity has served as a textbook model for meiotic dHJ resolution because such an activity could create non-COs (when the same pair of strands are

cleaved in both junctions) as well as obligate COs (when different strand pairs are cleaved at each intersection) (Fig. 4; Szostak et al. 1983). This model predicts that both COs and non-COs derive from dHJ intermediates. Classical HJ resolvases (like RuvC) cleave either pair of strands with equal probability, which is consistent with observations in *S. cerevisiae* and *C. elegans*, in which half of the meiotic DSBs are converted into COs. However, several observations challenge the idea that the orientation of HJ resolution accounts for the relative frequencies of COs and non-COs. For example, several mutations have been found in yeast that reduce CO recombination without affecting either the number of non-COs or the formation of DSBs (Whitby 2005). Moreover, in worms defective in SDSA, all meiotic DSBs appear to be converted into COs (Youds et al. 2010). This indicates that COs and non-COs derive from independent pathways of DSB repair. In fact, current models suggest that dHJs are resolved exclusively as COs, although the underlying mechanism is still unknown (Fig. 4).

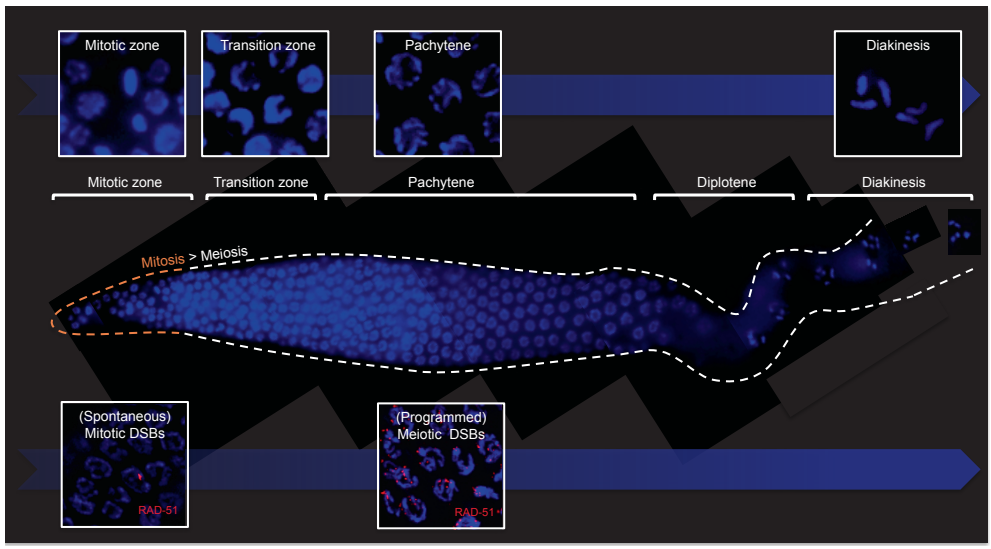

Fig. 4 Different models for CO formation. Schematic representation of the DSB repair model as postulated by Szostak et al. in 1983, in which CO/non-CO outcome is determined by the orientation of dHJ resolution (left), and the current model, in which CO/non-CO designation occurs before dHJ formation (right)

An important set of proteins involved in HJ resolution are the so-called ZMM (Zip1, Zip2, Zip3, Msh4, Msh5 and Mer3) proteins, among which ZHP-3, MSH-4, and MSH-5 are the best-studied members in *C. elegans* (Bhalla et al. 2008; Colaiacovo et al. 2003; Winand et al. 1998). In yeast, ZMM proteins appear to stabilize single-end invasion intermediates and promote dHJ formation and subsequently ensure that HJ resolution occurs with the appropriate bias to generate COs (Borner et al. 2004; Fung et al. 2004). Also, ZMM proteins localize to DSBs destined to be converted into COs, specifically those that are subject to CO interference (Lynn

et al. 2007). Accordingly, transgenic worms carrying a ZHP-3::GFP protein-fusion construct show six GFP foci in diplotene nuclei, one focus per chromosome pair (Bhalla et al. 2008). Moreover, worms carrying mutations in ZMM genes (e.g., *msh-4* or *msh-5* null mutants) are unable to generate the six obligate COs, resulting in 12 univalents at diakinesis (Kelly et al. 2000; Zalevsky et al. 1999). This strict requirement of ZMM proteins for proper meiotic CO formation is also seen in mammals; for instance Msh4-/- and Msh5-/- mice are infertile and exhibit defects in chromosome pairing during meiosis I (de Vries et al. 1999; Edelmann et al. 1999; Kneitz et al. 2000). While the exact role of the ZMM proteins remains to be elucidated, human MSH4-MSH5 heterodimers are thought to recognize HJs and encircle the adjacent duplex DNA, where they could serve to stabilize the HJ intermediate and/or recruit factors capable of resolving HJs (Snowden et al. 2004; Fig. 4).

In 2008, Ip and collaborators were the first to identify nucleases from budding yeast and human cells that promote HJ resolution *in vitro*, in a manner reminiscent of the bacterial HJ resolvase RuvC (Ip et al. 2008). Via extensive fractionation and mass spectrometry analysis of nuclear extracts derived from 200 liters of Hela cells, they discovered the human HJ resolvase GEN1. A parallel screen using a yeast gene fusion library yielded a similar Rad2/XPG nuclease called Yen1 (Ip et al. 2008). A mutant of the worm ortholog, g*en-1,* has recently been identified in the Gartner lab, using an unbiased forward genetic screen for DNA damage-induced cell cycle arrest (Bailly et al. 2010). Its function as an HJ resolvase appears to be conserved, since GEN-1 shows HJ resolution activity *in vitro*, and worms lacking *gen-1* are hypersensitive to DSB-inducing agents and show persistent RAD-51 foci after IR treatment, suggestive of inefficient DSB repair. However, *gen-1* null mutants are fertile and show no change in CO recombination, which suggests that *gen-1* functions primarily as a checkpoint gene in *C. elegans*, or that other factors exist that work redundantly to *gen-1* at the level of HJ resolution (Bailly et al. 2010).

In 2009, four studies reported the identification of a novel protein complex able to process HJs analogous to RuvC/GEN1. This complex consisted of the scaffold protein SLX4 and the endonuclease SLX1 (Andersen et al. 2009; Fekairi et al. 2009; Munoz et al. 2009; Svendsen et al. 2009). Human SLX4 is thought to act as a coordinating platform for multiple endonucleases to control cleavage of various damaged or branched substrates, including HJs (Fekairi et al. 2009; Svendsen et al. 2009). In vitro studies using SLX1 immunoprecipitates from human cells or SLX4/SLX1 complexes purified from *E. coli* suggest that the interaction between SLX4 and SLX1 is required for symmetric HJ resolution. Previous work in *Drosophila* had already identified a protein named MUS312, which was similar to SLX4 (and interacted with the fly XPF homolog MEI-9) and was needed for proper meiotic recombination, revealing the impact of SLX4 deficiency in a developing animal. Recently, such a role was substantiated by Saito and colleagues, who showed that the worm homolog SLX-4 was required for processing HR intermediates in both mitotic and meiotic nuclei in the *C. elegans* germline (Saito et al. 2009).

Slx-4 mutant animals show a reduction in CO recombination frequencies and increased levels of strand invasion intermediates (RAD-51 foci), accompanied by elevated germ cell apoptosis, unstable bivalent attachments, and chromosome non-disjunction. Still, homozygous *slx-4* mutants are able to produce viable offspring and frequently show six bivalents at the diakinesis stage, indicating that redundant activities exist that ensure CO formation in the absence of SLX-4. In accordance with the proposed "scaffold function" of its human counterpart, *C. elegans* SLX-4 also interacts with multiple structure-specific endonucleases, including SLX-1 and XPF-1 (Saito et al. 2009). At present, one deletion allele of *slx-1* is available, likely resulting in a truncated SLX-1 protein that still contains its highly conserved nuclease domain. Unfortunately, this allele is reported not to be a strong loss-of-function allele, hampering its use for *in vivo* analysis of SLX-1 function (Saito et al. 2009). In addition, the exact role of the interaction between SLX-4 and XPF-1 in meiotic CO formation is still unclear. Although x*pf-1*-deficient worms show meiotic defects similar to those observed in the absence of *slx-4* (including a reduction in CO frequency and elevated chromosomal non-disjunction), the phenotypes in *xpf-1* single mutants are clearly milder than those observed in *slx-4* single mutants (Saito et al. 2009).

Holliday junction processing

In addition to these HJ resolvases, other mechanisms have evolved to ensure CO formation. In *Schizosaccharomyces pombe*, CO formation mainly depends on another highly conserved endonuclease called Mus81. Mus81 mutants in fission yeast produce virtually no viable spores (<1% survival) due to defects in chromosome segregation during meiosis I (Boddy et al. 2000; Osman et al. 2000). In contrast, Mus81 mutants in budding yeast still produce 60% viable spores. Higher organisms seem to depend even less on Mus81 to repair meiotic DSBs, as *C. elegans mus-81* mutants produce up to 80% viable progeny and Mus81-/- mice are fertile and show only minor meiotic defects (Dendouga et al. 2005; McPherson et al. 2004; Saito et al. 2009). Recent studies have revealed overlapping roles for GEN1/Yen1 and Mus81 in HJ resolution at collapsed replication forks, as well as at meiotic DSBs (Lorenz et al. 2010; Tay and Wu 2010). The extreme dependence on Mus81 to process meiotic HJs, as observed in *S. pombe*, may be explained by the fact that this yeast species appears to lack an obvious Yen1 ortholog. In addition, fission yeast seems to be deprived of MSH4-MSH5 orthologs, which is also consistent with the observed lack of CO interference.

Several studies on Mus81 function indicate that this nuclease may act early during DSB repair, generating COs by processing non-dHJ intermediates (Heyer et al. 2003; Osman et al. 2003). In that vein, Mus81 in budding yeast has been shown to work together with the Bloom syndrome helicase Sgs1 to resolve aberrant joint molecules that may arise during meiotic recombination (Jessop and Lichten 2008; Oh et al. 2008). Such a function of MUS-81 could explain the fact that *C. elegans mus-81; rtel-1* double mutants are completely infertile and

exhibit many persistent RAD-51 foci in pachytene nuclei because, in the absence of RTEL-1, toxic strand invasion intermediates may arise that require MUS-81 function for their resolution. In keeping with the cooperative functions of Mus81 and Sgs1 in yeast, *him-6*; *rtel-1* double mutant worms also show an elevated level of meiotic RAD-51 foci and increased embryonic lethality compared with either single mutant (Barber et al. 2008). Although wild-type worms appear to depend exclusively on ZMM-mediated HJ resolution for CO formation, a recent study revealed that, in absence of *rtel-1*, ZMM-independent CO routes do exist in *C. elegans* (Youds et al. 2010). Similar to yeast, this ZMM-independent class of COs required *mus-81* (Hollingsworth and Brill 2004; Youds et al. 2010). Together, these data argue that MUS-81 does not function as a central HJ resolvase in *C. elegans*; however, it likely serves as an important backup to ensure proper HJ resolution.

Holliday junction dissolution

To complicate matters even further, nature has come up with another solution to resolve dHJs, *i.e.*, a process termed "dissolution" that does not require structure-specific nucleases. In dissolution, dHJs are untangled via ssDNA decatenation by a helicase–topoisomerase complex. In yeast, dissolution is performed by Sgs1, Top3, Rmi1, and RPA, and exclusively generates non-CO products (Chen and Brill 2007; Plank et al. 2006; Wu and Hickson 2003). The Sgs1 helicase has multiple redundant roles during HR, which are reflected by its many synthetic lethal interactors, including Dna2, Mus81, Slx4, and Srs2 (Pan et al. 2006). However, the Sgs1 helicase has non-redundant activities as well, illustrated by the fact that Sgs1 mutation results in reduced spore viability. Similarly, *C. elegans* single mutants lacking only the Sgs1 ortholog *him-6* show reduced progeny survival and elevated levels of chromosomal non-disjunction. In yeast, the predominant non-redundant meiotic function of this RecQ helicase seems to involve a non-CO pathway, as Sgs1 single mutants display an increase in CO frequency (Rockmill et al. 2003). On the contrary, worms deficient in *him-6* mainly exhibit phenotypes that suggest a key role in a CO pathway: *him-6* single mutants exhibit up to 50% reduction in CO recombination and severe defects in chiasmata formation (Wicky et al. 2004). Moreover, when all DSBs are skewed into CO pathways (e.g., by blocking the principal non-CO pathway in *C. elegans* via *rtel-1* mutation), meiotic nuclei seem to depend even more on HIM-6 for proper DSB repair (Barber et al. 2008). This suggests that, either the main function of this RecQ helicase has changed over the course of evolution, or the dependency on its specific functions has diverged between the different species.

In theory, the relative roles of the worm orthologs HIM-6 and TOP-3 during meiotic HJ resolution and/or dissolution could be assessed by epistasis analysis. Unfortunately, this is not feasible in the worm because *him-6; top-3* double mutants suffer from mitotic catastrophe, resulting in a massive increase in DSBs already in the mitotic zone of the germline (Wicky et al. 2004).

A long-standing question has concerned the mechanisms by which dHJ intermediates are resolved, and as described above, recent studies have led to the identification of many crucial factors involved (Figs. 1 and 4). Still, exciting times await us, since now, these pieces of the puzzle need to be placed correctly in the redundant networks that ensure proper HJ resolution. As a proven genetic model for metazoan meiosis, *C. elegans* will likely contribute in shaping this research field, e.g., by revealing the *in vivo* consequences of HJ resolution defects in complex genetic backgrounds.

Meiotic DSB repair via the sister chromatid

One of the interesting questions in the meiosis field concerns the choice of the two possible repair templates of programmed DSBs, *i.e.*, the sister chromatid or the homologous chromosome. Half of the DSBs are converted into COs and therefore use the homologous chromosome for repair. Repair of the other DSBs, via non-CO sub-routes of HR, does not necessarily involve the homologous chromosome: SDSA is the major non-CO repair route in the *C. elegans* germline, which could well use any homologous template (the sister or the homolog). As discussed earlier, most data thus far point towards the exclusive use of the homologous chromosome; however, inter-sister HR can also contribute to meiotic DSB repair. In 2008, Adamo and colleagues described the function of BRC-1, the homolog of the well-studied HR factor and breast cancer tumor suppressor BRCA1, and showed that it acts (almost) exclusively in inter-sister HR in the worm germline (Adamo et al. 2008). Null mutants of *brc-1* are viable, fertile, and exhibit the wild-type compliment of six bivalents in most diakinetic nuclei, indicative of successful CO recombination. However, *brc-1* mutants show persistent SPO-11-dependent RAD-51 foci at the late pachytene stage and a mild level of chromosome non-disjunction, revealing its role in meiotic DSB repair. Furthermore, *brc-1* mutant germlines are hypersensitive to DSB-inducing agents such as camptothecin and IR (Ward et al. 2007). When DSB repair via the homologous chromosome is not possible (e.g., in the absence of SC genes), loss of *brc-1* leads to severe chromosome fragmentation, suggesting that *brc-1* is crucial for meiotic DSB repair through inter-sister HR (Adamo et al. 2008). Notably, the vertebrate orthologs of *brc-1* and *com-1* (BRCA1 and CtIP, respectively) modulate DSB repair pathway choice during the different mitotic cell cycle phases (Yun and Hiom 2009). How exactly *brc-1* controls DSB repair during meiosis is still unclear, but it likely functions in concert with one of its many binding partners, as several recent proteomic and genetic studies have revealed the presence of various distinct BRCA1 complexes *in vivo*, each of which governs a specific cellular response to DNA damage (reviewed in Huen et al. 2009).

Recently, two other players, SMC-5 and SMC-6, have been described to have an important role in meiotic inter-sister HR (Bickel et al. 2010). The meiotic phenotypes of *smc-5/smc-6* mutants are very similar to *brc-1* mutants, including normal chiasmata formation, IR hypersensitivity, and severe chromosomal fragmentation upon loss of inter-homolog

HR. Then again, *smc-5/smc-6* single mutants already show a high degree of chromosome fragmentation at diakinesis stage, a phenotype rarely seen in *brc-1*-deficient germlines. This latter observation implies that a significant number of meiotic DSBs still need to be repaired via inter-sister HR to safeguard germ cell genomic integrity and that this process may not be completely disrupted in *brc-1* mutants (Bickel et al. 2010).

Signaling events in the germline

As portrayed above, DSB repair during meiosis requires many factors, which all need to be active only at a specific stage, location, and/or designated substrate. Importantly, HR (the principal repair route in the germline) is a dynamic process that involves both factors that favor recombination reactions and factors that counteract these intermediates. Tight regulation of the repair proteins involved is necessary to safeguard genomic stability and ensure the formation of the obligate COs. Posttranslational modifications, such as phosphorylation, ubiquitination, and SUMOylation are rapid, dynamic, and reversible means of regulation that could control many of the steps in meiotic prophase progression. Indeed, several highly conserved kinases have been shown to be crucial for proper DSB repair during meiosis.

Phosphorylation events in the germline

An important set of kinases implicated in the DSB response belong to the phosphatidylinositol-3 kinase related kinase (PIKK) family, among which ATM (*atm-1*) and ATR (*atl-1*) are the best-characterized in *C. elegans*. Both ATM and ATR are believed to be the primary sensors of DNA damage and phosphorylate numerous substrates involved in cell cycle checkpoint, apoptosis, and DNA repair (Matsuoka et al. 2007; Smolka et al. 2007). Although ATR and ATM share many of their downstream substrates, they primarily respond to different types of lesions and accordingly show different modes of activation and recruitment (Garcia-Muse and Boulton 2005; Hurley and Bunz 2007). In human mitotic cells, ATM mainly responds to IR-induced DSBs, whereas ATR primarily acts at lesions arising from replication fork stalling and UV damage (Cimprich and Cortez 2008; Czornak et al. 2008). A recent study that exploited the *C. elegans* germline to investigate the activation and recruitment of PIKKs after different types of DNA damage revealed an unexpected role for the RecQ helicase WRN-1 in the recruitment of ATM-1 to IR-induced damage (Lee et al. 2010). Although WRN helicases are well known for their roles in replication, DNA repair, and telomere maintenance, such an upstream role in DSB recognition and checkpoint activation had not been previously anticipated (Rossi et al. 2010). Whether the WRN helicase has a role in ATM activation also in human cells still awaits confirmation.

In budding yeast, the ATM/ATR homolog Mec1 is required for proper meiotic progression, as Mec1 mutants show a reduction in meiotic recombination, loss of inter-homolog bias, and defective CO control (Carballo and Cha 2007). PIKKs also seem to affect meiotic CO control

in higher organisms; for example, *Drosophila* mutants lacking the ATR homolog Mei-41 and Atm-/- mice both show altered CO distributions (Barchi et al. 2008; Gatti et al. 1980). In *C. elegans, atl-1* and *atm-1* single mutants display the normal six bivalents during diakinesis, indicating that ATR and ATM are not absolutely required for CO formation. However, these kinases could still play a role in CO interference. Interestingly, the protein sequence of RTEL-1 contains a putative ATM/ATR phosphorylation motif that is well conserved among flies, mice, and humans. Whether and how the PIKK kinases affect CO distribution in the worm still remains to be addressed.

With regard to possible downstream targets of ATM signaling, it should be noted that it is an outstanding question whether the H2Ax signaling cascade that amplifies the DNA damage response in mammals is "functionally" conserved in *C. elegans*. The genome of the worm does not encode an H2Ax ortholog nor is there an obvious motif present in, e.g., H2A that could serve as an ATM-dependent DSB chromatin mark. While other components involved in the more downstream part of this signaling cascade also seem to be missing (e.g., MDC1 and RNF8), some are likely conserved, as *hsr-9* encodes a protein that is closely related to 53BP1.

The polo-like kinase (PLK) family is another class of kinases that is important for faithful chromosome segregation and DSB response. For instance, Cdc5 (the sole PLK in yeast) promotes HJ resolution and proper chromosome separation during meiosis (Clyne et al. 2003; Sourirajan and Lichten 2008). Humans have four PLKs and while their role in mitosis is widely studied, their function during meiosis is largely unknown (Archambault and Glover 2009). The *C. elegans* genome contains three PLK paralogs, and mutations in *plk-1* and *plk-2* have recently been shown to display strong meiotic defects (Chase et al. 2000a, b; M. Zetka, personal communication). An additional kinase shown to control meiotic progression and affect genomic stability during worm gametogenesis is CHK-2; however, whether this protein has a direct role in DSB repair is unknown (MacQueen and Villeneuve 2001).

Ubiquitination events in the germline

In addition to these phosphorylation events, other modes of posttranslational modification (such as ubiquitination and SUMOylation) are likely to control DSB repair, as they do in other model organisms (Boulton 2009). For example, mammalian BRCA1 and its related binding partner BARD1 form a heterodimeric complex that acts as an ubiquitin E3 ligase (Hashizume et al. 2001). Since the enzymatic activity of the BRCA1/BARD1 complex is conserved over a broad phylogenetic range, it is thought to be critical for the central functions of BRCA1. However, Reid and coworkers recently revealed that key aspects of BRCA1 function in genome maintenance in mammalian ES cells, including its role in HR-mediated DSB repair, do not depend on the E3 ligase activity of BRCA1 (Reid et al. 2008). The *C. elegans* BRCA1 and BARD1 homologs (BRC-1 and BRD-1, respectively) have been shown to form an active ubiquitin ligase *in vitro* (Boulton et al. 2004; Polanowska et al. 2006). Notably, this BRC-1/

BRD-1 complex is activated on chromatin *in vivo* after IR damage and is responsible for many ubiquitination events at IR-induced lesions in the mitotic zone of the germline (Polanowska et al. 2006). Unfortunately, the identity of these IR-dependent BRC-1 substrates is still unknown. Moreover, the significance of these BRC-1-dependent ubiquitination events for genomic stability still needs to be addressed.

DSB repair and the mitotic cell cycle

Mitotic DSB repair and development

As described in the previous sections, HR pathways ensure genomic stability in meiotic cells by faithfully repairing all the programmed DSBs introduced by SPO-11. Maintaining genomic integrity in gametes is crucial to create viable offspring and thereby promotes species survival. However, the challenge does not end here, especially for multicellular organisms like *C. elegans* and humans, which must generate complex somatic tissues to support their germline. When two gametes merge to form a zygote, this single cell has to divide numerous times to form a healthy and fertile multicellular organism that is able to cope with the countless challenges it will encounter before it can complete its life cycle. During animal development and in tissues that are continuously replenished in adults (e.g., the human intestine and the hematopoietic system), many cells are actively cycling in order to create new diploid daughter cells.

Whereas DSBs can occur at any stage of the cell cycle, proper repair templates are not always available. During and after DNA replication, sister chromatids are held in close proximity to each other by cohesins, providing a convenient template for homology-based DSB repair (Nasmyth and Haering 2009). Accordingly, HR is mainly active in S/G2 (Beucher et al. 2009; Delacote and Lopez 2008). In contrast, NHEJ does not require a homologous template and has been shown to be active during all stages of the cell cycle (Beucher et al. 2009). Because HR is principally error-free and NHEJ is error-prone, cell cycle stage is an important determinant for DSB repair fidelity. In addition, cell fate is an important determinant for the consequences of unfaithful DSB repair: stem cells producing the germline harbor the genetic material that is passed on to the next generation and their genomic integrity is thus crucial to the identity and survival of the species. On the contrary, cells that form or replenish the soma are needed for the survival and fitness of the individual. For that reason, genomic stability in somatic cells determines the health of the individual and, with that, its ability to reproduce. Especially in long-lived animals, somatic genome instability can lead to the accumulation of genetic insults that may promote aberrant cellular behavior, ultimately leading to lethal diseases such as cancer. Even in short-lived animals that do not develop tumors, such as *C. elegans*, both cell cycle stage and cell fate have been demonstrated to greatly affect DSB repair.

DSB repair in the mitotic germline

In *C. elegans*, the germline is set apart from the soma already early during embryogenesis: during the first embryonic divisions only a few blastomeres (belonging to the so-called P-lineage) acquire germline potential, culminating in a single germline founder cell named P4 (Sulston et al. 1983). This P4 cell does not contribute to the soma, but divides to give rise to two primordial germ cells (named Z2 and Z3), which eventually will spawn all germline nuclei/cells (Fig. 2). Germline cells are the only cells in the adult animal that are mitotically proliferating; all other cells can be considered somatic (predominantly terminally differentiated) and are born through an invariant lineage mostly during *C. elegans* embryonic development, which for convenience can be divided into two distinct phases: an “early stage” that is marked by rapid mitotic divisions, resulting in approximately 550 cells in less than 6 h; and a “late stage” of 8 h that is virtually devoid of cell divisions (Fig. 5). Interestingly, in late-stage embryos, the mitotic primordial germ cells (Z2/Z3) arrest in G2, whereas the surrounding somatic cells temporarily halt in G1 (Clejan et al. 2006). Similar results have been observed in dauer larvae, which may have to store their non-dividing germline stem cells for weeks. This specific feature of germ cells could well be evolved to facilitate error-free HR in order to protect the genetic information passed on to future generations. Indeed, germ cells seem to depend exclusively on HR for IR resistance during all stages of development (Fig. 5; Clejan et al. 2006). In contrast, somatic cells have been shown to depend on HR as well as error-prone means of DSB repair to maintain genome stability (Fig. 5; Clejan et al. 2006; Pontier and Tijsterman 2009).

Many of the factors shown to be involved in meiotic HR are also contributing to mitotic HR. Accordingly, several mutants that exhibit defects in HR during the meiotic stages of the germline also display increased genomic instability in mitotic cells. As an example, previously discussed *him-6* and *xpf-1* mutants show elevated levels of RAD-51 foci also in the mitotic zone of the adult germline, suggesting that these HR factors act both on programmed meiotic DSBs and on spontaneous DSBs that arise in mitotic cells (Saito et al. 2009; Wicky et al. 2004). Another example: worms that lack factors involved in meiotic HJ resolution (e.g., SLX-4 or MUS-81) show elevated RAD-51 foci in the mitotic region of the germline (Saito et al. 2009). On the other hand, some HR steps seem to be differentially regulated at mitotic DSBs and meiotic DSBs. For instance, *rad-50* and *com-1* mutants show a number of strong RAD-51 foci in the mitotic zone but are completely incapable of loading RAD-51 at SPO-11-bound DSBs during meiosis (Hayashi et al. 2007; Penkner et al. 2007). While this could reflect the different natures of meiotic and mitotic DSBs, the distinct kinetics of RAD-51 loading at IR-induced DSBs suggests that DNA end resection is differently regulated in mitotic and meiotic cells (Hayashi et al. 2007). Downstream HR processes also seem to be differentially regulated, as *helq-1; rfs-1* double mutants are deficient in RAD-51 removal from meiotic DSBs but show no persistent RAD-51 foci in the mitotic compartment of the germline (Ward et al. 2010).

Apart from different genetic requirements for the repair of DSBs in mitotic versus meiotic cells, the intermediate DNA substrates onto which the various DSB repair proteins act may be fundamentally different. Although Bzymek and colleagues very recently reported DSB repair intermediates in mitotic yeast cells whose strand composition and size were identical to the dHJs that arise during meiosis, they also observed some fundamental differences (Bzymek et al. 2010): the joint molecules that arise during mitotic DSB repair preferentially occur between sister chromatids, whereas meiotic dHJs principally occur between homologous chromosomes. Moreover, dHJ intermediates seem to represent a minor pathway of DSB repair in mitotic cells, being detected at approximately tenfold lower levels (per DSB) than during meiotic recombination.

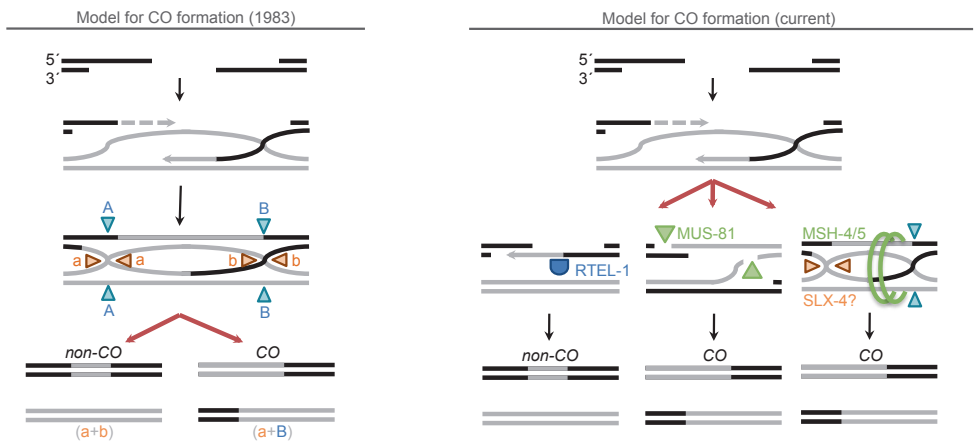

Fig. 5 Overview of the major DSB repair pathways that are active during C. elegans development. See text for details

DSB repair in somatic cells

Somatic cells do not depend solely on HR to repair a DSB, but instead use both high-fidelity and error-prone DSB repair pathways. An important and well-studied error-prone DSB repair pathway is NHEJ. In human cells, NHEJ requires, at the very least, the Ku70/Ku80 heterodimer complex for DSB recognition and the XRCC4–Ligase IV complex in order to seal the break. In addition, efficient NHEJ requires the protein kinase DNA–PKcs and DSB end-processing enzymes, such as Artemis (Burma et al. 2006; Fig. 1). Both the Ku proteins (CKU-70/CKU-80) and Ligase IV (LIG-4) are conserved in *C. elegans* and have been shown to be crucial for resistance to DSB-inducing agents during certain developmental stages (Clejan et al. 2006). Mammalian DNA–PKcs is able to bridge DSB ends *in vitro* (DeFazio et al. 2002) and is shown to be critical for NHEJ activity *in vivo* (Kurimasa et al. 1999). Remarkably, based on sequence identity, nematodes (and all yeast species) seem to lack an obvious DNA–PKcs homolog. Artemis is an SNM1-like exonuclease that, upon complex formation with DNA–PKcs, acquires endonucleolytic activity capable of processing complex DSBs, including the DSBs that occur in lymphocytes during V(D)J recombination (Pannicke et al. 2004). The *C. elegans* genome contains only a single gene that belongs to the SNM1 family: *mrt-1*. Surprisingly, worms lacking MRT-1 do not display the IR-induced somatic defects normally seen in strains deficient for any of the core NHEJ subunits *lig-4, cku-70*, or *cku-80* (Meier et al. 2009). Instead, *mrt-1* mutation results in hypersensitivity to DNA crosslinking agents; a phenotype shared with human SNM1 and many other HR factors (Meier et al. 2009). Together, these observations could suggest that the worm can do with a minimal set of NHEJ factors consisting only of three core proteins (CKU-70, CKU-80, and LIG-4); however, a saturated and unbiased screen for factors specifically affecting *in vivo* NHEJ activity has yet to be performed.

In 2006, Clejan and coworkers investigated the relative contribution of HR and NHEJ in somatic *C. elegans* cells by looking at developmental abnormalities induced by IR damage (Clejan et al. 2006; Fig. 2). Using several IR assays, they revealed that such cells employ both HR and NHEJ to repair exogenous DSBs (Fig. 5); however, these repair pathways were employed in different cellular contexts. When DSBs were introduced in highly proliferative somatic cells by irradiating “early stage” embryos, embryonic survival depended exclusively on HR factors, including the MRN complex components *rad-50* and *mre-11*, and downstream effectors *rad-51* and *rad-54*. The absence of NHEJ failed to enhance their hypersensitivity to IR (in both HR proficient and HR-depleted backgrounds), suggesting a non-redundant role for HR in the repair of IR-induced damage in the early embryo (Fig. 5). In contrast, when DSBs were introduced in non-cycling cells by irradiating “late stage” embryos, DSB repair depended primarily on NHEJ rather than HR (Fig. 5). Therefore, cell cycle progression clearly affects DSB repair pathway “choice”. Although irradiated late-stage embryos do hatch, they show a variety of severe post-embryonic defects, especially in tissues that require cell proliferation during larval development (Fig. 5). Similar to the situation during early embryogenesis, faulty DSB repair followed by cell cycle progression can result in major developmental defects.

IR is often used to study DSB repair because it is an efficient way of inflicting DSBs. However, IR actually induces many other types of DNA damage as well, including SSLs (Cadet et al. 2004). Our laboratory recently developed a transgenic reporter system that specifically detects DSB repair in the somatic cells of a developing worm (Pontier and Tijsterman 2009). This reporter system is based on inducible expression of the rare-cutting endonuclease I-SceI, which generates a single DSB specifically at the integrated reporter locus. Various well-known DSB repair factors (those needed for HR, NHEJ, or SSA) were probed for their relative contributions to DSB repair in somatic cells leading to the notion of a dynamic and robust network of DSB repair pathways that governs genome integrity during *C. elegans* development. For example, loss of HR (via either *rad-51* RNAi or *brc-1* mutation) resulted in a strong increase in SSA activity. Similarly, when crucial NHEJ factors were mutated, other DSB repair pathways (including SSA and MMEJ) compensated for the loss. In addition, Pontier revealed that *C. elegans* XPF-1 (in addition to its function in HR in the germline) has a conserved role in SSA in somatic cells, matching the SSA defects observed in Rad1/Xpf-deficient mitotic yeast cells (Klein 1988; Pontier and Tijsterman 2009; Prado and Aguilera 1995). Although this I-SceI-based reporter system revealed (error-prone) repair events in many different tissues, the exact identity of the cells involved and their proliferative states at the moment of DSB induction has yet to be determined (Figs. 2 and 5).

Concluding remarks

The toxicity of DSBs, which threatens all living organisms, has led to the evolution of various DSB repair pathways, including NHEJ, HR, MMEJ, and SSA. The fact that cells do not rely on a single DSB repair route, but instead have developed a complex network of redundant DSB repair mechanisms, underscores the risk of faulty DSB repair. Moreover, there seems to be immense evolutionary pressure on proper DSB repair, as many DSB repair factors are well-conserved from yeast to mammals. Paradoxically, the same evolutionary pressure has led to the existence of highly regulated developmental programs that induce endogenous DSBs to promote genetic variation and correct chromosome segregation. Several crucial components in DSB repair have recently been discovered, including factors involved in DSB formation, DSB recognition, DNA end resection, and dHJ resolution. *C. elegans* research has proven to be an excellent platform to elucidate DSB repair processes in a developmental context. Its convenient germline makeup, its suitability for genetic screens, and the fact that genetic mutants are relatively easily combined have already paid off in the identification of several crucial processes during meiotic DSB repair. Although somatic DSB repair is still largely unexplored in *C. elegans* research, this model organism has already led to important insights into the influence of cell fate and cell cycle progression on DSB repair during development.

Since many of the newly identified DSB repair genes are conserved from worms to humans and more and more tools are being developed to study DSB repair in the nematode, we expect that this little worm will contribute significantly to our understanding of DSB repair in multicellular animals.

Acknowledgments

We thank Daphne Pontier for providing the pictures of germline nuclei stained against RAD-51.We are also grateful to all members of the Tijsterman lab for discussions and to Nick Johnson for helpful comments on the manuscript. We apologize to authors whose research articles could not be cited due to space constraints.

References

Adamo A, Montemauri P, Silva N, Ward JD, Boulton SJ, La Volpe A (2008) BRC-1 acts in the inter-sister pathway of meiotic double- strand break repair. EMBO Rep 9:287–292

Alpi A, Pasierbek P, Gartner A, Loidl J (2003) Genetic and cytological characterization of the recombination protein RAD-51 in Caeno-rhabditis elegans. Chromosoma 112:6–16

Andersen SL, Bergstralh DT, Kohl KP, LaRocque JR, Moore CB, Sekelsky J (2009) Drosophila MUS312 and the vertebrate ortholog BTBD12 interact with DNA structure-specific endonucleases in DNA repair and recombination. Mol Cell 35:128–135

Archambault V, Glover DM (2009) Polo-like kinases: conservation and divergence in their functions and regulation. Nat Rev Mol Cell Biol 10:265–275

Bailly AP, Freeman A, Hall J, Declais AC, Alpi A, Lilley DM, Ahmed S, Gartner A (2010) The Caenorhabditis elegans homolog of Gen1/Yen1 resolvases links DNA damage signaling to DNA double-strand break repair. PLoS Genet 6:e1001025

Barber LJ, Youds JL, Ward JD, McIlwraith MJ, O'Neil NJ, Petalcorin MI, Martin JS, Collis SJ, Cantor SB, Auclair M, Tissenbaum H, West SC, Rose AM, Boulton SJ (2008) RTEL1 maintains genomic stability by suppressing homologous recombination. Cell 135:261–271

Barchi M, Roig I, Di Giacomo M, de Rooij DG, Keeney S, Jasin M (2008) ATM promotes the obligate XY crossover and both crossover control and chromosome axis integrity on autosomes. PLoS Genet 4:e1000076

Bennett CB, Lewis AL, Baldwin KK, Resnick MA (1993) Lethality induced by a single site-specific double-strand break in a dispensable yeast plasmid. Proc Natl Acad Sci USA 90:5613– 5617

Beucher A, Birraux J, Tchouandong L, Barton O, Shibata A, Conrad S,

Goodarzi AA, Krempler A, Jeggo PA, Lobrich M (2009) ATM and Artemis promote homologous recombination of radiation-induced DNA double-strand breaks in G2. EMBO J 28:3413–3427

Bhalla N, Wynne DJ, Jantsch V, Dernburg AF (2008) ZHP-3 acts at crossovers to couple meiotic recombination with synaptonemal complex disassembly and bivalent formation in C. elegans. PLoS Genet 4:e1000235

Bickel JS, Chen L, Hayward J, Yeap SL, Alkers AE, Chan RC (2010) Structural maintenance of chromosomes (SMC) proteins promote homolog-independent recombination repair in meiosis crucial for germ cell genomic stability. PLoS Genet 6:e1001028

Boddy MN, Lopez-Girona A, Shanahan P, Interthal H, Heyer WD, Russell P (2000) Damage tolerance protein Mus81 associates with the FHA1 domain of checkpoint kinase Cds1. Mol Cell Biol 20:8758–8766

Bolderson E, Tomimatsu N, Richard DJ, Boucher D, Kumar R, Pandita TK, Burma S, Khanna KK (2010) Phosphorylation of Exo1 modulates homologous recombination repair of DNA double-strand breaks. Nucleic Acids Res 38:1821–1831

Borner GV, Kleckner N, Hunter N (2004) Crossover/noncrossover differentiation, synaptonemal complex formation, and regulatory surveillance at the leptotene/zygotene transition of meiosis. Cell 117:29–45

Boulton SJ (2009) DNA repair: a heavyweight joins the fray. Nature 462:857–858

Boulton SJ, Martin JS, Polanowska J, Hill DE, Gartner A, Vidal M (2004) BRCA1/BARD1 orthologs required for DNA repair in Caenorhabditis elegans. Curr Biol 14:33–39

Brenner S (1974) The genetics of Caenorhabditis elegans. Genetics 77:71–94

Budd ME, Tong AH, Polaczek P, Peng X, Boone C, Campbell JL (2005) A network of multi-tasking proteins at the DNA replication fork preserves genome stability. PLoS Genet 1:e61

Buhler C, Borde V, Lichten M (2007) Mapping meiotic single-strand DNA reveals a new landscape of DNA double-strand breaks in Saccharomyces cerevisiae. PLoS Biol 5:e324

Burma S, Chen BP, Chen DJ (2006) Role of non-homologous end joining (NHEJ) in maintaining genomic integrity. DNA Repair (Amst) 5:1042–1048

Bzymek M, Thayer NH, Oh SD, Kleckner N, Hunter N (2010) Double Holliday junctions are intermediates of DNA break repair. Nature 464:937–941

Cadet J, Bellon S, Douki T, Frelon S, Gasparutto D, Muller E, Pouget JP, Ravanat JL, Romieu A, Sauvaigo S (2004) Radiation-induced DNA damage: formation, measurement, and biochemical fea- tures. J Environ Pathol Toxicol Oncol 23:33–43

Carballo JA, Cha RS (2007) Meiotic roles of Mec1, a budding yeast homolog of mammalian ATR/ATM. Chromosome Res 15:539– 550

Chase D, Golden A, Heidecker G, Ferris DK (2000a) Caenorhabditis elegans contains a third polo-like kinase gene. DNA Seq 11:327– 334

Chase D, Serafinas C, Ashcroft N, Kosinski M, Longo D, Ferris DK, Golden A (2000b) The polo-like kinase PLK-1 is required for nuclear envelope breakdown and the completion of meiosis in Caenorhabditis elegans. Genesis 26:26–41

Chen CF, Brill SJ (2007) Binding and activation of DNA topoisomerase III by the Rmi1 subunit. J Biol Chem 282:28971–28979

Chen PL, Chen CF, Chen Y, Xiao J, Sharp ZD, Lee WH (1998) The BRC repeats in BRCA2 are critical for RAD51 binding and resistance to methyl methanesulfonate treatment. Proc Natl Acad Sci USA 95:5287–5292

Chin GM, Villeneuve AM (2001) C. elegans mre-11 is required for meiotic recombination and DNA repair but is dispensable for the meiotic G(2) DNA damage checkpoint. Genes Dev 15:522– 534

Cimprich KA, Cortez D (2008) ATR: an essential regulator of genome integrity. Nat Rev Mol Cell Biol 9:616–627

Clejan I, Boerckel J, Ahmed S (2006) Developmental modulation of nonhomologous end joining in Caenorhabditis elegans. Genetics 173:1301–1317

Clerici M, Mantiero D, Lucchini G, Longhese MP (2005) The Saccharomyces cerevisiae Sae2 protein promotes resection and bridging of double strand break ends. J Biol Chem 280:38631– 38638

Clyne RK, Katis VL, Jessop L, Benjamin KR, Herskowitz I, Lichten M, Nasmyth K (2003) Polo-like kinase Cdc5 promotes chiasmata formation and cosegregation of sister centromeres at meiosis I. Nat Cell Biol 5:480–485

Colaiacovo MP, MacQueen AJ, Martinez-Perez E, McDonald K, Adamo A, La Volpe A, Villeneuve AM (2003) Synaptonemal complex assembly in C. elegans is dispensable for loading strand-exchange proteins but critical for proper completion of recombination. Dev Cell 5:463–474

Connolly B, Parsons CA, Benson FE, Dunderdale HJ, Sharples GJ, Lloyd RG, West SC (1991) Resolution of Holliday junctions *in vitro* requires the Escherichia coli ruvC gene product. Proc Natl Acad Sci USA 88:6063–6067

Couteau F, Nabeshima K, Villeneuve A, Zetka M (2004) A component of C. elegans meiotic chromosome axes at the interface of homolog alignment, synapsis, nuclear reorganization, and recombination. Curr Biol 14:585–592

Czornak K, Chughtai S, Chrzanowska KH (2008) Mystery of DNA repair: the role of the MRN complex and ATM kinase in DNA damage repair. J Appl Genet 49:383–396

Davies AA, Masson JY, McIlwraith MJ, Stasiak AZ, Stasiak A, Venkitaraman AR, West SC (2001) Role of BRCA2 in control of the RAD51 recombination and DNA repair protein. Mol Cell 7:273–282

de Vries SS, Baart EB, Dekker M, Siezen A, de Rooij DG, de Boer P, te Riele H (1999) Mouse MutS-like protein Msh5 is required for proper chromosome synapsis in male and female meiosis. Genes Dev 13:523–531

DeFazio LG, Stansel RM, Griffith JD, Chu G (2002) Synapsis of DNA ends by DNA-dependent protein kinase. EMBO J 21:3192–3200 Delacote F, Lopez BS (2008) Importance of the cell cycle phase for the choice of the appropriate DSB repair pathway for genome stability maintenance: the trans-S double-strand break repair model. Cell Cycle 7:33–38

Dendouga N, Gao H, Moechars D, Janicot M, Vialard J, McGowan CH (2005) Disruption of murine Mus81 increases genomic instability and DNA damage sensitivity but does not promote tumorigenesis. Mol Cell Biol 25:7569–7579

Dernburg AF, McDonald K, Moulder G, Barstead R, Dresser M, Villeneuve AM (1998) Meiotic recombination in C. elegans initiates by a conserved mechanism and is dispensable for homologous chromosome synapsis. Cell 94:387–398

Edelmann W, Cohen PE, Kneitz B, Winand N, Lia M, Heyer J, Kolodner R, Pollard JW, Kucherlapati R (1999) Mammalian MutS homologue 5 is required for chromosome pairing in meiosis. Nat Genet 21:123–127

Fekairi S, Scaglione S, Chahwan C, Taylor ER, Tissier A, Coulon S, Dong MQ, Ruse C, Yates JR 3rd, Russell P, Fuchs RP, McGowan CH, Gaillard PH (2009) Human SLX4 is a Holliday junction resolvase subunit that binds multiple DNA repair/recombination endonucleases. Cell 138:78–89

Fung JC, Rockmill B, Odell M, Roeder GS (2004) Imposition of crossover interference through the nonrandom distribution of synapsis initiation complexes. Cell 116:795–802

Garcia-Muse T, Boulton SJ (2005) Distinct modes of ATR activation after replication stress and DNA double-strand breaks in Caenorhabditis elegans. EMBO J 24:4345–4355

Garcia-Muse T, Boulton SJ (2007) Meiotic recombination in Caeno- rhabditis elegans. Chromosome Res 15:607–621

Gartner A, Boag PR, Blackwell TK (2008) Germline survival and apoptosis. WormBook: 1–20

Gatti M, Pimpinelli S, Baker BS (1980) Relationships among chromatid interchanges, sister chromatid exchanges, and meiotic recombination in Drosophila melanogaster. Proc Natl Acad Sci USA 77:1575–1579

Goodyer W, Kaitna S, Couteau F, Ward JD, Boulton SJ, Zetka M (2008) HTP-3 links DSB formation with homolog pairing and crossing over during C. elegans meiosis. Dev Cell 14:263–274

Grabowski MM, Svrzikapa N, Tissenbaum HA (2005) Bloom syndrome ortholog HIM-6 maintains genomic stability in C. elegans. Mech Ageing Dev 126:1314–1321

Gravel S, Chapman JR, Magill C, Jackson SP (2008) DNA helicases Sgs1 and BLM promote DNA double-strand break resection. Genes Dev 22:2767–2772

Hashizume R, Fukuda M, Maeda I, Nishikawa H, Oyake D, Yabuki Y, Ogata H, Ohta T (2001) The RING heterodimer BRCA1-BARD1 is a ubiquitin ligase inactivated by a breast cancer-derived mutation. J Biol Chem 276:14537–14540

Hayashi M, Chin GM, Villeneuve AM (2007) C. elegans germ cells switch between distinct modes of double-strand break repair during meiotic prophase progression. PLoS Genet 3:e191

Heyer WD, Ehmsen KT, Solinger JA (2003) Holliday junctions in the eukaryotic nucleus: resolution in sight? Trends Biochem Sci 28:548–557

Hillers KJ, Villeneuve AM (2003) Chromosome-wide control of meiotic crossing over in C. elegans. Curr Biol 13:1641–1647

Hoeijmakers JH (2009) DNA damage, aging, and cancer. N Engl J Med 361:1475–1485

Hoffenberg R (2003) Brenner, the worm and the prize. Clin Med 3:285–286

Hollingsworth NM, Brill SJ (2004) The Mus81 solution to resolution: generating meiotic crossovers without Holliday junctions. Genes Dev 18:117–125

Honma M, Zhang LS, Hayashi M, Takeshita K, Nakagawa Y, Tanaka N, Sofuni T (1997) Illegitimate recombination leading to allelic loss and unbalanced translocation in p53-mutated human lym- phoblastoid cells. Mol Cell Biol 17:4774–4781

Horvitz HR (2003) Worms, life, and death (Nobel lecture). Chem- biochem 4:697–711

Huen MS, Sy SM, Chen J (2009) BRCA1 and its toolbox for the maintenance of genome integrity. Nat Rev Mol Cell Biol 11:138–148

Huertas P (2010) DNA resection in eukaryotes: deciding how to fix the break. Nat Struct Mol Biol 17:11–16

Huertas P, Cortes-Ledesma F, Sartori AA, Aguilera A, Jackson SP (2008) CDK targets Sae2 to control DNA-end resection and homologous recombination. Nature 455:689–692

Hurley PJ, Bunz F (2007) ATM and ATR: components of an integrated circuit. Cell Cycle 6:414–417

Ip SC, Rass U, Blanco MG, Flynn HR, Skehel JM, West SC (2008) Identification of Holliday junction resolvases from humans and yeast. Nature 456:357–361

Jessop L, Lichten M (2008) Mus81/Mms4 endonuclease and Sgs1 helicase collaborate to ensure proper recombination intermediate metabolism during meiosis. Mol Cell 31:313–323

Johzuka K, Ogawa H (1995) Interaction of Mre11 and Rad50: two proteins required for DNA repair and meiosis-specific double- strand break formation in Saccharomyces cerevisiae. Genetics 139:1521–1532

Kang YH, Lee CH, Seo YS (2010) Dna2 on the road to Okazaki fragment processing and genome stability in eukaryotes. Crit Rev Biochem Mol Biol 45:71–96

Keeney S, Kleckner N (1995) Covalent protein-DNA complexes at the 5′ strand termini of meiosis-specific double-strand breaks in yeast. Proc Natl Acad Sci USA 92:11274–11278

Keeney S, Neale MJ (2006) Initiation of meiotic recombination by formation of DNA double-strand breaks: mechanism and regulation. Biochem Soc Trans 34:523–525

Keeney S, Giroux CN, Kleckner N (1997) Meiosis-specific DNA double-strand breaks are catalyzed by Spo11, a member of a widely conserved protein family. Cell 88:375–384

Kelly KO, Dernburg AF, Stanfield GM, Villeneuve AM (2000) Caenorhabditis elegans msh-5 is required for both normal and radiation-induced meiotic crossing over but not for completion of meiosis. Genetics 156:617–630

Klein HL (1988) Different types of recombination events are controlled by the RAD1 and RAD52 genes of Saccharomyces cerevisiae. Genetics 120:367–377

Klein HL, Symington LS (2009) Breaking up just got easier to do. Cell 138:20–22

Kneitz B, Cohen PE, Avdievich E, Zhu L, Kane MF, Hou H Jr, Kolodner RD, Kucherlapati R, Pollard JW, Edelmann W (2000) MutS homolog 4 localization to meiotic chromosomes is required for chromosome pairing during meiosis in male and female mice. Genes Dev 14:1085–1097

Kurimasa A, Kumano S, Boubnov NV, Story MD, Tung CS, Peterson SR, Chen DJ (1999) Requirement for the kinase activity of human DNA-dependent protein kinase catalytic subunit in DNA strand break rejoining. Mol Cell Biol 19:3877–3884

Lee BI, Shannon M, Stubbs L, Wilson DM 3rd (1999) Expression specificity of the mouse exonuclease 1 (mExo1) gene. Nucleic Acids Res 27:4114–4120

Lee MH, Han SM, Han JW, Kim YM, Ahnn J, Koo HS (2003) Caenorhabditis elegans dna-2 is involved in DNA repair and is essential for germ-line development. FEBS Lett 555:250–256

Lee SJ, Gartner A, Hyun M, Ahn B, Koo HS (2010) The Caenorhabditis elegans Werner syndrome protein functions upstream of ATR and ATM in response to DNA replication inhibition and double-strand DNA breaks. PLoS Genet 6:e1000801

Lewis LK, Karthikeyan G, Westmoreland JW, Resnick MA (2002) Differential suppression of DNA repair deficiencies of Yeast rad50, mre11 and xrs2 mutants by EXO1 and TLC1 (the RNA component of telomerase). Genetics 160:49–62

Li X, Heyer WD (2008) Homologous recombination in DNA repair and DNA damage tolerance. Cell Res 18:99–113

Lieber MR (2010) NHEJ and its backup pathways in chromosomal translocations. Nat Struct Mol Biol 17:393–395

Llorente B, Symington LS (2004) The Mre11 nuclease is not required for 5′ to 3′ resection at multiple HO-induced double-strand breaks. Mol Cell Biol 24:9682–9694

Lorenz A, West SC, Whitby MC (2010) The human Holliday junction resolvase GEN1 rescues the meiotic phenotype of a Schizosac- charomyces pombe mus81 mutant. Nucleic Acids Res 38:1866– 1873

Luo G, Santoro IM, McDaniel LD, Nishijima I, Mills M, Youssoufian H, Vogel H, Schultz RA, Bradley A (2000) Cancer predisposition caused by elevated mitotic recombination in Bloom mice. Nat Genet 26:424–429

Lynn A, Soucek R, Borner GV (2007) ZMM proteins during meiosis: crossover artists at work. Chromosome Res 15:591–605

MacQueen AJ, Villeneuve AM (2001) Nuclear reorganization and homologous chromosome pairing during meiotic prophase require C. elegans chk-2. Genes Dev 15:1674–1687 Manfrini N, Guerini I, Citterio A, Lucchini G, Longhese MP (2010) Processing of meiotic DNA double strand breaks requires cyclin-dependent kinase and multiple nucleases. J Biol Chem 285:11628–11637

Martin JS, Winkelmann N, Petalcorin MI, McIlwraith MJ, Boulton SJ (2005) RAD-51-dependent and -independent roles of a Caeno- rhabditis elegans BRCA2-related protein during DNA double- strand break repair. Mol Cell Biol 25:3127–3139

Martinez-Perez E, Villeneuve AM (2005) HTP-1-dependent con- straints coordinate homolog pairing and synapsis and promote chiasma formation during C. elegans meiosis. Genes Dev 19:2727–2743

Matsuoka S, Ballif BA, Smogorzewska A, McDonald ER 3rd, Hurov KE, Luo J, Bakalarski CE, Zhao Z, Solimini N, Lerenthal Y, Shiloh Y, Gygi SP, Elledge SJ (2007) ATM and ATR substrate analysis reveals extensive protein networks responsive to DNA damage. Science 316:1160–1166

Mazin AV, Mazina OM, Bugreev DV, Rossi MJ (2010) Rad54, the motor of homologous recombination. DNA Repair (Amst) 9:286–302

McKee AH, Kleckner N (1997) A general method for identifying recessive diploid-specific mutations in Saccharomyces cerevisiae, its application to the isolation of mutants blocked at intermediate stages of meiotic prophase and characterization of a new gene SAE2. Genetics 146:797–816

McPherson JP, Lemmers B, Chahwan R, Pamidi A, Migon E, Matysiak- Zablocki E, Moynahan ME, Essers J, Hanada K, Poonepalli A, Sanchez-Sweatman O, Khokha R, Kanaar R, Jasin M, Hande MP, Hakem R (2004) Involvement of mammalian Mus81 in genome integrity and tumor suppression. Science 304:1822–1826

McVey M, Lee SE (2008) MMEJ repair of double-strand breaks (director's cut): deleted sequences and alternative endings. Trends Genet 24:529–538

Meier B, Barber LJ, Liu Y, Shtessel L, Boulton SJ, Gartner A, Ahmed S (2009) The MRT-1 nuclease is required for DNA crosslink repair and telomerase activity *in vivo* in Caenorhabditis elegans. EMBO J 28:3549–3563

Mets DG, Meyer BJ (2009) Condensins regulate meiotic DNA break distribution, thus crossover frequency, by controlling chromo- some structure. Cell 139:73–86

Milman N, Higuchi E, Smith GR (2009) Meiotic DNA double-strand break repair requires two nucleases, MRN and Ctp1, to produce a single size class of Rec12 (Spo11)-oligonucleotide complexes. Mol Cell Biol 29:5998–6005

Mimitou EP, Symington LS (2008) Sae2, Exo1 and Sgs1 collaborate in DNA double-strand break processing. Nature 455:770–774

Moreau S, Morgan EA, Symington LS (2001) Overlapping functions of the Saccharomyces cerevisiae Mre11, Exo1 and Rad27 nucleases in DNA metabolism. Genetics 159:1423–1433

Mortimer RK, Contopoulou CR, King JS (1992) Genetic and physical maps of Saccharomyces cerevisiae, Edition 11. Yeast 8:817–902 Moynahan ME, Pierce AJ, Jasin M (2001) BRCA2 is required for homology-directed repair of chromosomal breaks. Mol Cell 7:263–272

Munoz IM, Hain K, Declais AC, Gardiner M, Toh GW, Sanchez- Pulido L, Heuckmann JM, Toth R, Macartney T, Eppink B, Kanaar R, Ponting CP, Lilley DM, Rouse J (2009) Coordination of structure-specific nucleases by human SLX4/BTBD12 is required for DNA repair. Mol Cell 35:116–127

Munz P (1994) An analysis of interference in the fission yeast Schizosaccharomyces pombe. Genetics 137:701–707

Nasmyth K, Haering CH (2009) Cohesin: its roles and mechanisms. Annu Rev Genet 43:525–558

Nimonkar AV, Ozsoy AZ, Genschel J, Modrich P, Kowalczykowski SC (2008) Human exonuclease 1 and BLM helicase interact to resect DNA and initiate DNA repair. Proc Natl Acad Sci USA 105:16906–16911

Ogawa H, Johzuka K, Nakagawa T, Leem SH, Hagihara AH (1995) Functions of the yeast meiotic recombination genes, MRE11 and MRE2. Adv Biophys 31:67–76

Oh SD, Lao JP, Taylor AF, Smith GR, Hunter N (2008) RecQ helicase, Sgs1, and XPF family endonuclease, Mus81-Mms4, resolve aberrant joint molecules during meiotic recombination. Mol Cell 31:324–336

O'Neil N, Rose A (2006) DNA repair. WormBook: 1-12

Osman F, Adriance M, McCready S (2000) The genetic control of spontaneous and UV-induced mitotic intrachromosomal recom- bination in the fission yeast Schizosaccharomyces pombe. Curr Genet 38:113–125

Osman F, Dixon J, Doe CL, Whitby MC (2003) Generating crossovers by resolution of nicked Holliday junctions: a role for Mus81- Eme1 in meiosis. Mol Cell 12:761–774

Pan X, Ye P, Yuan DS, Wang X, Bader JS, Boeke JD (2006) A DNA integrity network in the yeast Saccharomyces cerevisiae. Cell 124:1069–1081

Pannicke U, Ma Y, Hopfner KP, Niewolik D, Lieber MR, Schwarz K (2004) Functional and biochemical dissection of the structure- specific nuclease ARTEMIS. EMBO J 23:1987–1997

Pasierbek P, Jantsch M, Melcher M, Schleiffer A, Schweizer D, Loidl J (2001) A Caenorhabditis elegans cohesion protein with functions in meiotic chromosome pairing and disjunction. Genes Dev 15:1349–1360

Penkner A, Portik-Dobos Z, Tang L, Schnabel R, Novatchkova M, Jantsch V, Loidl J (2007) A conserved function for a Caeno- rhabditis elegans Com1/Sae2/CtIP protein homolog in meiotic recombination. EMBO J 26:5071–5082

Penkner AM, Fridkin A, Gloggnitzer J, Baudrimont A, Machacek T, Woglar A, Csaszar E, Pasierbek P, Ammerer G, Gruenbaum Y, Jantsch V (2009) Meiotic chromosome homology search involves modifications of the nuclear envelope protein Matefin/ SUN-1. Cell 139:920–933

Petalcorin MI, Sandall J, Wigley DB, Boulton SJ (2006) CeBRC-2 stimulates D-loop formation by RAD-51 and promotes DNA single-strand annealing. J Mol Biol 361:231–242

Petalcorin MI, Galkin VE, Yu X, Egelman EH, Boulton SJ (2007) Stabilization of RAD-51-DNA filaments via an interaction domain in Caenorhabditis elegans BRCA2. Proc Natl Acad Sci USA 104:8299–8304

Phillips CM, Meng X, Zhang L, Chretien JH, Urnov FD, Dernburg AF (2009) Identification of chromosome sequence motifs that mediate meiotic pairing and synapsis in C. elegans. Nat Cell Biol 11:934–942

Plank JL, Wu J, Hsieh TS (2006) Topoisomerase III alpha and Bloom's helicase can resolve a mobile double Holliday junction substrate through convergent branch migration. Proc Natl Acad Sci USA 103:11118–11123

Polanowska J, Martin JS, Garcia-Muse T, Petalcorin MI, Boulton SJ (2006) A conserved pathway to activate BRCA1-dependent ubiquitylation at DNA damage sites. EMBO J 25:2178–2188

Polo SE, Kaidi A, Baskcomb L, Galanty Y, Jackson SP (2010) Regulation of DNA-damage responses and cell-cycle progression by the chromatin remodelling factor CHD4. EMBO J 29:3130– 3139.

Pontier DB, Tijsterman M (2009) A robust network of double-strand break repair pathways governs genome integrity during C. elegans development. Curr Biol 19:1384–1388

Pothof J, van Haaften G, Thijssen K, Kamath RS, Fraser AG, Ahringer J, Plasterk RH, Tijsterman M (2003) Identification of genes that protect the C. elegans genome against mutations by genome-wide RNAi. Genes Dev 17:443–448

Prado F, Aguilera A (1995) Role of reciprocal exchange, one-ended invasion crossover and single-strand annealing on inverted and direct repeat recombination in yeast: different requirements for the RAD1, RAD10, and RAD52 genes. Genetics 139:109–123

Prinz S, Amon A, Klein F (1997) Isolation of COM1, a new gene required to complete meiotic double-strand break-induced re- combination in Saccharomyces cerevisiae. Genetics 146:781–795

Reddy KC, Villeneuve AM (2004) C. elegans HIM-17 links chromatin modification and competence for initiation of meiotic recombination. Cell 118:439–452

Reid LJ, Shakya R, Modi AP, Lokshin M, Cheng JT, Jasin M, Baer R, Ludwig T (2008) E3 ligase activity of BRCA1 is not essential for mammalian cell viability or homology-directed repair of double- strand DNA breaks. Proc Natl Acad Sci USA 105:20876–20881

Rockmill B, Fung JC, Branda SS, Roeder GS (2003) The Sgs1 helicase regulates chromosome synapsis and meiotic crossing over. Curr Biol 13:1954–1962

Rossi ML, Ghosh AK, Bohr VA (2010) Roles of Werner syndrome protein in protection of genome integrity. DNA Repair (Amst) 9:331–344

Rupnik A, Lowndes NF, Grenon M (2010) MRN and the race to the break. Chromosoma 119:115–135

Saito TT, Youds JL, Boulton SJ, Colaiacovo MP (2009) Caenorhab- ditis elegans HIM-18/SLX-4 interacts with SLX-1 and XPF-1 and maintains genomic integrity in the germline by processing recombination intermediates. PLoS Genet 5:e1000735

Sato A, Isaac B, Phillips CM, Rillo R, Carlton PM, Wynne DJ, Kasad RA, Dernburg AF (2009) Cytoskeletal forces span the nuclear envelope to coordinate meiotic chromosome pairing and synapsis. Cell 139:907–919

Severson AF, Ling L, van Zuylen V, Meyer BJ (2009) The axial element protein HTP-3 promotes cohesin loading and meiotic axis assembly in C. elegans to implement the meiotic program of chromosome segregation. Genes Dev 23:1763–1778

Sharples GJ, Lloyd RG (1991) Resolution of Holliday junctions in Escherichia coli: identification of the ruvC gene product as a 19- kilodalton protein. J Bacteriol 173:7711–7715

Shinohara M, Gasior SL, Bishop DK, Shinohara A (2000) Tid1/ Rdh54 promotes colocalization of rad51 and dmc1 during meiotic recombination. Proc Natl Acad Sci USA 97:10814– 10819

Smeenk G, Wiegant WW, Vrolijk H, Solari AP, Pastink A, van Attikum H (2010) The NuRD chromatin-remodeling complex regulates signaling and repair of DNA damage. J Cell Biol 190:741–749.

Smolikov S, Eizinger A, Schild-Prufert K, Hurlburt A, McDonald K, Engebrecht J, Villeneuve AM, Colaiacovo MP (2007) SYP-3 restricts synaptonemal complex assembly to bridge paired chromosome axes during meiosis in Caenorhabditis elegans. Genetics 176:2015–2025

Smolikov S, Schild-Prufert K, Colaiacovo MP (2008) CRA-1 uncovers a double-strand break-dependent pathway promoting the assembly of central region proteins on chromosome axes during C. elegans meiosis. PLoS Genet 4:e1000088

Smolka MB, Albuquerque CP, Chen SH, Zhou H (2007) Proteome- wide identification of *in vivo* targets of DNA damage checkpoint kinases. Proc Natl Acad Sci USA 104:10364–10369

Snowden T, Acharya S, Butz C, Berardini M, Fishel R (2004) hMSH4-hMSH5 recognizes Holliday junctions and forms a meiosis-specific sliding clamp that embraces homologous chro- mosomes. Mol Cell 15:437–451

Solinger JA, Heyer WD (2001) Rad54 protein stimulates the postsynaptic phase of Rad51 protein-mediated DNA strand exchange. Proc Natl Acad Sci USA 98:8447–8453

Sourirajan A, Lichten M (2008) Polo-like kinase Cdc5 drives exit from pachytene during budding yeast meiosis. Genes Dev 22:2627–2632

Sugawara N, Ira G, Haber JE (2000) DNA length dependence of the single-strand annealing pathway and the role of Saccharomyces cerevisiae RAD59 in double-strand break repair. Mol Cell Biol 20:5300–5309

Sulston JE (2003) Caenorhabditis elegans: the cell lineage and beyond (Nobel lecture). Chembiochem 4:688–696

Sulston JE, Schierenberg E, White JG, Thomson JN (1983) The embryonic cell lineage of the nematode Caenorhabditis elegans. Dev Biol 100:64–119

Svendsen JM, Smogorzewska A, Sowa ME, O'Connell BC, Gygi SP, Elledge SJ, Harper JW (2009) Mammalian BTBD12/SLX4 assembles a Holliday junction resolvase and is required for DNA repair. Cell 138:63–77

Szostak JW, Orr-Weaver TL, Rothstein RJ, Stahl FW (1983) The double- strand-break repair model for recombination. Cell 33:25–35

Tang L, Machacek T, Mamnun YM, Penkner A, Gloggnitzer J, Wegrostek C, Konrat R, Jantsch MF, Loidl J, Jantsch V (2010) Mutations in Caenorhabditis elegans him-19 show meiotic defects that worsen with age. Mol Biol Cell 21:885–896

Tay YD, Wu L (2010) Overlapping roles for Yen1 and Mus81 in cellular Holliday junction processing. J Biol Chem 285:11427–11432

Tran PT, Erdeniz N, Symington LS, Liskay RM (2004) EXO1-a multi- tasking eukaryotic nuclease. DNA Repair (Amst) 3:1549–1559

Tsai CJ, Mets DG, Albrecht MR, Nix P, Chan A, Meyer BJ (2008) Meiotic crossover number and distribution are regulated by a dosage compensation protein that resembles a condensin subunit. Genes Dev 22:194–211

van Haaften G, Romeijn R, Pothof J, Koole W, Mullenders LH, Pastink A, Plasterk RH, Tijsterman M (2006) Identification of conserved pathways of DNA-damage response and radiation protection by genome-wide RNAi. Curr Biol 16:1344–1350

Venkitaraman AR (2001) Chromosome stability, DNA recombination and the BRCA2 tumour suppressor. Curr Opin Cell Biol 13:338– 343.

Vilenchik MM, Knudson AG (2006) Radiation dose-rate effects, endogenous DNA damage, and signaling resonance. Proc Natl Acad Sci USA 103:17874–17879

Ward JD, Barber LJ, Petalcorin MI, Yanowitz J, Boulton SJ (2007) Replication blocking lesions present a unique substrate for homologous recombination. EMBO J 26:3384–3396

Ward JD, Muzzini DM, Petalcorin MI, Martinez-Perez E, Martin JS, Plevani P, Cassata G, Marini F, Boulton SJ (2010) Overlapping mechanisms promote postsynaptic RAD-51 filament disassem- bly during meiotic double-strand break repair. Mol Cell 37:259– 272

West SC (2009) The search for a human Holliday junction resolvase. Biochem Soc Trans 37:519–526

Whitby MC (2005) Making crossovers during meiosis. Biochem Soc Trans 33:1451–1455

Wicky C, Alpi A, Passannante M, Rose A, Gartner A, Muller F (2004) Multiple genetic pathways involving the Caenorhabditis elegans Bloom's syndrome genes him-6, rad-51, and top-3 are needed to maintain genome stability in the germ line. Mol Cell Biol 24:5016–5027

Winand NJ, Panzer JA, Kolodner RD (1998) Cloning and character- ization of the human and Caenorhabditis elegans homologs of the Saccharomyces cerevisiae MSH5 gene. Genomics 53:69–80

Wood WB (1988) The Nematode Caenorhabditis elegans. Cold Spring Harbor Laboratory Press

Wu L, Hickson ID (2003) The Bloom's syndrome helicase suppresses crossing over during homologous recombination. Nature 426:870– 874

Youds JL, Mets DG, McIlwraith MJ, Martin JS, Ward JD, ON NJ, Rose AM, West SC, Meyer BJ, Boulton SJ (2010) RTEL-1 enforces meiotic crossover interference and homeostasis. Science 327:1254–1258

Yuan SS, Lee SY, Chen G, Song M, Tomlinson GE, Lee EY (1999) BRCA2 is required for ionizing radiation-induced assembly of Rad51 complex *in vivo*. Cancer Res 59:3547–3551

Yun MH, Hiom K (2009) CtIP-BRCA1 modulates the choice of DNA double-strand-break repair pathway throughout the cell cycle. Nature 459:460–463

Zalevsky J, MacQueen AJ, Duffy JB, Kemphues KJ, Villeneuve AM (1999) Crossing over during Caenorhabditis elegans meiosis requires a conserved MutS-based pathway that is partially dispensable in budding yeast. Genetics 153:1271–1283

Zetka MC, Kawasaki I, Strome S, Muller F (1999) Synapsis and chiasma formation in Caenorhabditis elegans require HIM-3, a meiotic chromosome core component that functions in chromo- some segregation. Genes Dev 13:2258–2270

Zhu Z, Chung WH, Shim EY, Lee SE, Ira G (2008) Sgs1 helicase and two nucleases Dna2 and Exo1 resect DNA double-strand break ends. Cell 134:981–994

Zickler D (2006) From early homologue recognition to synaptonemal complex formation. Chromosoma 115:158–174

2

COM-1 promotes Homologous Recombination during *Caenorhabditis elegans* meiosis by antagonizing Ku-mediated Non-Homologous End Joining

Lemmens BB, Johnson NM, Tijsterman M

Adapted from Lemmens *et al.* PLoS Genet. 2013;9(2)

Abstract

Successful completion of meiosis requires the induction and faithful repair of DNA double-strand breaks (DSBs). DSBs can be repaired via homologous recombination (HR) or non-homologous end joining (NHEJ), yet only repair via HR can generate the interhomolog crossovers (COs) needed for meiotic chromosome segregation. Here we identify COM-1, the homolog of CtIP/Sae2/Ctp1, as a crucial regulator of DSB repair pathway choice during *Caenorhabditis elegans* gametogenesis. COM-1–deficient germ cells repair meiotic DSBs via the error-prone pathway NHEJ, resulting in a lack of COs, extensive chromosomal aggregation, and near-complete embryonic lethality. In contrast to its yeast counterparts, COM-1 is not required for Spo11 removal and initiation of meiotic DSB repair, but instead promotes meiotic recombination by counteracting the NHEJ complex Ku. In fact, animals defective for both COM-1 and Ku are viable and proficient in CO formation. Further genetic dissection revealed that COM-1 acts parallel to the nuclease EXO-1 to promote interhomolog HR at early pachytene stage of meiotic prophase and thereby safeguards timely CO formation. Both of these nucleases, however, are dispensable for RAD-51 recruitment at late pachytene stage, when homolog-independent repair pathways predominate, suggesting further redundancy and/or temporal regulation of DNA end resection during meiotic prophase. Collectively, our results uncover the potentially lethal properties of NHEJ during meiosis and identify a critical role for COM-1 in NHEJ inhibition and CO assurance in germ cells.

Author Summary

Sexually reproducing animals create germ cells via meiosis, a cell division program that requires the induction and faithful repair of DNA double-strand breaks (DSBs). Meiotic DSBs are typically repaired via homologous recombination (HR), an error-free repair pathway that generates transient links between homologous chromosomes, named crossovers (COs), which are needed for proper chromosome segregation. To date, it is unclear how germ cells channel these programmed DSBs into HR and not into error-prone DSB repair pathways such as non-homologous end joining (NHEJ). We used the genetically tractable animal model *Caenorhabditis elegans* to study the mechanisms underlying the strong HR bias in germ cells. Here, we identify COM-1, the worm homolog of CtIP, as a crucial regulator of meiotic DSB repair pathway choice: COM-1 effectively blocks the action of the NHEJ complex Ku, thereby assuring correct repair via HR. In addition, we show that unscheduled NHEJ activity during meiosis leads to a lack of COs, extensive chromosomal aggregation, and near-complete embryonic lethality. Further genetic dissection also revealed a redundant and stage-specific role for COM-1 in meiotic HR. Our work thus establishes COM-1/CtIP as a caretaker of germline genome stability and unveils meiotic NHEJ as a potent source of chromosomal aberrations in newborns.

Introduction

DNA double-strand breaks (DSBs) are toxic DNA lesions that, if not repaired correctly, can cause gross chromosomal alterations. For this reason, DSBs are potent inducers of cell death as well as malignant transformation [1]. Two major DSB repair mechanisms have evolved that are able to repair DSBs: an error-free pathway called homologous recombination (HR) and an efficient but error-prone pathway called non-homologous end joining (NHEJ) [2], [3]. Together NHEJ and HR safeguard genome integrity, however, on a mechanistic level, they are mutually exclusive. NHEJ is based on DNA end protection: the Ku70/Ku80 heterodimer stabilizes the double-strand (ds) DNA ends and prepares the DSB for direct ligation by DNA ligase IV [2]. In contrast, HR is based on DNA end resection: nucleases degrade the dsDNA ends to expose 3′ single strand (ss) DNA tails, which then form a nucleoprotein filament with the recombinase RAD51 that promotes strand invasion and subsequent DNA synthesis reactions [3]. Because of its conservative nature, HR is better suited for maintaining genome stability, but it requires an undamaged DNA template (*i.e.*, the sister chromatid or homologous chromosome), which is not always available. As a result, most human cells (especially non-cycling somatic cells) typically rely on NHEJ for DSB repair [2], [4].

DSB repair fidelity is particularly important in germ cells, as they harbor the genetic material that is passed on to the next generation. Germ cells create haploid gametes via a

specialized program of cell division called meiosis, in which a single round of DNA replication is followed by two subsequent rounds of chromosome segregation (named meiosis I and meiosis II). Separation of the parental/homologous chromosomes during meiosis I requires the induction of programmed DSBs [5]. Meiotic DSBs are introduced by SPO11, a highly conserved topoisomerase-like protein that, after cutting, remains covalently bound to the 5′ ends of the DSB. Loss of SPO11 function leads to severe chromosome missegregation and aneuploid gametes in many model systems, highlighting the importance of meiotic DSB formation for successful gametogenesis and species survival [5], [6].

Meiotic DSBs need to be repaired via HR, as only this pathway creates repair products known as crossovers (COs), which are required for the establishment of chiasmata, the transient links between homologous chromosomes. Chiasmata are essential for proper chromosome alignment and segregation during meiosis I [7]. Given that NHEJ competes with HR and does not lead to COs, this activity should be restricted in order to assure chromosome stability during gametogenesis. Previous studies have revealed that *Caenorhabditis elegans* (*C. elegans*) germ cells posses NHEJ activity, yet in wild-type germ cells this error-prone pathway seems to be inhibited very efficiently [8], [9], [10], [11].

Recent insights on mitotic DSB repair have led to the identification of several factors that are able to block NHEJ activity, including the tumor suppressor CtIP [12]. Studies on DSB repair pathway choice in meiotic cells are hampered by the fact that crucial regulators like CtIP are required for mammalian development, which precludes analysis of CtIP-deficient gametes [13]. Here, we exploited the *C. elegans* model system to explore if the CtIP homolog COM-1 is responsible for the robust HR bias in metazoan germ cells; maternal contribution of *com-1* gene products enables *com-1* mutant embryos to develop into adults that produce COM-1-deficient germ cells [14]. COM-1/CtIP is well conserved throughout evolution and homologous counterparts named Sae2 and Ctp1 have also been identified in the unicellular organisms *S. cerevisiae* and *S. pombe*, respectively [14], [15], [16]. In yeast, Sae2/Ctp1 is required for Spo11 removal and therefore is crucial for the initiation of meiotic DSB repair [17], [18].

Here, we show that COM-1 is dispensable for meiotic recombination *per se*, yet it is crucial to complete meiosis: COM-1 is required to block toxic Ku activity at meiotic DSBs and therefore is needed to prevent chromosome aggregation and CO failure. In addition, we reveal a role for COM-1 in interhomolog HR: COM-1 acts parallel to the nuclease EXO-1 to generate RAD-51-coated recombination intermediates at early/mid pachytene stage. We thus identified a dual role for COM-1 during metazoan meiosis: it blocks toxic NHEJ activity and guarantees the timely formation of interhomolog COs.

Results

COM-1–deficient germ cells bear chromosomal aggregates and univalent

In order to study the meiotic functions of COM-1 we obtained two different *com-1* mutant alleles previously identified by Penkner and colleagues (Figure S1) and [14]. In *C. elegans*, defects in repair of meiotic DSBs can be detected relatively easily, as these often manifest as chromosomal abnormalities in diakinesis nuclei of maturing oocytes (Figure 1A). Wild-type diakinesis nuclei typically have six rod-shaped DAPI-stained bodies named bivalents, which represent the six pairs of homologous chromosomes, each held together by chiasmata (Figure 1A and Figure 2A). In the absence of meiotic DSBs (e.g. in *spo-11* mutants) chiasmata are not formed, which can be detected by the presence of 12 DAPI-stained bodies, *i.e.* univalents [6]. When meiotic DSBs are induced but not repaired, chromosomal fragmentation occurs, typically resulting in ≥12 irregularly shaped DAPI-stained bodies at diakinesis [19], [20]. Surprisingly, *com-1* mutant oocytes exhibited a different chromosomal pattern: the diakinesis nuclei contained 1 to 12 DAPI-stained entities [14]. We validated this finding by careful inspection of COM-1-deficient diakinesis nuclei (Figure 1C and 1D). These diakinesis nuclei occasionally showed chromosomal fragments, albeit only in 2% of the oocytes (Figure 3C). We argued that the low frequency of chromosomal fragmentation in *com-1* mutants is inconsistent with a conserved role for COM-1 in SPO-11 removal, given that SPO-11-bound DSBs are refractory to repair. Based on the diakinesis studies we envisaged a different scenario in which *com-1* mutants are able to repair meiotic DSBs, yet do so in an error-prone manner, ultimately resulting in chromosomal aggregates and failed chiasmata formation. Several observations supported this hypothesis: Firstly, unlike *spo-11* mutants, *com-1* mutant oocytes hardly ever contained exactly 12 univalents, which indicated that DSBs were induced. Secondly, all diakinesis nuclei had fewer than 12 DAPI-stained bodies and rarely contained small chromosomal fragments, arguing that most programmed DSBs are repaired. Thirdly, the diakinesis nuclei often contained more than 6 DAPI-stained bodies and frequently exhibited DAPI bodies that morphologically resembled univalents, which implied that chiasmata formation was impaired. Finally, many diakinesis nuclei had fewer than six DAPI-stained bodies, potentially reflecting chromosomal entanglements and/or fusions between non-homologous chromosomes.

Loss of Ku restores chiasmata formation and viability in *com-1* mutant animals

To test if the chromosomal aggregation events in *com-1* mutant oocytes were due to inappropriate NHEJ activity, we crossed *com-1* mutants with worms lacking the NHEJ factor CKU-80. Strikingly, *cku-80* deficiency led to a >20 fold increase in viability among *com-1* mutant progeny: while *com-1* single mutants produced 0–2% viable embryos, *com-1 cku-80* double mutants produced 30–40% viable progeny (Figure 1B). Moreover, nearly all hatchlings of *com-1 cku-80* double mutants successfully developed into adults, while *com-1* single mutant hatchlings typically died as arrested L1/L2 larvae.

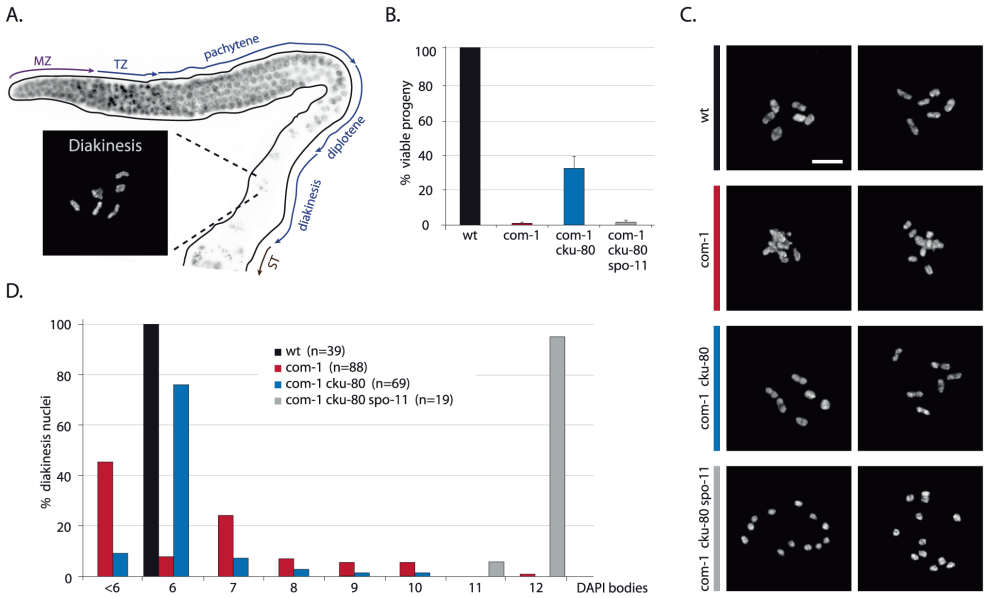

Figure 1. Loss of *cku-80* prevents chromosomal aggregation and restores chiasmata formation and embryonic survival in *com-1(t1626)* mutants.
(A) Schematic overview of the *C. elegans* germline, in which different zones correspond to the successive stages of meiotic prophase. MZ: mitotic zone; TZ: transition zone; ST: spermatheca. Blow-up shows a typical wild-type diakinesis nucleus with six bivalents. (B) Percentage progeny survival of animals of the indicated genotype; values are the average of 3 independent experiments, error bars represent S.E.M. (C) Two representative pictures of diakinesis nuclei of animals of the indicated genotype (D) Frequency distribution of DAPI-stained entities at diakinesis. n = number of germlines analyzed. Scale bars, 5 µm.

To verify these observations we crossed animals carrying another allele of *com-1* to worms lacking the other well-conserved Ku subunit CKU-70. The resultant *com-1(t1489) cku-70* double mutants showed identical phenotypes as the aforementioned *com-1(t1626) cku-80* double mutants, including elevated embryonic survival and restored larval development as compared to *com-1(t1489)* single mutants (Figure S1). We therefore conclude that *com-1* deficient animals suffer from toxic Ku activity and that in the absence of Ku, COM-1 is dispensable for *C. elegans* development and gametogenesis.

In contrast to the diakinesis nuclei of *com-1* single mutants, which hardly ever contain six DAPI-stained bodies, 70% of diakinesis nuclei of *com-1 cku-80* double mutants had the wild-type set of six bivalents (Figure 1C and 1D). We obtained similar results for *com-1 cku-70* double mutants (Figure S1). The fact that Ku deficiency restored bivalent formation in *com-1* mutant animals implies that both the univalents and the chromosomal aggregates in *com-1* deficient oocytes were due to Ku-mediated NHEJ. These observations also demonstrate that COM-1 is not required for chiasma formation *per se*. Notably, both bivalent formation and embryonic viability in *com-1 cku-80* double mutants were completely *spo-11*-dependent (Figure 1), which indicates that chiasma formation in *com-1* mutants occurs at programmed DSBs and not at spontaneous DSBs.

Based on these diakinesis studies we conclude that i) COM-1 is crucial to prevent NHEJ activity in meiotic cells; ii) Ku can act efficiently on meiotic DSBs (at least when COM-1 activity is perturbed); iii) a *com-1*-independent mechanism exists that is able to convert SPO-11-induced DSBs into proper chiasmata, and iv) in contrast to Sae2/Ctp1 in yeast, COM-1 is not required for SPO-11 removal in *C. elegans*.

Ku prevents CO formation in *com-1* mutant germlines

Since *com-1* single mutants fail to adequately form chiasmata and this defect can be restored by Ku loss (Figure 1), we reasoned that Ku might obstruct CO formation. In *C. elegans*, exactly one CO occurs per homolog pair and these presumptive CO sites can be visualized by specific recruitment of the fusion protein ZHP-3::GFP at late pachytene/diplotene stage [21], [22]. As shown in Figure 2B, wild-type animals had six ZHP-3::GFP foci in nearly all diplotene nuclei. In contrast, *com-1* single mutants on average had only two ZHP-3::GFP foci per diplotene nucleus (Figure 2A and 2B) and often exhibited persistent ZHP-3::GFP localization along the full length of the synaptonemal complex (SC) – a localization pattern characteristic of CO failure [21].

Importantly, loss of *cku-80* alleviated the ZHP-3::GFP localization defect of *com-1* mutant germlines: virtually all diplotene nuclei of *com-1 cku-80* double mutants had the normal complement of six ZHP-3::GFP foci (Figure 2A and 2B). We conclude that COM-1 is not needed for CO formation *per se*, yet COM-1 is essential to prevent interference by Ku and hence is critical for CO assurance.

The CO defect of *com-1* mutants is due to a scarcity of accessible DSBs

We hypothesized that Ku binds DSB ends and blocks DNA end resection and subsequent meiotic recombination. In order to test if the CO defect observed in *com-1* mutants is due to an insufficient number of DSBs available for HR, we subjected these animals to ionizing radiation (IR) to introduce additional DSBs. 70 Gy of IR did not alter the number of COs in wild-type animals: six ZHP-3::GFP foci were present per diplotene nucleus, irrespective of IR treatment (Figure 2C). Strikingly, 70 Gy of IR substantially increased CO formation in *com-1* mutant animals: while mock-treated *com-1* mutants had on average only two ZHP-3::GFP foci per diplotene nucleus, irradiated *com-1* mutants commonly contained six foci (Figure 2C).

Previous studies have shown that IR can increase CO frequencies only when meiotic DSBs are limiting, *e.g.* in *spo-11* mutants [6], [23], [24]. This effect is attributed to CO homeostasis mechanisms that ensure that meiotic cells receive at least one and only one CO per homolog pair [22], [24]. Our results imply that in the absence of *com-1* CO homeostasis mechanisms are still active and encourage the formation of the obligate COs, yet the substrates to do so are limited. A recent dose-response study estimated that 10 Gy of IR resulted in ~4 DSBs per chromosome pair, which was sufficient to consistently induce six CO foci in *spo-11* animals [23]. We exposed *com-1* mutants to 10 Gy, 50 Gy and 70 Gy of IR and found that only 70 Gy

resulted in a robust induction of six ZHP-3::GFP foci (Figure 2 and Figure S2). The observation that 10 Gy of IR was not sufficient to induce six CO foci in *com-1* mutants, suggests that Ku can also hijack SPO-11-independent DSBs. In support of this notion, IR resulted in increased levels of chromosomal aggregation in *com-1* deficient oocytes (Figure 2D) and [14]. Given the relatively high IR dose needed to allow six CO foci to be formed in COM-1-deficient animals, we propose that IR alleviates the CO defect, not because it introduces SPO-11-independent DSBs, but because it can introduce a total number of DSBs that exceeds the capacity of available Ku, leaving a subset of DSBs unblocked and available for HR. We conclude that both IR treatment and Ku deletion alleviated the CO deficit in *com-1* mutant animals, yet only Ku deletion restored the bias towards HR-mediated DSB repair.

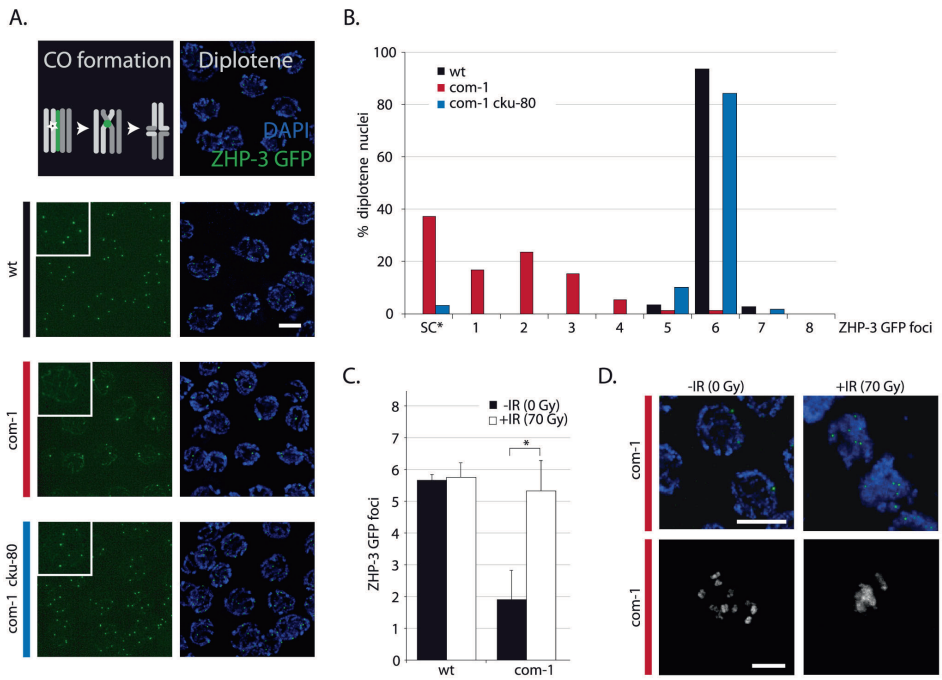

Figure 2. Loss of *cku-80* as well as γ-irradiation rescues the CO defect of *com-1* mutants.
(A) Localization pattern of ZHP-3::GFP at diplotene stage. Upper panel shows schematic overview of dynamic ZHP-3 re-localization (green) during CO formation; lower panels show representative pictures of diplotene nuclei of animals of the indicated genotype that express a ZHP-3::GFP transgene (left: GFP signal only, inset = blow-up of single nucleus; right: merge of GFP and DAPI signal). (B) Frequency distribution of ZHP-3::GFP foci in diplotene nuclei of animals of the indicated genotype; SC* = ZHP-3::GFP signal along the synaptonemal complex, no distinct foci (C) Average number of ZHP-3::GFP foci in diplotene nuclei of wild-type or *com-1* mutant animals 24 hours after mock/IR-treatment: 0 Gy (black bars)/70 Gy (white bars); Error bars represent SD, *the difference between mock- and IR-treated *com-1* mutants was highly significant ($p<0.001$ by Student's t-test, two tailed) (D) Upper panel: representative pictures of diplotene nuclei of mock/IR-treated *com-1* mutants that express a ZHP-3::GFP transgene (merge of GFP and DAPI signal); Lower panel: representative pictures of diakinesis nuclei of mock/IR-treated *com-1* mutants that express a ZHP-3::GFP transgene (DAPI signal only). Scale bars, 5 μm.

Loss of LIG-4 does not restore viability of *com-1* mutants

In *com-1* mutant animals Ku causes two problems: defective CO formation and chromosomal aggregation. We next set out to determine how Ku exerts these toxic effects. In classical NHEJ, Ku blocks DNA end resection, stabilizes the break ends and recruits the downstream factor LIG-4, which subsequently seals the DSB [2]. To assess if the Ku complex could be toxic independent of LIG-4-mediated ligation, we made *com-1 lig-4* double mutants and compared those to *com-1 cku-80* and *com-1 cku-70* double mutants. Interestingly, unlike *cku-70* and *cku-80*, the introduction of a *lig-4* null allele did not rescue progeny survival of *com-1* mutants (Figure 3B). Since either *lig-4* or *cku-70/cku-80* loss prevents NHEJ, blocking NHEJ *per se* is not sufficient to restore viability in *com-1* mutants. We therefore infer that Ku has toxic activities that are independent of NHEJ-mediated fusion.

Consistent with that notion, diakinesis nuclei of *com-1 lig-4* double mutants often showed more than six DAPI-stained bodies, indicating that CO formation remained perturbed (Figure 3A). While *lig-4* deletion did not restore the CO defect, it did prevent chromosomal aggregation: in contrast to *com-1* single mutants, the diakinesis nuclei of *com-1 cku-80* and *com-1 lig-4* double mutants rarely had fewer than six DAPI-stained bodies (Figure 1C and Figure 3A). These observations indicate that chromosomal aggregation in *com-1* mutants mainly depends on classical NHEJ.

Notably, diakinesis nuclei of *com-1 lig-4* double mutants frequently contained small DAPI-stained fragments, which are indicative of persistent DSBs (Figure 3A and 3C). We next established that these chromosomal fragments were the consequence of defective repair of programmed SPO-11-induced DSBs (and not of spontaneous DSBs): *com-1 lig-4; spo-11* triple mutant animals exhibited 12 intact univalents at diakinesis and no fragmentation (Figure 3A and 3C). Together, these results strongly suggest that in COM-1-deficient animals, Ku promotes LIG-4-mediated fusions and that in the absence of LIG-4 the Ku-bound DSBs remain unrepaired. We therefore propose that COM-1 needs to prevent Ku activity not only because Ku promotes classical NHEJ at meiotic DSBs, but mainly because Ku forestalls meiotic recombination directly.

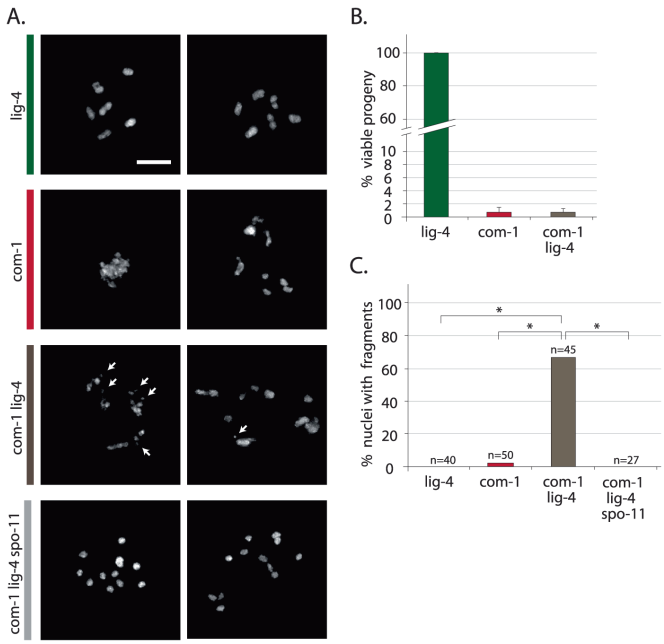

Figure 3. Loss of *lig-4* prevents chromosomal fusion in *com-1* mutants, but does not restore viability.
(A) Two representative pictures of diakinesis nuclei of animals of the indicated genotype. White arrows point out chromosomal fragments (B) Percentage progeny survival; values are the average of 3 independent experiments, error bars represent S.E.M. (C) Percentage of diakinesis nuclei that show chromosomal fragments; n = number of germlines analyzed. Scale bars, 5 μm. *The difference between these genotypes was highly significant ($p<0.001$ by Fisher's exact test, two tailed).

Ku acts at early/mid pachytene stage and blocks the formation of RAD-51 foci

We next determined how and when Ku prevents meiotic recombination. Based on their homologous counterparts, we expect CKU-70/CKU-80 to block DNA end resection. This scenario is consistent with the reported defect in RAD-51 recruitment in COM-1-deficient germlines [14]. Meiotic recombination is initiated in the transition zone where RAD-51-coated recombination intermediates become visible as distinct foci [25], [26]. In wild-type worms, the number of RAD-51 foci peaks at early/mid pachytene stage (Figure 4, zone 4+5) and as repair progresses, these RAD-51 foci disappear by late pachytene stage (Figure 4, zone 6+7) [27]. In *com-1* single mutants, however, we could not detect the typical rise of RAD-51 foci in early/mid pachytene nuclei, suggestive of a defect early in meiotic recombination (Figure 4C, zone 4+5). Strikingly, this defect was relieved by *cku-80* loss: *com-1 cku-80* double mutants did show the strong increase in RAD-51 foci at early/mid pachytene stage (Figure 4D, zone 4+5). These results demonstrate that, in the absence of COM-1, CKU-80 prevents efficient formation of RAD-51-coated HR intermediates, likely by inhibiting DNA end resection. Moreover, they reveal that CKU-80 can already act at early pachytene stage, which paradoxically is the stage where programmed DSBs need to be channeled into HR.

While *com-1 cku-80* double mutant germlines were proficient in RAD-51 loading, we noted a mild delay in RAD-51 focus formation compared to *cku-80* single mutant controls (Figure 4, zone 4+6). This delay suggests that COM-1 may also be required for efficient DNA end resection and thus the timely formation of interhomolog COs.

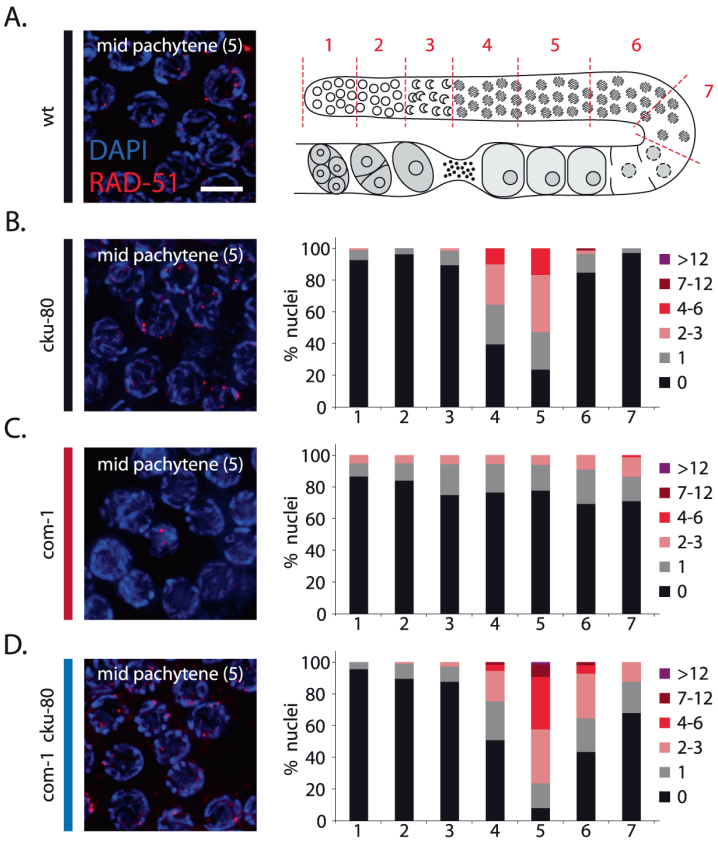

Figure 4. Loss of *cku-80* restores RAD-51 recruitment to meiotic DSBs in *com-1* mutant germlines. (A) Left: representative image of mid-pachytene nuclei in wild-type germlines stained with RAD-51 antibody; merge of RAD-51 (red) and DAPI signal (blue); Right: schematic overview of the C. elegans germline with indicated zones (1–7) used for RAD-51 foci analysis. (B)(C)(D) RAD-51 foci analysis of *cku-80, com-1* and *com-1 cku-80* double mutant germlines, respectively. Left: representative images of mid-pachytene nuclei (zone 5) stained with RAD-51 antibody, merge of RAD-51 (red) and DAPI signal (blue) Right: Stacked histograms depict the quantification of RAD-51 foci in germlines of the indicated genotypes. The number of RAD-51 foci per nucleus is categorized by the color code shown on the right. The percent of nuclei observed for each category (y-axis) are depicted for each zone along the germline axis (x-axis). Three independent gonads were scored for each genotype. Scale bars, 5 µm.

COM-1 and EXO-1 act redundantly to promote meiotic recombination

To find the factors responsible for COM-1-independent meiotic recombination, we searched for genes known to have overlapping functions with COM-1 or its homologs. In yeast, the sensitivity of Sae2-deficient mitotic cells to DSB-inducing agents can be rescued by overexpressing the 5′-3′ exonuclease Exo1 [28]. Furthermore, Exo1 transcription is highly induced during yeast meiosis and Exo1 promotes CO formation [29], [30], making Exo1 a suitable candidate for enabling *com-1*-independent CO formation.

A clear Exo1 homolog is present in *C. elegans*, F45G2.3, which we named *exo-1*. We used a deletion mutant of *exo-1*, which is predicted to express a severely truncated protein lacking the conserved nuclease domain (Figure 5A), to show that EXO-1 has a conserved role in HR-mediated DSB repair in germ cells. Firstly, *exo-1* mutant germlines were hypersensitive to IR, in a manner epistatic with the well-studied HR factor *brc-1* (Figure 5B) and secondly, *exo-1* mutants were hypersensitive to transposon-induced DSBs, *i.e. exo-1* deficiency significantly reduced embryonic survival in animals that have elevated levels of transposition in the germline (Figure S3). Despite the need for *exo-1* in repair of ectopic DSBs, unchallenged *exo-1* single mutants did not display major meiotic defects (Figure 5C and 5D), which suggests that EXO-1 does not act on SPO-11-induced DSBs or it operates in a redundant fashion.

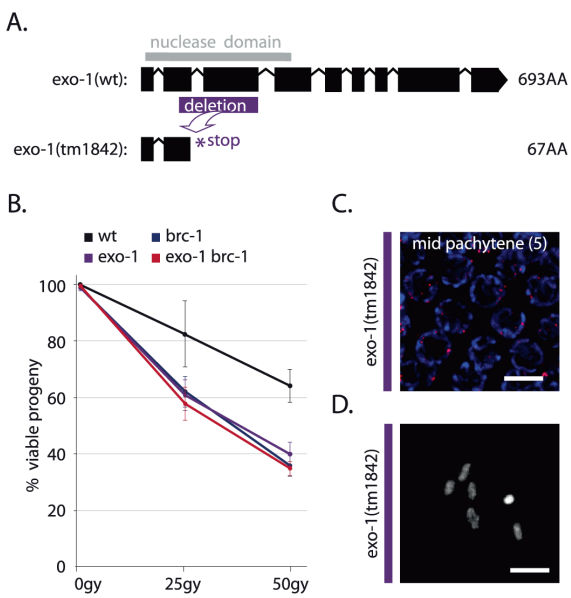

Figure 5. EXO-1 promotes DSB repair in germ cells.
(A) Gene model of wild-type F45G2.3 (*exo-1*) with the position of its catalytic domain (gray) and below its truncation allele *tm1842*; a 559 bp deletion (purple) results in a premature stop (B) Percentage progeny survival of animals of the indicated genotype treated with the indicated dose of IR; values are the average of 3 independent experiments, error bars represent S.E.M. (C) RAD-51 immunostaining of mid-pachytene nuclei (zone 5) in *exo-1* deficient germlines; merge of RAD-51 (red) and DAPI signal (blue) (D) Representative picture of a diakinesis nucleus of *exo-1* deficient animals.

To assess if EXO-1 is responsible for COM-1-independent meiotic recombination, we created *com-1 cku-80 exo-1* triple mutants and analyzed CO formation and progeny survival. In contrast to *com-1 cku-80* double mutants, which have robust CO formation (Figure 1C), *com-1 cku-80 exo-1* triple mutants fail to adequately produce COs, as illustrated by the scarcity of ZHP-3::GFP foci at diplotene (Figure 6A) and the lack of chiasmata at diakinesis (Figure 6B). Consequently, *com-1 cku-80 exo-1* animals typically produce aneuploid gametes and hardly any viable progeny (Figure 6D and 6E).

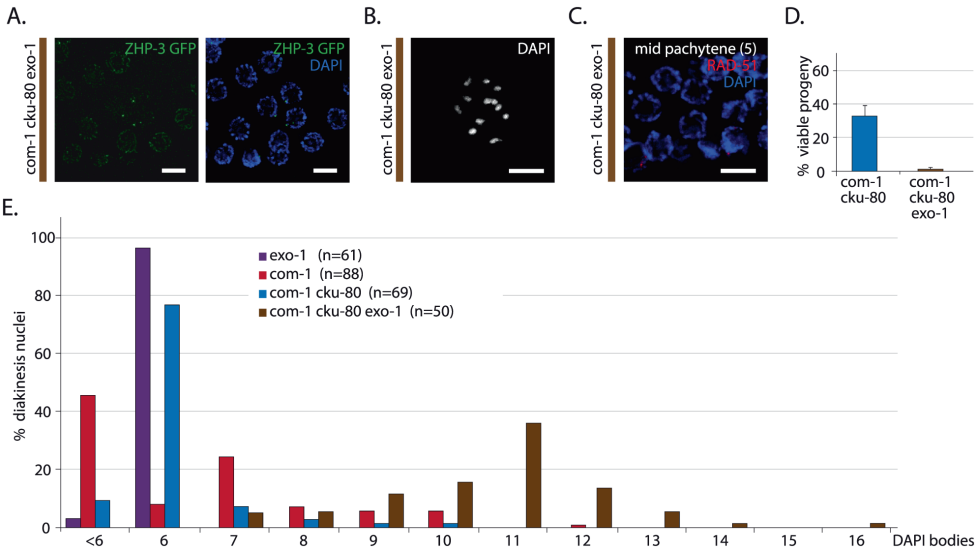

Figure 6. EXO-1 is required for meiotic recombination in absence of COM-1.
(A) Representative image of diplotene nuclei of *com-1 cku-80 exo-1* triple mutant animals that express a ZHP-3::GFP transgene (left: GFP signal only, right: merge of GFP and DAPI signal) (B) Representative picture of a diakinesis nucleus in *com-1 cku-80 exo-1* triple mutants germlines (C) RAD-51 immunostaining of mid-pachytene nuclei (zone 5) in *com-1 cku-80 exo-1* mutant germlines; merge of RAD-51 (red) and DAPI signal (blue) (D) Percentage progeny survival of animals of the indicated genotype; values are the average of 3 independent experiments*, error bars represent S.E.M. (E) Frequency distribution of DAPI-stained entities at diakinesis*. n = number of germlines analyzed. The *com-1 cku-80 exo-1* triple mutants occasionally showed >12 DAPI bodies due to chromosomal fragmentation. See Figure 7E for quantification. Scale bars, 5 µm. *These experiments were performed in parallel to those depicted in Figure 1B and 1D; reference values are depicted again here.

We next investigated how EXO-1 promotes CO formation in *com-1* deficient germlines. Recently, yeast Exo1 has been shown to promote CO formation via two distinct activities: i) by performing DNA end resection and ii) by resolving CO intermediates named double Holliday Junctions (dHJs) [30]. These two Exo1 activities affect HR at different steps: DNA end resection promotes the formation of RAD-51 intermediates, whereas dHJ resolution supports the clearance of RAD-51 intermediates. We found that early/mid pachytene nuclei of *com-1 cku-80 exo-1* triples contained hardly any foci (Figure 6C), which contrasts the many RAD-51

foci observed in *com-1 cku-80* double mutants (Figure 4D). This implies that EXO-1 promotes *com-1*-independent CO formation mainly via its role in DNA end resection.

From these results it can be deduced that i) EXO-1 can act on meiotic DSBs and ii) EXO-1 and COM-1 act in parallel pathways to promote RAD-51 recruitment at early/mid pachytene stage and individually can assure timely CO formation. Furthermore, both COM-1 and EXO-1 are not essential for SPO-11 removal because we did not observe substantial chromosome fragmentation in the diakinesis nuclei of *com-1 cku-80 exo-1* triple mutants. Instead, we detected six to twelve regularly shaped DAPI-stained bodies (Figure 6B and 6E), which suggests some degree of DSB repair.

Homolog-independent HR does not depend on COM-1 and EXO-1

C. elegans germ cells switch between different DSB repair modes as they progress through meiosis [31]. In the early stages of meiotic prophase, the majority of meiotic DSBs are repaired using the homologous chromosome as a template [31], [32]. At late pachytene stage this dominance is thought to be relieved, allowing homolog-independent mechanisms to repair the meiotic DSBs [32], [33]. One example that supports this notion is that mutant animals defective in interhomolog HR (e.g. *syp-2* mutants) show persistent meiotic DSBs that are eventually repaired late in meiotic prophase in a *rad-51*-dependent manner [32]. Subsequent studies suggest that these remaining DSBs are repaired efficiently via intersister HR, ultimately giving rise to intact chromosomes at diakinesis [19], [34].

To investigate the contribution of COM-1 and EXO-1 to homolog-independent HR, we quantified RAD-51 focus formation throughout the germline. *com-1 cku-80* double mutants had many RAD-51 foci at early/mid pachytene stage (Figure 7A, zone 4+5), but very few RAD-51 foci at late pachytene stage (Figure 7A, zone 7), indicating that the majority of RAD-51 intermediates were resolved by that point. Conversely, *com-1 cku-80 exo-1* triple mutant germlines had very few RAD-51 foci at early/mid pachytene stage (Figure 7B, zone 4+5), but showed many RAD-51 foci at late pachytene stage (Figure 7B, zone 7). This abundance of RAD-51-coated recombination intermediates at late pachytene implies that COM-1 and EXO-1 are dispensable for DNA end resection at these later stages, which suggests further redundancy and/or temporal regulation of DNA end resection during meiotic prophase. Moreover, these findings imply that intersister HR may not be affected by *com-1* and *exo-1* loss.

To test if intersister HR is responsible for the residual repair activity in the triple mutant, we depleted the cohesin factor REC-8, which is proposed to promote both interhomolog as well as intersister HR [9], [20], [35]. REC-8 depletion caused extensive chromosomal fragmentation in *com-1 cku-80 exo-1* triple mutants (Figure 7D), implying that REC-8-dependent HR is active in the absence of COM-1 and EXO-1. REC-8 depletion, however, has documented pleiotropic effects, including altered SPO-11 activity, which may affect the levels of chromosome fragmentation [31]. We therefore substantiated these findings by deleting

Structural Maintenance of Chromosomes 5 *(smc-5)* in *com-1 cku-80 exo-1* animals. *Smc-5* has recently been shown to be specifically required for homolog-independent (presumably intersister) HR during *C. elegans* meiosis [34]. Analogous to REC-8 depletion, deletion of *smc-5* in *com-1 cku-80 exo-1* triple mutants resulted in high levels of chromosome fragmentation at diakinesis (Figure 7C and 7E). Similar results were obtained when deleting the SMC-5 complex partner SMC-6 (Figure S3). Together these observations strongly suggest that, while COM-1 and EXO-1 redundantly promote RAD-51 recruitment and subsequent CO formation at early/mid pachytene stage, at late pachytene stage both proteins are dispensable for RAD-51-mediated intersister HR.

Ku deficiency does not fully restore genome stability in *com-1* mutants

Despite the observation that HR is active and COs are formed in germlines lacking both COM-1 and CKU-80, progeny survival of *com-1 cku-80* double mutants was not restored to wild-type levels. In fact, ~70% of *com-1 cku-80* double mutant progeny died during embryonic development (Figure 1B). Moreover, the mutant animals that survived frequently displayed developmental abnormalities, including altered body morphology and faulty vulval development (Figure S4). These phenotypes suggest that Ku-deficient *com-1* mutants still suffered from genomic instability. In support of this notion, *com-1 cku-80* and *com-1 cku-70* double mutants exhibited high levels of X-chromosome non-disjunction, as revealed by a 50-fold increase in XO males among the surviving progeny (Figure S4). Careful analysis of *com-1 cku-80* deficient germlines revealed that the fidelity of meiotic DSB repair is incomplete: diakinesis nuclei of *com-1 cku-80* double mutants occasionally showed chromosomal abnormalities, including unstable bivalent attachments and chromosomal aggregates (Figure 1D and Figure S5). We detected similar chromosomal aberrations in *com-1 lig-4* double mutants (Figure S5), supporting the notion that an alternative mutagenic repair pathway exists that can provoke chromosomal aggregates in germ cells devoid of classical NHEJ [8]. We propose that Ku-deficient *com-1* mutants still suffer from (NHEJ-independent) error-prone repair events, which cause substantial chromosomal instability and embryonic lethality.

We next addressed whether these aberrant repair events in *com-1 cku-80* double mutants induced germ cell apoptosis. Interestingly, despite the high degree of chromosomal instability, the level of apoptosis was not observed to be increased in *com-1* single mutant germlines [14]. Although we cannot formally exclude that COM-1 by itself is required for the signaling of apoptosis, our cytological data argue that Ku blocks end resection in these animals and thus precludes the formation of ssDNA - a major trigger for the DNA damage checkpoint [36], [37]. To test this hypothesis further, we counted apoptotic cells, marked by transgenic CED-1::GFP, in *com-1 cku-80* deficient germlines. We observed a mild but statistically significant increase as compared to *com-1* single mutants (Figure S4). This result may reflect inefficient repair of a fraction of DSBs in *com-1 cku-80* double mutants, as was also suggested by the subtle delay in RAD-51 focus resolution during meiotic prophase (Figure 4, zone 6). These phenotypes

are however very mildly different from wild-type behavior [14], [27], [38]. We thus conclude that the vast majority of meiotic DSBs are repaired effectively in *com-1 cku-80* mutant germ cells, without activating the DNA damage checkpoint. The fidelity of repair, however, is clearly affected by *com-1* and *cku-80* loss.

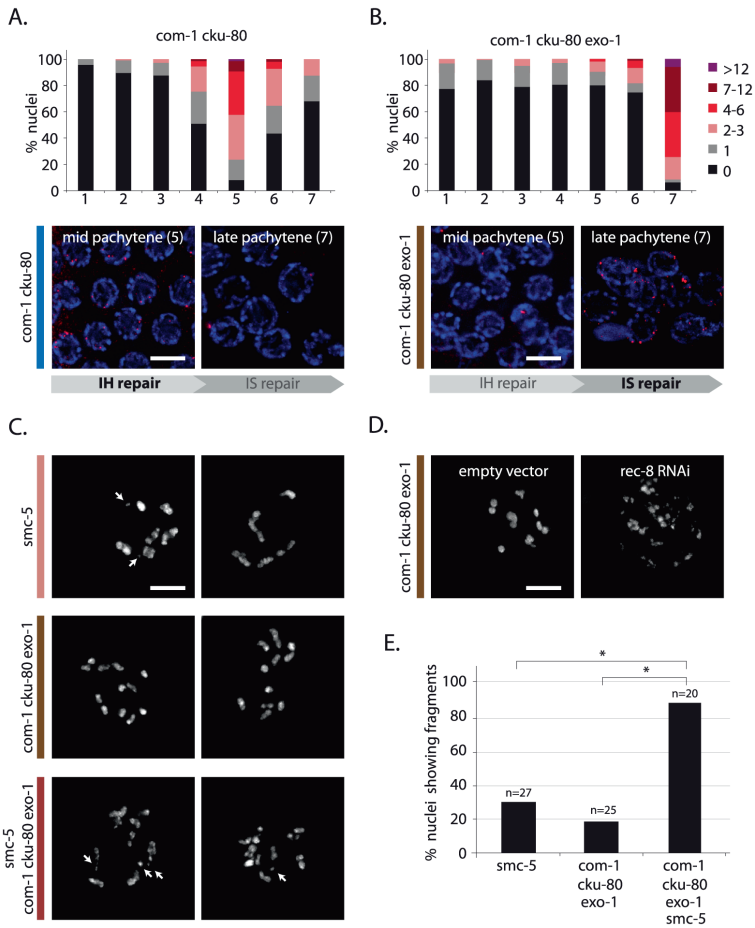

Figure 7. EXO-1 and COM-1 are needed for efficient interhomolog HR, but dispensable for intersister HR.
(A,B) RAD-51 foci analysis of *com-1 cku-80* double and *com-1 cku-80 exo-1* triple mutant germlines, respectively. Stacked histograms depict the quantification of RAD-51 foci in germlines of the indicated genotypes. See Figure 4 for details. Representative images of mid-pachytene nuclei (zone 5) and late pachytene nuclei (zone 7) stained with RAD-51 antibody (red). IH = interhomolog, IS = intersister (C) Two representative pictures of diakinesis nuclei of animals of the indicated genotype. White arrows point out chromosomal fragments (D) Representative picture of a diakinesis nucleus *of com-1 cku-80 exo-1* triple mutant animals, which are fed on E. coli strains carrying either a control- or rec-8 RNAi vector. (E) Percentage of diakinesis nuclei that show chromosomal fragments; n = number of germlines analyzed. *The difference between these genotypes was highly significant ($p<0.001$ by Fisher's exact test, two tailed). Scale bars, 5 µm.

Discussion

The conserved C-terminus of COM-1 counteracts Ku activity and thereby supports efficient meiotic recombination

We identified COM-1 as a crucial factor in preventing toxic Ku activity at meiotic DSBs. Both *com-1* alleles used in this study (*t1626* and *t1489*) are loss-of-function alleles and encode for C-terminally truncated proteins [14]. Although sequence analysis of the *t1489* allele revealed a different mutation than previously annotated, both alleles still contain a premature stop that prohibits expression of the conserved C-terminus (Figure S1).

Previously, Penkner and colleagues claimed that COM-1 was required specifically to repair SPO-11-induced DSBs but not IR-induced DSBs – suggestive of a conserved role for COM-1 in SPO-11 removal [14]. However, the data we present here reveals that COM-1-deficient germlines are able to repair SPO-11-induced DSBs both via NHEJ and HR. Moreover, we show that COM-1 is not required for meiotic recombination *per se*, but instead is needed to prevent Ku activity at early pachytene stage to allow DNA end resection and CO formation to take place.

Despite the high conservation of the C-terminal domain of Sae2/COM-1, the contribution of these proteins to SPO-11 removal has clearly diverged between yeast and metazoans: while in yeast a single point mutation in the C-terminus of Sae2 can block Spo11 removal and subsequent HR reactions [39], removal of the entire C-terminus of COM-1 does not prohibit meiotic recombination in *C. elegans*. Spo11 removal in yeast not only requires Sae2, but also the highly conserved nuclease Mre11 [18], [40]. Perhaps metazoan MRE-11 is able to remove SPO-11 independently of COM-1. In that scenario, MRE-11 would create free DSB ends that could act as a substrate for both HR and NHEJ (Figure 8). In *C. elegans*, MRE-11 is needed for meiotic DSB formation, however, this requirement can be bypassed by the depletion of meiotic cohesin [41], [42]. Meiotic DSB induction in absence of MRE-11 results in severe chromosome fragmentation, suggesting that MRE-11 is also required for SPO-11 removal in *C. elegans* [42].

We show here that COM-1 is not required for the initiation of meiotic DSB repair, but is needed to channel the programmed DSBs into HR. When COM-1 function is perturbed, Ku blocks EXO-1-mediated resection and promotes LIG-4-mediated fusion. How COM-1 prevents Ku activity on a molecular level is unknown to date, but based on the current models of DNA end resection at meiotic DSBs and the observations described here, we propose that COM-1 cleaves off Ku-bound DSB ends and thereby enables EXO-1 to perform DNA end resection (Figure 8).

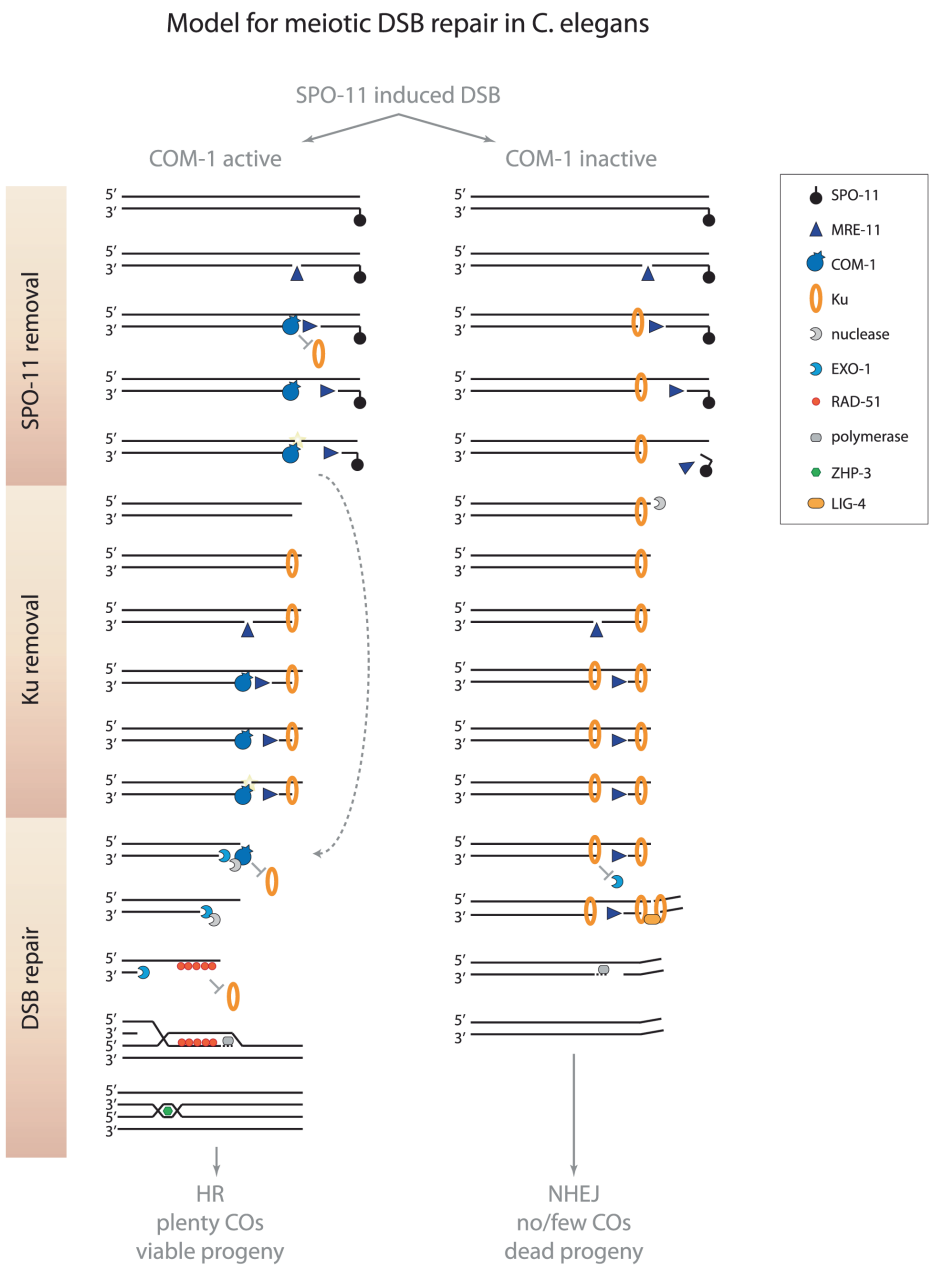

Figure 8. Model for meiotic recombination in *C. elegans*.
In wild-type germlines, MRE-11 may create substrates at meiotic DSBs that allow COM-1 to efficiently remove Ku (and SPO-11). When COM-1 function is perturbed, MRE-11 mediated processing may still release SPO-11 bound oligos. However, MRE-11 activity alone is not sufficient to counteract Ku binding and prevent toxic NHEJ activity. Without COM-1 and Ku, SPO-11 is removed and EXO-1 promotes DNA end resection and allows the obligate COs to be formed. See text for further details.

A model for COM-1–dependent Ku removal

Recent work on yeast meiosis has led to a new model for initiation of meiotic recombination that is based on bidirectional DNA end resection [43]. In this model Mre11 creates a single-strand nick up to 300 nucleotides from the meiotic DSB end. This nick then acts as a substrate for both Exo1 and Mre11: Exo1 starts resection in the 5′-3′ direction (away from the DSB) and Mre11 initiates resection in the 3′-5′ direction (towards the DSB end). Accordingly, the 3′-5′ exonuclease activity of Mre11 is critical for the efficient release of Spo11 oligos and subsequent meiotic recombination [43]. Mre11 is proposed to also remove Ku from DSB ends, since Ku (like Spo11) blocks DSB ends and prevents HR-mediated repair [43]. However, recent *in vitro* studies have revealed that human MRE11 cannot compete with Ku for DNA binding nor is able to displace Ku from DSB ends [44]. In these reactions, Ku efficiently prevented EXO1 from performing DNA end resection, even in the presence of MRE11. Our *in vivo* model is consistent with such an interaction, as MRE-11-proficient, but COM-1-deficient, germlines are able to remove SPO-11, but are not able to prevent Ku from hijacking meiotic DSBs (Figure 1 and Figure 2). Our observations imply that SPO-11 removal and Ku exclusion are two distinct activities. Based on the bidirectional nature of DNA end resection and the fact that the affinities of Ku to ssDNA nicks and dsDNA ends are almost equal [45], [46], we propose that Ku may act at the upstream nick to prevent EXO-1-mediated end resection. In such a scenario, MRE-11 may still be able to progress towards the DSB end to remove SPO-11, thus creating a free DSB end that allows NHEJ-mediated repair (Figure 8). The notion that Ku may block 5′-3′ resection by EXO-1, but not 3′-5′ resection by MRE-11 is supported by the fact that the 3′-5′ exonuclease activity of mammalian MRE11 promotes deletion formation during classical NHEJ [47].

We hypothesize that COM-1 prevents Ku occupancy at meiotic DSBs and therefore safeguards proper 5′-3′ DNA end resection and CO formation (Figure 8). While our study reveals that MRE-11, in the absence of COM-1, is not sufficient to prevent Ku activity at meiotic DSBs, we cannot exclude that COM-1 requires MRE-11 activity to counteract Ku. In fact, COM-1 may cut the gapped DNA structure that arises when MRE-11 progresses towards the DSB end, which would release both MRE-11 and Ku from the break site (Figure 8). In support of this model, Sae2 has been shown to possess intrinsic endonuclease activity on gapped DNA substrates *in vitro* and this activity is proportional to the length of exposed ssDNA [48]. Moreover, Sae2 mutants accumulate both Mre11 and Ku at DSB ends [49], [50].

Ku can act at early pachytene stage and competes with interhomolog HR

Several studies have found evidence of NHEJ-mediated chromosomal aggregates in *C. elegans* germ cells, however, the biological relevance of these NHEJ events has been uncertain, since they were evident only when meiotic recombination was completely abolished (e.g. by *rad-51*, *brc-2* or *msh-4* mutation) and were detected only at diakinesis, the final

stage of meiotic prophase [8], [9], [10]. Here we report that Ku can act even when meiotic recombination is proficient and that it does so early in meiosis, at early/mid pachytene stage. Moreover, we reveal that meiotic Ku activity can result in toxic chromosomal aggregates and a fatal lack of obligate COs.

The capacity of Ku to block meiotic recombination is maybe best illustrated by the low levels of ZHP-3::GFP foci observed in COM-1-deficient animals – a phenotype that can be completely alleviated by Ku loss (Figure 2). ZHP-3::GFP localizes to presumptive CO sites and forms six distinct foci in wild-type diplotene nuclei [21]. A recent study by Rosu and colleagues revealed that although each *C. elegans* meiotic nucleus may undergo up to 40 programmed DSBs, a single DSB per chromosome pair is largely sufficient to assure CO formation [51]. Given that more than a third of the COM-1-deficient nuclei are not able to form a single ZHP-3::GFP focus, and the ones that do only form on average 2–3 ZHP-3::GFP foci, we predict that in the absence of COM-1 nearly all meiotic DSBs are blocked by Ku. To shed more light on this subject, we tried to outcompete Ku by creating many extra DSBs using IR. Only when *com-1* mutants were treated with a relatively high dose of IR (estimated to inflict ~170 DSBs per nucleus [23]) the majority of diplotene nuclei had six CO foci. Based on these experiments we estimate that Ku is able to block ~97% of all meiotic DSBs when COM-1 function is impaired.

Despite this high toxic capacity of Ku, wild-type worms exhibit very robust CO formation and at least a hundred-fold bias towards HR over NHEJ-mediated repair of germline DSBs [51], [52]. This suggests that COM-1 is very potent in either blocking or removing Ku at meiotic DSBs. Given the striking affinity of Ku towards DNA ends [45] and the detrimental effects of meiotic NHEJ on species survival [this study], additional levels of regulation might be necessary to guarantee the strong HR bias in germ cells. In mouse spermatocytes, Ku protein levels drop significantly at early/mid pachytene stage, revealing that Ku activity can be prevented both by COM-1 activity and at the level of transcription/translation [53]. Interestingly, recently identified COM1 mutants in rice also displayed many non-homologous chromosome entanglements in meiotic cells, indicating that COM-1-mediated NHEJ inhibition may be a common phenomenon among eukaryotes [54].

COM-1 and EXO-1 promote the timely formation of CO substrates

In addition to its role in NHEJ inhibition, COM-1 also supports DNA end resection during early/mid pachytene stage (Figure 4 and Figure 7). In yeast, DNA end resection at meiotic DSBs is performed by Exo1 and Sgs1/Dna2, with Exo1 having the major role [39]. Accordingly, Exo1 mutants show subtle but significant meiotic defects including reduced spore viability and a two-fold decrease in CO recombination [55]. We show here that COM-1-proficient worms do not rely on EXO-1 for meiotic recombination, as *exo-1* single mutants form both meiotic RAD-51 foci and bivalents normally (Figure 5). When COM-1 is absent however, EXO-1 becomes essential for RAD-51 loading at early/mid pachytene stage and subsequent CO formation

(Figure 6). Thus meiotic germ cells require either COM-1 or EXO-1 to perform timely DNA end resection. How COM-1 promotes extensive DNA end resection is still unclear, as COM-1 homologs are implicated only in the onset of resection [49]. COM-1 may be needed for the recruitment of other nucleases to meiotic DSBs. For instance, recruitment of the nuclease DNA2 to DSBs strongly depends on CtIP in human cells [56]. In line with this suggestion, we found a strong synthetic lethal interaction between *exo-1* and *dna-2* (unpublished observations). We also demonstrated that HR via the sister chromatid is not abolished by *com-1* and *exo-1* mutation, revealing another activity that is able to resect meiotic DSBs independent of COM-1 and EXO-1, but only in late pachytene nuclei (Figure 7). Why this activity does not support meiotic recombination and CO formation at early pachytene stage is still an open question.

Implications of mutagenic NHEJ activity in germ cells

COM-1 is dispensable for meiotic recombination *per se*, however without it, many meiotic DSBs will be repaired via NHEJ, a mutagenic DSB repair pathway that generates non-CO products. The scarcity of COs, combined with the extensive chromosomal aggregation, provides a cogent explanation for the poor fertility of *com-1* mutant animals and reveals the deleterious nature of unscheduled NHEJ during meiosis.

How NHEJ is kept in check during human meiosis remains to be addressed. Recent studies have revealed that a subclass of so-called Seckel and Jawad syndrome patients express truncated CtIP variants that typically lack the conserved C-terminus [57], which are very reminiscent of the *com-1* alleles used for this study (Figure S1). Although these patients suffer from severe mental retardation and skeletal abnormalities, it is unknown to date if they also have fertility defects.

Multicellular animals rely heavily on NHEJ to maintain genome stability in somatic tissues, but the efficacy of this repair pathway seems to come with a price: uncontrolled NHEJ activity has been shown to drive tumorigenesis in mice [58] and the data presented here uncover its toxic properties during meiosis. Recent advances in genome-wide sequencing have revealed that many complex chromosomal rearrangements that occur *de novo* in human germlines show typical NHEJ footprints [59], [60], which suggests that incomplete inhibition of NHEJ during gametogenesis may affect genome evolution in many organisms, including humans, and could lead to pathogenic chromosomal alterations that cause serious inborn diseases.

Materials and Methods

Worm strains and culture conditions

All strains were maintained at 15°C using standard *C. elegans* techniques [61]. The wild-type background was Bristol N2. In case of mutant strains that carried a linked *unc-32(e189)* allele, matched *unc-32(e189)* homozygotes served as controls. The following mutations,

transgenes and genetic balancers were used: LGII: *smc-5(ok2421)*, *smc-6(ok3294)*, *dna-2* [62], *mln1*[*dpy-10* mls14]. LGIII: *com-1(t1626)* [14], *com-1(t1489)* [14], *unc-32(e189)*, *cku-80(ok861)*, *cku-70(tm1524)*, *lig-4(ok716)*, *exo-1(tm1842)*, *brc-1(tm1145)*, hT2[*let-? qIs48*]. LG IV: *spo-11(ok79)*, *jfIs2*[ZHP-3::GFP] [21].

Y-irradiation and progeny survival/him assays

Synchronized L4 worms were either left unchallenged or irradiated using an x-ray generator (200 kV; 10 mA; 11 Gy/min dose rate; YXLON International) to create germline DSBs. Three (irradiated) hermaphrodites were pooled on an OP50 seeded NGM plate and cultured at 20°C to produce progeny. After 40 hrs mothers were removed and the ratio between dead eggs/hatched larvae was assessed 24 hrs later. For Him assay, the percentage of males among the hatched progeny was determined. For all survival/him assays, at least three independent plates were scored per condition. Figures provide mean values of three independent experiments.

DAPI staining and ZHP-3::GFP analysis

Synchronized L4 worms were picked and allowed to age 20–24 hrs. Gonad dissection was carried out in 1× EBT (25 mM HEPES-Cl pH 7.4, 118 mM NaCl, 48 mM KCl, 2 mM CaCl, 2 mM MgCl, 0.1% Tween 20 and 20 mM sodium azide). An equal volume of 4% formaldehyde in EBT was added (final concentration is 2% formaldehyde) and allowed to incubate for 5 min. The dissected worms were freeze-cracked in liquid nitrogen for 10 min, incubated in methanol at −20°C for 10 min, transferred to PBS/0.1% Tween (PBST), washed 3×10 min in PBS/1%Triton-X and stained 10 min in 0.5 µg/ml DAPI/PBST. Finally samples were de-stained in PBST for 1 h and mounted with Vectashield. Diakinesis nuclei of −1 position oocytes (closest to the spermatheca) were analyzed using Leica DM6000 microscope. To examine CO formation, ZHP-3::GFP foci were analyzed in ~15 most proximal pachytene/diplotene nuclei of at least six independent germlines (~100 nuclei).

Immunofluorescence and RAD-51 focus quantification

RAD-51 protein was detected by indirect immunofluorescence. Germlines were dissected and fixed for whole-mount staining as described above, then blocked with 1% BSA in PBST and incubated overnight at 4°C with rabbit anti-RAD-51 antibody (Novus Biologicals) diluted 1:200. Primary antibody was detected using Alexa488 Goat anti-rabbit antibody (Invitrogen) diluted 1:1000 and DNA was counter-stained with 0.5 µg/ml DAPI. RAD-51 foci were imaged using a Leica DM6000 deconvolution microscope collecting 0.5 µm Z-sections. The number of foci per nucleus was counted for each of the seven zones of the germline [27]. Three to five germlines were quantified per condition.

Supporting Information

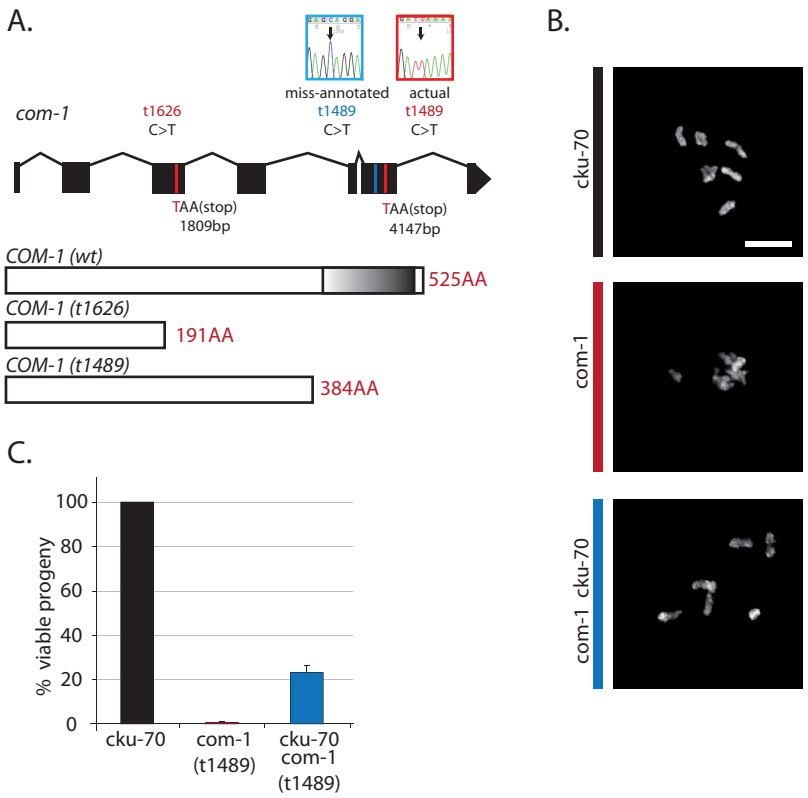

Figure S1. Loss of *cku-70* prevents chromosomal aggregation and restores chiasmata formation and embryonic survival in *com-1(t1489)* mutants. (A) Gene model of C44B9.5 (*com-1*) with the position of the non-sense mutations t1626 and t1489 in the third and sixth exon, respectively. Although the annotation of the t1626 allele is correct, the t1489 allele is miss-annotated: no C>T mutation was detected 4030 bp upstream of the ATG (supposedly resulting in an 'amber' stop and a 345AA COM-1 peptide). Instead, we found a C>T mutation 4147 bp upstream of the ATG, which leads to a 'ochre' stop and a 384AA truncated COM-1 peptide. Notably, both the t1626 and t1489 stops are upstream of the sequence coding for COM-1's well-conserved C- terminal domain. (B) A representative picture of diakinesis nuclei of animals of the indicated genotype. Scale bars, 5 µm. (C) Percentage progeny survival of animals of the indicated genotype; values are the average of 3 independent experiments; error bars represent S.E.M.

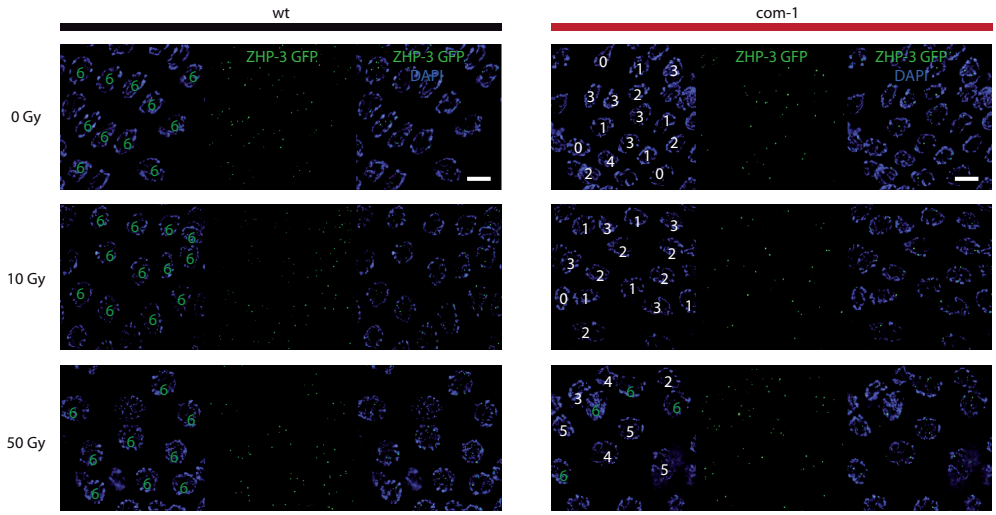

Figure S2. Dose-response analysis of ZHP-3::GFP foci formation upon exposure to IR Representative pictures of ZHP-3::GFP foci in diplotene nuclei from either wild-type germlines (left) or *com-1(t1626)* mutant germlines (right), exposed to indicated IR doses. Panels depict, from left to right, DAPI signal with numbers of foci in each nucleus indicated, GFP signal only, and DAPI/GFP merge). Scale bars, 5 µm.

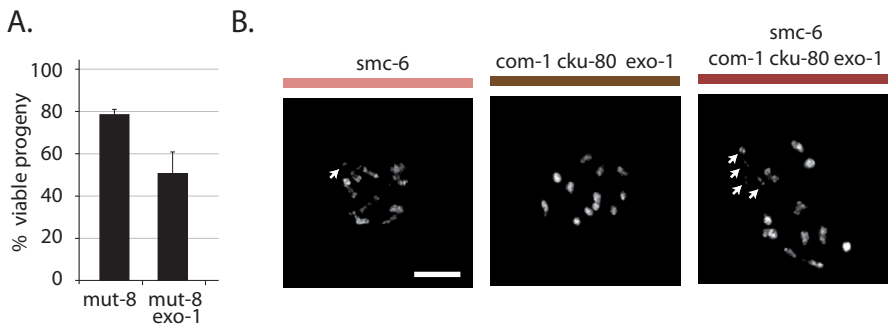

Figure S3. EXO-1 promotes DSB repair in *C. elegans* germ cells. (A) Percentage progeny survival of animals of the indicated genotype. Mut-8 mutation activates transposition in the germline. (B) A representative picture of diakinesis nuclei of animals of the indicated genotype. White arrows point out chromosomal fragments. Scale bar, 5 µm.

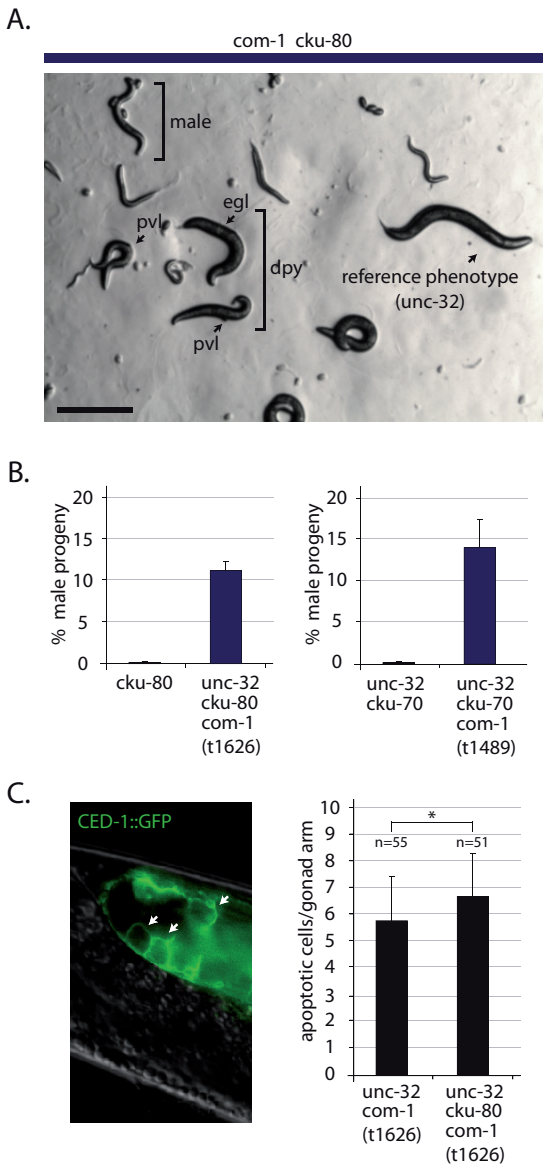

Figure S4. Ku deficient *com-1* mutants show various signs of chromosomal instability but only a mild increase in germline apoptosis. (A) Various somatic defects observed in second-generation *com-1 cku-80* double mutants, including dumpy morphology (dpy), egg laying deficiency (egl) and protruding vulvas (pvl). Black scale bar, 50 µm (B) Percentage male progeny of animals of the indicated genotype; values are the average of 3 independent experiments, error bars represent S.E.M. (C) Left: a representative picture of a CED-1:GFP expressing germline (left), with apoptotic cells indicated by white arrows; Right: Average number of apoptotic cells (surrounded by CED-1::GFP) per gonad arm in *com-1(t1626)* and *com-1(t1626) cku-80* mutant animals. Error bars represent SD, n = number of germlines analyzed. *The increase in apoptotic cells was statistically significant ($p<0.01$ by Student's t-test, two tailed).

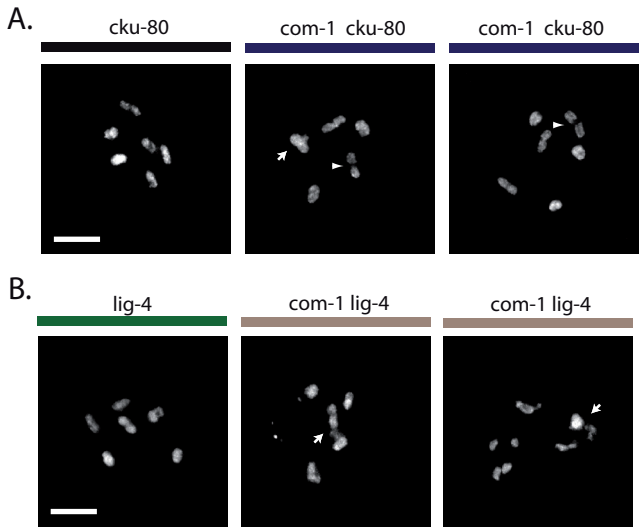

Figure S5. NHEJ deficient *com-1* mutants still exhibit chromosomal instability in the germline. (A) Examples of diakinesis nuclei showing chromosomal aberrations in *com-1(t1626) cku-80* mutant germlines. White arrowheads indicate unstable attachments between homologs; white arrows indicate odd-shaped DAPI bodies that may represent chromosomal fusions. Scale bar, 5 μm (B) Examples of diakinesis nuclei showing chromosomal aberrations in *com-1(t1489) lig-4* mutant germlines. White arrows indicate odd-shaped DAPI bodies that may represent chromosomal fusions. Scale bar, 5 μm.

Acknowledgments

The authors wish to thank Jane van Heteren for helpful comments on the manuscript and the Caenorhabditis Genetics Center, *C. elegans* Gene Knockout Consortium, and Dr. Shohei Mitani for providing worm strains.

Author Contributions

Conceived and designed the experiments: BBLGL. Performed the experiments: BBLGL NMJ. Analyzed the data: BBLGL NMJ MT. Contributed reagents/materials/analysis tools: MT. Wrote the paper: BBLGL NMJ MT.

References

1. McKinnon PJ, Caldecott KW (2007) DNA strand break repair and human genetic disease. Annu Rev Genomics Hum Genet 8: 37–55. doi: 10.1146/annurev.genom.7.080505.115648

2. Lieber MR (2010) The mechanism of double-strand DNA break repair by the nonhomologous DNA end-joining pathway. Annu Rev Biochem 79: 181–211. doi: 10.1146/annurev.biochem.052308.093131

3. Symington LS, Gautier J (2011) Double-strand break end resection and repair pathway choice. Annu Rev Genet 45: 247–271. doi: 10.1146/annurev-genet-110410-132435

4. Shahar OD, Ram EV, Shimshoni E, Hareli S, Meshorer E, et al. (2011) Live imaging of induced and controlled DNA double-strand break formation reveals extremely low repair by homologous recombination in human cells. Oncogene doi: 10.1038/onc.2011.516

5. Keeney S, Giroux CN, Kleckner N (1997) Meiosis-specific DNA double-strand breaks are catalyzed by Spo11, a member of a widely conserved protein family. Cell 88: 375–384. doi: 10.1016/s0092-8674(00)81876-0

6. Dernburg AF, McDonald K, Moulder G, Barstead R, Dresser M, et al. (1998) Meiotic recombination in C. elegans initiates by a conserved mechanism and is dispensable for homologous chromosome synapsis. Cell 94: 387–398. doi: 10.1016/s0092-8674(00)81481-6

7. Hunter N (2006) Meiotic recombination; Aguilera A, and Rothstein, R., eds., editor. Heidelberg: Springer-Verlag.

8. Martin JS, Winkelmann N, Petalcorin MI, McIlwraith MJ, Boulton SJ (2005) RAD-51-dependent and -independent roles of a Caenorhabditis elegans BRCA2-related protein during DNA double-strand break repair. Mol Cell Biol 25: 3127–3139. doi: 10.1128/mcb.25.8.3127-3139.2005

9. Smolikov S, Eizinger A, Hurlburt A, Rogers E, Villeneuve AM, et al. (2007) Synapsis-defective mutants reveal a correlation between chromosome conformation and the mode of double-strand break repair during Caenorhabditis elegans meiosis. Genetics 176: 2027–2033. doi: 10.1534/genetics.107.076968

10. Adamo A, Collis SJ, Adelman CA, Silva N, Horejsi Z, et al. (2010) Preventing nonhomologous end joining suppresses DNA repair defects of Fanconi anemia. Mol Cell 39: 25–35. doi: 10.1016/j.molcel.2010.06.026

11. Clejan I, Boerckel J, Ahmed S (2006) Developmental modulation of nonhomologous end joining in Caenorhabditis elegans. Genetics 173: 1301–1317. doi: 10.1534/genetics.106.058628

12. Yun MH, Hiom K (2009) CtIP-BRCA1 modulates the choice of DNA double-strand-break repair pathway throughout the cell cycle. Nature 459: 460–463. doi: 10.1038/nature07955

13. Chen PL, Liu F, Cai S, Lin X, Li A, et al. (2005) Inactivation of CtIP leads to early embryonic lethality mediated by G1 restraint and to tumorigenesis by haploid insufficiency. Mol Cell Biol 25: 3535–3542. doi: 10.1128/mcb.25.9.3535-3542.2005

14. Penkner A, Portik-Dobos Z, Tang L, Schnabel R, Novatchkova M, et al. (2007) A conserved function for a Caenorhabditis elegans Com1/Sae2/CtIP protein homolog in meiotic recombination. EMBO J 26: 5071–5082. doi: 10.1038/sj.emboj.7601916

15. Limbo O, Chahwan C, Yamada Y, de Bruin RA, Wittenberg C, et al. (2007) Ctp1 is a cell-cycle-regulated protein that functions with Mre11 complex to control double-strand break repair by homologous recombination. Mol Cell 28: 134–146. doi: 10.1016/j.molcel.2007.09.009

16. Sartori AA, Lukas C, Coates J, Mistrik M, Fu S, et al. (2007) Human CtIP promotes DNA end resection. Nature 450: 509–514. doi: 10.1038/nature06337

17. Keeney S, Kleckner N (1995) Covalent protein-DNA complexes at the 5′ strand termini of meiosis-specific double-strand breaks in yeast. Proc Natl Acad Sci U S A 92: 11274–11278. doi: 10.1073/pnas.92.24.11274

18. Hartsuiker E, Mizuno K, Molnar M, Kohli J, Ohta K, et al. (2009) Ctp1CtIP and Rad32Mre11 nuclease activity are required for Rec12Spo11 removal, but Rec12Spo11 removal is dispensable for other MRN-dependent meiotic functions. Mol Cell Biol 29: 1671–1681. doi: 10.1128/mcb.01182-08

19. Adamo A, Montemauri P, Silva N, Ward JD, Boulton SJ, et al. (2008) BRC-1 acts in the inter-sister pathway of meiotic double-strand break repair. EMBO Rep 9: 287–292. doi: 10.1038/sj.embor.7401167

20. Severson AF, Ling L, van Zuylen V, Meyer BJ (2009) The axial element protein HTP-3 promotes cohesin loading and meiotic axis assembly in C. elegans to implement the meiotic program of chromosome segregation. Genes Dev 23: 1763–1778. doi: 10.1101/gad.1808809

21. Bhalla N, Wynne DJ, Jantsch V, Dernburg AF (2008) ZHP-3 acts at crossovers to couple meiotic recombination with synaptonemal complex disassembly and bivalent formation in C. elegans. PLoS Genet 4: e1000235 doi:10.1371/journal.pgen.1000235.

22. Hillers KJ, Villeneuve AM (2003) Chromosome-wide control of meiotic crossing over in C. elegans. Curr Biol 13: 1641–1647. doi: 10.1016/j.cub.2003.08.026

23. Yokoo R, Zawadzki KA, Nabeshima K, Drake M, Arur S, et al. (2012) COSA-1 Reveals Robust Homeostasis and Separable Licensing and Reinforcement Steps Governing Meiotic Crossovers. Cell 149: 75–87. doi: 10.1016/j.cell.2012.01.052

24. Youds JL, Mets DG, McIlwraith MJ, Martin JS, Ward JD, et al. (2010) RTEL-1 enforces meiotic crossover interference and homeostasis. Science 327: 1254–1258. doi: 10.1126/science.1183112

25. Alpi A, Pasierbek P, Gartner A, Loidl J (2003) Genetic and cytological characterization of the recombination protein RAD-51 in Caenorhabditis elegans. Chromosoma 112: 6–16. doi: 10.1007/s00412-003-0237-5

26. Mets DG, Meyer BJ (2009) Condensins regulate meiotic DNA break distribution, thus crossover frequency, by controlling chromosome structure. Cell 139: 73–86. doi: 10.1016/j.cell.2009.07.035

27. Saito TT, Youds JL, Boulton SJ, Colaiacovo MP (2009) *Caenorhabditis elegans* HIM-18/SLX-4 interacts with SLX-1 and XPF-1 and maintains genomic integrity in the germline by processing recombination intermediates. PLoS Genet 5: e1000735 doi:10.1371/journal.pgen.1000735.

28. Mimitou EP, Symington LS (2010) Ku prevents Exo1 and Sgs1-dependent resection of DNA ends in the absence of a functional MRX complex or Sae2. EMBO J 29: 3358–3369. doi: 10.1038/emboj.2010.193

29. Szankasi P, Smith GR (1995) A role for exonuclease I from S. pombe in mutation avoidance and mismatch correction. Science 267: 1166–1169. doi: 10.1126/science.7855597

30. Zakharyevich K, Ma Y, Tang S, Hwang PY, Boiteux S, et al. (2010) Temporally and biochemically distinct activities of Exo1 during meiosis: double-strand break resection and resolution of double Holliday junctions. Mol Cell 40: 1001–1015. doi: 10.1016/j.molcel.2010.11.032

31. Hayashi M, Chin GM, Villeneuve AM (2007) *C. elegans* germ cells switch between distinct modes of double-strand break repair during meiotic prophase progression. PLoS Genet 3: e191 doi:10.1371/journal.pgen.0030191.

32. Colaiacovo MP, MacQueen AJ, Martinez-Perez E, McDonald K, Adamo A, et al. (2003) Synaptonemal complex assembly in C. elegans is dispensable for loading strand-exchange proteins but critical for proper completion of recombination. Dev Cell 5: 463–474. doi: 10.1016/s1534-5807(03)00232-6

33. Martinez-Perez E, Villeneuve AM (2005) HTP-1-dependent constraints coordinate homolog pairing and synapsis and promote chiasma formation during C. elegans meiosis. Genes Dev 19: 2727–2743. doi: 10.1101/gad.1338505

34. Bickel JS, Chen L, Hayward J, Yeap SL, Alkers AE, et al. (2010) Structural maintenance of chromosomes (SMC) proteins promote homolog-independent recombination repair in meiosis crucial for germ cell genomic stability. PLoS Genet 6: e1001028 doi:10.1371/journal.pgen.1001028.

35. Pasierbek P, Jantsch M, Melcher M, Schleiffer A, Schweizer D, et al. (2001) A Caenorhabditis elegans cohesion protein with functions in meiotic chromosome pairing and disjunction. Genes Dev 15: 1349–1360. doi: 10.1101/gad.192701

36. Zou L, Elledge SJ (2003) Sensing DNA damage through ATRIP recognition of RPA-ssDNA complexes. Science 300: 1542–1548. doi: 10.1126/science.1083430

37. Bailly A, Gartner A (2013) Germ cell apoptosis and DNA damage responses. Adv Exp Med Biol 757: 249–276. doi: 10.1007/978-1-4614-4015-4_9

38. Jaramillo-Lambert A, Engebrecht J (2010) A single unpaired and transcriptionally silenced X chromosome locally precludes checkpoint signaling in the Caenorhabditis elegans germ line. Genetics 184: 613–628. doi: 10.1534/genetics.109.110338

39. Manfrini N, Guerini I, Citterio A, Lucchini G, Longhese MP (2010) Processing of meiotic DNA double strand breaks requires cyclin-dependent kinase and multiple nucleases. J Biol Chem 285: 11628–11637. doi: 10.1074/jbc.m110.104083

40. Moreau S, Ferguson JR, Symington LS (1999) The nuclease activity of Mre11 is required for meiosis but not for mating type switching, end joining, or telomere maintenance. Mol Cell Biol 19: 556–566.

41. Chin GM, Villeneuve AM (2001) C. elegans mre-11 is required for meiotic recombination and DNA repair but is dispensable for the meiotic G(2) DNA damage checkpoint. Genes Dev 15: 522–534. doi: 10.1101/gad.864101

42. Baudrimont A, Penkner A, Woglar A, Mamnun YM, Hulek M, et al. (2011) A new thermosensitive smc-3 allele reveals involvement of cohesin in homologous recombination in C. elegans. PLoS ONE 6: e24799 doi:10.1371/journal.pone.0024799.

43. Garcia V, Phelps SE, Gray S, Neale MJ (2011) Bidirectional resection of DNA double-strand breaks by Mre11 and Exo1. Nature 479: 241–244. doi: 10.1038/nature10515

44. Sun J, Lee KJ, Davis AJ, Chen DJ (2011) Human Ku70/80 blocks Exonuclease1-mediated DNA resection in the presence of human Mre11 or Mre11/Rad50 complex. J Biol Chem doi: 10.1074/jbc.m111.306167

45. Blier PR, Griffith AJ, Craft J, Hardin JA (1993) Binding of Ku protein to DNA. Measurement of affinity for ends and demonstration of binding to nicks. J Biol Chem 268: 7594–7601.

46. Falzon M, Fewell JW, Kuff EL (1993) EBP-80, a transcription factor closely resembling the human autoantigen Ku, recognizes single- to double-strand transitions in DNA. J Biol Chem 268: 10546–10552.

47. Zhuang J, Jiang G, Willers H, Xia F (2009) Exonuclease function of human Mre11 promotes deletional nonhomologous end joining. J Biol Chem 284: 30565–30573. doi: 10.1074/jbc.m109.059444

48. Lengsfeld BM, Rattray AJ, Bhaskara V, Ghirlando R, Paull TT (2007) Sae2 is an endonuclease that processes hairpin DNA cooperatively with the Mre11/Rad50/Xrs2 complex. Mol Cell 28: 638–651. doi: 10.1016/j.molcel.2007.11.001

49. Shim EY, Chung WH, Nicolette ML, Zhang Y, Davis M, et al. (2010) Saccharomyces cerevisiae Mre11/Rad50/Xrs2 and Ku proteins regulate association of Exo1 and Dna2 with DNA breaks. EMBO J 29: 3370–3380. doi: 10.1038/emboj.2010.219

50. Kim HS, Vijayakumar S, Reger M, Harrison JC, Haber JE, et al. (2008) Functional interactions between Sae2 and the Mre11 complex. Genetics 178: 711–723. doi: 10.1534/genetics.107.081331

51. Rosu S, Libuda DE, Villeneuve AM (2011) Robust crossover assurance and regulated interhomolog access maintain meiotic crossover number. Science 334: 1286–1289. doi: 10.1126/science.1212424

52. Robert VJ, Davis MW, Jorgensen EM, Bessereau JL (2008) Gene conversion and end-joining-repair double-strand breaks in the Caenorhabditis elegans germline. Genetics 180: 673–679. doi: 10.1534/genetics.108.089698

53. Goedecke W, Eijpe M, Offenberg HH, van Aalderen M, Heyting C (1999) Mre11 and Ku70 interact in somatic cells, but are differentially expressed in early meiosis. Nat Genet 23: 194–198. doi: 10.1038/13821

54. Ji J, Tang D, Wang K, Wang M, Che L, et al. (2012) The role of OsCOM1 in homologous chromosome synapsis and recombination in rice meiosis. Plant J doi: 10.1111/j.1365-313x.2012.05025.x

55. Kirkpatrick DT, Ferguson JR, Petes TD, Symington LS (2000) Decreased meiotic intergenic recombination and increased meiosis I nondisjunction in exo1 mutants of Saccharomyces cerevisiae. Genetics 156: 1549–1557.

56. Peterson SE, Li Y, Chait BT, Gottesman ME, Baer R, et al. (2011) Cdk1 uncouples CtIP-dependent resection and Rad51 filament formation during M-phase double-strand break repair. J Cell Biol 194: 705–720. doi: 10.1083/jcb.201103103

57. Qvist P, Huertas P, Jimeno S, Nyegaard M, Hassan MJ, et al. (2011) CtIP Mutations Cause Seckel and Jawad Syndromes. PLoS Genet 7: e1002310 doi:10.1371/journal.pgen.1002310.

58. Bunting SF, Callen E, Wong N, Chen HT, Polato F, et al. (2010) 53BP1 inhibits homologous recombination in Brca1-deficient cells by blocking resection of DNA breaks. Cell 141: 243–254. doi: 10.1016/j.cell.2010.03.012

59. Kloosterman WP, Guryev V, van Roosmalen M, Duran KJ, de Bruijn E, et al. (2011) Chromothripsis as a mechanism driving complex de novo structural rearrangements in the germline. Hum Mol Genet 20: 1916–1924. doi: 10.1093/hmg/ddr073

60. Chiang C, Jacobsen JC, Ernst C, Hanscom C, Heilbut A, et al. (2012) Complex reorganization and predominant non-homologous repair following chromosomal breakage in karyotypically balanced germline rearrangements and transgenic integration. Nat Genet 44: 390–397. doi: 10.1038/ng.2202

61. Brenner S (1974) The genetics of Caenorhabditis elegans. Genetics 77: 71–94.

62. Lee MH, Hollis SE, Yoo BH, Nykamp K (2011) Caenorhabditis elegans DNA-2 helicase/endonuclease plays a vital role in maintaining genome stability, morphogenesis, and life span. Biochem Biophys Res Commun 407: 495–500. doi: 10.1016/j.bbrc.2011.03.045

3

A Role for the Malignant Brain Tumour (MBT) Domain Protein LIN-61 in DNA Double-Strand Break Repair by Homologous Recombination

Johnson NM, Lemmens BB, Tijsterman M.

Adapted from Johnson *et al.* PLoS Genet. 2013;9(3)

Abstract

Malignant brain tumour (MBT) domain proteins are transcriptional repressors that function within Polycomb complexes. Some MBT genes are tumour suppressors, but how they prevent tumourigenesis is unknown. The *Caenorhabditis elegans* MBT protein LIN-61 is a member of the synMuvB chromatin-remodelling proteins that control vulval development. Here we report a new role for LIN-61: it protects the genome by promoting homologous recombination (HR) for the repair of DNA double-strand breaks (DSBs). *lin-61* mutants manifest numerous problems associated with defective HR in germ and somatic cells but remain proficient in meiotic recombination. They are hypersensitive to ionizing radiation and interstrand crosslinks but not UV light. Using a novel reporter system that monitors repair of a defined DSB in *C. elegans* somatic cells, we show that LIN-61 contributes to HR. The involvement of this MBT protein in HR raises the possibility that MBT–deficient tumours may also have defective DSB repair.

Author Summary

The genome is continually under threat from exogenous sources of DNA damage, as well as from sources that originate within the cell. DNA double-strand breaks (DSBs) are arguably the most problematic type of damage as they can cause dangerous chromosome rearrangements, which can lead to cancer, as well as mutation at the break site and/or cell death. A complex network of molecular pathways, collectively referred to as the DNA damage response (DDR), have evolved to protect the cell from these threats. We have discovered a new DDR factor, LIN-61, that promotes the repair of DSBs. This is a novel and unexpected role for LIN-61, which was previously known to act as a regulator of gene transcription during development.

Introduction

DNA is maintained in the cell as chromatin: double-stranded DNA wrapped around core histone octomers to form nucleosome subunits. Chromatin folds into higher order structures depending on how tightly DNA is wrapped around the histones and how closely the nucleosomes interact [1]. Condensed chromatin acts as a physical barrier that restricts DNA access and therefore must be remodelled to enable various cellular processes such as gene transcription, DNA replication and DNA repair [2]. This is principally achieved by post-translational modification to the N-terminal tails of histones. One example of this is the methylation of lysine residues, which alters the degree of chromatin compaction and provides a binding site for the recruitment of non-histone proteins such as malignant brain tumour (MBT) domain proteins [2]. Once bound to histones, MBT domain proteins condense chromatin and repress transcription of target genes [3]. The MBT domain is a highly conserved motif of approximately 100 amino acids in length found throughout metazoans from *C. elegans* to humans [4].

Some MBT domain proteins act together with Polycomb group (PcG) repressor complexes that are best known for establishing and maintaining gene expression patterns during development [4]. The *C. elegans* MBT protein LIN-61 is also implicated in transcriptional regulation. It is a member of the synthetic multivulva (synMuv) class B group of proteins that act redundantly with synMuvA proteins to repress transcription of *lin-3* EGF and *lin-60* Ras [5]–[7]. Separate to its role within the synMuvB pathway, we found *lin-61* is also involved in maintaining genome stability. Worms depleted of *lin-61* have elevated rates of germline and somatic mutation, including small DNA insertions and deletions, but how LIN-61 maintains genome fidelity was unknown [8]. Intriguingly, other MBT proteins have been shown to act as tumour suppressors: *lethal(3)malignant brain tumour* [*l(3)mbt*)] mutants of *Drosophila* develop malignant transformations of the adult optic neuroblast and ganglion mother cells of the larval brain [9]; furthermore, the human MBT domain genes *L3MBTL2*, *L3MBTL3* and *SCML2* are mutated in rare cases of medulloblastoma [10]. Also, depletion of L3MBTL1 (another

LIN-61-related protein) causes genome instability [11]. Therefore it appears MBT proteins may have a general role in genome stability. It is not known how these proteins prevent tumourigenesis or protect the genome, but their ability to repress transcription likely plays a central role considering that the *l(3)mbt* malignancies of *Drosophila* ectopically express germline genes, the expression of which is required for tumour growth [12]. Preventing the expression of germline genes in somatic tissues may be a conserved function of MBT proteins because *lin-61* mutants also express germline genes in the soma in a temperature-dependent manner [13].

As well as regulating transcription, an increasing number of chromatin-remodelling proteins (including PcG proteins) have been found to act within the DNA damage response (DDR). These proteins accumulate at sites of DNA damage where they locally modify chromatin to allow the recruitment of DNA repair proteins [14]. In the present study we investigate the cause of genomic instability in *lin-61* mutants. We show that LIN-61 acts within the DDR where it is needed for efficient double-strand break (DSB) repair in both the germline and somatic cells of *C. elegans*. LIN-61 promotes DSB repair by homologous recombination (HR), but not the competing pathways, non-homologous end joining (NHEJ) or single-strand annealing (SSA). Despite the requirement for LIN-61 in HR, it is dispensable for meiotic recombination and the DNA damage checkpoints (cell cycle arrest and apoptosis) in the germline. We also use a novel GFP-based HR reporter assay that confirms LIN-61 is needed for HR. This reporter monitors the repair of a single defined DSB and is a new tool for measuring HR in *C. elegans* somatic cells. This is the first report demonstrating that an MBT protein promotes DNA repair and provides an explanation for why MBT-deficient cells have genomic instability.

Results

Genomic instability in *lin-61* mutants

To investigate how LIN-61 contributes to genomic stability, we obtained three independently generated null alleles of *lin-61* (*n3809*, *pk2225* and *tm2649*; Figure 1A and Text S1). The fourth MBT domain [essential for binding H3K9me2/3; [15]] is truncated or deleted in each of the mutant LIN-61 proteins. Moreover, *lin-61* mRNA is reduced approximately four-fold in *n3809* and *pk2225*, likely due to nonsense-mediated decay (Figure 1B). Each of the three mutants produced small broods (17–24% fewer progeny than wild-types; Figure 1C). This can be symptomatic of genomic instability as DNA repair mutants such as *brc-1*, *rfs-1*, *blm-1* and *smc-5/-6* also have small broods [16]–[19]. In accordance with their reduced fecundity, *lin-61* mutants had considerably smaller germlines than wild-types and contained fewer nuclei in the mitotic compartment (Figure 1D–1E). What is more, there were signs of DNA damage in these cells: their mitotic nuclei contained considerably more spontaneous RAD-51 foci than those of wild-types (Figure 1F). RAD-51 is the DNA strand exchange protein, which accumulates at DSBs and blocked replication forks, and therefore is a marker for DNA damage [20]–[22].

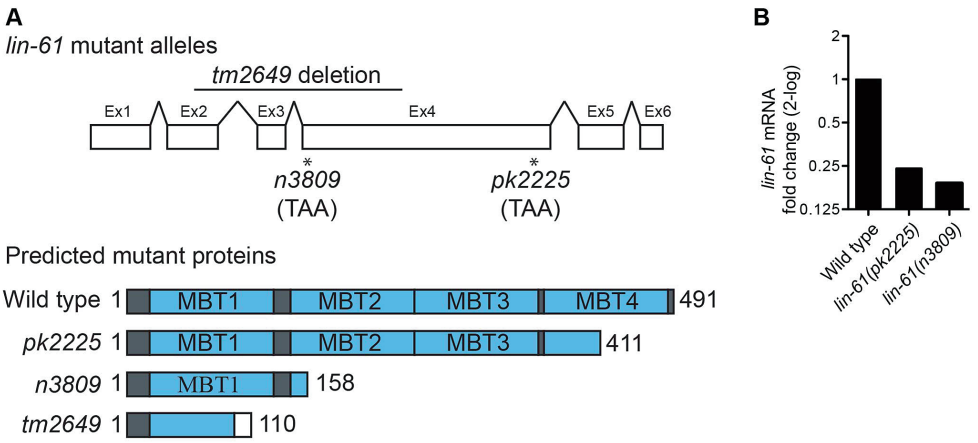

C

Genotype	Mean brood size (+/- std. dev.)	Percentage unviable embryos (total no. embryos scored)	Percentage male (total no. adults scored)
wild type	305 (+/- 45)	0.1 (4722)	0.02 (5415)
lin-61(pk2225)	233 (+/- 42)	1.4 (3413)	0.73 (4085)
lin-61(n3809)	254 (+/- 48)	n.d.	0.31 (3258)
lin-61(tm2649)	236 (+/- 36)	n.d.	0.18 (2726)

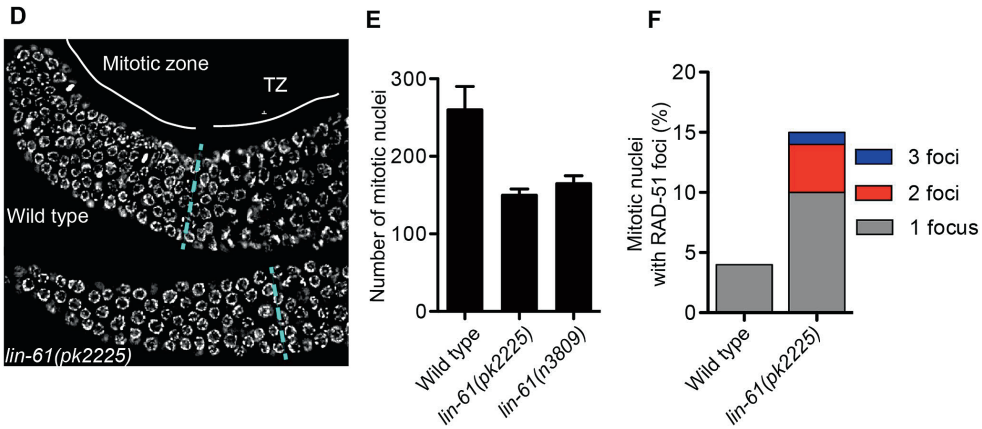

Figure 1. *lin-61* mutants display signs of genome instability and replication stress. (A) *lin-61* gene model (above) showing the location of *n3809*, *pk2225* and *tm2649* and predicted protein translations (below). Ex, exon. (B) Quantification of *lin-61* mRNA by qRT-PCR. Data is normalised to wild-type. (C) Table listing brood sizes, including proportion of male progeny and unhatched embryos. n.d., not determined. (D) Dissected and DAPI-stained germlines from young adults. A single layer of nuclei is shown for clarity. The blue dashed line separates the mitotic zone from the transition zone (TZ). (E) Histogram depicting the average number of nuclei per mitotic zone. Error bars represent s.d. (F) Stacked histogram showing the percentage of mitotic nuclei containing RAD-51 foci.

LIN-61 is required for resistance to ionizing radiation but dispensable for meiotic recombination

Since *lin-61* mutant germ cells displayed genomic instability and signs of persistent spontaneous DSBs, we wondered whether *lin-61* mutants were sensitive to ectopically induced DSBs. We found that the germ cells of *lin-61* mutants were hypersensitive to ionizing radiation (IR), which is a potent inducer of DSBs (Figure 2A). Also primordial germ cells that are arrested in the G2 stage of the cell cycle in L1 stage larvae, are hypersensitive to IR in *lin-61* mutants animals (Figure S1).

The LIN-61 paralog, called MBTR-1 (Malignant Brain Tumour Repeat containing protein 1), shares a high degree of sequence conservation with LIN-61 and both proteins are comprised almost entirely of four MBT domains (Figure S2A). We wondered whether MBTR-1 too might be needed for resistance to IR-induced DSBs. To test this, we challenged *mbtr-1(n4775)* mutants with IR but found that they were not more sensitive than wild-type controls (Figure S2B). Therefore LIN-61, but not the closely related MBT domain protein MBTR-1, is required for resistance to IR-induced DSBs in germ cells.

The IR-hypersensitivity of *lin-61* mutant germlines suggested that LIN-61 might be required for DSB repair during gametogenesis. We therefore investigated if LIN-61 also had a role in the repair of programmed DSBs that arise during meiosis. Meiotic DSB repair is required for the proper segregation of chromosomes to gametes and involves the repair of programmed DSBs introduced by the topoisomerase-like protein SPO-11 [23]. These DSBs are repaired by HR using the homologous chromosome as the repair template (interhomolog HR). The progression of DSB repair can be monitored in meiosis by following RAD-51 foci, which first appear at prophase, peak at early/mid-pachytene, and are resolved by late pachytene once DSB repair is completed [24]. The distribution of RAD-51 foci in *lin-61* meiotic cells was indistinguishable from those of wild-types (Figure S3). This indicated that repair of SPO-11-introduced DSBs was unperturbed in *lin-61* mutants. Interhomolog HR enables crossover (CO) formation, which establishes the physical connection (chiasmata) that holds homologs together until their separation at the first meiotic cell division. Diakinesis stage oocytes of *lin-61* mutants contained the correct complement of six bivalents (paired homologs), which indicated that CO formation was competent in these mutants. Furthermore, *lin-61* mutants produced mostly viable progeny and did not display an increased incidence of males (Him) phenotype (Figure 1C). Failed meiotic recombination causes nondisjunction and aneuploidy due to the uncontrolled segregation of chromosomes to gametes, which manifests as embryonic lethality and the Him phenotype [25]. We conclude that LIN-61 is necessary for the repair of IR-induced DSBs but dispensable for CO formation and meiotic recombination. This phenotype is paralleled by the HR mutant *brc-1* and the cohesin-like mutants *smc-5/-6*. These mutants are IR hypersensitive due to defective DSB repair by HR that uses the sister chromatid (intersister HR) [19], [26], [27]. Our observation that *lin-61* mutants were hypersensitivity to IR suggested that LIN-61 might also contribute to intersister HR.

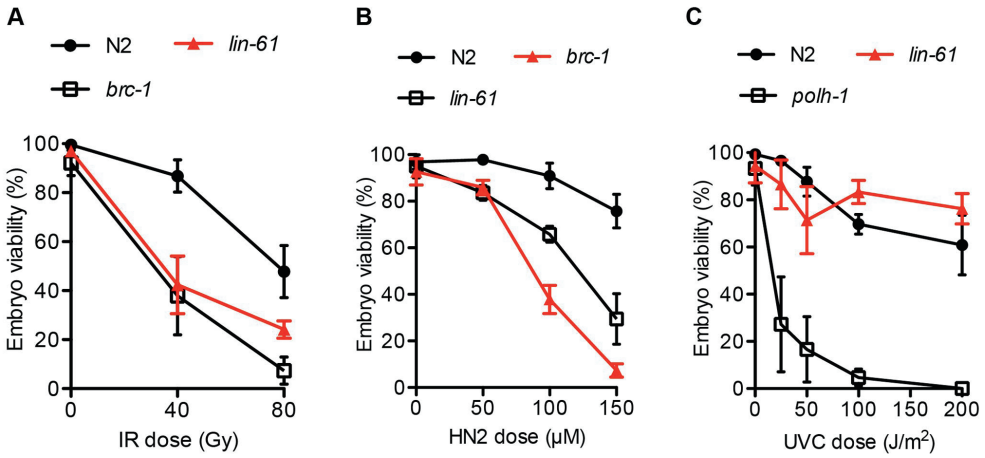

Figure 2. *lin-61* mutants are sensitive to IR and HN2, but not UV-C.
L4 stage animals were challenged with (A) IR, ionizing radiation; and young adults were treated with (B) HN2, nitrogen mustard or (C) UVC, ultraviolet light subtype C. The average percentage of viable eggs is plotted. Error bars represent s.d.

lin-61 mutants are hypersensitive to interstrand crosslinks but not UV lesions

In addition to repairing IR-induced DSBs, intersister HR is needed for repair of interstrand crosslinks (ICLs). ICLs are particularly cytotoxic lesions that block the replication fork by covalently linking opposing strands of double-stranded DNA [28]. During ICL repair, the crosslinked lesion is excised, thus producing a DSB substrate for intersister HR [29]. HR-deficient mutants like *brc-1*, or the *rad-51* paralog *rfs-1* are therefore hypersensitive to ICLs [21]. Consistent with LIN-61 having a possible role in intersister HR, we found that *lin-61* mutants were hypersensitive to nitrogen mustard (HN2), which is a potent inducer of ICLs (Figure 2B).

Other DNA lesions that block replication forks (such as bulky photoadducts made by UV light) do not cause a DSB and do not require HR for repair. Instead, translesion synthesis (TLS) DNA polymerases such as POLH-1 bypass these lesions to allow replication to proceed [30]. *polh-1* mutants are therefore hypersensitive to UV-C [31] but HR-deficient mutants such as *rfs-1* are not [21]. We found that *lin-61* mutants were not hypersensitive to UV-C (Figure 2C). The sensitivity of *lin-61* mutants to IR and HN2, but not UV-C, suggested that LIN-61 may promote DNA repair through HR, but is not required for the repair of other replication-blocking lesions such as photoadducts.

LIN-61 has a role in HR, but not NHEJ, in somatic cells

LIN-61 is broadly expressed in somatic and germ cells throughout development [6]. To determine if LIN-61 contributes to DSB repair in somatic cells, as it does in germ cells, we used established assays that test the proficiency of HR, as well as the other major DSB repair

route, NHEJ [32]. Somatic cells use either HR or NHEJ depending on developmental context and phase of the cell cycle. HR is active during S and G2 phases (when sister chromatids are closely aligned), whereas NHEJ can be performed throughout the duration of the cell cycle, but is especially important during G1 when HR is unavailable [33]. Early stage embryonic cells (<6 hours post fertilisation) rapidly transition between S phase and M phase, without G1 and G2 gap phases [34], [35] and are particularly reliant on HR for DSB repair [32] (Figure 3A). Accordingly, early stage embryos of HR-deficient mutants are very sensitive to IR, while those of NHEJ-deficient mutants are not [32]. To test whether *lin-61* promotes HR in somatic cells, we scored the viability of γ-irradiated early stage *lin-61* embryos. These embryos were indeed hypersensitive to IR, which was indicative of an HR defect (Figure 3B). Their degree of IR sensitivity was similar to that of HR-deficient *brc-1* embryos. While HR is the dominant DSB repair route in early embryos, NHEJ is the major repair pathway in late stage embryos and arrested L1 larvae because most of their cells are arrested in G1 [32] (Figure 3C). NHEJ-deficient L1 larvae have delayed or arrested growth in response to IR [32]. We found that wild type, *lin-61(n3809)* and *lin-61(pk2225)* L1 larvae did not display substantial growth delay following IR, whereas most NHEJ-deficient *cku-80* mutants failed to develop to the L4 stage 48 hours after irradiation (Figure 3D). L1 larvae of the HR-deficient mutant, *brc-1*, were also not hypersensitive to IR (Figure S4). Taken together, these results suggest that LIN-61 has a role in repairing DSBs by HR, but not NHEJ, in somatic cells.

LIN-61 is not required for intersister HR in meiotic nuclei

Although *lin-61* mutants phenocopy *brc-1* mutants in many aspects of genome stability, they also differ in some important aspects. For example, *brc-1* mutants display the Him phenotype, while *lin-61* mutants do not. Him is an indication of problems with chromosome segregation at meiosis. Like *brc-1* mutants, *lin-61* mutants are able to successfully complete meiosis, indicating that their interhomolog HR is proficient. However, by genetically disrupting the synaptonemal complex (SC), and thereby preventing interhomolog HR, it has been possible to demonstrate that BRC-1 contributes to meiotic intersister HR [27]. Adamo and colleagues observed that chromosomal fragments appear in the diakinesis stage nuclei of *brc-1* mutants that were depleted of key SC components [27]. Using this approach we tested whether LIN-61 also has a role in meiotic intersister HR. In contrast to *brc-1* mutants, neither the oocytes of *lin-61(pk2225)* or *lin-61(n3809)* contained chromosomal fragmentation after depletion of the core SC component, SYP-2 (Figure 4A). These data, together with those showing normal RAD-51 kinetics and successful chiasmata formation in *lin-61* mutants (Figure S3 and Figure 4A), indicate that LIN-61 is dispensable for HR in meiotic cells.

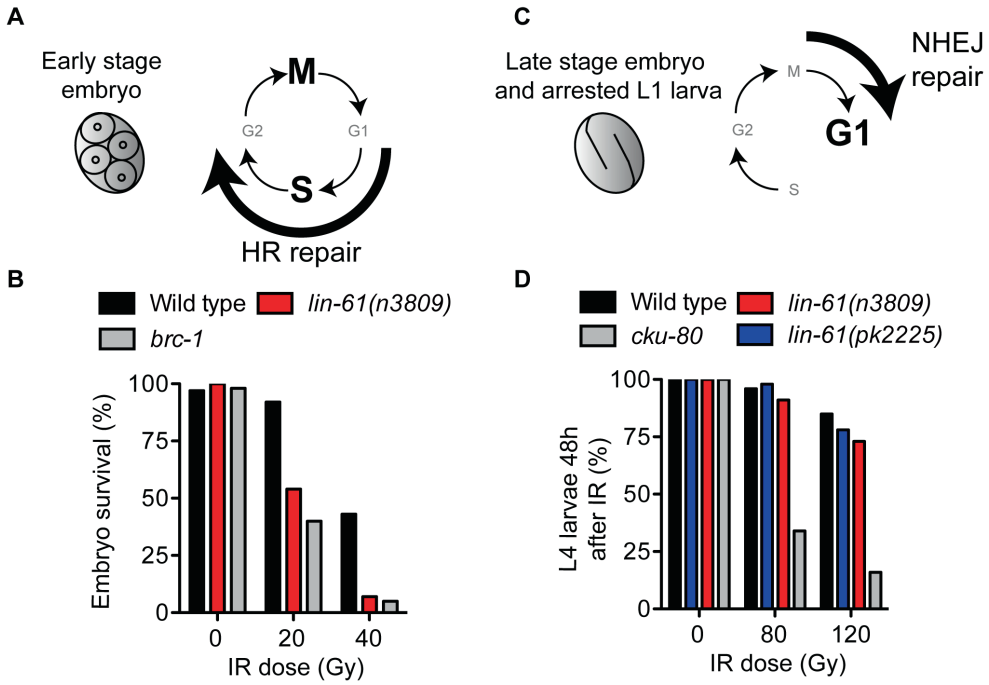

Figure 3. LIN-61 is needed for HR, but not NHEJ, in somatic cells.
(A) Early stage embryos rapidly cycle between mitosis (M) and DNA synthesis (S), without gap phases (G1 and G2). HR is the prominent repair pathway in these cells. (B) Survival rates of IR-treated early stage embryos. (C) Most cells of late stage embryos and arrested L1 larvae are held in G1 phase. NHEJ is the principal DSB repair pathway in these cells. (D) The proportion of animals that developed to the L4 stage 48 hours after being γ-irradiated as L1 larvae.

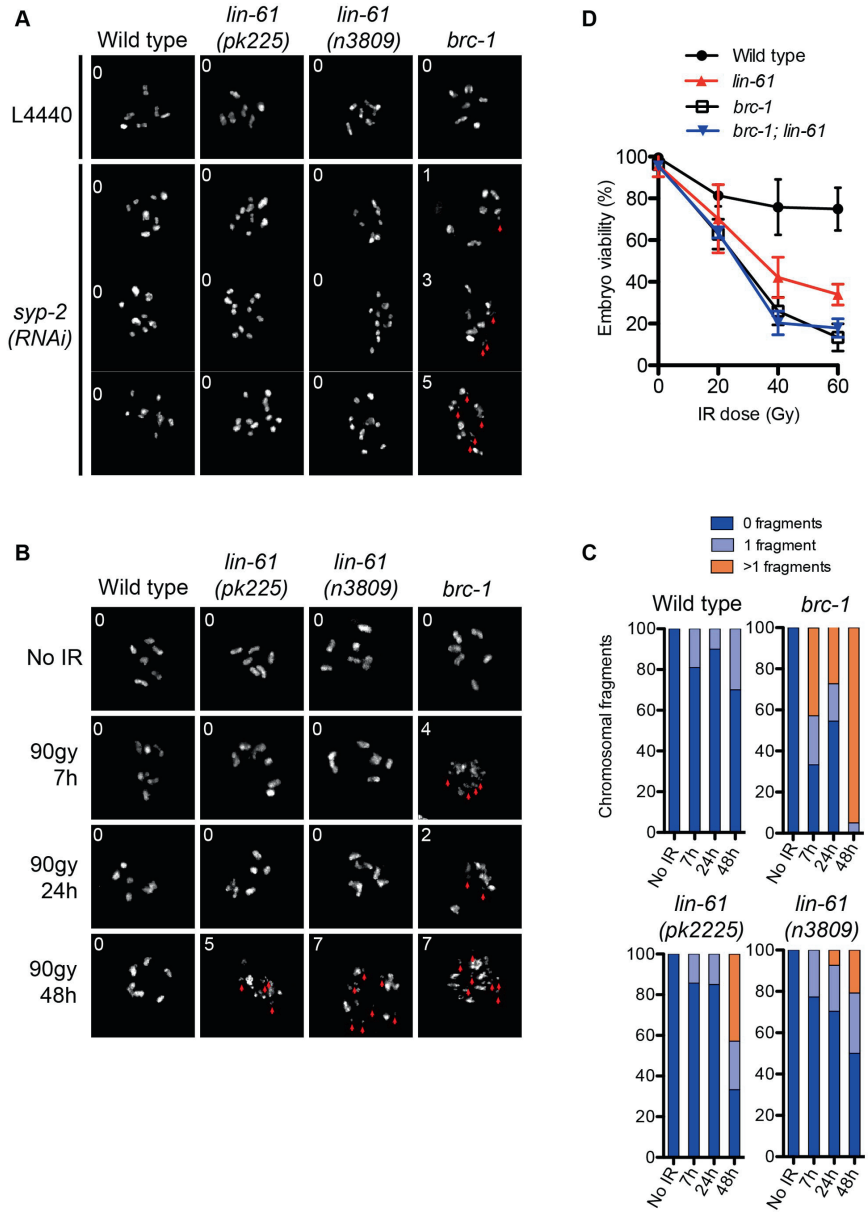

Figure 4. LIN-61 contributes to HR in mitotic cells, but is dispensable for meiotic HR.
(A) DAPI-stained DNA bodies in diakinesis stage oocytes of animals mock treated (L4440) or depleted of SYP-2 by RNAi. (B) Time course of chromosomal fragmentation in response to 90 Gy dose of IR. In (A) and (B), the red arrowheads indicate chromosomal fragments and the inset number corresponds to the number of small fragments visible in the image. (C)
Quantification of the chromosomal fragmentation. (D) Epistatic analysis of *brc-1* and *lin-61(pk2225)* IR sensitivity. L4 larvae were irradiated with the indicated dose. The percentage of viable embryos is plotted. Error bars represent s.d.

LIN-61 contributes to DSB repair in mitotic germ cells but not meiotic germ cells

lin-61 mutants are proficient in the repair, at meiosis, of SPO-11-introduced DSBs (using both intersister and interhomolog repair) but are hypersensitive to IR. To confirm that LIN-61 is required for DSB repair specifically in mitotic germ cells we used an assay that directly tests whether DSBs are adequately repaired in irradiated germ cells. Completion of DSB repair can be determined in germ cells by observing chromosomes at diakinesis because chromosome fragments are present if DSBs are unrepaired [36]. In the absence of exogenous damage, the diakinesis stage oocytes of *lin-61* mutants contained six bivalents and were not fragmented (Figure 4B). This demonstrated that DSBs induced by SPO-11 were efficiently repaired in *lin-61* mutants, as discussed earlier. Strikingly however, both *lin-61* mutants and the HR-deficient mutant *brc*-1 had severely fragmented chromosomes 48 hours after γ-irradiation (Figure 4B–4C). We anticipated that these nuclei could have been located within the mitotic zone at the time of irradiation, having subsequently migrated to the diakinesis stage 48 hours later. Failure to repair the introduced DSBs could therefore be due to defective HR whilst in the mitotic zone, or later whilst in the meiotic zone, or both. To distinguish between these possibilities we analysed earlier time points following irradiation (7 h and 24 h). For these time points, the nuclei being analysed were in meiosis when DSBs were introduced. We found that *brc-1* mutants had fragmented chromosomes at these earlier time points (7 h and 24 h) (Figure 4B–4C), which is consistent with BRC-1 acting in meiotic DSB repair [27]. In contrast, *lin-61* mutants, like wild-types, rarely had fragmented chromosomes at early time points following irradiation (Figure 4B–4C). Thus while BRC-1 contributes to DSB repair in both mitotic and meiotic cells, LIN-61 seems to promote DSB repair only in mitotic cells. In accordance with that notion, we found that *brc-1* mutants were more sensitive to IR than *lin-61* mutants (Figure 4D). Moreover, *lin-61; brc-1* double mutants were no more sensitive to IR than *brc-1* single mutants suggesting that *lin*-61 acts within the *brc-1* genetic pathway (Figure 4D).

LIN-61 is dispensable for RAD-51 focus formation

Having established that LIN-61 promotes DSB repair via HR, we looked to address which step of HR fails in *lin-61* mutants. The first stages of HR involve the nucleolytic processing at the DSB to expose single stranded 3′ overhangs (DNA end resection) and subsequent coating of these overhangs with RAD-51. RAD-51 foci rapidly formed in the γ-irradiated mitotic germ cells of both wild-types and *lin-61* mutants (Figure 5A). Foci were detected at a very early time point after γ-irradiation (10 minutes), which showed that DNA end resection was unperturbed in these cells (Figure 5A). The loading of RAD-51 at SPO-11-induced DSBs was also normal in *lin-61* meiotic cells, as discussed earlier (Figure S3). Together this showed that DNA end resection at IR-induced and SPO-11-induced DSBs, as well as the loading of RAD-51 on resected DNA, was normal in *lin-61* mutants. The number of RAD-51 foci that formed in γ-irradiated germ cells was similar between wild-types and *lin-61* mutants (4–5 foci per

nucleus) (Figure 5B). Since the DNA in wild-type and *lin-61* nuclei were equally susceptible to IR, the hypersensitivity of these mutants was not due to an elevated damage load.

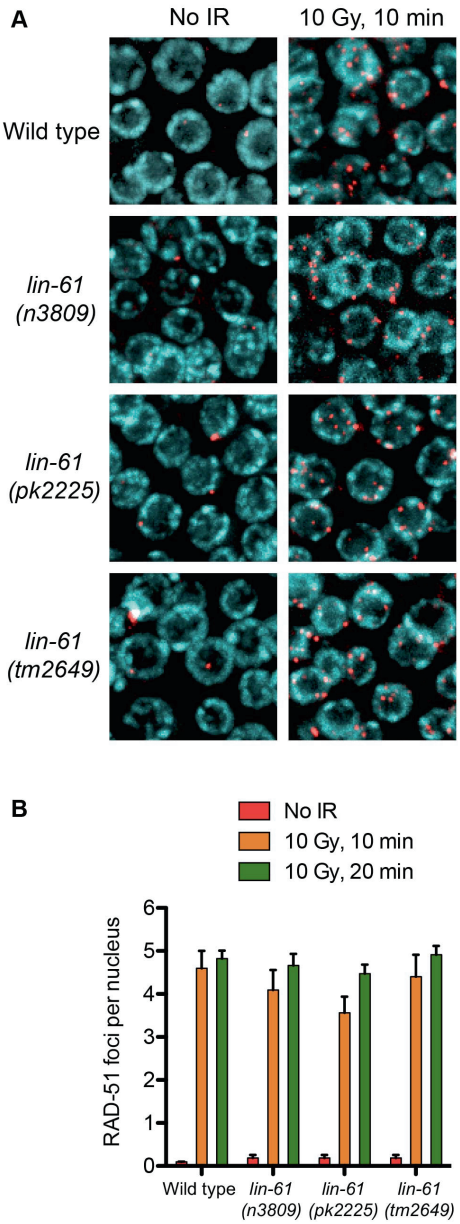

Figure 5. RAD-51 is loaded efficiently in irradiated *lin*-61 mutants.
(A) RAD-51 foci (red) in mitotic nuclei (DNA is blue) of wild-type and *lin-61* mutants 10 minutes after 10 Gy IR, or mock treatment. (B) Quantification of RAD-51 foci in mitotic nuclei. Error bars are S.E.M.

A novel GFP-based HR reporter system confirms that LIN-61 is required for HR in somatic cells

While IR is a potent source of DSBs, it also causes oxidative damage to proteins and cell membranes [37]. To confirm that the hypersensitivity displayed by *lin-61* mutants was due to defective DSB repair (and not other types of damage), we developed an assay that specifically measures HR-mediated repair of a defined DSB. This assay was based on the DR-GFP reporter system, which has been used extensively to measure HR proficiency in cultured human cells [38]. Such an assay was previously unavailable to the *C. elegans* researcher. The new *C. elegans* reporter consisted of a *gfp* gene in which part of the open reading frame had been deleted and replaced by an I-SceI endonuclease recognition site, which rendered the GFP non-functional, and provided the defined location where the DSB could be introduced (Figure 6A). A fragment of *gfp* containing the sequences disrupted by the I-SceI site (but by itself non-functional) was located downstream of the reporter and served as a template for synthesis-dependent strand annealing (SDSA) (Figure 6A). SDSA is a sub-pathway of HR that results in gene conversion rather than a CO and is the most common HR pathway used to repair two-sided DSBs [39]. The reporter was designed such that repair of the DSB by SDSA (but not a CO pathway) would be able to restore expression to the corrupted *gfp* gene. Non-HR pathways such as NHEJ or SSA are unable to produce functional GFP (Figure 6B).

We created a transgenic strain that carried both the HR reporter and heat-shock inducible I-SceI endonuclease. I-SceI was fused to mCherry so that its expression could be easily monitored by epifluorescence. Since it is thought HR does not occur in postmitotic cells (*i.e.* G1/G0 stage cells), we chose to express the reporter in intestinal cells using the *elt-2* promoter as their nuclei undergo endoreplication (S phase without mitosis) at several points during post-embryonic development [40]. We first confirmed that induction of mCherry::I-SceI resulted in GFP expression. 60–80% of wild-type worms expressed GFP in intestinal nuclei 24 hours after mCherry::I-SceI expression. Importantly, reporter activation was dependent upon DSB induction because non-heat shocked worms did not express GFP (data not shown). Also, GFP expression was dependent upon the donor *gfp* sequences since a disabled version of the HR reporter, which lacked these sequences, was not able to express GFP (Figure S5). To confirm that GFP expression depended on HR, we tested the effect *brc-1* mutation had on the reporter. BRC-1 promotes intersister HR in meiotic cells [27], and likely in somatic cells as well [41]. Indeed, *brc-1* mutants had significantly reduced frequency of HR reporter activation (Figure 6C–6D). This confirmed that the assay provided a measure of HR proficiency. We also used an *rtel-1* mutation to test whether reporter activation was dependent on the SDSA pathway. RTEL-1 is thought to influence HR pathway choice by removing the invaded DNA strand from its homologous template, which has the effect of promoting SDSA at the expense of CO outcomes [42]. The role of *rtel-1* in somatic cells was previously untested but we found that *rtel-1* mutants also had significantly reduced rates of HR reporter activation (Figure

6D). Therefore RTEL-1 likely promotes SDSA in somatic cells as it does in meiotic cells. A previous study showed that DSB repair pathways are dynamic and are in competition in *C. elegans* somatic cells such that the inhibition of one pathway caused increased activity in the others [41]. We therefore reasoned that inhibiting NHEJ should increase the frequency of HR reporter activation. As predicted, blocking NHEJ by *cku-80* mutation resulted in substantial elevation of HR activity. More *cku-80* animals expressed GFP than wild-types (Figure 6D). This increase was likely an underestimation of HR activity as the GFP was also expressed much more brightly in *cku-80* mutants than wild-types. Brighter GFP likely results from multiple HR reporter genes being activated within a single cell. These experiments demonstrated that the HR reporter is able to measure relative changes in HR activity, in both HR-deficient and HR-hyperactive mutants.

Importantly, we found that both *lin-61(n3809)* and *lin-61(pk2225)* mutants showed a substantial reduction in the frequency of HR reporter activation compared with wild-types (Figure 6D). In fact HR activation in *lin-61* mutants was reduced to *brc-1* levels. This confirmed LIN-61 is needed for DSB repair by the HR pathway. Further, it indicated that IR hypersensitivity of *lin-61* mutants was likely due to defective DSB repair rather than other types of IR-induced cellular damage. While HR repairs DSBs in an error-free way, other DSB repair pathways such as NHEJ and SSA are error-prone processes. To test whether LIN-61 contributes to mutagenic DSB repair routes, we constructed a second reporter gene that specifically monitored SSA. This SSA reporter was similar to the HR reporter as both were expressed in intestinal nuclei and both received a single DSB from the mCherry::I-SceI enzyme, however the SSA reporter could only become active following an SSA event, and not an HR event (Figure S6A). We found that *lin-61* mutants did not have reduced SSA activity but actually had increased SSA reporter activation compared to wild-types (Figure S6B–S6C), in line with *lin-61* mutants being HR-defective. A similar shift towards SSA has previously been found for DSB repair in *brc-1* mutant animals [41]. We conclude that LIN-61 is necessary for efficient HR in somatic cells but is dispensable for SSA in somatic intestinal cells. Assays that measure sensitivity to DNA-damaging agents revealed that embryonic and germline cells of *lin-61* mutants are defective for DSB repair (Figure 2 and Figure 3). The data generated using the HR and SSA reporters demonstrated that cell types other than those of the germline and embryo are defective for DSB repair in *lin-61* mutants. Together, these complementary experiments suggested that *lin-61* mutants have a systemic defect in DSB repair.

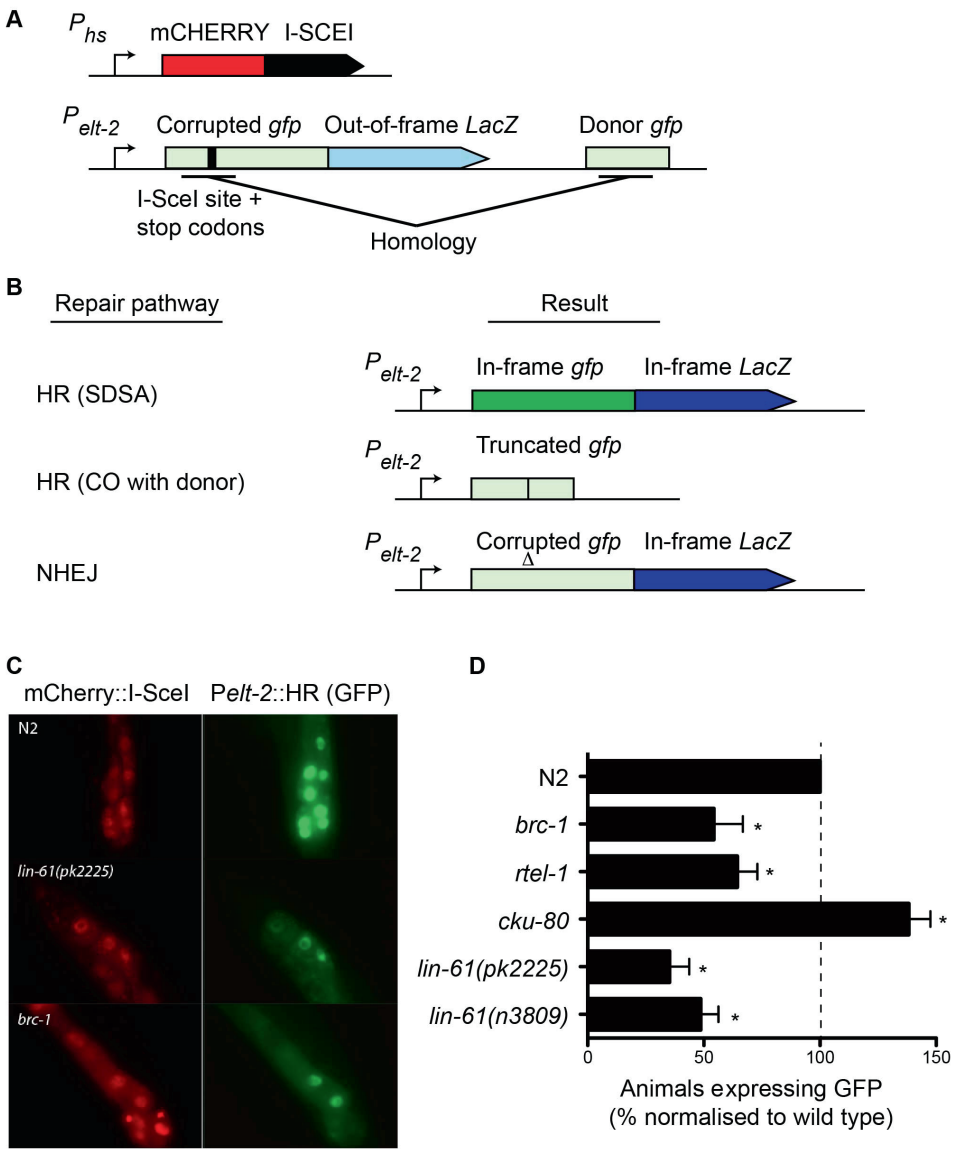

Figure 6. A novel GFP-based HR reporter system shows LIN-61 is needed for HR in somatic cells. (A) Schematic diagram of P*heatshock*::mCherry::I-SceI and the P*elt-2*::HR reporter. (B) Repair the of I-SceI-induced DSB can result in various outcomes depending upon which repair pathway is used. GFP expression is only restored by the HR-subpathway, synthesis-dependent strand annealing (SDSA). HR repair resulting in a CO between the reporter and the donor cannot restore GFP expression. Non-homologous end joining (NHEJ) cannot restore the *gfp* ORF, but can result in LacZ expression if stop codons are deleted. Light green and light blue represents out-of-frame/non-functional *gfp* and *LacZ*, respectively. Dark green and dark blue represents in-frame *gfp* and *LacZ*. (C) Images of mCherry::I-SceI (red) and GFP (green) expression in intestinal nuclei. (D) The percentage of animals with at least one intestinal nucleus expressing GFP after DSB repair. All data is normalised to N2 wild-types (set to 100%). Average data from these experiments. Error bars represent s.d. * $p<0.001$.

DNA damage checkpoints are proficient in *lin-61* mutants

Sensitivity to DNA damage can be caused by failure to activate DNA damage checkpoints [43]. The G2/M checkpoint is triggered in response to DNA damage and keeps mitotic germ cells in G2 phase to provide sufficient time for DNA repair (Figure 7A) [44]. Arrested cells do not divide, but continue to grow, making them readily identifiable by their enlarged size [43]. Following exposure to IR, all three *lin-61* mutants displayed proficient cell cycle arrest. Like wild-type worms (and *mbtr*-1 mutants that are not IR sensitive), the *lin-61* mutants had enlarged mitotic nuclei and a reduced number of germ cells 24 hours after γ-irradiation (Figure 7B–7C).

In addition to the G2/M checkpoint, DNA damage also triggers apoptosis in pachytene stage meiotic cells via a process dependent upon the p53 homologue, CEP-1 [43], [45]. Upon challenge with IR, apoptotic corpses accumulated in the germlines of wild-type, *lin-61(n3809)* and *lin-61(pk2225)* animals, while *cep-1* mutants failed to undergo DNA damage-dependent apoptosis (Figure 6D–6E). CEP-1 drives the apoptotic programme by up-regulating *egl-1*/BH3-only transcription [43], [45], [46]. In response to IR, *egl-1* expression was increased in wild-type and *lin-61* worms, but not *cep-1* mutants, as determined by qRT-PCR (Figure 7F). Together these results indicated that the activation of DNA damage checkpoints (cell cycle arrest and apoptosis) was normal in *lin-61* mutants. The hypersensitivity of *lin-61* mutants to IR could therefore not be attributed to defective checkpoint activation.

DNA repair genes are expressed at normal levels in *lin-61* mutants

Since LIN-61 is a transcriptional repressor, we checked whether DDR genes were appropriately expressed in *lin-61* mutants, as this could be the underlying cause of their HR defect. Using microarrays, we compared the expression profiles of wild-types and *lin-61* animals. Young adult worms (24 hours post L4) were analysed in order to increase the proportion of germ cells present in the samples, considering LIN-61 is needed for repair of DSBs in both somatic and germ cells. Microarrays were performed on two different *lin-61* alleles *(n3809* and *pk2225)* in order to control for changes in gene expression that were due by background mutations present within only one of the single strains. 58 genes were identified that, in both mutants, had a 1.5-fold or greater change in expression level (p-value<0.01) (Table S1). Most of these alternatively expressed genes were upregulated in *lin-61* mutants (52 genes, 90%), with only 6 genes (10%) downregulated. This is consistent with LIN-61 acting as a transcriptional repressor. Importantly, none of the genes alternatively expressed in *lin-61* mutants were implicated in DNA repair. The *lin-61* transcript served as a positive control in the microarray analysis as we had previously shown, using qRT-PCR, that this transcript was reduced approximately 4-fold in *lin-61* mutants, likely due to nonsense-mediated decay (Figure 1B). According to the microarray data, *lin-61* mRNA was reduced 3.25-fold, which in good agreement with the qRT-PCR data. The expression analysis showed that while LIN-61 does indeed act as a transcriptional repressor, *lin-61* mutation by itself (in the absence of an

additional synMuvA mutation) has only a minor effect on global gene transcription. Finally, since these experiments indicated that DNA repair genes are expressed at normal levels in *lin-61* mutants, it is likely that LIN-61 influences DSB repair directly and not by ensuring that other DDR genes are appropriately expressed.

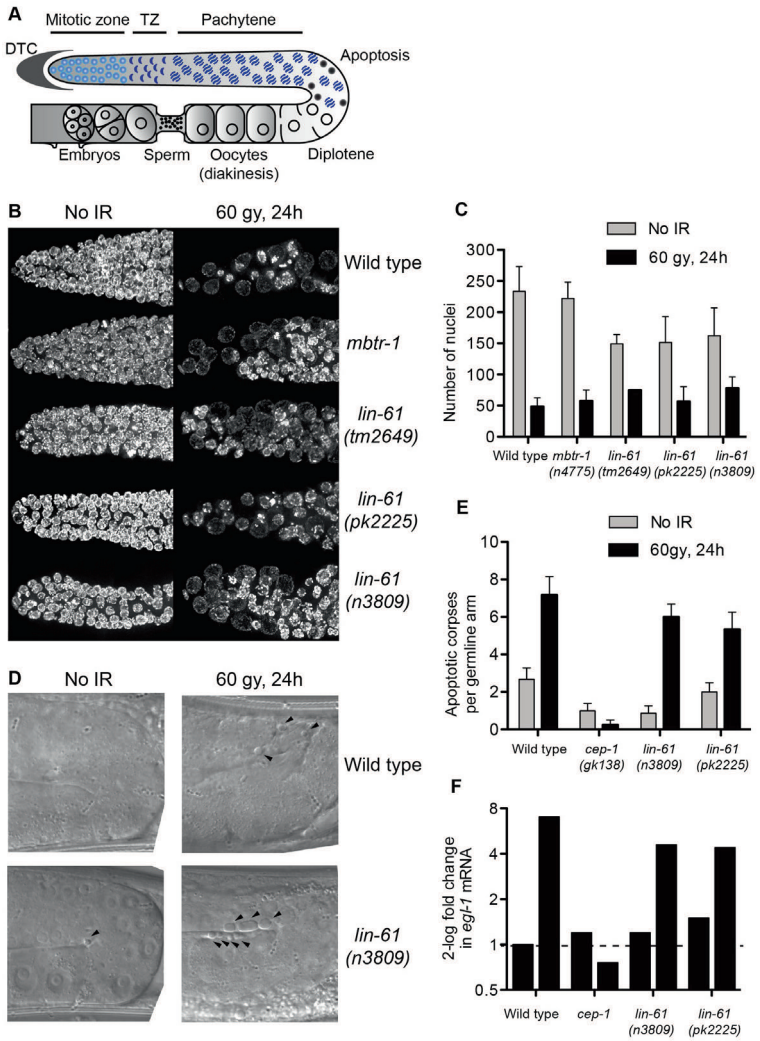

Figure 7. LIN-61 is dispensable for DNA damage checkpoints in the germline.
(A) Schematic diagram of the hermaphrodite germline. Cell cycle arrest (as in B–C) occurs in the mitotic zone and apoptosis (D–E) occurs at the bend of the germline. DTC, distal tip cell; TZ, transition zone. (B) Maximum projections of DAPI-stained mitotic nuclei 24 hours after irradiation with 60 Gy or mock-treatment. (C) Quantification of mitotic cell cycle arrest, error bars are s.d. (D) DIC images of pachytene stage nuclei 24 hours after irradiation with 60 Gy or mock-treatment. Arrowheads mark apoptotic corpses. (E) Quantification of apoptotic corpses per germline arm. Error bars represent s.d. (F) Quantification of *egl-1* mRNA by qRT-PCR, normalised to untreated wild-types. Total RNA was isolated from mixed populations of developmentally staged young adults 24 hours after irradiation with 120 Gy, or mock treatment.

Discussion

In this study we have identified the underlying cause of genomic instability in *lin-61* mutants: DSBs are not adequately repaired due to defective HR. Accordingly, these animals are hypersensitive to IR and nitrogen mustard and DSBs remain unrepaired in diakinesis oocytes of γ-irradiated *lin-61* mutants. LIN-61 contributes to HR in mitotic cells but it is dispensable for DSB repair during meiosis. Sensitivity of *lin-61* germ cells to DSBs is not due to faulty DNA damage checkpoints as both cell cycle arrest and apoptosis are functional. Moreover, DNA repair genes are not inappropriately expressed in *lin-61* mutants. The role of LIN-61 in HR is not restricted to germ cells because the somatic cells of early stage embryo are also very sensitive to IR. Also, later in development, intestinal cells are HR defective, as determined by the GFP-based HR reporter system. HR is essential for genome stability, as it is the principal DSB repair route in germ cells. It is also an error-free repair pathway. Blocking HR enables mutagenic and toxic repair routes to become active, which likely contributes to genomic instability in *lin-61* mutants.

The role of LIN-61 in HR is restricted to mitotic cells

LIN-61 is expressed in all nuclei, both in the germline and somatic tissues [6]. Despite this, several observations suggests that LIN-61 contributes to HR only in mitotic cells and is dispensable for both meiotic interhomolog and intersister HR. Meiotic cells rely on interhomolog HR to repair at least one programmed DSBs per chromosome pair so that the obligate CO will be established [47]. Meiotic recombination is not defective in *lin-61* mutants as they form chiasmata normally and produce nearly completely viable broods. What is more, RAD-51 foci that appear in prophase are resolved by late pachytene in both wild-type and *lin-61* mutants, indicative of the successful repair of programmed DSBs. The proficiency of intersister HR can be tested in meiotic cells by disrupting the SC in order to prevent interhomolog HR. In this situation, DSBs remain unrepaired if intersister HR too is defective, which manifests as chromosomal fragmentation at diakinesis. Unlike *brc-1* and *smc-5/-6* mutants [19], [27,27], *lin-61* mutants depleted of the SC component SYP-2 do not have fragmented diakinesis chromosomes, indicating that intersister HR is proficient in the meiotic cells of these mutants. Moreover, DSBs introduced by IR into *lin-61* meiotic cells, but not *brc-1* meiotic cells, are efficiently repaired.

While *lin-61* mutants are proficient in meiotic HR, their mitotic cells are defective in HR. These cells display signs of persistent and spontaneous DNA damage. Further, γ-irradiation of mitotic germ cells causes severe chromosome fragmentation in *lin-61* mutants. Finally, *lin-61* mutants are also hypersensitive to ICLs and the repair of these lesions occurs in S/G2 phase using the newly synthesised sister chromatid as the HR repair template [29]. The somatic (mitotic) cells of *lin-61* are also hypersensitive to IR and mitotic cells exclusively use the sister

chromatid for HR [39]. Together, these observations indicate that LIN-61 contributes to DSB repair via intersister HR in mitotic cells but does not participate in meiotic HR.

How does LIN-61 promote DSB repair?

Considering that the transcriptional profile of *lin-61* mutants cannot explain their HR defect, LIN-61 likely acts directly at sites of DNA damage to promote DSB repair. This is an attractive hypothesis considering that chromatin can act as a physical barrier that must be remodelled to allow access of DDR factors to sites of damage. In addition, many proteins that alter chromatin structure have recently been implicated in the DDR including NuRD components MTA1, MTA2, CHD4, HDAC1 and HDAC2 [48]–[50]; and PcG proteins BMI1, RING1, RING2 and HP1 [51]–[55]. Each of these proteins is rapidly recruited to DNA damage and is necessary for DNA repair. The *C. elegans* counterparts of these proteins are also synMuvB proteins like LIN-61. Intriguingly, L3MBTL2, the putative human orthologue of LIN-61, is part of a PcG-like complex (PRC1L4) that shares RING1, RING2 and HP1γ as partner members [56]. Moreover, human cells depleted of RING2 [55], and *C. elegans hlp-2* HP1 mutants [53], are radiosensitive like *lin-61* mutants. PRC1L4, or a related L3MBTL2-containing PcG complex, may therefore act in DSB repair like LIN-61. Using immunofluorescence, we were not able to detect a change in LIN-61 intracellular localisation upon IR (data not shown). However LIN-61 is abundantly present and localised at chromatin in all cells, which may conceal its relocalisation around sites of DNA damage. Recruitment to sites of DNA damage has also not been observed for any other *C. elegans* synMuvB proteins, likely for similar reasons.

It is unknown how PcG activity promotes DSB repair but it is argued that inhibiting transcription locally at the DSB may be important as the transcriptional machinery could interfere with repair proteins or with DNA repair intermediates [50], [57]. PRC1L4 represses transcription of target genes by monoubiquitinating lysine 119 of histone H2A via its E3 ubiquitin ligase activity [56]. This histone mark is also implicated in the DDR as it was recently shown to rapidly accumulate at DSBs [52], [58]. It will be of interest to determine whether L3MBTL2 and the other members of PRC1L4 are involved in DSB repair in human cells.

One possible explanation we considered for why *lin-61* mutants were HR-defective was that they might have altered expression of DDR genes. But contrary to this, microarray expression analysis did not reveal any alternatively expressed DDR genes in these mutants. Some alternatively expressed genes were identified but none are implicated in DNA repair. The vast majority of the alternatively expressed genes were upregulated rather than downregulated, which is in accordance with LIN-61 being a transcriptional repressor. A previous study found that germline genes were ectopically expressed in the somatic tissues of *lin-61* mutants, but only when maintained at the relatively high temperature of 26°C [13]. In line with this, we found that *lin-61* mutants grown at the normal laboratory temperature of 20°C had only minor changes in gene expression and did not overexpress germline genes. Importantly, *lin-61*

mutants grown at 20°C displayed a profound HR defect, which further indicated that altered gene expression was not the cause of defective DNA repair. The microarrays were performed using RNA from a mixed population of germ and somatic cells. We cannot strictly exclude the possibility that a distinct population of cells had altered DDR gene expression that went undetected. This is unlikely though, as the defect in DSB repair was systemic, occurring in multiple tissues and at various stages of development, and not isolated to a small number of cells.

A novel GFP-based HR reporter system for *C. elegans*

In this study we introduce a novel reporter system for monitoring HR in *C. elegans* somatic cells. The reporter confirmed that LIN-61 is needed for HR. This tool was previously unavailable for *C. elegans* researchers. We propose it as a method for testing candidate HR genes, for example it confirmed that both BRC-1 and RTEL-1 have roles in HR in somatic cells, analogous to their functions previously only described in meiotic germ cells. Our experiments with the HR reporter also supported previous findings that suggested DSB repair pathways are dynamic and are in competition in somatic cells [41] since mutations that blocked NHEJ, increased HR reporter activity.

Though this system is a new tool that provides for the readout of repair, probably by an SDSA mechanism, of a defined DSB, it does have limitations. For example, the HR reporter does not easily allow for dissection of the biochemical processes that underpin HR pathways. These approaches are not well suited to *C. elegans*. Also, in its current form the HR reporter is expressed only in intestinal cells, which in contrast to most *C. elegans* somatic cells still cycle postembryoniccally. This choice of cell type was largely motivated by the likely need for S- and G2 phase dependent DNA end resection at DSBs for HR type of repair to occur. However, when interpreting the data it must be considered that these cells are atypical because they progress and grow through cycles of endoreduplication and not via canonical cell cycle stages including mitosis. It is thus possible that the response to the HR reporter is cell type-dependent. Finally, since formation of the DSB relies on expression of the I-SceI transgene using the heat-shock promoter, any possible differences in heat-shock response must be carefully controlled for as these differences may affect the level of DSB induction.

Implications for HR deficiency in MBT mutants

This is the first report showing that an MBT protein is needed for DSB repair. Genes encoding MBT proteins have previously been linked with tumourigenesis and can act as tumour suppressor genes. However, their contribution to DNA repair and genome stability is unknown. Our finding that LIN-61 is required for efficient HR may have implications for the treatment of MBT-deficient tumours, which may also be HR defective. HR-deficient tumours, such as those with BRCA1 or 2 hypomorphic mutations, are very susceptible to poly(ADP ribose)

polymerase (PARP) inhibitors [39]. It will be important to determine whether the role of LIN-61 in DSB repair is conserved in human MBT proteins and whether MBT mutated tumours, such as medulloblastomas with mutations in *L3MBTL2*, *L3MBTL3* or *SCML2* [10], are HR deficient as they too may prove responsive to treatment with PARP inhibitors.

Materials and Methods

Genetics

The Bristol N2 strain was used as the wild-type strain and maintained at 20°C according to standard protocols [59]. Alleles used in the study include LG I: *lin-61(n3809)* [6], *lin-61(pk2225)* (this study), *lin-61(tm2649)* [15], *mbtr-1(n4775)* [6], *cep-1(gk138)* [60] and *rtel-1(tm1866)* [61]; LG III: *brc-1(tm1145)* [62], *cku-80(ok861)* [63], *polh-1(lf31)* [31], *lfIs129 [elt-2::HR-reporter; hsp16-41::mCherry::I-SceI]* (this study); and LG X: *lfIs82 [elt-2::SSA-reporter; hsp16-41::mCherry::I-SceI]* (this study). To determine brood sizes, L4 larvae were singled on 6 cm plates with OP50 *E. coli* and transferred each day for three days. The number of viable progeny and unhatched eggs were counted, as well as the number of males in the brood.

DNA damage sensitivity, checkpoint activation, and chromosome fragmentation assays

All γ-irradiation was performed with a dose rate of 15 Gy/minute using an electronic X-ray generator set to 200 kV 12 mA (XYLON International). For L4 larval IR sensitivity, three L4 animals per plate (three plates per condition) were treated with various doses of γ-irradiation. For UV-C sensitivity, young adult (24 post L4 stage) worms were exposed to UV (254 nm lamp, Philips). HN2 sensitivity assays were performed as described [64]. γ-irradiation of embryos and L1 larvae was preformed as described [32]. Apoptosis assays were performed in as [45]. Cell cycle arrest and fragmentation assays were as in [36]. *syp-2* RNAi was performed as in [19]. For cell cycle arrest, 4–5 germlines were analysed per condition, except for irradiated *lin-61(tm649)* for which a single germ line was scored.

Germline dissections and RAD-51 immunofluorescence

Germlines were dissected in egg salts, Tween, levamisole and fixed in 2% paraformaldehyde for 5 minutes at room temperature, and snap frozen on dry ice, then placed in methanol at −20°C for 10 minutes, washed three times for 10 minutes in PBS with 1% Triton X-100 and blocked in PBST (PBS with 0.1% Tween 20) and 1% BSA for 30 minutes at room temperature. Samples were incubated overnight at 4°C with rabbit anti-RAD-51 antibodies (Novus Biologicals) diluted 1:200 in PBST 1% BSA and detected with Alexa488 goat anti-rabbit antibodies (Invitrogen) diluted 1:1000. DNA was counterstained with 0.5 µg/ml DAPI and samples were mounted with VectaShield. RAD-51 foci were imaged with a Leica DM6000 deconvolution microscope collecting 0.5 µm Z-sections. The number of foci per nucleus was

counted for each of the seven zones of the germline as described [64]. Three to five germlines were quantified per condition.

Microarray and qRT–PCR

Worms were synchronised as L1 larvae by bleaching and grown to the L4 stage. Total RNA was isolated with Trizol reagent (Invitrogen), and cleaned with RNeasy kit (Qiagen). Service XS (Leiden, NL) performed the Affymetrix expression analysis according to standard protocols. Data was analysed with the MAS 5.0 algorithm using Tukey's biweight estimator. Significance (p-value) was determined using Wilcoxon's rank test. Sequence of qRT-PCR primers is available in Text S1.

P*elt-2*::HR and P*elt-2*::SSA reporter

Details on construction of the P*elt-2*::HR and P*elt-2*::SSA reporter strains are provided in Text S1. For HR reporter assays, expression of mCherry::ISce-I was induced in L4 larvae by heat-shock twice at 34°C for 1 hour (with 30 min rest at 20°C). 24 hours after induction, worms were mounted on agarose pads and their intestinal nuclei were scored for GFP expression using a Leica DM6000 microscope with 63× objective. Experiments were performed in triplicate with 50–100 animals tested for each condition. Statistical significance was tested using the Cochran-Mantel-Haenszel test.

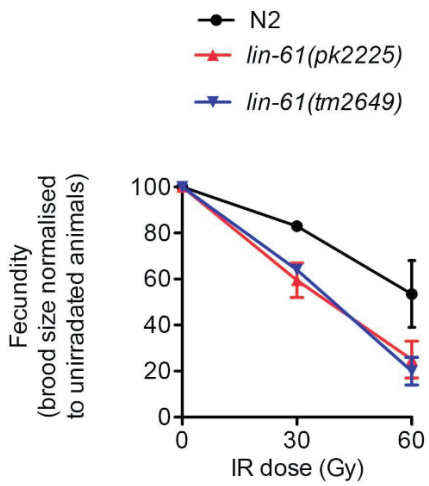

Figure S1. The primordial germ cells of *lin-61* mutants are hypersensitive to IR.
L1 larvae were irradiated with the indicated dose of IR and grown to adulthood before their brood sizes was determined. The average brood size of five adults was counted for each condition. Depicted is the average brood size from two experiments, normalised to the brood size of unirradiated animals. Error bars are standard error of the mean.

A

```
MBTR-1 ------------------------------------------------------------
LIN-61 MLKLVILCFALFYNTVSSTRFLFGVEVKCDFDEVFQLTVSHWEDDGNTFWDRDEDITGRM 60

MBTR-1 --MEKSSSNFIQNGKR-----------------DHGGKLRQYNYKLEEAEYRYFTEERLF 41
LIN-61 TMFARKKIFFYQDGHHGFEFGKLEPYGWFLHNCTKNGNFREYRHGLSSTSGSNGLEYIEY 120

MBTR-1 YRRRNPVEKIAQRIPKPQIEGTFTWSDELRCNYDGNTQFLPVEALEGCLPLEKLNQHLKP 101
LIN-61 TMSEFLKIVRANKKSDRKLDKTYLWESYLHQFEKGKTSFIPVEAFNRNLTVN-FNECVKE 179
          .      *:: .. ::: *: *.. *:    .*:*.*:****::  *.:: :*: :*
MBTR-1 GFRLEVVVRPSLDPSITTKSPEIRWFGEVTAVCGFYVAIKFVGELNRRPCWFHMLSEDIF 161
LIN-61 GVIFETVVH---DYDKNCDSIQVRWFARIEKVCGYRVLAQFIGADTK--FWLNILSDDMF 234
       *. :*.**:   * . . .* ::***..:  ***: *  :*:*  .:   *:::**:*:*
MBTR-1 DIGSGLKQDPAMKWLQYR-PLSLLKPMQCPKFWRRGSTPAPPVPRPTEEILDEFQAELHE 220
LIN-61 GLANAAMSDPNMDKIVYAPPLAINEEYQN---------------DMVNYVNNCIDGEIVG 279
       .:...  .** *. : *  **:: :  *                    .: : : ::.*:
MBTR-1 NRISEPKIFDQLRHLAHRPSRFRLNQRVELLNYLEPTEIRVARILRILGRRLMVMVTAQD 280
LIN-61 -QTSLSPKFDEGKALLSK-HRFKVGQRLELLNYSNSTEIRVARIQEICGRRMNVSITKKD 337
        : * .  **: : *  :  **::.**:***** :.******** .* ***: * :* :*
MBTR-1 YPEDLPSVEAKDRQVQHENVEFWVDESSFFLFPVGFAMINGLRTKATEGYLEHSRRIAEG 340
LIN-61 FPESLPDADD-DRQVFSSGSQYWIDEGSFFIFPVGFAAVNGYQLNAKKEYIEHTNKIAQA 396
       :**.**..:  ****  .. ::*:**.***:****** :** : :*.: *:**:.:**:.
MBTR-1 SGS-----YHKDDVTFEQLFAGKPDISAEKLNLLKVGQKFELLDPLSDLRQSFCVATIRK 395
LIN-61 IKNGENPRYDSDDVTFDQLAKDP--IDPMIWRKVKVGQKFELIDPLAQQFNNLHVASILK 454
         .     *..*****:**  .   *..   . :********:***::  :.: **:* *
MBTR-1 ICKTPGFLIISPDETESDDESFPIHIDNHFMHPVGYAEKFGIKLDRLAGTEPGKFKWEGY 455
LIN-61 FCKTEGYLIVGMDGPDALEDSFPIHINNTFMFPVGYAEKYNLELVPPD-EFKGTFRWDEY 513
       :*** *:**:. * .:: ::******:* **.*******:.::*        *.*:*: *
MBTR-1 LKEKQAEKIPDEMLRPLPSKERRHMFEFGRVLEAVGQNETYWISPASVEEVHGRTVLIEF 515
LIN-61 LEKESAETLPLDLFKPMPSQERLDKFKVGLRLEAADMCENQFICPATVKSVHGRLINVNF 573
       *:::.**.:* ::::*:**:** . *:.*  ***..  *. :*.**:*:.**** : ::*
MBTR-1 QGWDSEFSELYDMDSHDLLPAGWCEFFNFKLRHPVLPVNDPNAENGEYD 564
LIN-61 DGWDEEFDELYDVDSHDILPIGWCEAHSYVLQP-------PKKYN--Y- 612
       :***.**.****:****:** **** ..: *:        *:  *  *
```

B

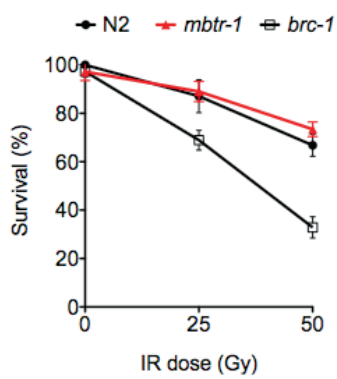

Figure S2. mbtr-1 mutants are not sensitive to IR.
(A) Protein sequence alignment of LIN-61 and MBTR-1. Asterisk (*), semicolon (:) and full stop (.) denote identical residues, conserved substitutions and semi-conservative substitutions, respectively. Residues present in the four MBT domains are coloured red, blue, green and purple. (B) *mbtr-1* mutants are not sensitive to IR. The percentage of viable progeny laid by irradiated L4 larvae is plotted. Error bars represent standard deviation.

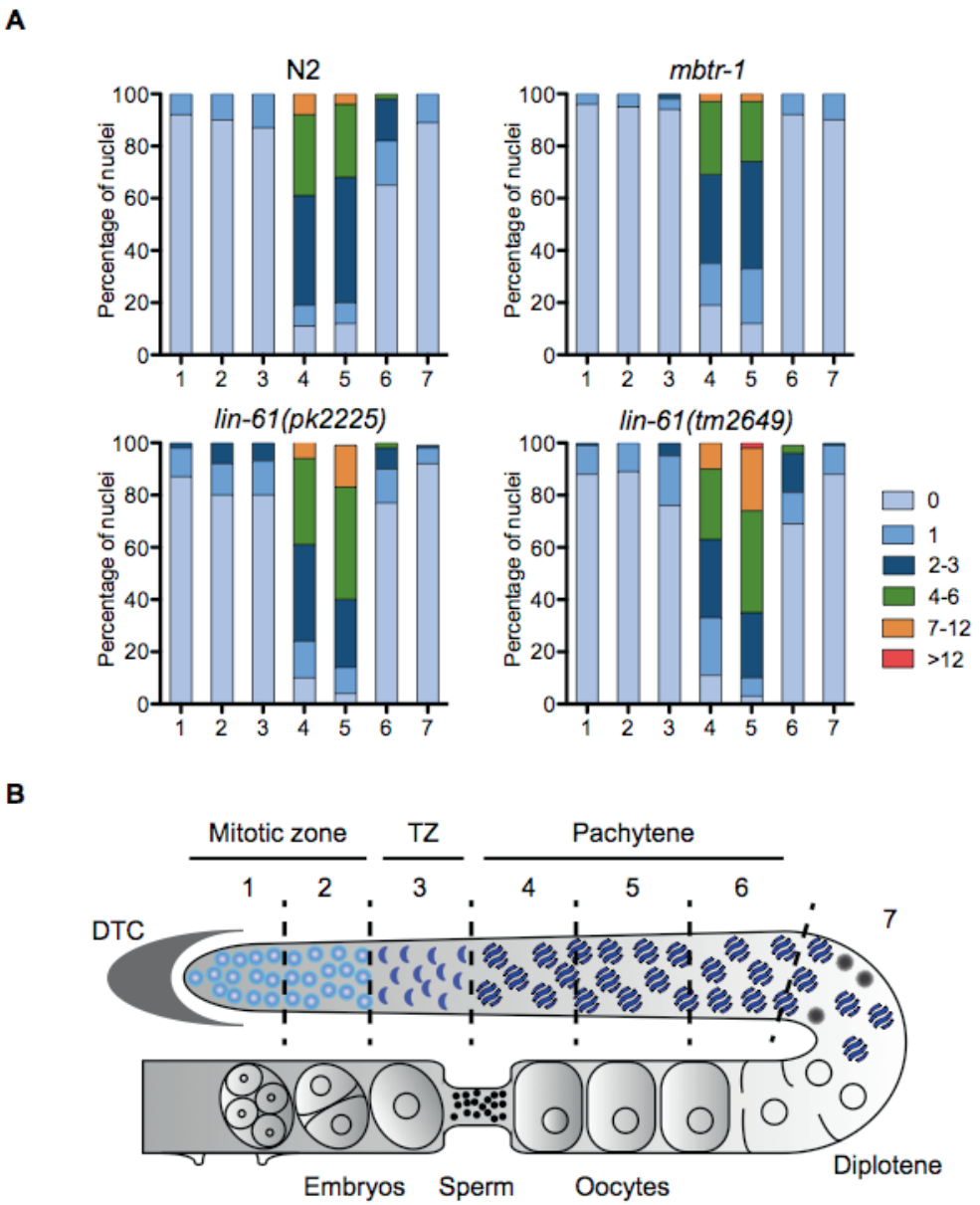

Figure S3. Quantification of RAD-51 foci in lin-61 germlines.
(A) Stacked histograms showing the average number of RAD-51 foci per nucleus present in each of the seven zones of the germline. (B) Diagram depicting the germline divided into seven zones. Zones one and two include the mitotic zone; zone three is the transition zone (TZ); zones four and five are early-mid pachytene; zone six is late pachytene; and zone seven is late pachytene/diplotene. DTC, distal tip cell.

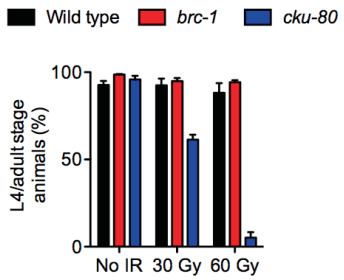

Figure S4. *brc-1* L1 larvae do not display developmental delay following IR.
Depicted is the proportion of animals that developed to the L4 stage 48 hours after being γ-irradiated as L1 larvae with the indicated dose. Error bars are s.d.

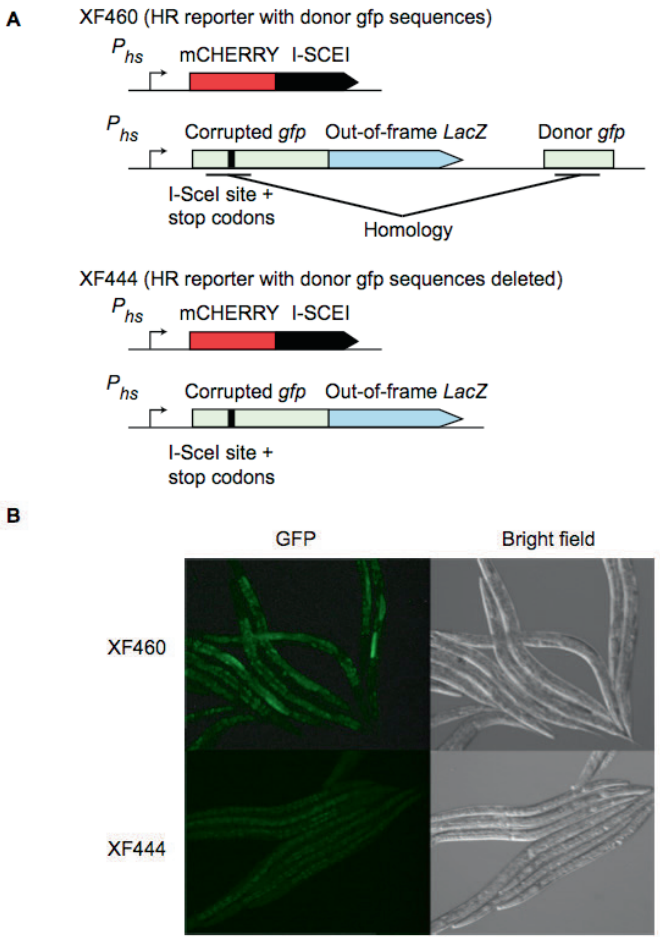

Figure S5. HR reporter activation requires donor sequence for activation.
(A) Schematic diagram of versions of the HR reporter that contain (upper panel; strain XF460) or lack (lower panel; strain XF444) the gfp donor cassette. These reporters are expressed using the heat-shock promoter. (B) Epifluorescence and brightfield images of adult worms 24 hours after DSB induction. GFP is visible in intestinal cells in XF460, but not XF444.

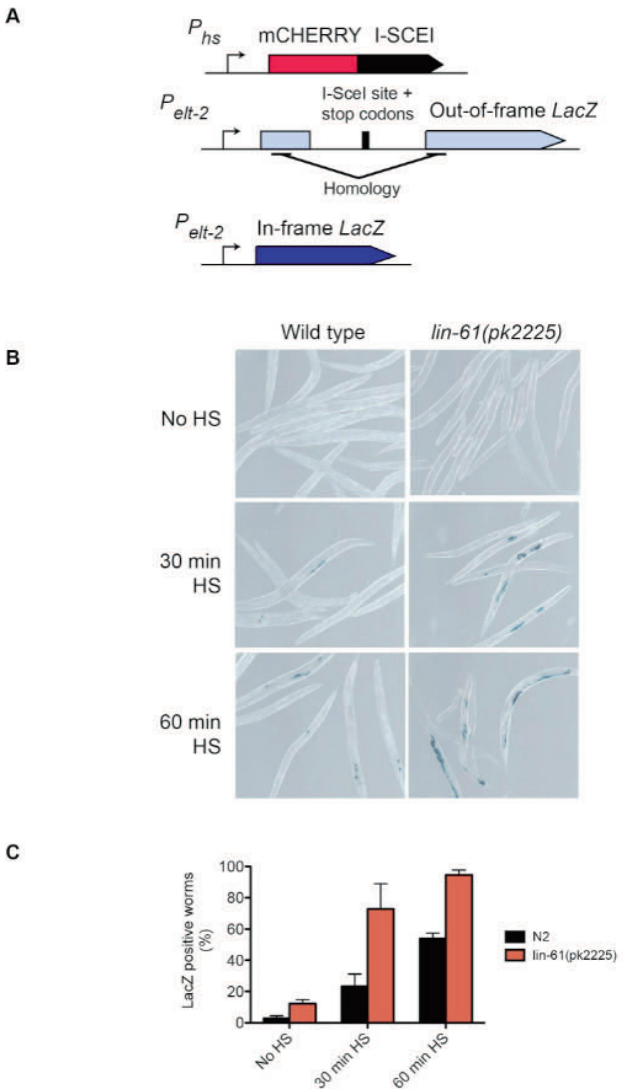

Figure S6. Pelt-2::SSA reporter.
(A) Schematic showing the Pelt-2::SSA reporter. The Pelt-2::SSA reporter consists of an out-of-frame LacZ gene, disrupted by an I-SceI sites and stop codons in all three frames. A region of LacZ is duplicated and located between the elt-2 promoter and the I-SceI site, and provides homologous sequences for SSA. A DSB is introduced in the centre of the reporter by expressing Pheatshock::mCherry::I-SceI. Repair of the DSB by SSA places the LacZ gene in-frame and deletes the sequences between the homologous repeats (including the I-SceI site and stop codons). (B) LacZ (β-galactosidase) activity was visualised by the conversion of X-gal to 5,5′-dibromo-4,4′-dichloro-indigo, which has an intense blue colour. Shown are representative bright field images of L4/young adult worms expressing LacZ in their intestinal cells (C) Graph showing the percentage of worms containing at least one blue intestinal cell. Induction of mCherry::I-SceI was achieved by heat-shocking L1 stage worms for 30 or 60 min. These worms were stained for LacZ expression 48 hours after heat-shock. Error bars represent standard deviation.

Table S1. Genes alternatively expressed in *lin-61* mutants.

This table lists the genes alternatively expressed in L4 stage *lin-61* mutants compared with wild-types, as determined by Affymetrix expression analysis.

	Fold change	Direction	Gene	Description	p-value
1	3.25	down	*lin-61*	MBT domatin protein	0.70015
2	2.88	down	*fbxa-106*	F-box A protein	0.79353
3	2.72	down	*bath-29*	BTB and MATH domain containing	0.79353
4	2.53	down	F45D11.14, ,	Gene of unknown function	0.79353
5	1.96	down	C33G8.3	Gene of unknown function	0.79353
6	1.57	down	C10B5.1	WD40 domain protein	0.38141
7	9.15	up	C18D4.6	Gene of unknown function	0.00159
8	6.97	up	F15D4.5	Gene of unknown function	0.00229
9	5.14	up	*ccb-1*	Calcium channel	0.00010
10	4.18	up	Y55F3AM.11	Gene of unknown function	0.00089
11	3.65	up	*spe-15*	unconventional myosin	0.00616
12	3.48	up	*dmd-9*	DM (Doublesex/MAB-3) Domain	0.00103
13	3.47	up	C33C12.3	glucosylceramidase	0.00228
14	3.32	up	H14E04.3	Gene of unknown function	0.00636
15	3.09	up	W06A11.4	Gene of unknown function	0.00052
16	3.06	up	*dhcr-7*	7-dehydrocholesterol reductase	0.00933
17	2.96	up	Y54G2A.21	Gene of unknown function	0.00912
18	2.94	up	R09A1.2	Kelch-like protein 13-homologue	0.00233
19	2.72	up	*fkb-8*	FKBP-type peptidylprolyl isomerase	0.00868
20	2.71	up	C33C12.4	Gene of unknown function	0.00162
21	2.55	up	T04D3.8	Gene of unknown function	0.00384
22	2.55	up	W06A11.4,	Gene of unknown function	0.00908
23	2.44	up	ZK849.5	Putative membrane protein	0.00270
24	2.35	up	*ceh-91*	Protein with a THAP domain	0.00649
25	2.28	up	Y54G2A.4	Gene of unknown function	0.00332
26	2.26	up	Y73B3A.11	Gene of unknown function	0.00276
27	2.12	up	C27C7.1	Gene of unknown function	0.00378
28	2.05	up	*fmo-5*	Flavin-containing MonoOxygenase	0.00247
29	2.03	up	K08C9.7	Ubiquitin-40S ribosomal protein	0.00125
30	2.03	up	K08A2.4	Gene of unknown function	0.00269
31	2.01	up	Y37E3.13	Immunoglobulin domain protein	0.00770
32	1.99	up	*srr-2*	Serpentine Receptor, class R	0.00005
33	1.98	up	*nstp-6*	Nucleotide Sugar TransPorter	0.00304
34	1.97	up	W04C9.5	Small GTPase	0.00330
35	1.97	up	*gst-20*	Glutathione S-Transferase	0.00545
36	1.96	up	Y94H6A.4	Glutathione peroxidase	0.00068
37	1.96	up	F21A9.2	zinc finger protein	0.00169
38	1.95	up	*ubc-15*	E2 ubiquitin-conjugating enzyme	0.00867
39	1.92	up	*dyb-1*	DYstroBrevin homolog	0.00657
40	1.90	up	Y66D12A.11	Gene of unknown function	0.00536
41	1.89	up	K08A2.4	lin-8 (synMuvA) paralog	0.00221

42	1.88	up	C06A5.10	Gene of unknown function	0.00070
43	1.86	up	*npp-8*	Nuclear Pore complex Protein	0.00236
44	1.85	up	*bath-45*	BTB and MATH domain containing	0.00516
45	1.84	up	*gale-1*	UDP-GALactose 4-Epimerase	0.00189
46	1.82	up	Y54F10BM.9	Gene of unknown function	0.00717
47	1.75	up	*clec-48/49*	C-type LECtin	0.00735
48	1.73	up	K06B9.4	Gene of unknown function	0.00643
49	1.70	up	H05C05.2	Gene of unknown function	0.00720
50	1.70	up	Y39B6A.1	Gene of unknown function	0.00738
51	1.63	up	Y22D7AL.9	Tetratricopeptide	0.00394
52	1.62	up	*lin-17*	Frizzled-homologue, Wnt receptor	0.00407
53	1.60	up	*ceh-44*	Homeobox	0.00075
54	1.58	up	F08A8.5	alpha-1,2-fucosyltransferase	0.00369
55	1.56	up	*spe-6*	defective SPErmatogenesis	0.00905
56	1.52	up	C03B8.3	Gene of unknown function	0.00702
57	1.51	up	T28F2.2	Gene of unknown function	0.00247
58	1.51	up	*haf-4*	lysosomal peptide ABC transporter	0.00447

Text S1. Supporting Experimental Procedures.

Description of *lin-61* mutant alleles

n3809 is a CAA to TAA nonsense mutation (Q159ochre) located in the fourth exon that truncates the LIN-61 protein by removing the second, third and fourth MBT domains and causes a highly penetrant synMuv phenotype (Harrison et al., 2007) The second allele, *pk2225,* was isolated from an EMS mutagenesis library (Cuppen et al., 2007) and identified using a reverse genetics approach by sequencing PCR amplicons of the *lin-61* gene. *pk2225* is also a CAA to TAA mutation (Q412ochre) and, coincidently, is identical to another allele (*n3446*) isolated in a screen for mutants that have a synMuv phenotype when combined with *lin-15A* (Ceol et al., 2006). The synMuv phenotype of *n3446* was as penetrant as *n3809* (Harrison et al., 2007), therefore *pk2225* is also likely to have a strong synMuv phenotype. The third allele (*tm2649*) is a large deletion within *lin-61* with breakage points located in the second exon and at a position in the fourth exon that places the remaining exons out-of-frame (Figure 1A). *lin-61(tm2649)* also causes a highly penetrant synMuv phenotype (Koester-Eiserfunke and Fischle, 2011).

Construction of P*elt-2*::HR reporter, P*elt-2*::SSA reporter and P*hsp16-41*::mCherry::ISce-I

pLM44 (P*elt-2*::SSA reporter) was constructed by transferring the cassette containing LacZ (interrupted by an I-SceI site) from pRP1879 (Pontier and Tijsterman, 2009) to pJM67 (P*elt-2*::gfp::lacZ) using AgeI and XhoI sites. pLM17 (P*hsp16-41*::mCherry::ISceI) was constructed by inserting an mCherry cassette into pRP3001 (P*hsp16-41*::ISceI) using a single XmaI site to produce an in-frame N-terminal fusion. The plasmids were injected together at 2 ng/µl along with pRF4 (dominant *rol-6(su1006)* marker) and genomic DNA to generate transgenic strains carrying low-copy extrachromosomal arrays. Extrachromosomal arrays were integrated by g-irradiation with 50 Gy and F2 progeny were selected for 100% inheritance of the Rol-6 phenotype. Mapping analysis showed that the array was integrated in chromosome III.

SSA reporter assay

Worms were bleached to obtain synchronized L1 larvae. mCherry::I-SceI was induced by heat-shock at 34˚C for 30 minutes or 60 minutes. Correct induction of mCherry::I-SceI was determined by visualizing mCherry epifluorescence. Two days after heat-shock, L4 larvae/ young adult worms were rinsed off plates, washed twice with water and dried in a speedyvac, before being fixed in acetone. LacZ staining was performed with X-gal solution (0.04% X-gal, 5 mM ferricyanide, 5 mM ferrocyanide, 0.3% formamide, 166 mM Na_2HPO_4, 33 mM NaH_2PO_4, 0.2 mM $MgCl_2$, 0.004% SDS, 75 µg/ml kanamycin)

qRT-PCR primers

Sequence of qRT-PCR primers are as follows: *lin-61* tgctgacatgtgtgaaaatcagtt and catgggagtccacatcatacagtt; *egl-1* actcgggatttttgatgactctg and aaaaagtccagaagacgatggaag; tbg-1 attcaatccgctatctctcctgtt and tcattcgaagtggtttaagcatgt. All data was normalized to tubulin beta (*tbg-1*) expression levels.

L1 larvae IR assay

Assay was performed as in Bailly et al 2010 but L1 worms were obtained by bleaching rather than from growing populations using Millipore filters.

Acknowledgments

The authors thank Shohei Mitani (National Bioresource Project, Japan) and the Caenorhabditis Genetics Center for strains; Sophie Roerink and Carine Stapel for HR reporter construction and data; Ron Romeijn, Kristy Okihara, and Jennemiek van Arkel for technical support; and Joris Pothof for isolation of *pk2225*.

Author Contributions

Conceived and designed the experiments: NMJ MT. Performed the experiments: NMJ BBLGL. Analyzed the data: NMJ BBLGL MT. Wrote the paper: NMJ MT.

References

1. Tremethick DJ (2007) Higher-order structures of chromatin: the elusive 30 nm fiber. Cell 128: 651–654 doi:10.1016/j.cell.2007.02.008.

2. Kouzarides T (2007) Chromatin modifications and their function. Cell 128: 693–705 doi:10.1016/j.cell.2007.02.005.

3. Trojer P, Li G, Sims RJ, Vaquero A, Kalakonda N, et al. (2007) L3MBTL1, a histone-methylation-dependent chromatin lock. Cell 129: 915–928 doi:10.1016/j.cell.2007.03.048.

4. Bonasio R, Lecona E, Reinberg D (2010) MBT domain proteins in development and disease. Semin Cell Dev Biol 21: 221–230 doi:10.1016/j.semcdb.2009.09.010.

5. Saffer AM, Kim DH, van Oudenaarden A, Horvitz HR (2011) The Caenorhabditis elegans Synthetic Multivulva Genes Prevent Ras Pathway Activation by Tightly Repressing Global Ectopic Expression of lin-3 EGF. PLoS Genet 7: e1002418 doi:10.1371/journal.pgen.1002418.

6. Harrison MM, Lu X, Horvitz HR (2007) LIN-61, one of two Caenorhabditis elegans malignant-brain-tumor-repeat-containing proteins, acts with the DRM and NuRD-like protein complexes in vulval development but not in certain other biological processes. Genetics 176: 255–271 doi:10.1534/genetics.106.069633.

7. Poulin G, Dong Y, Fraser AG, Hopper NA, Ahringer J (2005) Chromatin regulation and sumoylation in the inhibition of Ras-induced vulval development in Caenorhabditis elegans. EMBO J 24: 2613–2623 doi:10.1038/sj.emboj.7600726.

8. Pothof J, van Haaften G, Thijssen K, Kamath RS, Fraser AG, et al. (2003) Identification of genes that protect the C. elegans genome against mutations by genome-wide RNAi. Genes Dev 17: 443–448 doi:10.1101/gad.1060703.

9. Wismar J, Löffler T, Habtemichael N, Vef O, Geissen M, et al. (1995) The Drosophila melanogaster tumor suppressor gene lethal(3)malignant brain tumor encodes a proline-rich protein with a novel zinc finger. Mech Dev 53: 141–154. doi: 10.1016/0925-4773(95)00431-9

10. Northcott PA, Nakahara Y, Wu X, Feuk L, Ellison DW, et al. (2009) Multiple recurrent genetic events converge on control of histone lysine methylation in medulloblastoma. Nat Genet 41: 465–472 doi:10.1038/ng.336.

11. Gurvich N, Perna F, Farina A, Voza F, Menendez S, et al. (2010) L3MBTL1 polycomb protein, a candidate tumor suppressor in del(20q12) myeloid disorders, is essential for genome stability. Proc Natl Acad Sci USA 107: 22552–22557 doi:10.1073/pnas.1017092108.

12. Janic A, Mendizabal L, Llamazares S, Rossell D, Gonzalez C (2010) Ectopic Expression of Germline Genes Drives Malignant Brain Tumor Growth in Drosophila. Science 330: 1824–1827 doi:10.1126/science.1195481.

13. Petrella LN, Wang W, Spike CA, Rechtsteiner A, Reinke V, et al. (2011) synMuv B proteins antagonize germline fate in the intestine and ensure C. elegans survival. Development 138: 1069–1079 doi:10.1242/dev.059501.

14. Luijsterburg MS, van Attikum H (2011) Chromatin and the DNA damage response: The cancer connection. Mol Oncol doi:10.1016/j.molonc.2011.06.001.

15. Koester-Eiserfunke N, Fischle W (2011) H3K9me2/3 binding of the MBT domain protein LIN-61 is essential for Caenorhabditis elegans vulva development. PLoS Genet 7: e1002017 doi:10.1371/journal.pgen.1002017.

16. Youds JL, O'Neil NJ, Rose AM (2006) Homologous recombination is required for genome stability in the absence of DOG-1 in Caenorhabditis elegans. Genetics 173: 697–708 doi:10.1534/genetics.106.056879.

17. Grabowski MM, Svrzikapa N, Tissenbaum HA (2005) Bloom syndrome ortholog HIM-6 maintains genomic stability in C. elegans. Mech Ageing Dev 126: 1314–1321 doi:10.1016/j.mad.2005.08.005.

18. Yanowitz JL (2008) Genome integrity is regulated by the Caenorhabditis elegans Rad51D homolog rfs-1. Genetics 179: 249–262 doi:10.1534/genetics.107.076877.

19. Bickel JS, Chen L, Hayward J, Yeap SL, Alkers AE, et al. (2010) Structural maintenance of chromosomes (SMC) proteins promote homolog-independent recombination repair in meiosis crucial for germ cell genomic stability. PLoS Genet 6: e1001028 doi:10.1371/journal.pgen.1001028.

20. Alpi A, Pasierbek P, Gartner A, Loidl J (2003) Genetic and cytological characterization of the recombination protein RAD-51 in Caenorhabditis elegans. Chromosoma 112: 6–16 doi:10.1007/s00412-003-0237-5.

21. Ward JD, Barber LJ, Petalcorin MI, Yanowitz J, Boulton SJ (2007) Replication blocking lesions present a unique substrate for homologous recombination. EMBO J 26: 3384–3396 doi:10.1038/sj.emboj.7601766.

22. Hayashi M, Chin GM, Villeneuve AM (2007) C. elegans germ cells switch between distinct modes of double-strand break repair during meiotic prophase progression. PLoS Genet 3: e191 doi:10.1371/journal.pgen.0030191.

23. Dernburg AF, McDonald K, Moulder G, Barstead R, Dresser M, et al. (1998) Meiotic recombination in C. elegans initiates by a conserved mechanism and is dispensable for homologous chromosome synapsis. Cell 94: 387–398. doi: 10.1016/s0092-8674(00)81481-6

24. Colaiácovo MP, MacQueen AJ, Martinez-Perez E, McDonald K, Adamo A, et al. (2003) Synaptonemal complex assembly in C. elegans is dispensable for loading strand-exchange proteins but critical for proper completion of recombination. Dev Cell 5: 463–474. doi: 10.1016/s1534-5807(03)00232-6

25. Hodgkin J, Horvitz HR, Brenner S (1979) Nondisjunction Mutants of the Nematode CAENORHABDITIS ELEGANS. Genetics 91: 67–94.

26. Boulton SJ, Martin JS, Polanowska J, Hill DE, Gartner A, et al. (2004) BRCA1/BARD1 orthologs required for DNA repair in Caenorhabditis elegans. Current Biology 14: 33–39. doi: 10.1016/j.cub.2003.11.029

27. Adamo A, Montemauri P, Silva N, Ward JD, Boulton SJ, et al. (2008) BRC-1 acts in the inter-sister pathway of meiotic double-strand break repair. EMBO Rep 9: 287–292 doi:10.1038/sj.embor.7401167.

28. Deans AJ, West SC (2011) DNA interstrand crosslink repair and cancer. Nat Rev Cancer 11: 467–480 doi:10.1038/nrc3088.

29. Long DT, Räschle M, Joukov V, Walter JC (2011) Mechanism of RAD51-dependent DNA interstrand cross-link repair. Science 333: 84–87 doi:10.1126/science.1204258.

30. Ciccia A, Elledge SJ (2010) The DNA damage response: making it safe to play with knives. Mol Cell 40: 179–204 doi:10.1016/j.molcel.2010.09.019.

31. Roerink SF, Koole W, Stapel LC, Romeijn RJ, Tijsterman M (2012) A Broad Requirement for TLS Polymerases η and κ, and Interacting Sumoylation and Nuclear Pore Proteins, in Lesion Bypass during C. elegans Embryogenesis. PLoS Genet 8: e1002800 doi:10.1371/journal.pgen.1002800.

32. Clejan I, Boerckel J, Ahmed S (2006) Developmental modulation of nonhomologous end joining in Caenorhabditis elegans. Genetics 173: 1301–1317 doi:10.1534/genetics.106.058628.

33. Jackson SP, Bartek J (2009) The DNA-damage response in human biology and disease. Nature 461: 1071–1078 doi:10.1038/nature08467.

34. Kipreos ET (2005) C. elegans cell cycles: invariance and stem cell divisions. Nat Rev Mol Cell Biol 6: 766–776 doi:10.1038/nrm1738.

35. Edgar LG, McGhee JD (1988) DNA synthesis and the control of embryonic gene expression in C. elegans. Cell 53: 589–599. doi: 10.1016/0092-8674(88)90575-2

36. Bailly AP, Freeman A, Hall J, Déclais A-C, Alpi A, et al. (2010) The Caenorhabditis elegans homolog of Gen1/Yen1 resolvases links DNA damage signaling to DNA double-strand break repair. PLoS Genet 6: e1001025 doi:10.1371/journal.pgen.1001025.

37. Krisko A, Radman M (2010) Protein damage and death by radiation in Escherichia coli and Deinococcus radiodurans. Proc Natl Acad Sci USA 107: 14373–14377 doi:10.1073/pnas.1009312107.

38. Pierce AJ, Johnson RD, Thompson LH, Jasin M (1999) XRCC3 promotes homology-directed repair of DNA damage in mammalian cells. Genes Dev 13: 2633–2638. doi: 10.1101/gad.13.20.2633

39. Helleday T, Lo J, van Gent DC, Engelward BP (2007) DNA double-strand break repair: from mechanistic understanding to cancer treatment. DNA Repair 6: 923–935 doi:10.1016/j.dnarep.2007.02.006.

40. Hedgecock EM, White JG (1985) Polyploid tissues in the nematode Caenorhabditis elegans. Dev Biol 107: 128–133. doi: 10.1016/0012-1606(85)90381-1

41. Pontier DB, Tijsterman M (2009) A robust network of double-strand break repair pathways governs genome integrity during C. elegans development. Current biology: CB 19: 1384–1388 doi:10.1016/j.cub.2009.06.045.

42. Youds JL, Mets DG, McIlwraith MJ, Martin JS, Ward JD, et al. (2010) RTEL-1 enforces meiotic crossover interference and homeostasis. Science 327: 1254–1258 doi:10.1126/science.1183112.

43. Gartner A, Milstein S, Ahmed S, Hodgkin J, Hengartner MO (2000) A conserved checkpoint pathway mediates DNA damage–induced apoptosis and cell cycle arrest in C. elegans. Mol Cell 5: 435–443. doi: 10.1016/s1097-2765(00)80438-4

44. Moser SC, Elsner von S, Büssing I, Alpi A, Schnabel R, et al. (2009) Functional dissection of Caenorhabditis elegans CLK-2/TEL2 cell cycle defects during embryogenesis and germline development. PLoS Genet 5: e1000451 doi:10.1371/journal.pgen.1000451.

45. Schumacher B, Hofmann K, Boulton S, Gartner A (2001) The C. elegans homolog of the p53 tumor suppressor is required for DNA damage-induced apoptosis. Current biology: CB 11: 1722–1727. doi: 10.1016/s0960-9822(01)00534-6

46. Conradt B, Horvitz HR (1998) The C. elegans protein EGL-1 is required for programmed cell death and interacts with the Bcl-2-like protein CED-9. Cell 93: 519–529. doi: 10.1016/s0092-8674(00)81182-4

47. Hillers KJ, Villeneuve AM (2003) Chromosome-wide control of meiotic crossing over in C. elegans. Current biology: CB 13: 1641–1647 doi:10.1016/j.cub.2003.08.026.

48. Miller KM, Tjeertes JV, Coates J, Legube G, Polo SE, et al. (2010) Human HDAC1 and HDAC2 function in the DNA-damage response to promote DNA nonhomologous end-joining. Nat Struct Mol Biol doi:10.1038/nsmb.1899.

49. Smeenk G, Wiegant WW, Vrolijk H, Solari AP, Pastink A, et al. (2010) The NuRD chromatin-remodeling complex regulates signaling and repair of DNA damage. J Cell Biol

50. Chou DM, Adamson B, Dephoure NE, Tan X, Nottke AC, et al. (2010) A chromatin localization screen reveals poly (ADP ribose)-regulated recruitment of the repressive polycomb and NuRD complexes to sites of DNA damage. Proc Natl Acad Sci USA 107: 18475–18480 doi:10.1073/pnas.1012946107.

51. Facchino S, Abdouh M, Chatoo W, Bernier G (2010) BMI1 confers radioresistance to normal and cancerous neural stem cells through recruitment of the DNA damage response machinery. J Neurosci 30: 10096–10111 doi:10.1523/JNEUROSCI.1634-10.2010.

52. Ginjala V, Nacerddine K, Kulkarni A, Oza J, Hill SJ, et al. (2011) BMI1 is recruited to DNA breaks and contributes to DNA damage-induced H2A ubiquitination and repair. Mol Cell Biol 31: 1972–1982 doi:10.1128/MCB.00981-10.

53. Luijsterburg MS, Dinant C, Lans H, Stap J, Wiernasz E, et al. (2009) Heterochromatin protein 1 is recruited to various types of DNA damage. J Cell Biol 185: 577–586 doi:10.1083/jcb.200810035.

54. Ismail IH, Andrin C, McDonald D, Hendzel MJ (2010) BMI1-mediated histone ubiquitylation promotes DNA double-strand break repair. J Cell Biol 191: 45–60 doi:10.1083/jcb.201003034.

55. Pan M-R, Peng G, Hung W-C, Lin S-Y (2011) Monoubiquitination of H2AX Protein Regulates DNA Damage Response Signaling. J Biol Chem 286: 28599–28607 doi:10.1074/jbc.M111.256297.

56. Trojer P, Cao AR, Gao Z, Li Y, Zhang J, et al. (2011) L3MBTL2 protein acts in concert with PcG protein-mediated monoubiquitination of H2A to establish a repressive chromatin structure. Mol Cell 42: 438–450 doi:10.1016/j.molcel.2011.04.004.

57. Iacovoni JS, Caron P, Lassadi I, Nicolas E, Massip L, et al. (2010) High-resolution profiling of gammaH2AX around DNA double strand breaks in the mammalian genome. EMBO J 29: 1446–1457 doi:10.1038/emboj.2010.38.

58. Shanbhag NM, Rafalska-Metcalf IU, Balane-Bolivar C, Janicki SM, Greenberg RA (2010) ATM-dependent chromatin changes silence transcription in cis to DNA double-strand breaks. Cell 141: 970–981 doi:10.1016/j.cell.2010.04.038.

59. Brenner S (1974) The genetics of Caenorhabditis elegans. Genetics 77: 71–94.

60. Hofmann ER, Milstein S, Boulton SJ, Ye M, Hofmann JJ, et al. (2002) Caenorhabditis elegans HUS-1 is a DNA damage checkpoint protein required for genome stability and EGL-1-mediated apoptosis. Current Biology 12: 1908–1918. doi: 10.1016/s0960-9822(02)01262-9

61. Barber LJ, Youds JL, Ward JD, McIlwraith MJ, O'Neil NJ, et al. (2008) RTEL1 maintains genomic stability by suppressing homologous recombination. Cell 135: 261–271 doi:10.1016/j.cell.2008.08.016.

62. Polanowska J, Martin JS, Garcia-Muse T, Petalcorin MIR, Boulton SJ (2006) A conserved pathway to activate BRCA1-dependent ubiquitylation at DNA damage sites. EMBO J 25: 2178–2188 doi:10.1038/sj.emboj.7601102.

63. Dmitrieva NI, Celeste A, Nussenzweig A, Burg MB (2005) Ku86 preserves chromatin integrity in cells adapted to high NaCl. Proc Natl Acad Sci USA 102: 10730–10735 doi:10.1073/pnas.0504870102.

64. Saito TT, Youds JL, Boulton SJ, Colaiácovo MP (2009) Caenorhabditis elegans HIM-18/SLX-4 interacts with SLX-1 and XPF-1 and maintains genomic integrity in the germline by processing recombination intermediates. PLoS Genet 5: e1000735 doi:10.1371/journal.pgen.1000735.

4

PNN-1 and UAF-1 link RNA splicing to DNA repair by Non-Homologous End Joining

Lemmens BB, van Schendel R, Tijsterman M.

Abstract

Non-homologous End Joining (NHEJ) is the major DNA double strand break (DSB) repair route in somatic tissues and is vital to ensure genomic stability and proper animal development. Accordingly, NHEJ deficiency syndromes are characterized by severe developmental abnormalities and hypersensitivity to DSB-inducing agents such as ionizing radiation (IR). Given its highly effective but error-prone nature, NHEJ needs to be tightly regulated during development. In recent years RNA binding proteins (RBPs) have emerged as important regulator of genome stability, yet how and if they control DSB repair is unknown to date. Here, we constructed a transgenic reporter assay in *C. elegans* that allows detection of NHEJ activity *in vivo* and performed unbiased forward genetics screens to identify novel regulators of NHEJ. We found the THO ribonucleoprotein complex (*thoc-2*, *thoc-5* and *thoc-7*) and the RNA splicing regulator Pinin (*pnn-1*) to be required for efficient NHEJ and IR resistance in somatic tissues. In-depth transcriptome analysis revealed strikingly similar RNA expression alterations among the NHEJ mutants, including exon-specific splicing defects. Moreover, we found THO mutants to suffer from reduced expression of the essential splicing factor U2AF65 (*uaf-1*) of which depletion by RNA interference mimics the DSB repair defects in THO mutants. The identification of the splicing factors PNN-1 and UAF-1 in NHEJ regulation sets the stage for further dissection of RNA processing mechanisms during animal development and implicates potentially new roles of alternative RNA transcripts in DSB repair.

Introduction

During animal development cells are exposed to numerous DNA damaging agents that may hamper cellular function, ultimately leading to developmental defects, pathologies and reduced fitness. One of the most toxic DNA lesions a cell can encounter is a DNA double strand break (DSB); left unrepaired a DSB can cause chromosome segregation defects and cell death and its incorrect repair can lead to gross chromosomal aberrations, including deletions and translocations that promote oncogenic transformation (McKinnon and Caldecott 2007). To neutralize the toxic effects of DSBs an elaborate network of proteins has evolved that either can repair the damage or minimalize the consequences for animal development (Phillips and McKinnon 2007). Recent proteomic studies have revealed a vast amount of proteins being post-translationally modified upon DSB induction, including factors required for DSB repair, cell cycle arrest, chromatin modification and apoptosis (Aslanian *et al.* 2014; Beli *et al.* 2012; Jungmichel and Blasius 2013; Jungmichel *et al.* 2013; Matsuoka *et al.* 2007). Surprisingly, another major class of proteins modified during the DNA damage response consists of RNA binding proteins (RBPs), yet if and how these RBPs affect DSB repair is still an open question (Dutertre *et al.* 2014; Lenzken *et al.* 2013).

Eukaryotic cells posses a versatile toolbox of DNA repair factors that can act in different chromatin contexts, cell cycle stages and on a wide range of DNA substrates and repair templates. Accordingly, DSBs can be repaired via several different repair mechanisms, including non-homologous end joining (NHEJ), homologous recombination (HR) or single strand annealing (SSA), which all have unique abilities and limitations. For instance, NHEJ can seal DSBs independent of DNA sequence context, while both HR and SSA require a homologous DNA template to repair DSBs.

NHEJ is the major DSB repair route in human cells and also the pathway of choice in somatic tissues of the animal model *Caenorhabditis elegans (C. elegans) (Clejan et al. 2006; Lieber 2010)*. The core NHEJ machinery is well conserved and is based on DSB recognition by the Ku70/Ku80 heterodimer (CKU-70/CKU-80 in *C. elegans*) and subsequent recruitment of DNA ligase IV (LIG-4), which seals the break. Although this pathway is very efficient, there is no quality control and occasionally some nucleotides are lost or inserted, making it an error-prone repair route. Reduced *in vivo* NHEJ activity is associated with several human developmental disorders and is characterized by cellular radiosensitivity, microcephaly and severe immunodeficiency due to loss of NHEJ-dependent genetic variation among lymphocytes (McKinnon and Caldecott 2007). Although DSB repair via NHEJ is crucial to maintain genomic stability during development, it can also have detrimental toxic effects when left unrestrained. In fact, uncontrolled NHEJ activities can corrupt error-free repair by HR, promoting chromosomal abnormalities, tumorigenesis and infertility in animals (Adamo *et al.* 2010; Bunting *et al.* 2010; Lemmens *et al.* 2013). The activity of DSB repair pathways can

be regulated in many ways, for instance at the level of the DNA substrate chromatin status or protein modification, but also at the level of mRNA expression, localization and stability (Chapman *et al.* 2012; Hu and Gatti 2011; Lenzken *et al.* 2013).

In order to identify new regulators of NHEJ activity during animal development we performed an unbiased forward genetics screen in *C. elegans*. We constructed a dual reporter-based assay that allowed us to read-out NHEJ activity *in vivo* and identified both known NHEJ genes as well as factors not implicated in NHEJ before. Notably, we found three components of the THO ribonucleoprotein complex (*thoc-2*, *thoc-5* and *thoc-7*) and splicing-regulator Pinin (*pnn-1*) to be required for NHEJ in *C. elegans*, implying an important role for RBPs for NHEJ efficacy during development. Next to defective repair of endonuclease-induced DSBs, all mutants identified were hypersensitive to ionizing radiation (IR) during development, a characteristic also seen in NHEJ deficient human patients (Dvorak and Cowan 2010). Epistasis analysis with canonical NHEJ mutants confirmed a specific requirement for repair via NHEJ for these RBPs. To investigate possible effects on mRNA stability of canonical NHEJ factors, we performed genome-wide RNAseq in *thoc-5*, *thoc-7* and *pnn-1* mutants and found a small but very specific subset of transcripts to be affected in these mutant backgrounds. In-dept expression analysis revealed striking similarity between both THO and PNN-1 mutants including exon-specific splicing defects. Interestingly, we found the expression of the essential splicing factor UAF-1/U2AF to be reduced in THO mutants and UAF-1 depletion mimics the DSB repair defects in THO mutants, including reduced NHEJ and increased SSA activity. All together these results reveal a close link between mRNA splicing and *in vivo* NHEJ activity and set the stage for the analysis of potential novel mRNA isoforms that control DSB repair efficacy.

Results

Dual reporter system to measure NHEJ activity in *C. elegans*

In recent years the *C. elegans* model system has become a powerful tool to study DNA damage responses in a developmental context, leading to important insights in DSB repair in somatic as well as germline tissues (Lemmens and Tijsterman 2011). While classical DNA damage sensitivity assays and transgenic reporter systems uncovered robust and tissue-specific DSB repair mechanisms (Clejan *et al.* 2006; Pontier and Tijsterman 2009), cytological approaches revealed several regulators of DSB repair pathway choice, including suppressors of NHEJ (Adamo *et al.* 2010; Lemmens *et al.* 2013). We recently developed a variety of transgenic reporter systems based on site-specific DSB induction by the I-SceI meganuclease, which allowed us to measure both HR and SSA activities during worm development (Johnson *et al.* 2013; Pontier and Tijsterman 2009). Although these reporter systems can be used to examine HR and SSA activity directly, they can also be used to study NHEJ in an indirect manner, given that NHEJ defects result in a stark increase in compensatory pathways such as HR and SSA

(Johnson *et al.* 2013; Pontier and Tijsterman 2009). Yet such indirect measurements can be obscured by other repair defects that result in similar shifts in pathway usage, e.g. defective HR can also increase SSA activity.

We therefore developed a new I-SceI-based reporter that measures classical NHEJ activity directly (Figure 1A). This NHEJ reporter is based on restored expression of an out-of-frame GFP/LacZ sequence due to mutagenic repair of an upstream I-SceI target site: error-prone repair by NHEJ resulting in +1 or -2 frame shifts results in pharyngeal GFP/LacZ expression. We chose to measure DSB repair in pharyngeal muscle tissue because these cells are already terminally differentiated at the first larval stage and in contrast to cycling cells lack alternative end joining activities (D. Pontier and M. Tijsterman unpublished data). This provides us the unique possibility to measure mutagenic end joining *in vivo* that depends completely on classical NHEJ. Accordingly, DSB induction during larval development resulted in robust pharyngeal GFP/LacZ expression that was completely abolished by *lig-4* mutation (Figure 1B). To internally control for NHEJ efficacy within the same animal we combined the NHEJ reporter transgene with a well-characterized SSA reporter transgene, creating a dual reporter system that can detect *in vivo* NHEJ activity directly (by measuring NHEJ in non-replicating pharyngeal cells) and indirectly (by measuring SSA in various replicating somatic cells). We combined both reporter transgenes with a heat-shock inducible mCherry I-SceI fusion transgene allowing us to govern and monitor nuclear meganuclease expression (Figure 1A and 1C).

Inactivating NHEJ in dual reporter animals by *lig-4* mutation resulted in a dramatic shift in LacZ staining pattern: while LacZ staining disappeared in the pharynx, LacZ staining increased strongly in various other somatic tissues. Moreover, this pattern was extremely robust among reporter animals: while 0% of *lig-4* mutants showed GFP/LacZ positive pharynxes, nearly 100% of wild-type animals showed pharyngeal GFP/LacZ ORF correction within 24 hours post DSB induction (Figure 1D).

Forward genetics screen for regulators of NHEJ

Having such a distinct phenotype depending on classical NHEJ provided us with the opportunity to search for possible new regulators of NHEJ. To this end, we performed forward genetics screens in which we induced random mutations in dual reporter animals by ethyl methanesulfonate (EMS) and assessed NHEJ activity among mutant progeny (*i.e.* complex F3 populations were screened for animals with reduced pharyngeal GFP signal) (Figure 1E and S1). These GFP^{low} animals were selected and their clonal progeny was again tested for NHEJ activity to exclude stochastic events and identify heritable traits that affect pharyngeal GFP expression. To exclude false-positive mutants with reduced DSB induction or defective NHEJ transgenes we analyzed mCherry-I-SceI expression as well as SSA activity in all mutant candidates. Only NHEJ mutants that also showed increased SSA activity, indicative of repair defects post DSB induction, were selected for further analysis (Figure 1E).

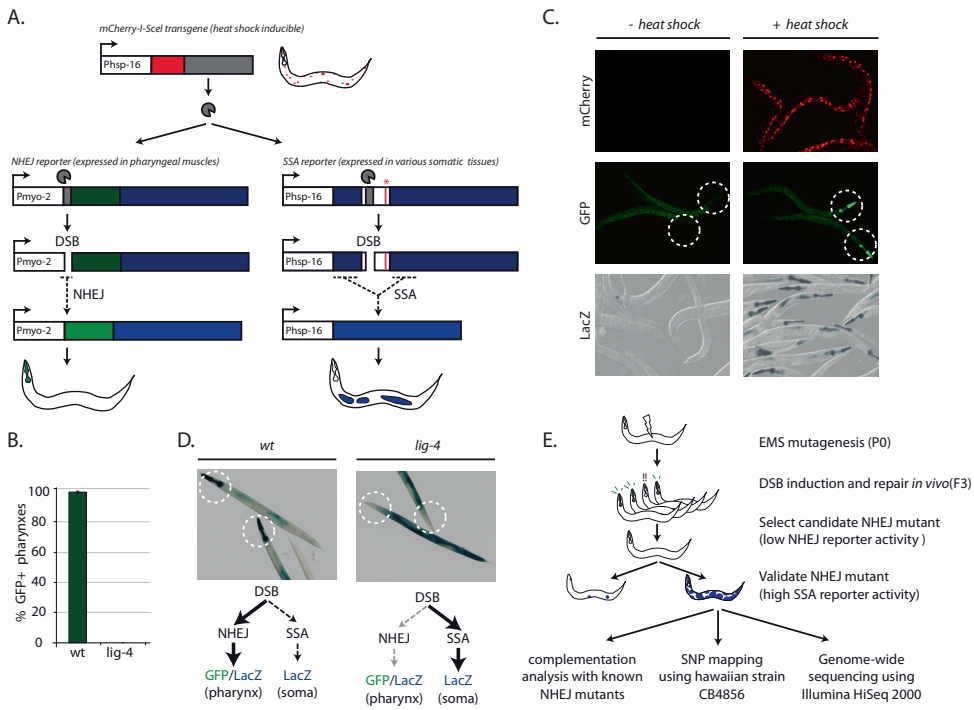

Figure 1. Dual reporter assay to measure NHEJ activity in developing *C. elegans*
A. Schematic diagram of dual reporter system based on heat-shock-inducible expression of mCherry::I-SceI and DSB repair-mediated ORF restoration at two multi-copy reporter transgenes. Mutagenic NHEJ is measured by GFP/LacZ ORF correction in non-dividing pharyngeal cells, while SSA is measured by LacZ ORF correction in dividing somatic cells. Asterisk indicates stop codon. **B.** Quantification of GFP-positive pharynxes in synchronized wild-type and *lig-4* deficient dual reporter animals, heat-shocked for 180 minutes at L1 stage and measured in adults. Average of three populations (n>200) is depicted; error bars represent S.E.M. **C.** Representative pictures of animals expressing nuclear mCherry::I-SceI (6 hours post adult heat-shock), pharyngeal GFP (3 days post L1 heat-shock, yet prior to adult heat-shock) and somatic LacZ (3 hours post adult heat-shock). Synchronized animals were heat-shocked for 180 minutes at L1 stage (to induce I-SceI expression /DSB formation) and at adult stage (to express the SSA reporter). **D.** LacZ expression patterns 3 hours post adult heat-shock of synchronized wild-type and *lig-4* deficient dual reporter animals, heat-shocked for 180 minutes at L1 and adult stage. **E.** Setup of forward genetics screen (more elaborate setup is depicted in Figure S1).

By screening ~9000 haploid genomes we found seven *bona fide* NHEJ mutants: four showing reduced GFP expression and three showing no pharyngeal GFP at all. We next quantified both NHEJ activity (GFP expression) and SSA activity (somatic LacZ expression) of synchronized mutant populations and observed the expected inverse correlation between NHEJ defect severity and increased compensatory SSA activity: *lf151*, *lf152* and *lf153* having no detectable NHEJ activity and a strong (>4-fold) increase in SSA activity, and *lf158*, *lf160* and *lf161* having detectable but significantly reduced NHEJ activity and a milder (~3-fold) increase in SSA activity (Figure 2A). The seventh mutant *lf159* was also characterized in detail

but these results will be discussed later. All together these results indicate that our screening setup allowed us to find null alleles for essential NHEJ factors as well as modifier alleles that either partially impair essential NHEJ factors or fully block the function of non-essential NHEJ regulators.

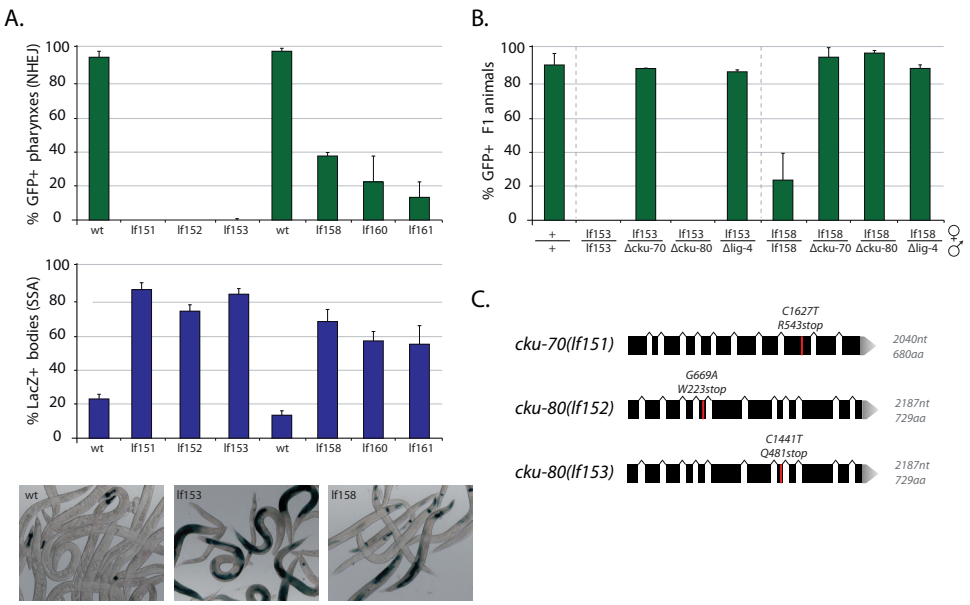

Figure 2. Characterization and complementation analysis of novel NHEJ mutants
A. Quantification of GFP-positive pharynxes and non-pharyngeal LacZ staining in clonal mutant populations of synchronized dual reporter animals, heat-shocked for 120 minutes at L1 and adult stage and measured in adults. Average of three populations (n>200) is depicted; error bars represent S.E.M. Lower panels depict LacZ expression patterns three hours post adult heat-shock. **B.** Quantification of GFP-positive pharynxes in trans-heterozygous F1 cross progeny, heat-shocked for 120min and measured in adults. Average percentage of GFP-positive pharynxes of three independent F1 populations is depicted. **C.** Gene models and newly identified alleles of *cku-70* and *cku-80*.

Screen validation

In order to identify the causal mutations and test if the new alleles affected the function of known NHEJ genes in *C. elegans*, we performed complementation analysis using null alleles of *lig-4*, *cku-80* and *cku-70*. All six mutants were crosses with *lig-4*, *cku-80* and *cku-70* mutant males and the trans-heterozygous F1 progeny was tested for NHEJ activity. As illustrated in Figure 2B, NHEJ activity of the *lf153* allele could be rescued by *lig-4* and *cku-70* mutant males, but not but *cku-80* mutants, implying that *lf153* affected *cku-80* function. Indeed, sequencing analysis of *lf153* mutants revealed a typical EMS induced C>T transversion in *cku-80*, leading to a premature stop codon that prevents expression of the well conserved C-terminus of CKU-80. Similarly, we found the NHEJ defect in *lf151* and *lf152* mutants to be caused by nonsense

mutations in *cku-70* and *cku-80*, respectively (Figure 2C). The identification of canonical NHEJ genes using this unbiased approach validated both our dual reporter system as well as our screening setup. Interestingly, although the NHEJ defect of all three null alleles *lf151, lf15*2 and *lf153* could be explained by mutations in known NHEJ genes, the NHEJ defect of the modifier alleles *lf158*, *lf160* and *lf161* was not caused by mutations in canonical NHEJ genes. For instance, paternally derived genomes containing *cku-70*, *cku-80* or *lig-4* null alleles could still restore NHEJ activity in *lf158* trans-heterozygotes (Figure 2B). These results suggest that we also picked up mutations in genes not described before to regulate NHEJ during *C. elegans* development.

THO complex is required for efficient NHEJ in *C. elegans*

To find the causal mutations in the NHEJ modifier strains we combined classical positional mapping and next generation sequencing techniques. We mapped the chromosomal regions responsible for the NHEJ defect using single nucleotide polymorphisms (SNPs) between a Hawaiian mapping strain CB4856 and Bristol dual reporter mutants, and found the causal genes of *lf158* and *lf161* to be located on the center of chromosome III and *lf161* on the right arm of chromosome IV (Figure 3A). Although located on the same chromosome, complementation analysis between *lf158* and *lf161* revealed that the causal mutations were in different genes (data not shown). Parallel to the mapping studies we used whole-genome sequencing to find non-synonymous SNPs that were unique for every mutant and were located in the mapped regions, culminating to a relatively small set of 4-7 candidate genes per mutant. Strikingly, we found that all three mutants carried a candidate mutation in a gene belonging to the THO complex, strongly suggesting that defective THO complex function was causing reduced NHEJ activity in *C. elegans* (Figure 3A).

The THO complex is a highly conserved ribonucleoprotein complex that has been implicated in transcription elongation, non-coding RNA metabolism, mRNA splicing and mRNA export (Luna *et al.* 2012). Intriguingly, defective THO complex function is shown to result in genome instability in various species, including yeast, worms and man, which in part could be explained by its role in preventing the formation of RNA:DNA hybrids throughout the genome (Castellano-Pozo *et al.* 2012b; Dominguez-Sanchez *et al.* 2011; Huertas and Aguilera 2003). The identification of several THO mutants in our NHEJ screen adds another possible link between these conserved RBPs and genome instability.

Here we identified a missense mutation in *thoc-2* (*lf158*) and *thoc-7* (*lf160*) and a nonsense mutation in *thoc-5* (*lf161*). While both the *thoc-5* and *thoc-7* alleles affected highly conserved residues and thus may reflect null alleles, the *thoc-2* allele affected a non-conserved amino acid, likely retaining some THOC-2 activity (Figure 3B). In fact, *lf158* animals are fertile while *thoc-2* null mutants are reported to be completely sterile, suggesting that we acquired either a hypomorfic or separation-of-function allele of *thoc-2* (Castellano-Pozo *et al.* 2012b).

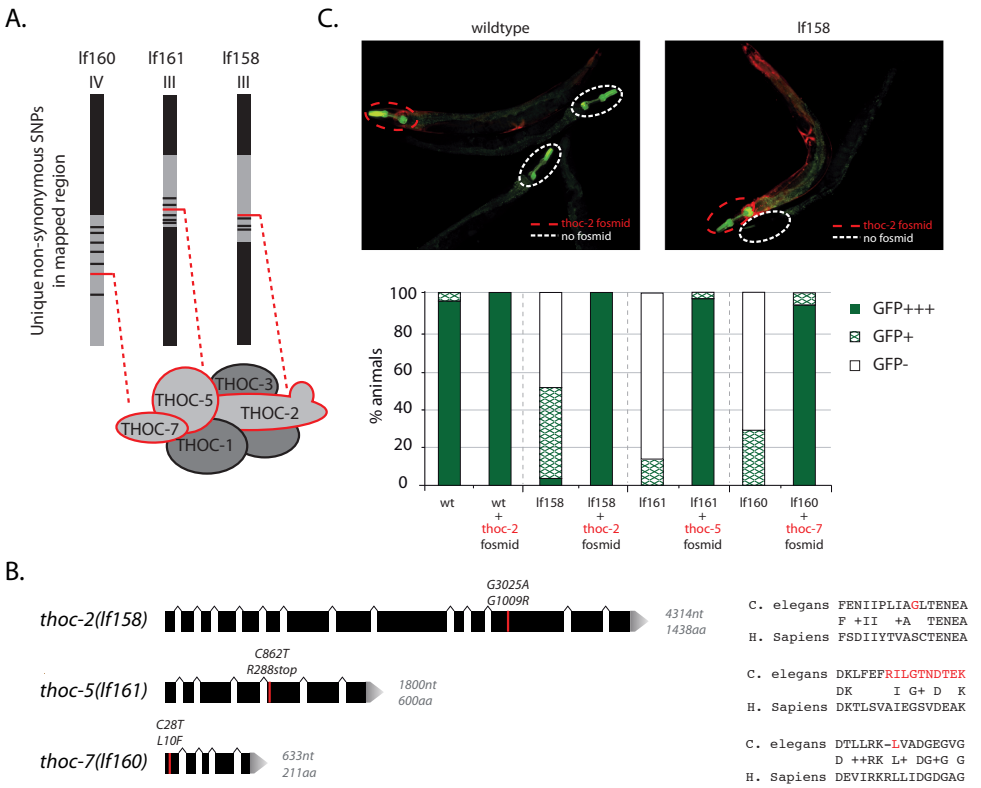

Figure 3. THO mutations cause reduced NHEJ activity in *C. elegans*
A. Schematic diagram of chromosomes III and IV in three NHEJ mutants; regions found to cause NHEJ defect based on Hawaiian SNP mapping in grey; black/red horizontal lines represent unique non-synonymous mutations. All three mutants bear mutations in THO genes **B.** Gene models and newly identified alleles of *thoc-2*, *thoc-5* and *thoc-7*. Right panel depicts amino acid context and conservation of THO mutations. **C.** Complementation analysis using fosmid arrays carrying wild-type THO genes and mCherry expression markers. Representative picture of synchronized populations of wildtype and lf158 animals with (red circle) or without (white circle) *thoc-2* fosmid array; animals were heat-shocked for 180 minutes at L1 stage. Histogram shows quantification of GFP-positive pharynxes in adults of the different genetic backgrounds. NHEJ activity was restored to wild-type levels by complementing the THO mutants with functional THO genes. Average percentage of GFP-positive pharynxes of three independent populations (n>150) is depicted.

To establish causality between the THO complex mutations and *in vivo* NHEJ efficacy we set out to complement the mutant dual reporter worms with functional THO genes. We performed fosmid microinjections to create animals carrying inheritable extra-chromosomal arrays harboring wild-type gene products of the mutated THO genes (Figure S2). These extra-chromosomal arrays also carried mCherry expression markers to be able to identify transgenic animals that express the functional THO genes. We next crossed the mCherry-marked fosmid arrays to the corresponding mutants: a *thoc-2* expression array to *lf158* animals, a *thoc-5*

expression array to *lf161* animals, and a *thoc-7* expression array to *lf161* animals. Both THO mutant and wild-type counterparts were isolated from each cross and NHEJ activity was measured in mCherry positive as well as mCherry negative progeny. Importantly, the presence of functional THO genes NHEJ activity in all three corresponding mutants, indicating that the NHEJ defect in these animals was indeed caused by impaired THO complex function (Figure 3C). Furthermore, we confirmed NHEJ restoration in complemented animals by analyzing SSA reporter activity and found somatic LacZ expression to be reduced in complemented animals ($mCherry^+$) compared to THO mutant controls ($mCherry^-$), further supporting a specific role for THO complex genes in NHEJ and DSB repair dynamics (Figure S3A). Moreover, we could increase SSA activity by reducing THOC-2 expression by RNA interference, suggesting that reduced THO gene expression, like THO gene mutations, affects NHEJ efficacy *in vivo* (Figure S3B).

PCR-based assay confirms role for the THO complex in mutagenic NHEJ

We next assayed DSB repair more directly and independent of reporter transcription via a PCR-based assay (Figure 4A). We heat-shocked synchronized L1 larva of two wild-type controls and four different NHEJ mutants (*i.e.* two Ku complex mutants and two THO complex mutants) to induce I-SceI expression and create DSBs at the NHEJ reporter locus. After allowing *in vivo* DSB repair for 24 hours, we isolated genomic DNA of all larva and PCR-amplified the genomic region surrounding the I-SceI target site. Subsequently, the PCR products were digested *in vitro* with recombinant I-SceI enzyme and restriction products were resolved on a polyacrylamide gel. As shown in Figure 4B, PCR products derived from non-heat-shocked animals were all susceptible to I-SceI cleavage, which indicated that the I-SceI site was intact in all the strains prior to DSB induction. However, after heat-shock induction different digestion patterns became apparent: while the majority of PCR products (~67%) derived from wild-type control animals became resistant to I-SceI cleavage (suggestive of mutagenic repair events at the DSB site), nearly all PCR products derived from both Ku mutants were susceptible to I-SceI cleavage (Figure 4C). This indicates that the resistant fraction in wild-type animals is dependent on Ku and likely reflects the error-pone activity of classical NHEJ. Notably, the majority of PCR products derived from both *thoc-5* and *thoc-7* mutants was still susceptible to I-SceI cleavage and only a minor fraction was I-SceI resistant (~36%), indicating that some mutagenic NHEJ activity is still present in these animals but that this activity is significantly reduced compared to wild-type animals (Figure 3C). Accordingly, both these THO mutants are able to restore GFP expression in an I-SceI dependent manner, but do so at a severely reduced level compared to wild-type animals (Figure 1 and 2).

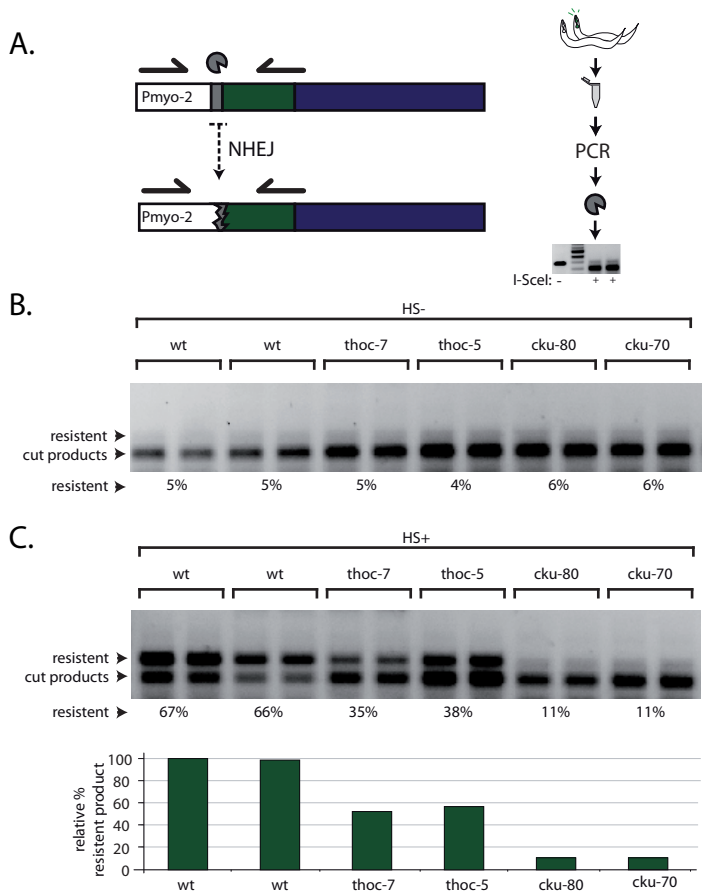

Figure 4. PCR-based assay confirms reduced mutagenic DSB repair in THO mutants
A. Setup of PCR-based assay to measure mutagenic DSB repair at NHEJ reporter transgene. Genomic I-SceI target sites of synchronized heat-shocked populations were PCR amplified and digested *in vitro* with recombinant I-SceI enzyme. Mutagenic repair of I-SceI-induced DSBs *in vivo* creates I-SceI resistant PCR products. **B.** Representative gel and band intensity quantification of I-SceI resistant fractions of synchronized untreated animals (non-heat shock controls). **C.** Representative gel and band intensity quantification of I-SceI resistant fractions of synchronized animals heat-shocked twice for 180 minutes. Histogram depicts I-SceI resistant fractions relative to wild-type controls (reflecting mutagenic DSB repair activity).

THO deficient somatic tissues are hypersensitive to IR

Given the NHEJ defect at endonuclease-induced DSBs in THO mutant animals, we wondered if the THO complex was also needed for efficient repair of DSBs inflicted throughout the genome by IR. IR sensitivity can be read-out by two different assays in *C. elegans*: a so-called 'L1 assay' in which somatic cells of L1 larva are irradiated and consequent developmental defects are analyzed, or a 'L4 assay' in which germ cells of L4 larva are irradiated and progeny

survival is analyzed (Figure 5A). While NHEJ mutants are hypersensitive in the L1 assay, most HR mutants are not, reflecting the key role of NHEJ in DSB repair in somatic cells (Clejan *et al.* 2006). In contrast, HR mutants are typically hypersensitive in the L4 assay, while NHEJ mutants are not, reflecting the strong HR bias in germ cells (Clejan *et al.* 2006; Johnson *et al.* 2013; Robert *et al.* 2008).

In line with previous studies, we found animals deficient for BRC-1 (the ortholog of well-established human HR factor BRCA1) to be hypersensive to IR in the L4 assay, while animals lacking the canonical NHEJ factor CKU-80 behaved like wild-types in this assay (Figure 5B) (Johnson *et al.* 2013; Lemmens *et al.* 2013). Similar to NHEJ mutants, germ cells defective for THOC-5 or THOC-7 were not hypersensitive to IR, indicating that lack of these THO factors does not sensitize genomes to IR *per se* (Figure 5B). However, when we subjected these animals to the L1 assay, we observed the inverse pattern. While *brc-1* mutants showed a very mild increase in IR-induced somatic defects, *cku-80, thoc-5* and *thoc-7* mutants were very sensitive in this assay, resulting into ~75%, 65% and 55% of animals having defective vulva development after 60Gy of IR, respectively (Figure 5C). Similar to canonical NHEJ mutants, *thoc-5* and *thoc-7* mutants showed various IR-dependent vulval defects, including protruding vulvas, ruptured vulvas and so-called “bag-of-worms” where progeny hatches within the mother because of an egg laying defect, all culminating to less progeny on the plate (Figure 5D). These data indicate that THOC-5 and THOC-7 are needed for IR resistance in somatic cells, like the vulval precursor cells, but not in germ cells, suggesting a specific need for the THO complex in DSB repair via NHEJ. This notion is also strongly supported by our previous data acquired via the transgenic DSB repair assays, where these THO mutants were specifically defective for NHEJ but not in other repair pathways such as SSA (Figure 2A). Moreover, both the IR sensitivity assays and the I-SceI-based reporter assays revealed a partial defect in NHEJ in THO mutants compared to CKU-80 null mutants, indicating that these THO alleles do not completely abolish THO function or that the THO complex promotes NHEJ in a non-essential manner.

While the read-out for *in vivo* NHEJ activity using the transgenic reporter system was completely saturated in NHEJ null mutants (showing no pharyngeal GFP at all), the L1 assay (measuring vulval defects) was not saturated, even when NHEJ was completely abolished (Figure 1 and 5). This attribute of the L1 assay allowed us to do epistasis analysis between the different NHEJ mutants and delineate the pathways involved. We created *thoc-5 thoc-7* and *cku-80; thoc-7* double mutants and analyzed IR sensitivity parallel to the single mutants described above. As expected, we found the *thoc-5; thoc-7* double mutants and *thoc-5* single mutants to be equally sensitive to IR, implying that THOC-5 and THOC-7 act in the same pathway/protein complex that confers IR resistance (Figure 5E). Notably, we also found *cku-80; thoc-7* double mutants and *cku-80* single mutants to be equally sensitive to IR, indicating that CKU-80 and THOC-7 also act in the same pathway that confers IR resistance in somatic cells (Figure 5F).

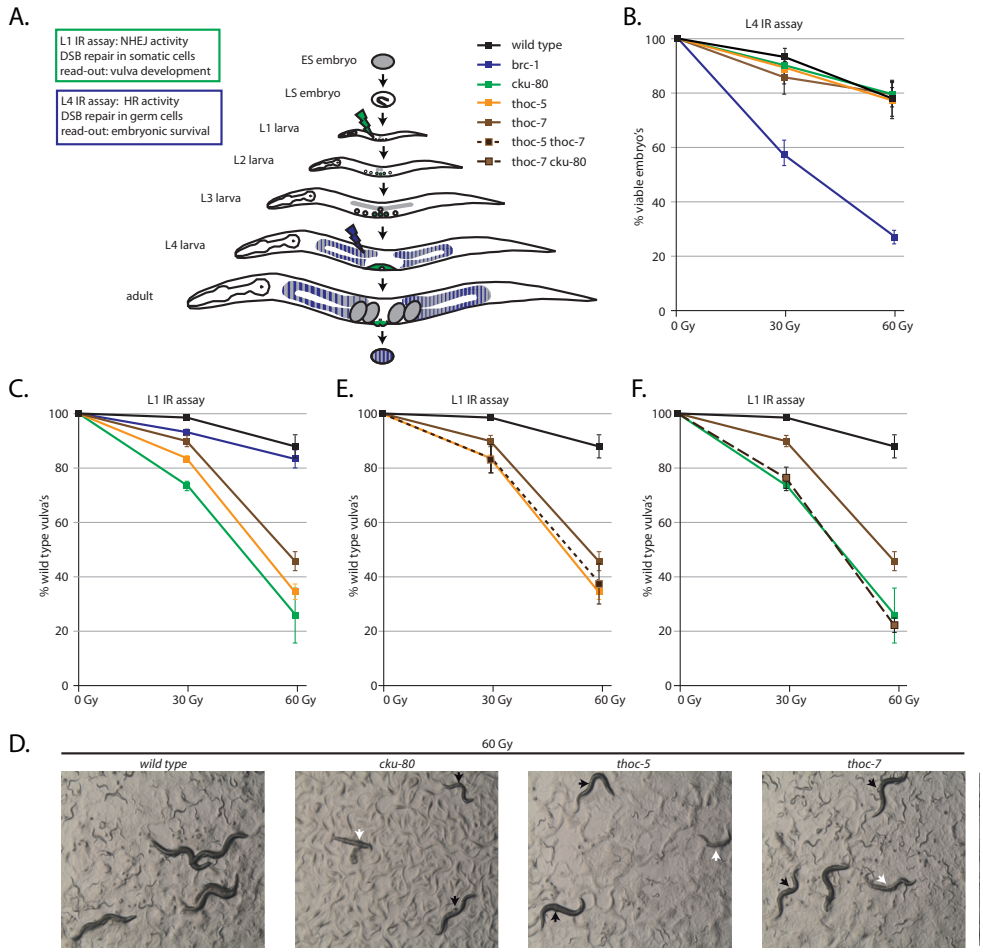

Figure 5. THO deficient somatic tissues are hypersensitive to IR

A. Schematic representation of two different IR assays in the context of the *C. elegans* life cycle and challenged tissues. While the L1 assay measures IR-resistance of arrested vulva precursor cells and mainly reflects NHEJ activity, the L4 assay measures IR-resistance of germ cells and typically reflects HR activity. **B.** L4 assay; L4 animals were challenged by the indicted dose of IR and percentage of viable progeny is plotted, see figure 5A for legends. Values depict the average of three independent experiments and error bars represent S.E.M. **C.** L1 assay; L1 animals were challenged by the indicted dose of IR and percentage of wild-type vulvas is plotted, see figure 5A for legends. Values depict the average of three independent experiments and error bars represent S.E.M. **D.** Representative pictures of synchronized animal populations 5 days post IR (60 Gy at L1 stage). Black arrows indicate protruding vulvas. White arrows indicate severe vulva defects resulting in germline extrusion or internal hatchlings/ bag-of-worms. **E. F.** L1 assay; Percentage of wild-type vulvas of double mutants treated as in Figure 5C; results of reference strains are depicted again, see figure 5A for legends. Values depict the average of three independent experiments and error bars represent S.E.M.

Given that *thoc-7* deficiency cannot increase IR sensitivity of NHEJ null mutants also suggests that THOC-7 loss does not result in additional (IR-induced) DSBs, which may be expected if RNA:DNA hybrids were to be abundant in the genome (Gomez-Gonzalez *et al.* 2011). In accordance with this notion, we found that increased SSA in *thoc-7* mutants depended on I-SceI-induced DSB formation and thus was not due to increased spontaneous DSBs (Figure S3C). All together, these data strongly argue for a role of the THO complex post DSB induction and at the level of DSB repair via classical NHEJ.

Splicing regulator PNN-1 is required for efficient NHEJ in *C. elegans*

The identification of the THO complex as an NHEJ regulator raised the intriguing question of how RBPs promote DNA repair? Interestingly, we identified one other NHEJ mutant (allele *lf159*), which based on epistasis and mapping studies was not affected in known NHEJ genes nor in THO complex genes. Subsequent genome-wide sequencing analysis revealed a candidate nonsense mutation in R186.7 (*pnn-1)*, the *C. elegans* homolog of Pinin/DRS/memA (Figure 6A and 6B). Pinin was first identified as a desmosome-associated protein involved in cell adhesion, but later was found to have nuclear functions as well, including regulation of mRNA splicing (Li *et al.* 2003; Wang *et al.* 2002). Notably, both the THO complex and Pinin associate with spliceosomes and have been implicated in pre-mRNA processing and mRNA export (Chi *et al.* 2013; Li *et al.* 2003). Given the potential functional overlap between PNN-1 and the THO complex, we investigated the putative role for PNN-1 in NHEJ regulation. To address if the NHEJ defect in *lf159* animals was caused by the early stop mutation in *pnn-1*, we crossed *lf159* hermaphrodites with wild-type males and males homozygous for a *pnn-1* deletion allele (*ok1872*). While NHEJ activity was restored in heterozygous cross progeny from wild-type males (*lf159/+)*, NHEJ activity in trans-heterozygous cross progeny (*lf159/ok1872)* was still defective, strongly arguing for a causal role for PNN-1 in NHEJ regulation (Figure 6C). Moreover, animals homozygous for the independently derived *pnn-1* null allele (*ok1872*) showed reduced NHEJ activity (pharyngeal LacZ) and increased SSA activity (somatic LacZ), revealing attenuated DSB repair and repair pathway specificity (Figure 6B and 6D).

To validate a role for PNN-1 in somatic NHEJ, we challenged *pnn-1* mutant larva with IR-induced DSBs during development. Like *thoc-5* mutants, *pnn-1* deletion mutants were hypersensitive to IR (Figure 6E and 6F). Interestingly, animals defective for both *thoc-5* and *pnn-1* were even more sensitive to IR than the respective single mutants, indicating that the THO complex and PNN-1 can act cooperatively to promote NHEJ (Figure 6F). This notion was confirmed using the dual reporter system: *thoc-5; pnn-1* double mutants showed reduced pharyngeal GFP (NHEJ) and increased somatic LacZ (SSA) compared to either single mutant (Figure 6D). Notably, *thoc-5; pnn-1* double mutants were nearly as sensitive to IR as *lig-4* deficient animals and showed severely reduced NHEJ reporter activity, illustrating the significance for these RBPs for efficient NHEJ *in vivo*.

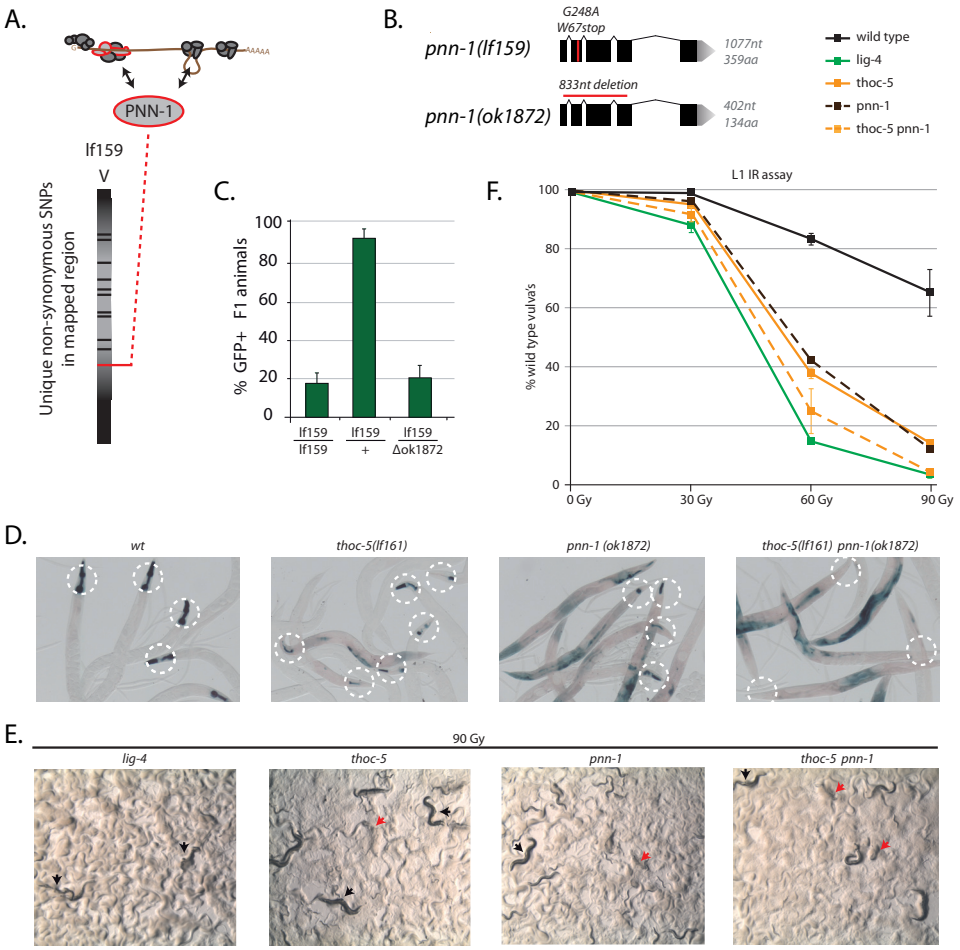

Figure 6. PNN-1 deficiency causes reduced NHEJ activity in *C. elegans*

A. Schematic diagram of chromosomes V in lf159 mutants; regions found to cause NHEJ defect based on Hawaiian SNP mapping in grey; black/red horizontal lines represent unique non-synonymous mutations. lf159 mutants have a nonsense mutation in *pnn-1*, a gene implicated in mRNA metabolism **B.** Gene model and alleles of pnn-1. **C.** Quantification of GFP-positive pharynxes in trans-heterozygous F1 cross progeny, heat-shocked for 120 minutes and measured in adults. **D.** LacZ expression patterns of synchronized dual reporter animals of the indicated genotype; animals were heat-shocked for 180 minutes at L1 and adult stage and stained three hours after the second heat-shock. **E.** Representative pictures of synchronized animal populations 6 days post IR (90 Gy at L1 stage). Black arrows indicate protruding vulvas. Red arrows indicate severe vulva defects resulting in germline extrusion or internal hatchlings/bag-of-worms. Wild-type control populations were starved under these conditions as they still had high fecundity. **F.** L1 assay; L1 animals were challenged by the indicted dose of IR and percentage of wild-type vulvas is plotted, see figure 5B for legends. Values depict the average of three independent experiments and error bars represent S.E.M.

PNN-1 and THO regulate mRNA stability of a specific set of transcripts

RBPs have been implicated in genome instability via the formation of RNA:DNA hybrids as well as their direct role in expression of specific DNA repair factors (Chan *et al.* 2014; Savage *et al.* 2014). Here we found Pinin/THO deficient L1 larva to be defective in NHEJ of both nuclease- and IR-induced DSBs. In order to search for gene expression alterations that may explain the NHEJ defect in these mutants, we extracted total RNA from unchallenged L1 larva from wild-type, *thoc-5*, *thoc-7* and *pnn-1* mutants and performed genome-wide RNAseq. We found total RNA levels not to be significantly different between the genotypes tested, implying that PNN-1 and these THO complex factors are not essential for transcription and stability of bulk RNA (Figure S4A). However, PNN-1 as well as THO deficiency resulted in altered expression of a specific set of genes, leading to both elevated and reduced expression patterns (Figure 7A). While THOC-5 loss resulted in slightly more down-regulated transcripts (535↓ versus 438↑), PNN-1 loss resulted in more up-regulated transcripts (195↓ versus 330↑), implying different roles for these RBPs in mRNA metabolism (Figure 7A). However, we also found a highly significant overlap in affected transcripts between the NHEJ mutants: *thoc-7* and *thoc-5* mutants shared 67% and 71% of up-regulated and down-regulated transcripts, and *pnn-1* and *thoc-5* shared 20% and 50% of up-regulated and down-regulated transcripts, respectively (Figure 7A). Thus PNN-1 and THOC-5/7 control mRNA stability in a similar but non-identical manner and both act highly selectively, affecting less than 5% of the transcriptome.

Since all three mutants were defective in NHEJ, we first focused on the genes of which the expression was significantly affected in all mutants, culminating to a common list of 18 up-regulated and 41 down-regulated transcripts (Figure 7A and S5). Interestingly, a quarter of the up-regulated genes was implicated in RNA metabolism and transcription, and 2 out of 18 up-regulated genes (11%) are known to interact with THO and promote mRNA splicing and export, potentially reflecting an *in vivo* response on a mRNA processing defect in these animals (Figure 7B) (Castellano-Pozo *et al.* 2012a; Chi *et al.* 2013). Surprisingly, none of the shared up-regulated and down-regulated genes were linked to DNA repair, cell cycle checkpoint or DNA damage signaling, suggesting that altered mRNA stability (by itself) was not the main cause for the NHEJ defect in these mutants (Figure S5).

Reduced LIG-4 levels in THO mutants do not limit NHEJ

Among the significantly down-regulated genes in *thoc-5* mutants, we found *lig-4* mRNA to be reduced to 36% of wild-type levels. Also *thoc-7* (68%) and *pnn-1* (86%) mutants seemed to suffer for reduced *lig-4* expression, yet this reduction was not statistically significant (Figure S4B). In contrast, *cku-80* and *cku-70* mRNA levels were not significantly affected in any of the RBP mutants, hinting towards a possible specific defect in *lig-4* mRNA metabolism (Figure S4C). To investigate if the NHEJ defect in THO mutants was due to low *lig-4* expression, we constructed several functional *lig-4* cDNA overexpression arrays and crossed these into the

different genetic backgrounds. While the *lig-4* cDNA arrays effectively restored NHEJ activity in *lig-4* mutants, they did not in *thoc-5* mutants, arguing that LIG-4 is not limiting in THO deficient animals (Figure S4D). Parallel approaches using fosmids or vectors expressing the full length *lig-4* ORF lead to similar results, further supporting the notion that reduced *lig-4* expression was not the cause of the NHEJ defect in *thoc-5* mutants. Besides, reducing functional *lig-4* transcripts by 50%, like in lig-4(ok719) heterozygotes (Figure 2B), also did not impede NHEJ efficacy, arguing that the residual *lig-4* mRNA levels in THO mutants (36-68%) are likely sufficient for efficient NHEJ.

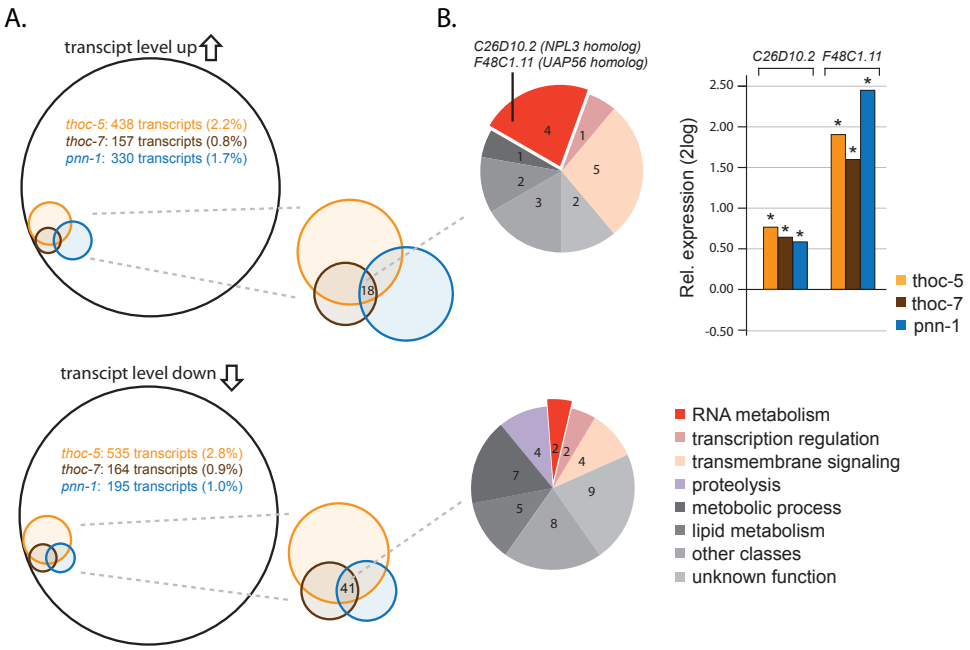

Figure 7. Transcriptome analysis by RNAseq of *thoc-5*, *thoc-7* and *pnn-1* mutants
A. Venn diagrams of significantly affected transcripts found by RNAseq in synchronized L1 animals of the indicated genotype. Upper Venn diagram depicts the number up-regulated transcripts; Lower Venn diagram depicts the number of down-regulated transcripts. Only a small fraction of the ~19.000 different transcripts identified was affected by *thoc-5*, *thoc-7* or *pnn-1* deficiency (% indicated between parentheses). A significant overlap was found between affected transcripts in *thoc-5*, *thoc-7* or *pnn-1* mutants, culminating in 18 and 41 common transcripts being up or down regulated, respectively. **B.** Pie-charts of the commonly affected transcripts in *thoc-5*, *thoc-7* or *pnn-1* mutants categorized by gene function, see bottom right for legends. Among the few up regulated transcripts, two encoded for genes that had orthologs implicated in RNA splicing and export: C26D10.2 and F48C1.11. Histogram depicts relative expression changes of C26D10.2 and F48C1.11 in the indicated genotypes compared to wild-type; asterisks indicates significance $q \leq 0.05$.

PNN-1 and THO deficiency results in alternative splicing at specific genes

Since Pinin and THO were also linked to mRNA splicing, we examined the genome-wide RNAseq data for splicing alterations that may explain the NHEJ defect. To identify putative splicing defects in these animals, we analyzed the relative expression of exons within the ~19.000 transcripts identified (Figure 8A). As expected, we identified altered expression patterns in the *pnn-1* gene itself, only in the strains carrying the *pnn-1* deletion allele, validated our bioinformatics analysis and substantiated the notion that we detected bona-fide exon-specific expression changes (Figure 8B). While the total number of transcripts with altered exon expression was relatively low in all three NHEJ mutants (*i.e.* 87, 17 and 19 transcripts in *thoc-5*, *thoc-7* and *pnn-1* mutants, respectively), the overlap in affected transcripts between the NHEJ mutants was strikingly large, being 100% between *thoc-7* and *thoc-5* and 42% between *pnn-1* and *thoc-5* (Figure 8A). Thus THOC5/7 and PNN-1 are highly selective regulators of mRNA metabolism, affecting exon expression of less than 0.5% of the transcriptome. This high selectivity was even seen at the level of individual exons: often the very same exons were included or excluded in THO and PNN-1 mutants, suggestive of highly specific splicing defects (Figure 8C). For example, all the NHEJ modifiers showed increased inclusion of the second exon of *oxi-1,* which encodes a well-conserved E3 ubiquitin ligase reported to be alternatively spliced in humans (Gong *et al.* 2003).

Although our RNAseq analysis revealed a common role for THOC5/7 and PNN-1 in RNA metabolism, they also revealed subtle differences. For instance, *thoc-5*, *thoc-7* and *pnn-1* mutants all showed alternative splicing of *tos-1*, resulting in the inclusion of the first intron; yet only the THO mutants showed additional expression defects of the latter three exons of *tos-1*, suggestive of a THO-specific alternative transcript (Figure 8D). The fact that THO and PNN-1 control mRNA metabolism in similar but non-identical ways may explain their cooperative functions in NHEJ regulation, as correct splicing of NHEJ genes may require both PNN-1 and the THO complex (Figure 6 and 8).

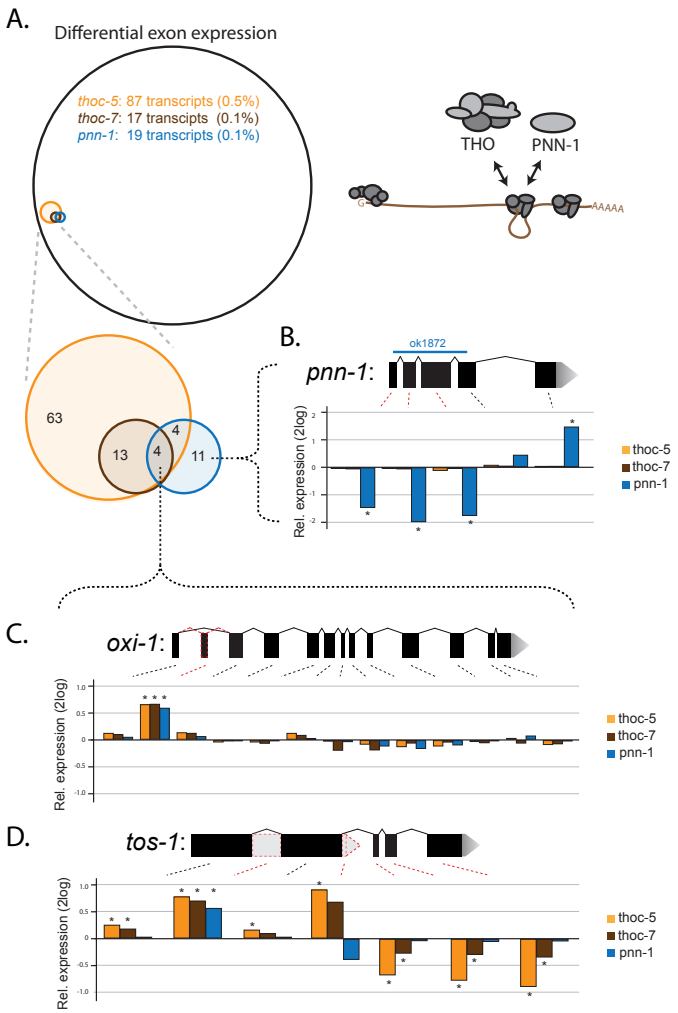

Figure 8. Differential exon expression in *thoc-5*, *thoc-7* and *pnn-1* mutants
A. Venn diagram of transcripts bearing significantly affected exons found by RNAseq in synchronized L1 animals of the indicated genotype. Only a small fraction of the ~19.000 transcripts identified had differentially expressed exons (% indicated between parentheses). Venn diagram blowup depicts unique and shared number of transcripts; a significant overlap was found between affected transcripts in *thoc-5*, *thoc-7* or *pnn-1* mutants, suggestive of rare but highly specific splicing defects. **B.** Gene model of *pnn-1* illustrates the position of the genomic deletion present in the *pnn-1* mutant (blue line). Histogram depicts relative expression changes of exons of the *pnn-1* transcript compared to wild-type as identified by DexSeq in the indicated genotypes; asterisks points out significance q ≤ 0.05. **C.** Gene model of *oxi-1*, a gene bearing alternatively expressed exons in *thoc-5*, *thoc-7* and *pnn-1* mutants. Histogram depicts relative expression changes of exons of *oxi-1* transcripts compared to wild-type as identified by DexSeq in the indicated genotypes; asterisks points out significance q ≤ 0.05. All three NHEJ mutants have increased inclusion of the second exon. **D** Gene model of *tos-1*, a gene bearing alternatively expressed exons in *thoc-5*, *thoc-7* and *pnn-1* mutants. Histogram depicts relative expression changes of exons of *tos-1* transcripts compared to wild-type as identified by DexSeq in the indicated genotypes; asterisks points out significance q ≤ 0.05. All three NHEJ mutants have increased inclusion of the first intron.

Reduced expression of splicing factor UAF-1 in THO mutants impedes NHEJ

Previous studies on alternative splicing have led to the identification of novel splicing regulators in *C. elegans*, including MFAP-1 and the ortholog of human U2AF large subunit UAF-1 (Ma *et al.* 2012; Ma and Horvitz 2009). Interestingly, *uaf-1* mutants have reported splicing defects reminisced to the ones occurring in the Pinin/THO mutants described here. In fact, *uaf-1* deficient animals also included the first intron of the endogenous splicing reporter gene *tos-1* (Ma *et al.* 2012). Our RNAseq analysis revealed that both *thoc-5* and *thoc-7* deficient L1 animals, but not *pnn-1* mutants, suffered from reduced *uaf-1* expression, implying that the splicing defects observed on the THO mutants may be caused (partially) by UAF-1 deficiency (Figure 9A and 9B). In order to establish a functional link between UAF-1 expression and *in vivo* DSB repair, we depleted *uaf-1* expression in dual DSB repair reporter animals by RNAi. Similar to THO mutation, *uaf-1* depletion by RNAi resulted in lower NHEJ activity and elevated SSA activity, strongly arguing for a causal link between altered UAF-1 levels and NHEJ efficacy (Figure 9C and 9D). All together these data suggest that both the splicing alterations and NHEJ defects in THO mutant animals can be readily explained by reduced expression of the essential splice factor UAF-1. The identification of selective splicing factors such as PNN-1 and UAF-1 in controlling *in vivo* NHEJ efficacy reveals another layer of regulation of error-prone DSB repair activities during animal development and sets the stage to discover alternative gene products that contribute to genome stability.

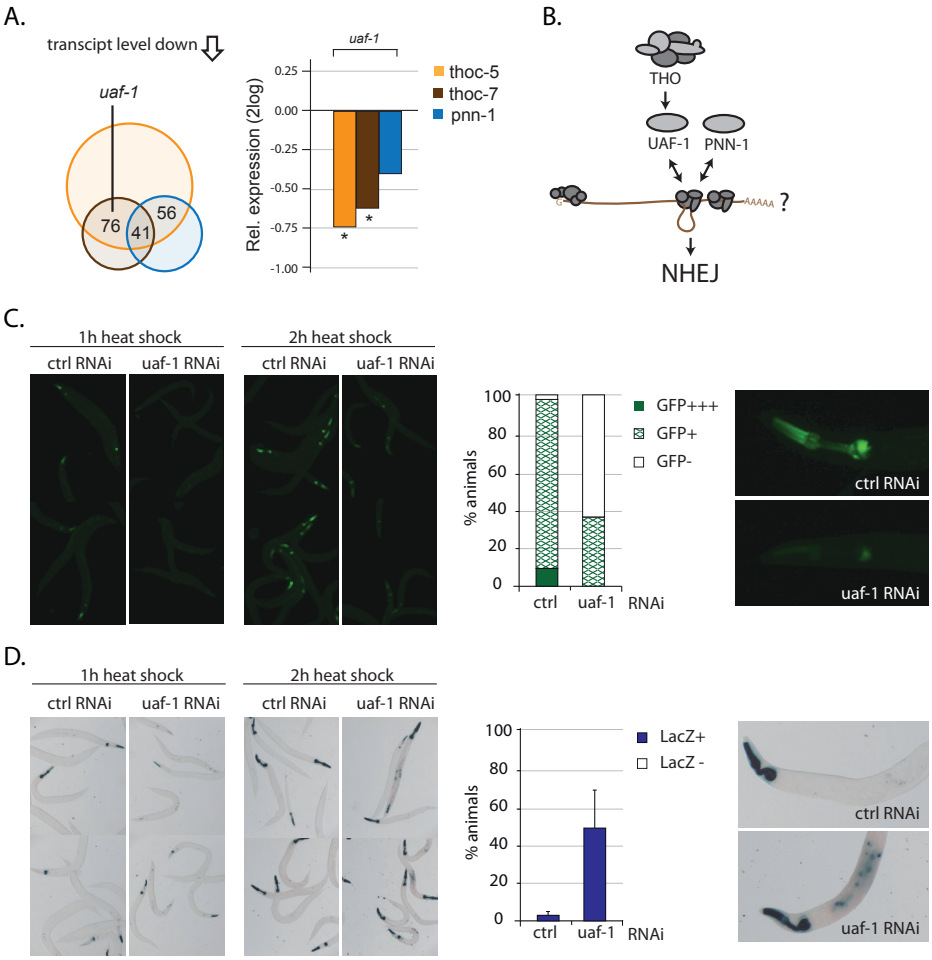

Figure 9. Reduced expression of splicing factor UAF-1 in THO mutants impedes NHEJ
A. Venn diagram of significantly down regulated transcripts compared to wild-type control as found by RNAseq in synchronized L1 animals deficient for *thoc-5* (orange), *thoc-7* (brown) and *pnn-1* (blue); numbers of commonly affected transcripts are indicated. Histogram depicts relative expression changes of *uaf-1* transcripts in the indicated genotypes compared to wild-type; asterisks indicates significance q ≤ 0.05. **B.** Putative model for the cooperative action of PNN-1 and the THO complex in NHEJ regulation. **C.** Representative pictures and quantifications of GFP-positive pharynxes in synchronized populations of dual reporter animals fed bacteria carrying empty vectors of *uaf-1* RNAi vectors. L4 animals were heat-shocked for 60 or 120 minutes and GFP was measured in adults. Histogram depicts average percentage of GFP-positive pharynxes of three independent populations (n>150) heat-shocked for 60 minutes. Right panels show representative pharyngeal GFP patterns in control and UAF-1 RNAi animals that were qualified as GFP+++ and GFP+, respectively. **D.** Representative pictures and quantifications of non-pharyngeal LacZ staining patterns in synchronized populations of dual reporter animals fed bacteria carrying empty vectors of *uaf-1* RNAi vectors. L4 animals were heat-shocked for 60 or 120min and stained 24 hours later. Histogram depicts average percentage of LacZ positive animals of three independent populations (n>150) heat-shocked for 120 minutes. Error bars represent S.E. Right panels show representative LacZ patterns in control and UAF-1 RNAi animals that were qualified as LacZ- and LacZ+, respectively.

Discussion

Recent large-scale genetic and molecular studies identified RBPs as important players in the maintenance of genome stability, either because they directly affect DNA repair or because they control proper expression of crucial DNA repair factors (Dutertre *et al.* 2014; Lenzken *et al.* 2013). At the same time several studies have shown that uncontrolled DSB repair activities can be detrimental for animal development and human health, ultimately leading to severe diseases such as cancer (Bunting *et al.* 2010; McKinnon and Caldecott 2007). How the activity of error-prone repair routes like NHEJ are controlled during development and if RBPs play a role in this regulation is unknown to date. We performed an unbiased forward genetics screen to find factors required for efficient DSB repair in *C. elegans* and identified the well-conserved RBPs PNN-1 and THOC-2/5/7 to promote NHEJ (Figure 1, 2, 3 and 6). Multiple transgenic DSB repair reporter assays and independent IR-sensitivity assays confirmed a specific requirement of these RBPs for efficient NHEJ but not DSB repair via HR/SSA (Figure 2, 5 and 6). Subsequent genome-wide transcriptome analysis revealed that the novel NHEJ mutants suffered from highly specific splicing defects, implying a functional link between NHEJ regulation and mRNA splicing. This notion was substantiated by the fact that the essential splicing factor UAF-1/U2AF was mis-expressed in THO deficient animals and the NHEJ defects seen in THO mutants could be mimicked by reduced expression of UAF-1. We propose that altered processing of specific mRNAs could provide means to affect the activity of essential gene products and may compromise DSB repair efficacy in somatic tissues.

Notably, many cancer-associated genes are regulated through alternative splicing, arguing for a significant role of this post-transcriptional regulatory mechanism in the production of oncogenes and tumor suppressors. Recently, more intimate links between splicing and DNA repair complexes became apparent, as for instance the tumor suppressor BRCA1 was found to be part of a DNA damage-induced splicing complex that controlled the activity of multiple DNA repair genes (Savage *et al.* 2014). Moreover, reduced expression of U2AF was shown to result in IR hypersensitivity in human cells, which could be partially restored by overexpression of specific DNA repair genes, suggesting a conserved but indirect role for U2AF in regulating DSB repair (Savage *et al.* 2014). Interestingly, Pinin was recently found to be part of a novel RNA-processing complex that recruits U2AF to specific mRNAs (Bracken *et al.* 2008) and both Pinin and U2AF are phosphorylated upon DNA damage (Beli *et al.* 2012). In support of a post-transcriptional role for such splicing factors in DNA repair, Pinin is redistributed upon DNA damage but is excluded from DNA damage sites (Beli *et al.* 2012; Lenzken *et al.* 2013). Alternative splicing factors are known to respond to external and internal stimuli and recent high-throughput screenings in human cells and budding yeast revealed many RNA processing factors to be targets of DNA damage checkpoint kinases. In fact, human THOC5 is also directly phosphorylated by ataxia-telangiectasia-mutated (ATM) kinase upon DNA damage

and this modification impaired THOC5/mRNA complex formation, drastically decreasing the cytoplasmic pool of THOC5-dependent mRNAs (Ramachandran *et al.* 2011). We show here that deficiencies of several well-conserved RNA processing factors, including PNN-1 and THOC-5 can result in highly selective splicing defects that are paralleled by specific defects in NHEJ, including somatic IR hypersensitivity. Given that RNA processing factors are often deregulated in response to genotoxic treatments and many chemotherapeutic therapies are based on DNA-damaging agents, alternative splicing can be an important determinant of how tumor cells respond to therapy (Ladomery 2013; Lenzken *et al.* 2013). The identification of the abovementioned RBPs in NHEJ sets the stage for further dissection of mRNA processing mechanisms during development and potentially will reveal important roles of alternative RNA transcripts in DSB repair.

Materials and Methods

Genetics

All strains were cultured according to standard *C. elegans* procedures (Brenner 1974). Alleles used in this study include: *LGIII: cku-70(tm1524), cku-80(ok861), lig-4(ok716), brc-1(tm1145), cku-70(lf151), cku-80(lf152), cku-80(lf153), thoc-2(lf158), thoc-5/Y32H12A.2(lf161), LGIV: thoc-7/B0513.2(lf160), LGV: pnn-1/R186.7(lf159), pnn-1/R186.7(ok1872), LGX: pkIs2379 [Phsp-16.41::I-SceI-ORF; rol-6(su1006)], pkIs2170 [SSA reporter Phsp-16.41::ATG::LacZ::I-SceI-site::stops::LacZ-ORF); unc-119(+)], lfIs104 [NHEJ reporter Pmyo-2::ATG::I-SceI-site:GFP-ORF::LacZ-ORF, Phsp-16.41::mCherry::I-SceI-ORF; rol-6(su1006)], lfEx164 [thoc-2 fosmid WRM0614bD12; Pmyo-3::mCherry; Prab-3::mCherry], lfEx166 [thoc-7 fosmid WRM0640bD11; Pmyo-3::mCherry; Prab-3::mCherry], lfEx164 [thoc-5 fosmid WRM0617bE04; Pmyo-3::mCherry; Prab-3::mCherry], lfEx190 [lig-4 fosmid WRM0634bF07; Pmyo-3::mCherry; Prab-3::mCherry], lfEx195 [Prpl-28::lig-4-cDNA; Pmyo-3::mCherry; Prab-3::mCherry], lfEx196 [Prpl-28::lig-4-ORF; Pmyo-3::mCherry; Prab-3::mCherry].* All transgenic strains were obtained by microinjection of plasmid/fosmid DNA into the germ line and data presented are from a single representative transgenic line unless noted otherwise. The parental NHEJ reporter transgene *lfIs104* was obtained via IR-mediated genomic integration and combined with *pkIs2379* and *pkIs2170* to create the dual reporter strain XF540, which served as the starting strain for the forward genetics screen.

DSB repair reporter assays

Synchronized L1 animals were obtained by harvesting eggs from hypochlorite-treated gravid adults and overnight starvation in M9 solution (Lewis and Fleming 1995). Hatched L1 larvae were transferred on NGM plates seeded with either *E. coli* OP50 or HT115 bacteria (Kamath and Ahringer 2003). In order to insure complete RNAi before DSB induction, L1 worms were

cultured at 20°C for at least 20hrs. Heat-shock driven I-SceI expression was induced by putting the worms at 34°C for 60-180 minutes, as indicated. After the heat-shock procedure, worms were cultured at 20°C to allow DSB formation, DSB repair and worm development. NHEJ activity was measured by scoring pharyngeal GFP expression using a Leica M165FC fluorescence dissecting-microscope. Experiments were performed in triplicate with 50-200 animals tested for each condition. After GFP quantification, ~25 adult animals were transferring onto microscope slides with 3% agarose pads and representative pictures were acquired using a Leica DM6000 microscope with 10X objective. SSA activity was measured by scoring animals showing LacZ positive cells in non-pharyngeal somatic tissues (Pontier and Tijsterman 2009). One hour prior fixation/LacZ staining, young adults were heat-shocked at 34°C for 120 minutes to induce SSA reporter expression.

Forward genetics screen

Dual reporter larvae (XF540) were mutagenized with ethyl methanesulfonate (EMS) using standard procedures (Brenner 1974). Complex F2 populations, each derived from 50 mutagenized P0s, were bleached and synchronized L1 larvae (F3) were seeded on NGM/OP50 plates. On two consecutive days larvae were heat-shocked at 34°C for 180 minutes in order to maximize GFP ORF correction. GFP^{low} F3 animals were selected using a Leica M165FC fluorescence dissecting-microscope and clonal F4 populations were tested again for NHEJ activity. Populations showing reduced GFP expression were fixed and stained with X-gal as described previously (Pontier and Tijsterman 2009).

Positional cloning, genome-wide sequencing and transgenesis

Causal mutations in *thoc-2*, *thoc-5* and *thoc-7* were mapped by crossing the respective mutants (Bristol) to the related Hawaiian strain CB4856 and performing single-nucleotide-polymorphism mapping on NHEJ proficient versus NHEJ deficient F2 lines (Davis *et al.* 2005). Unique EMS-induced genetic alterations in the mapped regions were identified by comparing genome-wide paired-end sequencing data of the parental mutant strains using the Illumina Hiseq 2000 platform, the *C. elegans* reference genome (Wormbase version 225) and MaqGene software (Bigelow *et al.* 2009). Causality was established by complementation analysis using wild-type fosmid arrays. Complemented regions spanned by the fosmids contained only one non-synonymous SNP (Figure S2). To create transgenic animals carrying fosmid arrays an injection mix containing 100 ng/µl pBluescript, 10 ng/µl pGH8 (Prab-3::mCherry::unc-54-3′UTR), 5 ng/µl pCFJ104 (Pmyo-3::mCherry::unc-54-3′UTR) and 10-50 ng/µl fosmid DNA (lig-4 WRM0634bF07, thoc-2 WRM0614bD12, thoc-7 WRM0640bD11, thoc-5 WRM0617bE04, pnn-1 WRM0637aA06) was injected into the gonads of young adults. For lig-4 cDNA and lig-4 ORF containing vectors, 5 ng/µl plamsid DNA was added instead of the fosmid DNA.

PCR-based DSB repair assay

Synchronized L1 larvae were seeded on NGM/OP50 plates and heat-shocked at 34°C for 180 minutes at L1 and L2 stage. Genomic DNA of L3 larvae was extracted using DNeasy Blood & Tissue kit (Qiagen) and 100ng of genomic DNA was digested for 2 hours at 37°C with 7.5 units I-SceI (New England Biolabs) to enrich for cleavage-resistant sites. PCR on pre-digested DNA was performed in duplicate (2x 50ng) using primers flanking the I-SceI target site of the NHEJ reporter: CTCGCGCATCCCACCGAGCGG and CAGGTAGTTTTCCAGTAGTGC. PCR products were purified (QIAquick) and digested for 2 hours at 37°C with 7.5 units I-SceI (New England Biolabs) and analyzed on a 2% agarose gel. Band intensities were quantified using ImageJ software.

IR sensitivity assays

All IR experiments were performed with a dose rate of 10Gy/minute using an electronic X-ray generator (XYLON International). Figures provide mean values of three independent experiments. L4 assay: three L4 animals per plate were treated with various doses of IR (three plates per condition) and progeny survival was scored 2 days post IR. L1 assay: ~200 L1 larvae per plate were treated with various doses of IR (three plates per condition) and vulval phenotypes were scored 5 days post IR. Representative pictures of irradiated populations were acquired using a Leica DFC295 camera/M165FC microscope.

Transcriptome sequencing

To obtain clean L1 populations and remove dead corpses, o/n starved L1 progeny from hypochlorite-treated gravid adults were filtered using 10µm nylon filters (Millipore). Total RNA of >3000 L1s per sample was extracted as follows: L1 animas were collected in 100µl M9, 400µl Trizol was added, vortexed 2 minutes, followed by 4 snap freeze/thaw cycles at -196°C/37°C, 200µl Trizol was added, incubated 5 minute RT, 120ul chloroform was added, incubated 2 minute at RT, centrifuged 15 minutes at 4°C (16000 rcf), 350µl supernatant was mixed with 70% ethanol (1:1) and total RNA was purified using Purelink® RNA columns (Ambion) and stored at -80°C. Total RNA was DNAse treated (Turbo DNA-free, Ambion) and RNA quality was verified using RNA 6000 Pico kit (Agilent).

RNA-Seq was performed on an Illumina HiSeq 2000 platform using standard reagents. Raw reads were aligned by TopHat on Wormbase assembly 238, which allows for reads to be split over splice junctions. Next, we used Cuffdiff, part of the Cufflinks package, to identify differentially expressed transcripts ($q \leq 0.05$) (Trapnell *et al.* 2012). For differential exon expression, DEXSeq was used using standard settings ($p_{adjust} \leq 0.05$) (Anders *et al.* 2012). For each mutant two or three samples were sequenced to account for variation between isogenic L1 populations.

Supporting Information

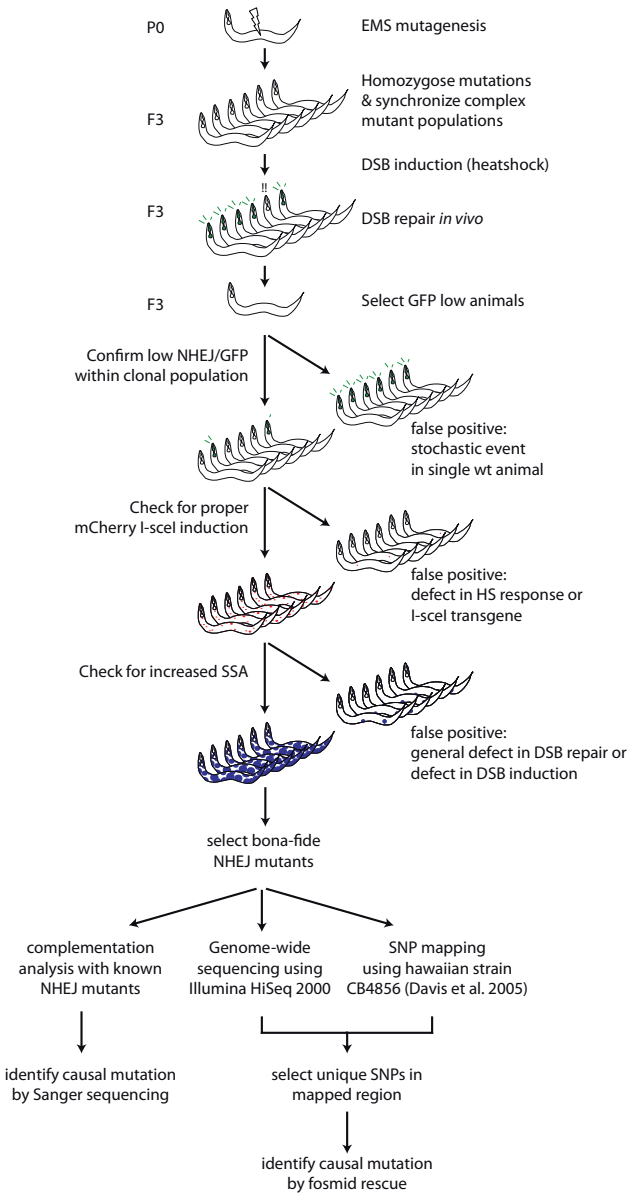

Figure S1. Schematic setup of forward genetics screens to identify NHEJ mutants

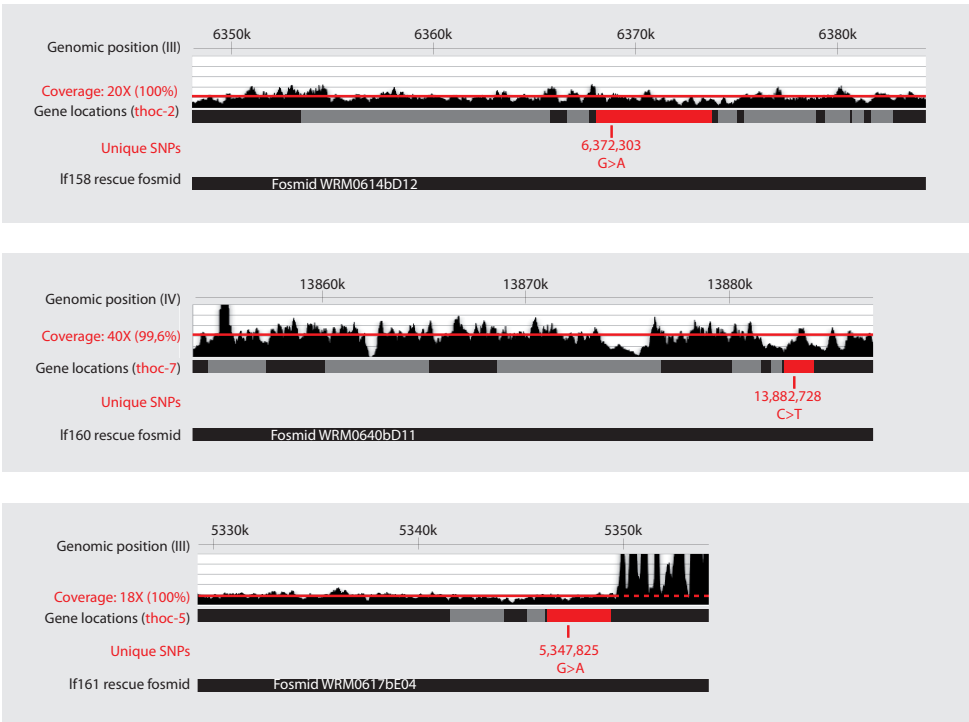

Figure S2. Sequencing coverage and genomic context of regions spanned by rescue fosmids Unique non-synonymous SNPs in the genomic regions spanned by the rescue fosmids (highlighted in red). Despite high sequence coverage, no other unique variants than those in the THO genes were found in the respective NHEJ mutants, strongly suggesting that we specifically complemented THO deficiency despite the use of 2-4kb fosmids.

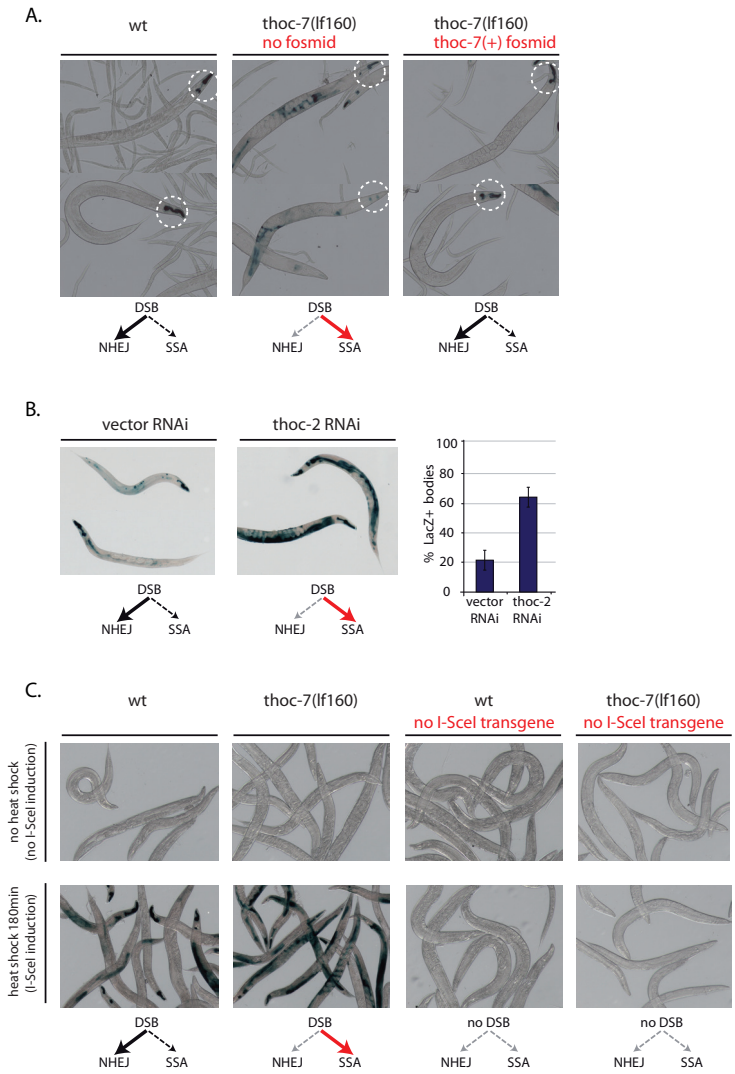

Figure S3 THO deficiency results in increased DSB repair via SSA

A. Representative pictures of synchronized and LacZ-stained dual-reporter animals of the indicated genotype. For the *thoc-7* mutant lines carrying the mCherry-marked *thoc-7* fosmid arrays, mCherry negative and mCherry positive clonal populations were grown and synchronized by bleaching. Animals were heat-shocked for 90 min at L1 stage and stained for LacZ expression as adults. While mCherry negative populations typically showed low pharyngeal LacZ (NHEJ) and increased levels of somatic LacZ (SSA), mCherry positive populations often showed animals having high levels of pharyngeal LacZ (NHEJ). These animals typically also had low levels of somatic LacZ (SSA), indicative of systemic restoration of functional NHEJ **B.** Representative pictures and quantification of LacZ-stained dual-reporter animals treated by feeding RNAi. Synchronized L1 animals were fed on *thoc-2*/empty vector RNAi plates, heat-shocked for 120 minutes at L4 stage and stained as adults. **C.** Representative pictures of transgenic populations of the indicated genotype. Synchronized animals were heat-shocked 0 or 120 minutes at L1 stage and adults were stained for LacZ expression. Increased somatic LacZ (SSA) in *thoc-7* mutants required heat-shock-driven I-SceI expression and the presence of the I-sceI transgene.

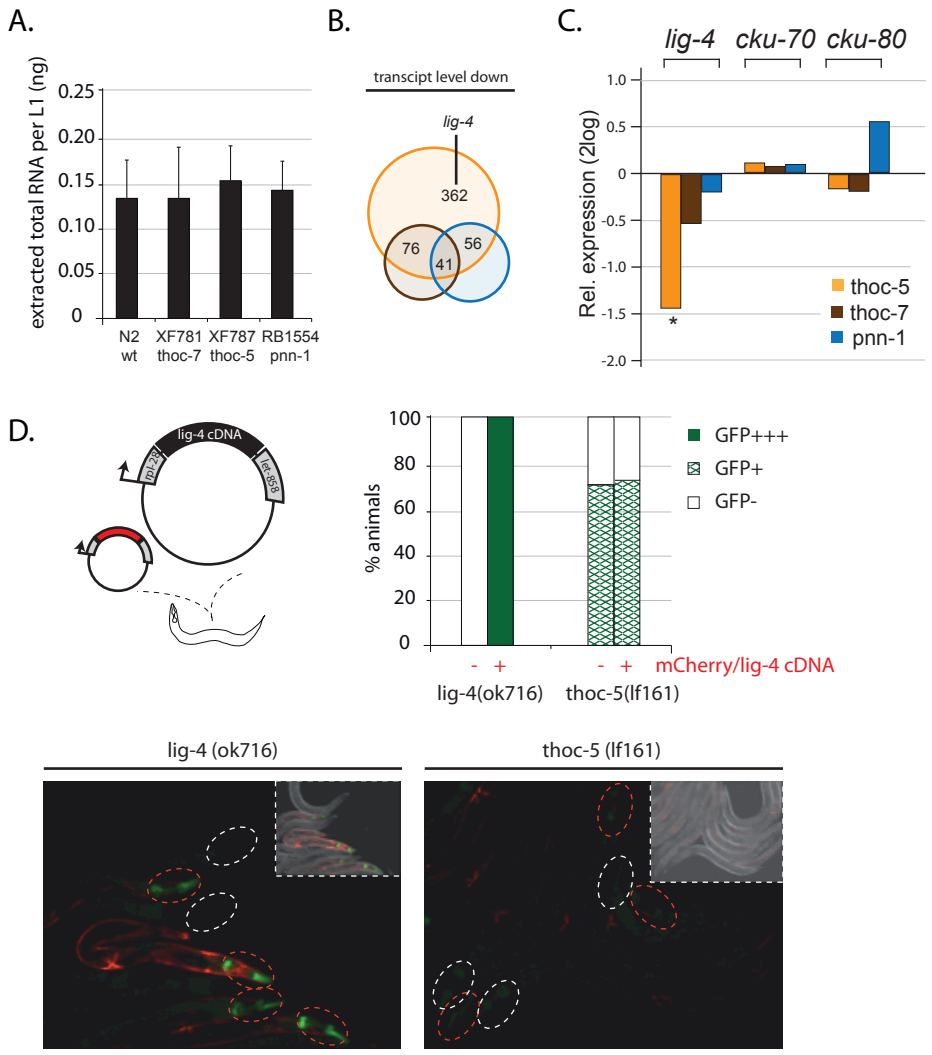

Figure S4 Reduced LIG-4 levels in THO mutants do not limit NHEJ

A. Average total RNA yield per L1 animal determined from four independent L1 populations of the indicated genotype. **B.** Venn diagram of significantly down-regulated transcripts compared to wild-type control as found by RNAseq in synchronized L1 animals deficient for *thoc-5* (orange), *thoc-7* (brown) and *pnn-1* (blue); numbers of commonly affected transcripts are indicated. **C.** Histogram depicts relative expression changes of *lig-4, cku-70* and *cku-80* transcripts in the indicated genotypes compared to wild-type; asterisks indicates significance q ≤ 0.05. **D.** Extra-chromosomal multi-copy arrays carrying P*rpl-28*::*lig-4* cDNA expression constructs and mCherry-based markers were made by micro-injection and crossed to *lig-4(ok716)* and *thoc-5(lf161)* mutants. Histogram shows quantification of GFP-positive pharynxes in adults of the different genetic backgrounds. Average percentage of GFP-positive pharynxes of three independent populations (n>100) is depicted. The presence of the *lig-4* overexpression array (mCherry^{+}) fully restored NHEJ activity in *lig-4* null mutants but did not improve NHEJ in *thoc-5* mutants. Lower panels are representative pictures of synchronized populations of *lig-4* and *thoc-5* deficient animals with (red circle) or without (white circle) *lig-4* overexpression constructs; animals were heat-shocked for 180min at L1 stage.

DOWN	
Transcript	*Function*
Y39B6A.1	*Ca ion binding*
F23H12.4	*cuticle formation*
F53E10.4	*infection response*
T08A9.12	*infection response*
T01C3.4	*lipid metabolism*
W02A2.2	*lipid metabolism*
W03G1.7	*lipid metabolism*
Y51H4A.5	*lipid metabolism*
Y65B4BR.1	*lipid metabolism*
B0310.5	*metabolic process*
F55F3.2	*metabolic process*
F58A6.1	*metabolic process*
K05B2.4	*metabolic process*
T01G1.4	*metabolic process*
T02B5.1	*metabolic process*
ZK550.6	*metabolic process*
M04B2.4	*oxidation respons*
R10E8.6	*protein binding*
T12B5.6	*protein binding*
F36D3.9	*proteolysis*
F44B9.1	*proteolysis*
F59D6.3	*proteolysis*
Y75B8A.4	*proteolysis*
M04B2.1	*RNA binding*
M04B2.2	*RNA binding*
M04B2.3	*transcription regulation*
R07B7.3	*transcription regulation*
C03G6.3	*transmembrane signalling/transport*
E03H4.10	*transmembrane signalling/transport*
R07E3.4	*transmembrane signalling/transport*
ZK666.7	*transmembrane signalling/transport*
C48D1.1	*ubiquitin binding*
C17F4.7	*unknown*
C26E1.2	*unknown*
F46C5.10	*unknown*
K07A9.4	*unknown*
K09F6.6	*unknown*
M04B2.6	*unknown*
Y38C1AA.12	*unknown*
Y51F10.7	*unknown*
ZK1290.13	*unknown*

UP	
Transcript	*Function*
Y48G1C.8	development
ZC168.5	*intercellular signalling*
B0285.9	*lipid metabolism*
Y38E10A.7	*lipid metabolism*
Y50D7A.3	*metabolic process*
WBGene00022951	*ncRNA*
C26D10.2	*RNA binding*
D2030.6	*RNA binding*
F48C1.11	*RNA binding*
B0213.2	*RNA binding?*
C13C4.3	*transcription regulation*
C10F3.3	*transmembrane signalling/transport*
F44F4.4	*transmembrane signalling/transport*
F54F12.1	*transmembrane signalling/transport*
T11G6.3	*transmembrane signalling/transport*
Y80D3A.7	*transmembrane signalling/transport*
F48C1.9	*unknown*
T02G5.14	*unknown*

Figure S5. Common transcripts affected significantly in *thoc-5*, *thoc-7* and *pnn-1* mutants
List of significantly affected transcipts (q ≤ 0.05) that are shared by *thoc-5*, *thoc-7* and *pnn-1* mutants. Putative protein functions based on orthologs or structural domains are indicated.

Acknowledgements
The authors thank Shohei Mitani (National Bioresource Project, Japan) and the Caenorhabditis Genetics Center for strains; Jennemiek van Arkel and Evelina Papaioannou for technical support.

References

Adamo, A., S. J. Collis, C. A. Adelman, N. Silva, Z. Horejsi *et al.*, 2010 Preventing nonhomologous end joining suppresses DNA repair defects of Fanconi anemia. Mol Cell **39:** 25-35.

Anders, S., A. Reyes and W. Huber, 2012 Detecting differential usage of exons from RNA-seq data. Genome Res **22:** 2008-2017.

Aslanian, A., J. R. Yates, 3rd and T. Hunter, 2014 Mass spectrometry-based quantification of the cellular response to methyl methanesulfonate treatment in human cells. DNA Repair (Amst) **15:** 29-38.

Beli, P., N. Lukashchuk, S. A. Wagner, B. T. Weinert, J. V. Olsen *et al.*, 2012 Proteomic investigations reveal a role for RNA processing factor THRAP3 in the DNA damage response. Mol Cell **46:** 212-225.

Bigelow, H., M. Doitsidou, S. Sarin and O. Hobert, 2009 MAQGene: software to facilitate C. elegans mutant genome sequence analysis. Nat Methods **6:** 549.

Bracken, C. P., S. J. Wall, B. Barre, K. I. Panov, P. M. Ajuh *et al.*, 2008 Regulation of cyclin D1 RNA stability by SNIP1. Cancer Res **68:** 7621-7628.

Brenner, S., 1974 The genetics of Caenorhabditis elegans. Genetics **77:** 71-94.

Bunting, S. F., E. Callen, N. Wong, H. T. Chen, F. Polato *et al.*, 2010 53BP1 inhibits homologous recombination in Brca1-deficient cells by blocking resection of DNA breaks. Cell **141:** 243-254.

Castellano-Pozo, M., T. Garcia-Muse and A. Aguilera, 2012a The Caenorhabditis elegans THO complex is required for the mitotic cell cycle and development. PLoS One **7:** e52447.

Castellano-Pozo, M., T. Garcia-Muse and A. Aguilera, 2012b R-loops cause replication impairment and genome instability during meiosis. EMBO Rep **13:** 923-929.

Chan, Y. A., P. Hieter and P. C. Stirling, 2014 Mechanisms of genome instability induced by RNA-processing defects. Trends Genet **30:** 245-253.

Chapman, J. R., M. R. Taylor and S. J. Boulton, 2012 Playing the end game: DNA double-strand break repair pathway choice. Mol Cell **47:** 497-510.

Chi, B., Q. Wang, G. Wu, M. Tan, L. Wang *et al.*, 2013 Aly and THO are required for assembly of the human TREX complex and association of TREX components with the spliced mRNA. Nucleic Acids Res **41:** 1294-1306.

Clejan, I., J. Boerckel and S. Ahmed, 2006 Developmental modulation of nonhomologous end joining in Caenorhabditis elegans. Genetics **173:** 1301-1317.

Davis, M. W., M. Hammarlund, T. Harrach, P. Hullett, S. Olsen *et al.*, 2005 Rapid single nucleotide polymorphism mapping in C. elegans. BMC Genomics **6:** 118.

Dominguez-Sanchez, M. S., S. Barroso, B. Gomez-Gonzalez, R. Luna and A. Aguilera, 2011 Genome instability and transcription elongation impairment in human cells depleted of THO/TREX. PLoS Genet **7:** e1002386.

Dutertre, M., S. Lambert, A. Carreira, M. Amor-Gueret and S. Vagner, 2014 DNA damage: RNA-binding proteins protect from near and far. Trends Biochem Sci **39:** 141-149.

Dvorak, C. C., and M. J. Cowan, 2010 Radiosensitive severe combined immunodeficiency disease. Immunol Allergy Clin North Am **30:** 125-142.

Gomez-Gonzalez, B., M. Garcia-Rubio, R. Bermejo, H. Gaillard, K. Shirahige *et al.*, 2011 Genome-wide function of THO/TREX in active genes prevents R-loop-dependent replication obstacles. EMBO J **30:** 3106-3119.

Gong, T. W., L. Huang, S. J. Warner and M. I. Lomax, 2003 Characterization of the human UBE3B gene: structure, expression, evolution, and alternative splicing. Genomics **82:** 143-152.
Hu, H., and R. A. Gatti, 2011 MicroRNAs: new players in the DNA damage response. J Mol Cell Biol **3:** 151-158.

Huertas, P., and A. Aguilera, 2003 Cotranscriptionally formed DNA:RNA hybrids mediate transcription elongation impairment and transcription-associated recombination. Mol Cell **12:** 711-721.

Johnson, N. M., B. B. Lemmens and M. Tijsterman, 2013 A role for the malignant brain tumour (MBT) domain protein LIN-61 in DNA double-strand break repair by homologous recombination. PLoS Genet **9:** e1003339.

Jungmichel, S., and M. Blasius, 2013 Rapid and transient protein acetylation changes in response to DNA damage. Cell Cycle **12:** 1993.

Jungmichel, S., F. Rosenthal, M. Altmeyer, J. Lukas, M. O. Hottiger *et al.*, 2013 Proteome-wide identification of poly(ADP-Ribosyl)ation targets in different genotoxic stress responses. Mol Cell **52:** 272-285.

Kamath, R. S., and J. Ahringer, 2003 Genome-wide RNAi screening in Caenorhabditis elegans. Methods **30:** 313-321.

Ladomery, M., 2013 Aberrant Alternative Splicing Is Another Hallmark of Cancer. Int J Cell Biol **2013:** 463786.

Lemmens, B. B., N. M. Johnson and M. Tijsterman, 2013 COM-1 promotes homologous recombination during Caenorhabditis elegans meiosis by antagonizing Ku-mediated non-homologous end joining. PLoS Genet **9:** e1003276.

Lemmens, B. B., and M. Tijsterman, 2011 DNA double-strand break repair in Caenorhabditis elegans. Chromosoma **120:** 1-21.

Lenzken, S. C., A. Loffreda and S. M. Barabino, 2013 RNA Splicing: A New Player in the DNA Damage Response. Int J Cell Biol **2013:** 153634.

Lewis, J. A., and J. T. Fleming, 1995 Basic culture methods. Methods Cell Biol **48:** 3-29.

Li, C., R. I. Lin, M. C. Lai, P. Ouyang and W. Y. Tarn, 2003 Nuclear Pnn/DRS protein binds to spliced mRNPs and participates in mRNA processing and export via interaction with RNPS1. Mol Cell Biol **23:** 7363-7376.

Lieber, M. R., 2010 The mechanism of double-strand DNA break repair by the nonhomologous DNA end-joining pathway. Annu Rev Biochem **79:** 181-211.

Luna, R., A. G. Rondon and A. Aguilera, 2012 New clues to understand the role of THO and other functionally related factors in mRNP biogenesis. Biochim Biophys Acta **1819:** 514-520.

Ma, L., X. Gao, J. Luo, L. Huang, Y. Teng *et al.*, 2012 The Caenorhabditis elegans gene mfap-1 encodes a nuclear protein that affects alternative splicing. PLoS Genet **8:** e1002827.

Ma, L., and H. R. Horvitz, 2009 Mutations in the Caenorhabditis elegans U2AF large subunit UAF-1 alter the choice of a 3' splice site *in vivo*. PLoS Genet **5:** e1000708.

Matsuoka, S., B. A. Ballif, A. Smogorzewska, E. R. McDonald, 3rd, K. E. Hurov *et al.*, 2007 ATM and ATR substrate analysis reveals extensive protein networks responsive to DNA damage. Science **316:** 1160-1166.

McKinnon, P. J., and K. W. Caldecott, 2007 DNA strand break repair and human genetic disease. Annu Rev Genomics Hum Genet **8:** 37-55.

Phillips, E. R., and P. J. McKinnon, 2007 DNA double-strand break repair and development. Oncogene **26:** 7799-7808.

Pontier, D. B., and M. Tijsterman, 2009 A robust network of double-strand break repair pathways governs genome integrity during C. elegans development. Curr Biol **19:** 1384-1388.

Ramachandran, S., D. D. Tran, S. Klebba-Faerber, C. Kardinal, A. D. Whetton *et al.*, 2011 An ataxia-telangiectasia-mutated (ATM) kinase mediated response to DNA damage down-regulates the mRNA-binding potential of THOC5. RNA **17:** 1957-1966.

Robert, V. J., M. W. Davis, E. M. Jorgensen and J. L. Bessereau, 2008 Gene conversion and end-joining-repair double-strand breaks in the Caenorhabditis elegans germline. Genetics **180:** 673-679.

Savage, K. I., J. J. Gorski, E. M. Barros, G. W. Irwin, L. Manti *et al.*, 2014 Identification of a BRCA1-mRNA Splicing Complex Required for Efficient DNA Repair and Maintenance of Genomic Stability. Mol Cell **54:** 445-459.

Trapnell, C., A. Roberts, L. Goff, G. Pertea, D. Kim *et al.*, 2012 Differential gene and transcript expression analysis of RNA-seq experiments with TopHat and Cufflinks. Nat Protoc **7:** 562-578.

Wang, P., P. J. Lou, S. Leu and P. Ouyang, 2002 Modulation of alternative pre-mRNA splicing *in vivo* by pinin. Biochem Biophys Res Commun **294:** 448-455.

5

A single unresolved G4 quadruplex structure spawns multiple genomic rearrangements during animal development

Lemmens BB, van Schendel R, Tijsterman M.

Abstract

Faithfull DNA replication is crucial to prevent genetic heterogeneity and malignant transformation. How cells deal with endogenous DNA lesions and DNA secondary structures that hamper DNA replication is poorly understood, especially in biological contexts in which the lesions are insufficient in amount to cause cell cycle arrest. Here, we studied the genetic consequences of persistent DNA secondary structures during *C. elegans* development and found that a single unresolved G4 quadruplex can survive mitotic divisions, causing numerous deletions in the descending cells. We demonstrate that DOG-1/FANCJ is the principle helicase to resolve G4 quadruplexes in *C. elegans* and that in its absence these endogenous DNA secondary structures persist *in vivo* to create substrates for polymerase Theta-Mediated End Joining, providing further mechanistic insight in the mode of mutagenesis of G4 structures. Our data indicate that low frequency replication barriers escape detection and active processing, allowing them to cause multiple genomic rearrangements in proliferating tissues

Introduction

Every time a cell divides it has to replicate its entire genome to provide both daughter cells with equal amounts of genetic material and it has to do so in an accurate manner to ensure genome stability. This is especially important for multicellular organisms where the single-cell embryo has to replicate its genome several times to form all adult tissues, risking the accumulation of genetic alterations that may result in cellular dysfunction and/or malignant transformation.

Replication fidelity is maintained by the use of highly accurate replicative polymerases, which are double-checked by efficient mismatch and post-replication repair mechanisms (Loeb and Monnat 2008; Jiricny 2013). Additionally, cells need to deal with damaged DNA bases and DNA secondary structures that can obstruct the replicative polymerase and thus may hamper the cell to replicate its genome successfully (Budzowska and Kanaar 2009). Replication errors are a major source of spontaneous mutagenesis and promote cancer progression, yet how cells deal with replication impediments and how this impacts the mutational landscape is still unclear (Preston *et al.* 2010). Especially, how low frequency replication barriers affect genome stability during development is largely unknown.

We have recently shown that endogenous DNA damage as well as DNA secondary structures like G4 quadruplexes can cause genomic rearrangements during *C. elegans* development and evolution, and that deficiencies in specialized DNA polymerases or DNA helicases that deal with replication barriers can result in high levels of genomic instability in this animal (Koole *et al.* 2014; Roerink *et al.* 2014). In fact, animals lacking the FANCJ helicase DOG-1 show a thousand fold increase in deletion formation at G4 sites, illustrating the mutagenic potential of these endogenous DNA sequences and revealing the importance of such helicases to ensure genome stability (De and Michor 2011; Koole *et al.* 2014). We recently also have uncovered a novel error-prone DSB repair pathway that limits the consequences of such replication blocks, which we named Theta-mediated end joining (TMEJ), as it requires the well-conserved DNA polymerase Theta/POLQ-1 (Koole *et al.* 2014). Genetic deficiencies either leading to inefficient bypass of damaged DNA bases or the inability to resolve G4 quadruplexes typically resulted in 50-300 base pair (bp) deletions throughout the genome, which all were the product of TMEJ (Kruisselbrink *et al.* 2008; Koole *et al.* 2014; Roerink *et al.* 2014). It has been proposed that these deletions arise because unresolved replication blocks lead to DNA double-strand breaks (DSBs) that are subsequently repaired by TMEJ. However, at present, nothing is known about the fate of the initial blocking lesion, nor how these lesions induce DSBs that fuel TMEJ-dependent deletions.

G4 quadruplexes have been shown to be potent replication blocks *in vitro (Howell et al. 1996; Han et al. 1999; Edwards et al. 2014)*, yet little is known about their impact on replication progression *in vivo*. Recent insights on UV-induced DNA damage suggest that

local impairments of polymerase activity are unlikely to stall overall replication progression, as most DNA will be replicated via the convergence of opposing replication forks or via re-priming mechanisms downstream of the lesion (Blow *et al.* 2011; Elvers *et al.* 2011; Helleday 2013). Both scenarios promote gross DNA replication but are predicted to result in small single-strand (ss) DNA gaps opposite to the blocking lesions. How these ssDNA gaps are detected and resolved *in vivo* is still an open question, but the typical small 50-300bp deletions directly flanking replication-stalling G4 sites could imply that such gapped structures are converted into TMEJ substrates (Koole *et al.* 2014; Roerink *et al.* 2014).

Two fundamentally different models might link polymerase blockage to deletion formation: i) a direct conversion model, in which the blocking lesion and the resultant gapped DNA structure are directly converted into a DSB, either because ssDNA is intrinsically unstable or via active processing by nucleases, or ii) a persistent lesion model, in which the blocking lesion escapes detection/processing and the opposing ssDNA gap persists, eventually resulting in a DSB during the next S-phase as the ssDNA gap is replicated (Figure 1A).

Both scenarios can explain the occurrence of DSBs that could fuel TMEJ-dependent deletions, yet their consequences for animal development are fundamentally different. If unresolved replication barriers are converted directly into DSBs, they are lost during the repair process and pose a threat to genome stability only once. However, if unresolved replication barriers escape detection and persist during the life of the individual, they can continuously fuel genomic instability among dividing cells.

Here we provide evidence for a persistent lesion model, in which low-frequency replication blocks result in pre-mutagenic lesions (e.g. 50-300bp ssDNA gaps) that are not detected nor processed, yet result in TMEJ-dependent deletions in subsequent replication rounds. By combining in-depth deletion footprint analysis and transgenic reporter assays we found that in the absence of DOG-1 helicase activity, G4 quadruplexes persist *in vivo* and create pre-mutagenic lesions that in turn spawn multiple deletions throughout animal development. This work provides a framework to investigate the consequences of low frequency replication barriers for animal development and reveals that a single persistent DNA structure can lead to multiple genomic rearrangements in proliferating tissues – a feature that may significantly contribute to tumor heterogeneity and malignant transformation.

Results

MUS-81 or XPF-1 nucleases are not required for G4-induced deletion formation

Recent studies suggest that hard-to-replicate loci known as “fragile sites” can be processed by specialized topoisomerase complexes as well as structure-specific nucleases (*i.e.* Sgs1/Top3/Rmi1 and Mus81 respectively), which either resolve stalled replication intermediates directly or convert them into DSBs that are repaired later on (Manthei and Keck 2013; Minocherhomji

and Hickson 2014). Although the exact nature of these nuclease/topoisomerase substrates is not known, we hypothesized that similar mechanisms may promote DSB induction at hard to replicate G4 sites, creating a substrate for TMEJ.

To investigate the genetic requirements for G4-induced deletion formation, we first studied the role of two highly conserved structure-specific nucleases, MUS81 and XPF. These nucleases have been implicated in DNA break formation at (yet-undefined) late replication intermediates and animals deficient for *xpf-1* and *mus-81* show elevated levels on genome instability in mitotic cells (Agostinho *et al.* 2013; O'Neil *et al.* 2013; Saito *et al.* 2013; Minocherhomji and Hickson 2014). We analyzed stochastic deletion formation in *dog-1* animals lacking either *mus-81* or *xpf-1* using a PCR-based assay that amplifies deletion products at endogenous G4 sites (e.g. Qua213 on chromosome I). Depletion of *mus-81* or *xpf-1* did not prevent G4 deletion formation in *dog-1* animals (Figure 1B). MUS-81 and XPF-1 are known to have (partially) redundant functions, which is exemplified by the fact that *mus-81; xpf-1* double mutants are synthetic lethal (Agostinho *et al.* 2013; O'Neil *et al.* 2013; Saito *et al.* 2013). However, the sensitivity of the PCR-based assay and the mutagenicity of such G4 sites allowed us to test G4 deletion formation in the few survivors of *dog-1 mus-81; xpf-1* triple mutants and found them still proficient in G4-induced deletion formation (Figure 1B). We therefore conclude that MUS-81 and XPF-1 are not required for G4-induced deletion formation.

Similarly, previous studies have found that neither the nuclease scaffold protein SLX-4 nor the Sgs1 homolog HIM-6 are needed for G4-induced deletion formation, further supporting the notion that unresolved G4 structures may not require direct processing to become mutagenic (Youds *et al.* 2006; Saito *et al.* 2009).

G4 deletion frequency reveals the presence of a persistent pre-mutagenic substrate

We next investigated a scenario where G4 quadruplexes are not processed in the absence of the DOG-1 helicase and therefore will persist during subsequent cellular divisions. In that case, the G4 will impose a physical block for the replicative polymerase during every S-phase, resulting in small ssDNA gaps in the nascent strand opposite of the stable G4. If these gaps are left unfilled, they are expected to collapse into DSBs during the next replication round, providing a substrate for TMEJ (Figure 1A). While TMEJ can repair the DSBs arising from the ssDNA gaps, it does not take away the replication-stalling lesion that caused the gap: the G4 quadruplex. This model therefore predicts that unresolved G4 structures will persist independent of the repair process and can cause new mutagenic events every time the cell divides.

A fundamental difference between the direct conversion model and the persistent lesion model is the fate of the G4 bearing DNA strand. In the first model the G4 bearing DNA strand is processed to form a deletion product, while in the latter scenario the G4 persists

and the gapped nascent strand provides the substrate for TMEJ (Figure 1A). Next to the obvious cellular implications, this difference in G4 fate will also affect the deletion frequency distribution within the animal population. While the direct conversion model predicts that an animal showing a deletion has lost the G4 structure, the persistent lesion model predicts that an animal showing a deletion still harbors a mutagenic G4, substantially increasing the chance of the occurrence of another deletion.

We set out to distinguish between these models by determining the stochastic deletion frequency of endogenous G4 sites per animal and correlate that to the frequency of animals bearing two unique deletions at the same genomic locus. The persistent lesion model predicts that the probability (and thus frequency) of a second deletion would be much higher than expected based on random chance. To be able to measure stochastic deletion frequencies among *dog-1* animals and at the same time capture multiple independent G4 deletion events within these animals, we devised a PCR-based assay on minimal dilutions of genomic DNA lysates (Figure 1C). In short, we extracted genomic DNA from individual animals (each consisting of ~900 somatic cells) and performed two independent nested PCRs, each on 1% of lysate, amplifying G4 sites on genetic material corresponding to ~9 somatic cells. To obtain stochastic deletions frequencies we extracted DNA from >190 *dog-1* proficient and >330 *dog-1* mutant animals and analyzed two endogenous G4 loci (*i.e.* Qua375 on chromosome I and Qua1277 on chromosome IV). For each locus, two independent PCR reactions were analyzed in parallel and unique deletion products were discriminated based on size by gel-electrophoreses (Figure 1C).

Using this approach we frequently detected two differently sized deletions per animals, suggesting that G4 deletions often co-occur during animal development (Figure 1D, highlighted in red). The identification of two different deletions per animal also indicated that the small sample size (corresponding to ~9 somatic cells) allowed us to amplify unique molecules and exclude potentially abundant/favored deletion products. While we found 4% and 6% of the *dog-1* deficient samples to have deletions at Qua375 and Qua1277, respectively, we detected no deletions in the *dog-1* proficient samples. Moreover, the deletions were randomly distributed over the animal population and no significant correlation was found between deletions at the two G4 loci (Figure S1). These data confirm DOG-1 as a potent suppressor of G4 deletions and indicate that we detected stochastic *in vivo* rearrangements.

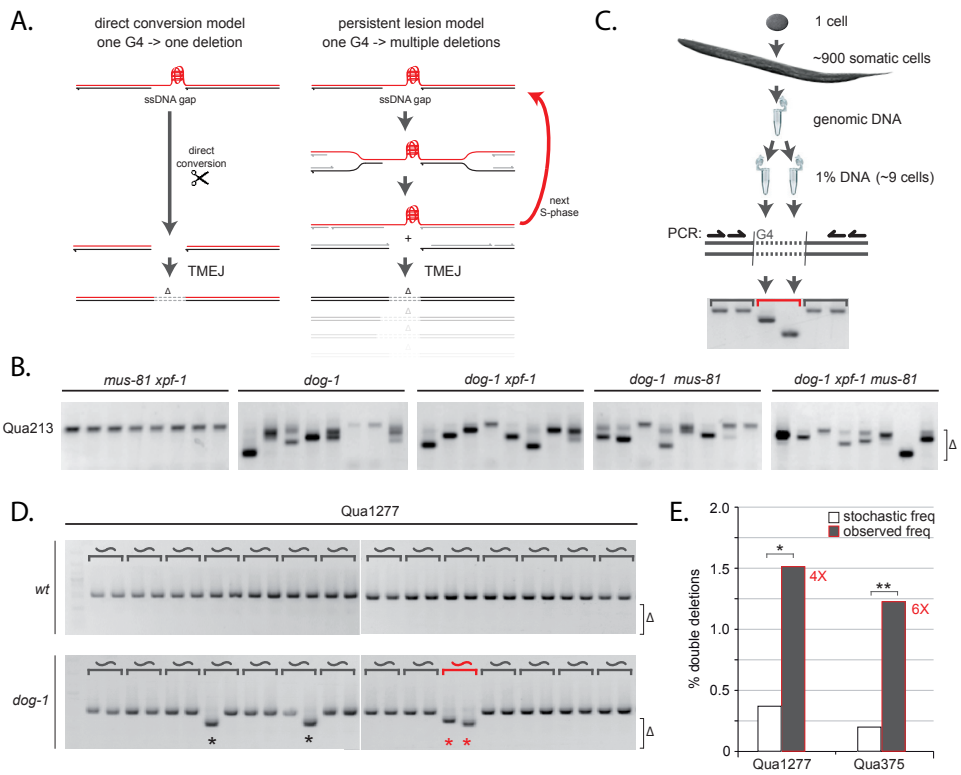

Figure 1. Overrepresentation of co-occurring G4 deletions in single animals

A. Two putative models for G4-induced deletions formation. In the "direct conversion model" the mutagenic G4 structure is lost during deletion formation, unlike the "persistent lesion model" where the G4 structure is maintained and can spawn multiple deletions in descending cells **B.** PCR analysis of G4 instability at endogenous G4 site Qua213; each well represents an independent PCR reaction on 10% single worm lysate; size-range of PCR-amplified deletions products is indicated by Δ. **C.** Schematic overview of PCR-based setup to identify multiple G4 deletions in single animals using parallel nested PCR reactions on 1% single worm lysates **D.** PCR analysis of G4 instability at endogenous G4 site Qua1277 in *dog-1* proficient (upper panel) and deficient animals (lower panel); Representative gel images are depicted used to determine the stochastic deletion frequencies among individual animals (asterisks) and directly extract the frequency of double deletions (red); each well represents an independent PCR reaction on 1% single worm lysate; size-range of PCR-amplified deletions products is indicated by Δ. ***E.*** Histogram depicts double deletion frequencies in 1% single animal lysates, as determined using the PCR-based assay depicted in Figure 1C. White bars represent expected double deletion frequencies based on the obtained stochastic deletion frequencies within the tested animal population (See methods section for details). Black bars represent double deletion frequencies that were identified directly (as highlighted in red in figure 1D). Asterisks indicate highly significant over-representation of the observed double deletion events within the tested population (*n=352 **n=576) as determined by hypergeometric testing (*p<0.003 **p<0.001).

To obtain the expected frequency of animals carrying two independent stochastic deletions we considered the two genomic fractions as independent tests and multiplied the deletion frequency in the first sample to the frequency of unique deletions in the second sample (Figure 1E and see methods section for details). This data set also allowed us to extract the double deletion frequency directly, as we readily detected single animals with two differently sized deletions (Figure 1D, highlighted in red). Strikingly, the actual frequency of double deletions was four to six fold higher than predicted based on random chance ($p<0.003$), indicating that an animal carrying a deletion has a much higher chance to acquire another deletion than one would expect based on the deletion frequency in the population (Figure 1E). The observation that animals bearing a deletion are predisposed to have an additional deletion at the same genomic locus strongly argues for the existence of a pre-mutagenic lesion. The continued mutagenicity of the pre-mutagenic lesion implies that the source of genomic instability is not resolved, but instead persists during animal development, allowing it to cause multiple DSBs that are processed into deletions through TMEJ.

Unresolved G4 structures cause multiple site-specific deletions in single animals

If in the absence of DOG-1 helicase activity G4 structures persist and remain mutagenic, one would predict that the G4 structures that arise early in development would cause many different deletions within one animal. To see if we could identify more than two G4 deletions in individual *dog-1* animals we subjected the single animal lysates to multiple deletion tests (Figure 2A). As predicted by the persistent lesion model, lysates positive for a Qua375 deletion (indicative of a persistent G4) often showed extra deletions at this very same locus (5/14= 36%). In contrast, lysates previously found negative for Qua375 deletions rarely showed additional deletions (1/16= 6%). Similarly, we subjected lysates having two different Qua213 deletions (indicative of potential early events) to multiple testing rounds and identified several animals that had three or even five differently sized deletions among eleven test samples (5/18= 27%), while lysates lacking Qua213 deletions in the first two tests displayed no additional deletions (0/5= 0%) (Figure 2C). These observations are in line with the presence of a pre-mutagenic substrate only in a subset of animals and suggest that G4-induced genomic rearrangements can be very abundant in certain individuals, likely when the G4 structure manifested early in the cell lineage.

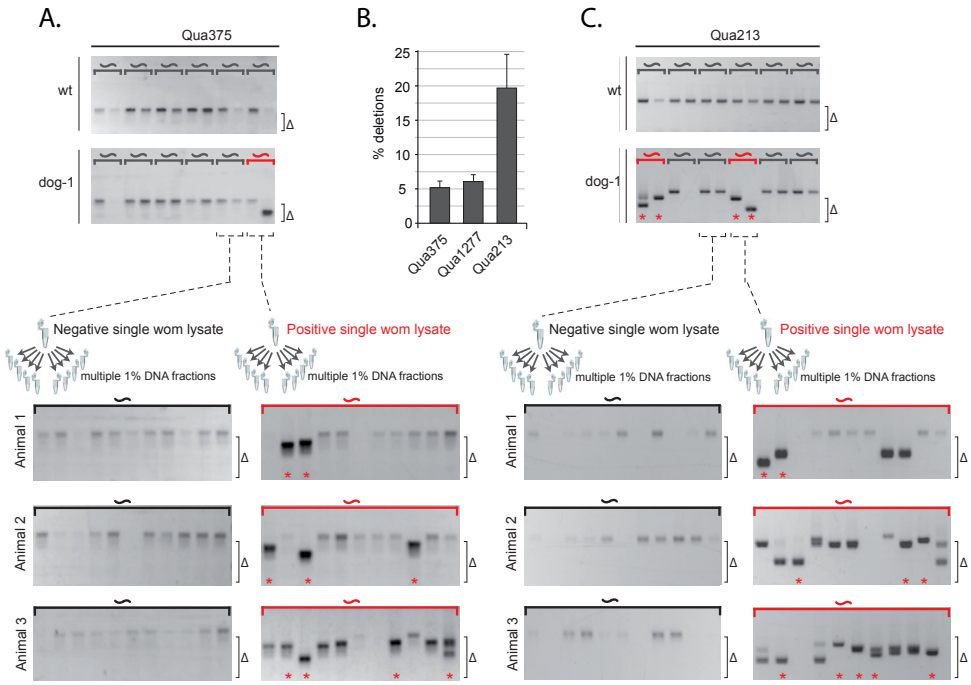

Figure 2. Co-occurrence of multiple locus-specific deletions in single animals
A. PCR analysis of G4 instability at endogenous G4 site Qua375 in wild-type and *dog-1* animals, upper and lower panel, respectively; each well represents an independent PCR reaction on 1% single worm lysate; size-range of PCR-amplified deletions products is indicated by Δ. Single worm lysates were first categorized based on the presence or absence of G4 deletions in two PCR test round and subsequently tested eleven times to test for additional G4 deletions. Three representative gel images for each category are depicted. Asterisk indicates unique deletion events based on product size. **B.** Histogram depicts double deletion frequencies in 1% single animal lysates, as determined using the PCR-based assay as depicted in Figure 1C. **C.** PCR analysis of G4 instability at endogenous G4 site Qua213 in wild-type and *dog-1* animals, upper and lower panel, respectively; each well represents an independent PCR reaction on 1% single worm lysate; size-range of PCR-amplified deletions products is indicated by Δ. Single worm lysates were first categorized based on the presence or absence of two unique G4 deletions in two PCR test round and subsequently tested eleven times to extract additional G4 deletions. Three representative gel images for each category are depicted. Asterisk indicates unique deletion events based on product size.

Recurrent 3′ deletion junctions in single animals argue for persistent replication blocks during development

Our observations thus far indicated that animals that cannot resolve G4 structures accumulate multiple site-specific deletions, suggestive of a local persistent entity that provokes deletion formation. To determine if the multiple deletion events within one animal were derived from a single persistent G4 structure, we needed to find unique characteristics of the causing lesion. Current technology does not allow direct monitoring of a single replication-blocking lesion

within a developing animal, a problem that has challenged research on endogenous (low frequency) replication barriers for years.

We nevertheless reasoned that each replication block could leave a unique genetic “scar” that would unveil its presence and exact genomic location. In fact, the exact position of G4 deletion junctions can serve as a distinctive mark, as we previously found that deletions at G4 sites are typically unidirectional with their 3′ junction close to the start of the G4 motif (Koole *et al.* 2014). The typical position of the 3′ deletion junctions, right at the start of the G4 motif, plausibly reflects the collision of the replicative polymerase with the stable G4 quadruplex (Figure 3A).

To more precisely mark the start of a G4 deletion and correlate that to the potential configuration of a stable quadruplex fold, we determined the spectra of 3′ junctions of G4 deletions at two endogenous G4 sites that can adopt only one possible three-stacked quadruplex configuration, Qua1465 and Qua1466, and indeed found a very sharp distribution of 3′ junctions immediately flanking the 3′ outermost G of the G4 motif (Figure 3B). This narrow distribution of 3′ deletion junctions suggests that the position of the replication block at minimal G4 sites is relatively fixed.

The genome, however, also harbors many mutagenic G4 sites like Qua915 or Qua1277 that can adopt many different quadruplex configurations that satisfy the G4 consensus G_{3-5}-N_{1-3}-G_{3-5}-N_{1-3}-G_{3-5}-N_{1-3}-G_{3-5} (Kruisselbrink *et al.* 2008). Such G4 sites may inflict differently positioned replication barriers within the population, which would provide a window to discriminate between individual DNA secondary structures that arise during animal development. In line with that notion, 3′ deletion junctions at Qua915 and Qua1277 show a much broader spectrum than seen at minimal G4 sites and are found not only at the 3′ flank of the G4 motif but also within the G4 sequence itself, reaching up to the 3′ border of the outermost minimal G4 motif (Figure 3B). The observation that most deletion junctions at Qua915 and 1277 are not positioned immediately upstream of the G4 sequence (like with minimal G4 loci), but instead are located within the G4 sequence yet upstream of the minimal G4 consensus, strongly suggests that the pre-mutagenic lesion is in fact a DNA secondary structure.

If an unresolved G4 structure will not be processed and will persist during the animal’s lifetime, it is predicted to block the replicative DNA polymerase at the very same genomic position in subsequent replication cycles. Importantly, the strong correlation between the anticipated G4 structure and the 3′ deletion junctions allows us to test this hypothesis: If the position of G4 quadruplexes varies among individuals, but such a DNA structure persists within an individual, one expects to find variable 3′ deletion junctions within the population but recurrent 3′ junctions within single animals (Figure 3A). Our PCR-based assay allows us to detect multiple G4 deletions in individual animals and analyze the deletion footprints at the nucleotide level. We first analyzed the 3′ deletion junctions of five animals in which we found two different Qua1277 deletions and plotted their relative position to the G4 motif

(Figure 3C). While the position of the 3′ deletion junctions varied significantly between the different animals, the deletions within the animals had a very similar position of the 3′ junction, suggesting that the G4 structure indeed persisted during animal development and spawned different deletions.

Although the distributions of 3′ deletion junctions are narrow at minimal G4 motifs, they still spread a few nucleotides, implying variable polymerase progression upon G4 collision and/or minimal DNA processing. This intrinsic variability complicates the identification of persistent lesions as it obscures the translation of fixed G4 structures to deletion footprints. To facilitate the discrimination between stochastic G4 folding events and persistent G4 structures we searched for endogenous G4 sites that showed a bimodal distribution of 3′ deletion junctions. Bimodal junction spectra imply two distinct G4 folding possibilities that are spatially separated enough to identify two differently positioned replication blocks. The endogenous G4 site Qua375 could fulfill such criteria since it consists of a minimal G4 sequence (G_{15}) and an upstream guanine triplet (G_3) that are separated by 4 nucleotides.

We analyzed Qua375 deletions in >20 *dog-1* animals and determined the 3′ deletion junctions and found that deletions at Qua375 indeed can occur right next to the G_{15} tract, but primarily start in front of the extra guanine triplet, thus >7 nucleotides away from the minimal G4 motif (Figure 3A). The resultant bimodal distribution of 3′ deletion junctions indicated that quadruplexes at Qua375 adopt two distinct folding types: one consisting merely of the minimal G_{15} tract and another type that includes both the G-tract and the guanine triplet (Figure 3A, right panel). After characterizing stochastic Qua375 deletions among individual *dog-1* animals, we set out to determine deletion junctions within single animals. Like for Qua1277, we extracted two Qua375 deletion products per animals using our PCR assay on 1% DNA fractions and determined the 3′ deletion junctions (Figure 3B). Strikingly, all deletion pairs from individual animals (12/12) were from the same type, *i.e.* the position of the first deletion had perfect predictive value for the position of the second deletion (p=0.004). This strong correlation between 3′ deletion junctions within individuals was not limited to two G4 deletions, as also the cases having three or four different Qua375 deletions had matching 3′ junctions (p=0.003) (Figure 3C). The highly significant correlation between 3′ deletion junctions within single animals and the typical position next to G4 motifs strongly suggest that these genomic deletions have a common ancestor and that their position is determined by the anticipated polymerase block - the 3′ leg of the quadruplex fold. These observations together with the overrepresentation of double deletions within animals (Figure 1E) provide further evidence that G4 structures can arise during animal development and argue strongly for a scenario in which the DOG-1/FANCJ helicase is essential to resolve DNA secondary structures that would otherwise persist throughout the animal's life and cause multiple deletions.

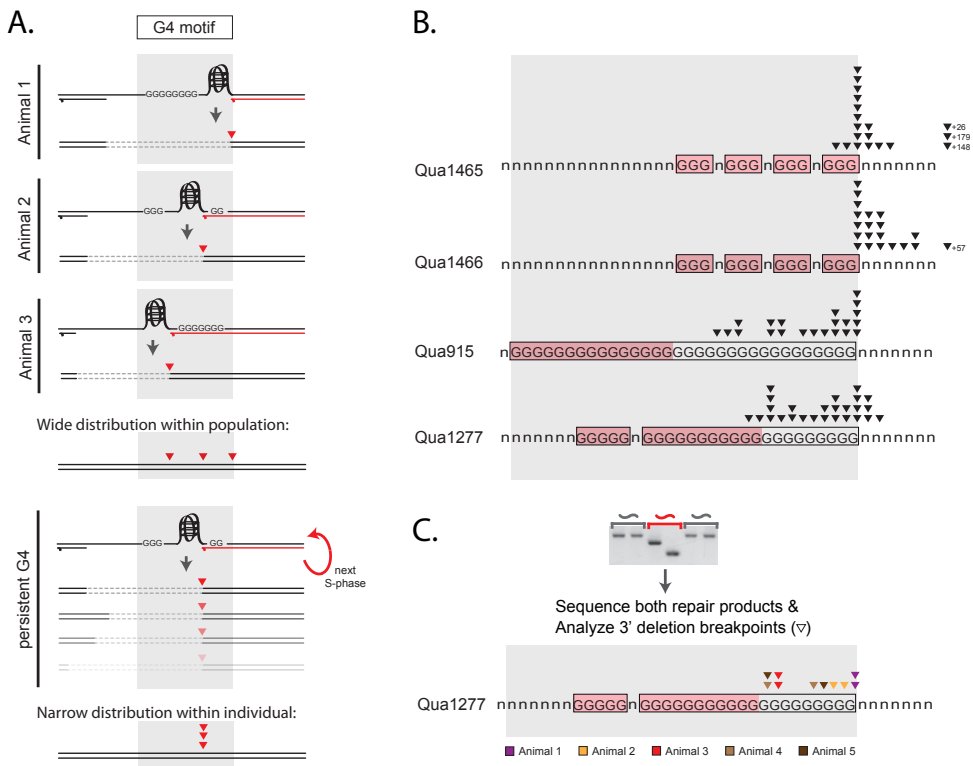

Figure 3. Spectra of 3′ deletion junctions correlate with G4 quadruplex configurations A. Schematic representation of possible G4 quadruplex positions in G-rich motifs and its strong association with 3′ deletion junction position (red triangle). While stochastic G4 folding events within the population are predicted to occur randomly along the possible folding positions and thus produce a wide spectrum of 3′ deletion junctions, persistent G4 structures are predicted to stay at one position and thus cause a very narrow spectrum of 3′ deletion junctions within individuals. **B.** Spectra of 3′ deletion junctions at indicated G4 loci. Each black triangle represents a 3′ deletion junction identified in a unique individual. **C.** Experimental setup and results of 3′ deletion junction analysis at Qua1277 in single *dog-1* deficient animals. The 3′ deletion junctions identified in 1% lysate fractions of the same individual are color-coded as indicated by the legends.

Although 3′ junctions of G4 deletions within an animal are very similar, no significant correlation was found for deletion size (Figure 4D). This observation suggests that the blocking lesion persists, but the resultant pre-mutagenic substrates (e.g. ssDNA gaps) can vary, leading to stochastic 5′ junctions. Similarly, we did not find any predictive value for the presence of flank insertions among double deletions, suggesting that subsequent repair events also occur on uniquely formed substrates. All together, these data imply that a single G4 structure can persist and give rise to various lesions that are processed independently by TMEJ.

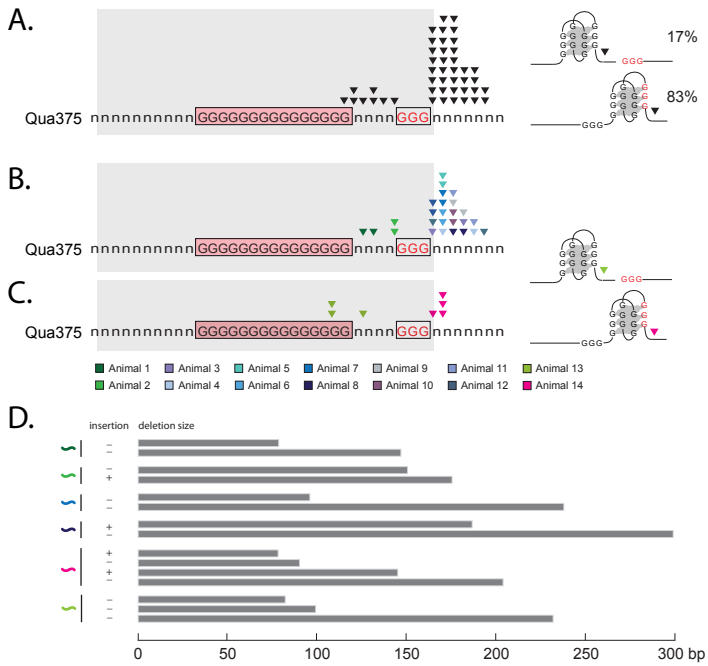

Figure 4. Recurrent 3′ deletion junctions at endogenous G4 site in single animals
A. Bimodal spectrum of 3′ deletion junctions at Qua375. Each black triangle represents a 3′ deletion junction identified in a unique individual. Illustrations on the right portray expected G4 quadruplex configurations at Qua375 and their relative frequencies **B and C.** Results of 3′ deletion junction analysis at Qua375 in single *dog-1* deficient animals. The 3′ deletion junctions identified in 1% lysate fractions of the same individual are color-coded as indicated. Illustrations on the right portray expected G4 quadruplex configurations at Qua375 in animal 13 and 14 in which several recurrent 3′ deletion junctions were identified. **D.** Histogram depicts sizes of G4 deletions in the individual animals of which the 3′ deletion junctions are depicted above. Individuals are color-coded as indicated in Figure 4C. Presence of flank insertions is indicated (+/-).

Visualization of multiple G4 deletion events during organ development

To substantiate our PCR-based findings we set out to visualize multiple G4 deletion events directly in single animals using a LacZ-based reporter system. We constructed transgenic animals that express LacZ only when a G4-induced deletion brings the reporter ORF in frame with the upstream ATG start codon (Figure 5A). The G4 reporter construct is driven by a *myo-2* promoter, which results in specific expression in pharyngeal muscle cells. The *C. elegans* pharynx is a well-characterized organ composed of cells with different embryonic origins and its muscle cells undergo approximately ten mitotic divisions after fertilization of the zygote. We hypothesized that also these cells could be subject to persistent lesions, resulting in multiple deletions in different cells of the pharynx.

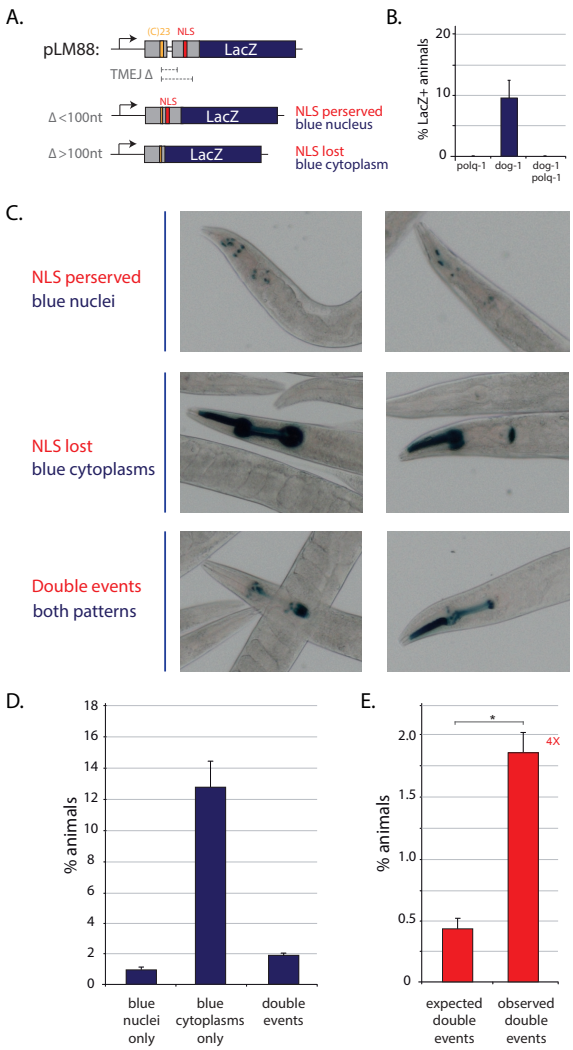

Figure 5. Transgenic G4 instability reporter reveals co-occurring deletions of different sizes during pharynx development

A. Schematic diagram of G4 instability reporter pLM88 and repair outcomes via TMEJ. While relative small deletions will keep the downstream nuclear localization signal (NLS) intact, larger deletions will exclude the NLS from the restored LacZ ORF. **B.** Histogram shows quantification of stochastic pLM88 ORF correction in three asynchronous populations measured by the percentage of LacZ positive animals of the indicated genotype. Average percentage of LacZ-positive animals of three independent experiments is depicted and error bars represent S.E.M. **C.** Representative pictures of stochastic LacZ expression patterns of *dog-1* deficient pLM88 animals. **D.** Histogram depicts quantification of stochastic LacZ patterns in synchronized populations of *dog-1* deficient pLM88 animals (as illustrated in figure 5C). Average percentage of LacZ-positive animals of three independent experiments is depicted and error bars represent S.E.M. **E.** Comparison of the observed frequency of double events and the expected frequency of double staining patterns based on the frequency of the individual nuclear/cytoplasmic LacZ patterns. Asterisk indicates highly significant over-representation of the observed double events within the population (n=1933) as determined by hypergeometric testing ($p<0.001$).

To discriminate unique deletion events in single animals we exploited the fact that deletions arising from a single replication block can be of different size; we cloned a nuclear localization signal (NLS) 90bp downstream of the G4 motif, allowing small deletions to keep the NLS intact and big deletions to exclude the NLS but still render the LacZ reporter gene functional. As expected, *dog-1* deficiency resulted in a stark increase in LacZ expressing cells and we detected both nuclear and cytoplasmic staining patterns (Figure 5B and 5C). In line with previous reports showing that >75% of G4 deletions are bigger than 100bp (Koole *et al.* 2014), we found the vast majority of LacZ expressing animals to display cytoplasmic LacZ patterns (~80%), indicating that often the NLS was lost (Figure 5D). Moreover, both LacZ patterns were *polq-1* dependent, indicating that TMEJ was indeed responsible for these deletion events (Figure 5B). We next determined the frequency of LacZ ORF correction events and found 15% of the animals to display cytoplasmic staining patterns and 3% to have nuclear LacZ staining patterns. Notably, animals harboring cells with nuclear LacZ often displayed additional cells with cytoplasmic staining, suggesting that they suffered (at least) two unique G4 deletion events (Figure 5D). Importantly, the frequency of such double events was significantly higher (>4 fold) than expected based on the stochastic frequencies of the individual patterns ($p<0.001$), confirming that G4 deletions co-occur during animal development (Figure 5E). These observations imply that somatic cells are prone to suffer from a G4 deletion when other cells in the lineage sustained a deletion at that very same locus, substantiating the notion that *dog-1* deficient animals harbor local pre-mutagenic substrates that promote the formation of multiple G4 deletions in descending cells. All together, these data argue that unresolved G4 structures can persist during animal development and present a potent source of genetic mosaicism in somatic tissues.

Discussion

Faithfull DNA replication is crucial to all life forms and is continuously challenged by lesions that can obstruct the replicative polymerase. Endogenous replication barriers are thought to be a major source of spontaneous mutagenesis, potentially promoting malignant transformation. However, little is known about the consequences of endogenous replication barriers for animal development, especially when present at low physiological levels. In recent years, several defense mechanisms are identified that promote DNA synthesis past replication barriers, including specialized translesion polymerases that can bypass damaged DNA bases (e.g. POLH/POLH-1) and helicases that can resolve DNA secondary structures (e.g. FANCJ/DOG-1). Deficiencies in these translesion polymerases or DNA helicases result in cancer prepositions syndromes in humans and increased spontaneous mutagenesis in *C. elegans* (Masutani *et al.* 1999; Levitus *et al.* 2005; Koole *et al.* 2014; Roerink *et al.* 2014). Recent studies imply a major role for TMEJ in repairing DSBs inflicted by unresolved replication

barriers, typically resulting in deletions of 50-300bp in size (Koole *et al.* 2014; Roerink *et al.* 2014). Yet how unresolved replication barriers promote the formation of genomic deletions on a mechanistic level remained elusive. Here, we provide evidence for a model in which low frequency replication barriers escape detection and direct processing, allowing them to spawn multiple TMEJ-mediated genomic rearrangements in descending cells.

We studied the mutagenic role of endogenous G4 quadruplexes: guanine-rich DNA secondary structures that are very stable under physiological conditions and potently block replication *in vitro* (Howell *et al.* 1996; Han *et al.* 1999; Huppert 2010). While the biochemical properties of G4 quadruplexes have been well characterized, their formation and putative function *in vivo* has remained elusive and a subject of debate ever since they were first described (Guschlbauer *et al.* 1990). While recent studies suggest that G4 quadruplexes may be functionally important to regulate transcription, DNA replication and/or telomere maintenance, the use of thermodynamically stable G4 quadruplexes as regulatory entities is controversial, mainly because such structures are intrinsically recombinogenic and would pose serious problems to many DNA metabolic processes (Tarsounas and Tijsterman 2013). Several DNA helicases are reported to resolve G4 quadruplexes *in vitro* (including *FANCJ, PIF1* and *BLM*), presenting several conceivable defense mechanisms to neutralize the malicious properties of G4 quadruplexes.

The data presented here indicate that G4 quadruplexes persist during *C. elegans* development in the absence of the DOG-1/FANCJ helicase, implying that effective redundant activities that can resolve these stable DNA structures *in vivo* are absent. Moreover, the persistent mutagenicity of G4 motifs suggests that G4 quadruplexes can be highly stable throughout the animal's lifetime and support the notion that these enigmatic DNA structures do occur *in vivo*.

The frequency and 3′ junction analysis of G4 deletions presented here argue that G4 quadruplexes arise stochastically within the animal population but remain stable in *dog-1* deficient individuals, resulting in several TMEJ-mediated deletions during animal development. These findings were substantiated by a LacZ-based reporter system able to detect different G4 deletions in single animals, showing that G4 deletions are prone to co-occur in somatic tissues. We propose a model where unresolved G4 quadruplexes block the replicative polymerase, leading to short stretches of unreplicated DNA opposite the persistent G4 structure (*i.e.* 50-300bp ssDNA gaps). These ssDNA gaps present pre-mutagenic lesions that might not stall mitotic division. Upon a second round of replication, the ssDNA gaps are converted into replication-born DSBs, which via TMEJ result into 50-300bp deletions. Importantly, the G4-bearing strand remains intact during the process of deletion formation, causing the replicative polymerase to run again into the persistent G4 quadruplex and create a new 50-300bp ssDNA gap. In agreement with this model we found the co-occurring deletions in single animals to have matching 3′ junctions (suggestive of a persistent polymerase block) but stochastic 5′

junctions (suggestive of independent ssDNA gap sizes/DSB substrates). Furthermore, the high co-occurrence of G4 deletions in single animals argues that the mutagenic lesions are not lost during deletion formation but instead promote G4 instability during animal development.

The persistence of unresolved G4 quadruplexes also implies that these DNA secondary structures are not processed directly by structure-specific nucleases to create DSBs and TMEJ-mediated deletions. The data presented here thus suggest that the biological consequences of low frequency replication barriers are fundamentally different to the replication stress induced via overall DNA polymerase inhibition (e.g. by aphidicolin) or nucleotide depletion (e.g. by hydroxyurea). The latter treatments impede efficient DNA replication, resulting in DNA breaks and gaps at hard to replicate chromosomal regions called “fragile sites”. Recent data indicate that break formation at fragile sites is an active process that requires structure-specific nucleases such as MUS81 and XPF (Minocherhomji and Hickson 2014). Here we found deletion formation at endogenous G4 sites to occur independent of these nucleases, suggestive of a different source of genome instability. We propose that inhibition of DNA synthesis by DNA polymerase inhibitors or nucleotide depletion may result in large sections of unreplicated DNA that are subject to nuclease cleavage, while low frequency replication barriers might inflict relatively small ssDNA gaps that escape detection and nuclease cleavage. This latter attribute allows unresolved replication barriers to persist during mitotic divisions and cause multiple ssDNA gaps that induce DSBs in subsequent replication rounds, ultimately resulting in numerous genomic rearrangements in proliferating tissues.

The persistent lesion model, as presented here, also provides an explanation why replication-born DSBs caused by unresolved replication barriers are not repaired via error-free mechanisms like homologous recombination (HR), but instead are repaired via mutagenic pathways such as TMEJ. If unresolved replication barriers remain present during the process of DSB formation, the replication-born DSBs (derived from the ssDNA gaps) cannot be repaired via HR using the sister-chromatid, because this template still contains the persistent lesion (Figure 1A). In contrast to HR, TMEJ does not require an undamaged repair template, allowing DSB repair in the presence of a lesion-bearing sister chromatid. Repair via TMEJ comes with a price, however, as it results in small deletions. The notion that a single unresolved replication barrier can cause multiple DSBs that are bound to be repaired via mutagenic means illustrates the potential hazard of such lesions and emphasizes the need for helicases such as DOG-1/FANCJ to safeguard genome stability in proliferating tissues.

The concepts mentioned above may also have important implications for cancer development, as the mutagenic burden of unresolved replication barriers is predicted to grow every time the cell divides, fueling genetic heterogeneity in fast proliferating tissues. We show here that a single unresolved G4 quadruplex can cause many deletions and promote genetic heterogeneity in somatic tissues, a feature often found in tumor tissues and known to correlate with poor prognosis (Burrell *et al.* 2013). Given the significant enrichment of G4 motifs at

structural genomic variations in cancer tissues (De and Michor 2011), unresolved replication barriers may present a potent source of genomic instability during cancer evolution.

Materials and Methods

Genetics

All strains were cultured according to standard *C. elegans* procedures (Brenner 1974). Alleles used in this study include: *LGI; dog-1(gk10), mus-81(tm1937), LGII; xpf-1(e1487), LGIII: polq-1(tm2026), LG unknown; lfIs77 [pLM88].*

PCR-based assays to identify G4 deletions at endogenous loci

Stochastic deletion formation at endogenous G4 DNA loci was assayed using a PCR-based approach. Genomic DNA was isolated either from single worms or pools of worms and subjected to nested rounds of PCRs with primers that flank a G4 motif; all amplicons are >1kb in size. PCR-based methods are highly sensitive and allows detection of low-frequency genomic rearrangements: G4 deletion products are preferentially amplified because they are smaller than the abundant wild-type products and lack the G4 motif that hampers DNA replication *in vitro* (Pontier *et al.* 2009).

To capture independent G4 deletion events in individuals, L4 stage animals were used (1 worm per 10ul lysis reaction) and ~0.1ul lysate (1%) was transferred into 15ul PCR reactions using a 384 pin replicator (Genetix X5050). Subsequently 0.2ul of PCR product was used for 15ul nested PCR reactions. PCR reactions were typically run for 35 cycles with 54°C primer annealing and 72°C extension for 120 seconds. x The following primers (5′-3′) were used: Qua213; ctcagccaaggctacaaac, gatacgtgtacatgaatagtc, ccggcaattacacatttgcc, caaaactgtcgcctgacctc,Qua1277;ggggagaagccgcatccaa,cacatggagacggagagaaac, cctgacaaacgcctactctc,gaatccctttaatttggcaatag,Qua375;ctagttcagggtatctggac, ccttctctcgaagcgcgacc, ggacggagagtcaataaaatc, cgaggtaaagtgcccgcaatc.

Deletion junctions were analyzed by Sanger sequencing.

To obtain stochastic deletions frequencies at Qua1277 and Qua375, we analyzed two independent PCR reactions on 1% lysate fractions of >190 *dog-1* proficient and >330 *dog-1* deficient L4 animals. Unique deletion products were discriminated based on size by gel-electrophoreses. To obtain the expected frequency of animals carrying two independent stochastic deletions we considered the two genomic lystate fractions as independent tests and multiplied the deletion frequency in the first sample to the frequency of unique deletions in the second sample. Dominant deletions products that resulted in identical deletions in both lysate fractions were assigned positive only in the first sample but not in the second, because these two deletions products did not represent independent stochastic events. In fact, subsequent testing of singe worm lysates that displayed two identical deletions resulted exclusively in

identical PCR products (5/5), indicating that such deletion products act dominantly in the PCR reaction and likely prevent the amplification of actual independent stochastic events, actually resulting in an underestimation of unique double deletion events. To determine whether there was significant over-representation of double deletion events, we used a hypergeometric test for overlap between the stochastic deletion frequency (based on the deletion frequency among independent individuals and size of the population) and the observed deletion frequency within the population sample carrying at least one unique deletion. This test returns the probability of a given number of sample successes, given the sample size, population successes and population size (hypergeometric p-value).

LacZ-based transgenic reporter assay to visualize G4 deletions

Transgenic strains were obtained by microinjection of reporter construct pLM88 [myo-2::C23::stops::NLS::LacZ] and mCherry-based co-expression markers pGH8 pCFJ104 to generate *lfIs77 (Frokjaer-Jensen et al. 2008)*. To visualize stochastic G4 deletions, clonal lines of *dog-1* deficient *lfIs77* animals were synchronized by bleaching and ~200 L1 animals were grown on OP50 plates and stained for LacZ expression three days later (Pothof *et al.* 2003). To obtain LacZ expression frequencies, >4 synchronized populations of three independent clonal *dog-1 lfIs77* lines were analyzed.

Supplementary information

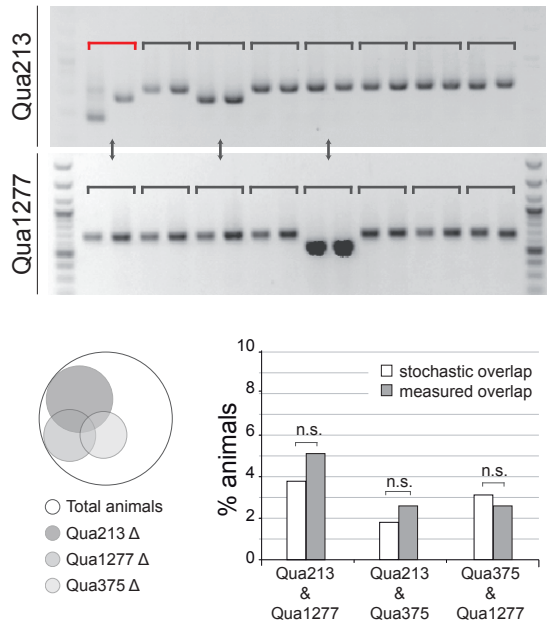

Figure S1. No significant correlation among G4 deletions detected at different genomic loci
PCR analysis of G4 instability at endogenous G4 loci Qua213, Qua1277 and Qua375. Representative gel images are depicted used to monitor stochastic deletions at Qua213 and Qua1277 in the same set of *dog-1* deficient animals (upper panels). Arrows illustrate no correlation between deletion events at the different loci in the same animal. Venn diagram shows distribution of G4 deletion events among 156 animals tested for all three loci. Histogram depicts expected frequencies of animals showing stochastic G4 deletions at both indicated G4 loci, assuming the deletion events are independent random events (white bars), as well as the observed frequencies of animals showing G4 deletions at both indicated G4 loci (grey bars). n.s. indicates a non-significant over-representation of the overlap between the indicated G4 deletion samples within the animal population (n=156) as determined by hypergeometric testing ($p > 0.20$), strongly suggesting that these are random independent events.

Acknowledgements

The authors thank Shohei Mitani (National Bioresource Project, Japan) and the Caenorhabditis Genetics Center for strains; Jane van Heteren, Ron Romeijn and Maartje van Kregten for valuable technical support.

References

Agostinho, A., B. Meier, R. Sonneville, M. Jagut, A. Woglar *et al.*, 2013 Combinatorial regulation of meiotic holliday junction resolution in C. elegans by HIM-6 (BLM) helicase, SLX-4, and the SLX-1, MUS-81 and XPF-1 nucleases. PLoS Genet 9**:** e1003591.

Blow, J. J., X. Q. Ge and D. A. Jackson, 2011 How dormant origins promote complete genome replication. Trends Biochem Sci 36**:** 405-414.

Brenner, S., 1974 The genetics of Caenorhabditis elegans. Genetics 77**:** 71-94.

Budzowska, M., and R. Kanaar, 2009 Mechanisms of dealing with DNA damage-induced replication problems. Cell Biochem Biophys 53**:** 17-31.

Burrell, R. A., N. McGranahan, J. Bartek and C. Swanton, 2013 The causes and consequences of genetic heterogeneity in cancer evolution. Nature 501**:** 338-345.

De, S., and F. Michor, 2011 DNA secondary structures and epigenetic determinants of cancer genome evolution. Nat Struct Mol Biol 18**:** 950-955.

Edwards, D. N., A. Machwe, Z. Wang and D. K. Orren, 2014 Intramolecular telomeric G-quadruplexes dramatically inhibit DNA synthesis by replicative and translesion polymerases, revealing their potential to lead to genetic change. PLoS One 9**:** e80664.

Elvers, I., F. Johansson, P. Groth, K. Erixon and T. Helleday, 2011 UV stalled replication forks restart by re-priming in human fibroblasts. Nucleic Acids Res 39**:** 7049-7057.

Frokjaer-Jensen, C., M. W. Davis, C. E. Hopkins, B. J. Newman, J. M. Thummel *et al.*, 2008 Single-copy insertion of transgenes in Caenorhabditis elegans. Nat Genet 40**:** 1375-1383.

Guschlbauer, W., J. F. Chantot and D. Thiele, 1990 Four-stranded nucleic acid structures 25 years later: from guanosine gels to telomer DNA. J Biomol Struct Dyn 8**:** 491-511.

Han, H., L. H. Hurley and M. Salazar, 1999 A DNA polymerase stop assay for G-quadruplex-interactive compounds. Nucleic Acids Res 27**:** 537-542.

Helleday, T., 2013 PrimPol breaks replication barriers. Nat Struct Mol Biol 20**:** 1348-1350.

Howell, R. M., K. J. Woodford, M. N. Weitzmann and K. Usdin, 1996 The chicken beta-globin gene promoter forms a novel “cinched” tetrahelical structure. J Biol Chem 271**:** 5208-5214.

Huppert, J. L., 2010 Structure, location and interactions of G-quadruplexes. FEBS J 277**:** 3452-3458.

Jiricny, J., 2013 Postreplicative mismatch repair. Cold Spring Harb Perspect Biol 5**:** a012633.

Koole, W., R. van Schendel, A. E. Karambelas, J. T. van Heteren, K. L. Okihara *et al.*, 2014 A Polymerase Theta-dependent repair pathway suppresses extensive genomic instability at endogenous G4 DNA sites. Nat Commun 5**:** 3216.

Kruisselbrink, E., V. Guryev, K. Brouwer, D. B. Pontier, E. Cuppen *et al.*, 2008 Mutagenic capacity of endogenous G4 DNA underlies genome instability in FANCJ-defective C. elegans. Curr Biol 18**:** 900-905.

Levitus, M., Q. Waisfisz, B. C. Godthelp, Y. de Vries, S. Hussain *et al.*, 2005 The DNA helicase BRIP1 is defective in Fanconi anemia complementation group J. Nat Genet 37**:** 934-935.

Loeb, L. A., and R. J. Monnat, Jr., 2008 DNA polymerases and human disease. Nat Rev Genet 9**:** 594-604.

Manthei, K. A., and J. L. Keck, 2013 The BLM dissolvasome in DNA replication and repair. Cell Mol Life Sci 70**:** 4067-4084.

Masutani, C., R. Kusumoto, A. Yamada, N. Dohmae, M. Yokoi *et al.*, 1999 The XPV (xeroderma pigmentosum variant) gene encodes human DNA polymerase eta. Nature 399**:** 700-704.

Minocherhomji, S., and I. D. Hickson, 2014 Structure-specific endonucleases: guardians of fragile site stability. Trends Cell Biol 24**:** 321-327.

O'Neil, N. J., J. S. Martin, J. L. Youds, J. D. Ward, M. I. Petalcorin *et al.*, 2013 Joint molecule resolution requires the redundant activities of MUS-81 and XPF-1 during Caenorhabditis elegans meiosis. PLoS Genet 9**:** e1003582.

Pontier, D. B., E. Kruisselbrink, V. Guryev and M. Tijsterman, 2009 Isolation of deletion alleles by G4 DNA-induced mutagenesis. Nat Methods 6**:** 655-657.

Pothof, J., G. van Haaften, K. Thijssen, R. S. Kamath, A. G. Fraser *et al.*, 2003 Identification of genes that protect the C. elegans genome against mutations by genome-wide RNAi. Genes Dev 17**:** 443-448.

Preston, B. D., T. M. Albertson and A. J. Herr, 2010 DNA replication fidelity and cancer. Semin Cancer Biol 20**:** 281-293.

Roerink, S. F., R. van Schendel and M. Tijsterman, 2014 Polymerase theta-mediated end joining of replication-associated DNA breaks in C. elegans. Genome Res 24**:** 954-962.

Saito, T. T., D. Y. Lui, H. M. Kim, K. Meyer and M. P. Colaiacovo, 2013 Interplay between structure-specific endonucleases for crossover control during Caenorhabditis elegans meiosis. PLoS Genet 9**:** e1003586.

Saito, T. T., J. L. Youds, S. J. Boulton and M. P. Colaiacovo, 2009 Caenorhabditis elegans HIM-18/SLX-4 interacts with SLX-1 and XPF-1 and maintains genomic integrity in the germline by processing recombination intermediates. PLoS Genet 5**:** e1000735.

Tarsounas, M., and M. Tijsterman, 2013 Genomes and G-quadruplexes: for better or for worse. J Mol Biol 425**:** 4782-4789.

Youds, J. L., N. J. O'Neil and A. M. Rose, 2006 Homologous recombination is required for genome stability in the absence of DOG-1 in Caenorhabditis elegans. Genetics 173**:** 697-708.

6

Homology-directed repair bypasses polymerase Theta-mediated end joining of G quadruplex-induced DNA breaks

Lemmens BB, van Schendel R, Tijsterman M

Abstract

Damaged DNA bases and DNA secondary structures such as G4 quadruplexes impede DNA replication and promote the occurrence of deleterious DNA double strand breaks (DSBs). In recent years, several alternative repair mechanisms have been found to repair DSBs parallel to the heavily studied pathways non-homologous end joining (NHEJ) and homologous recombination (HR). Yet how these pathways interact and what dictates pathway choice remains poorly understood. We recently identified polymerase Theta mediated end joining (TMEJ) to be the major pathway responsible for mutagenic repair of replication-born DSBs in *C. elegans* and to prevail over NHEJ and HR in the repair of G4-induced DSBs. Here we establish that DNA sequence context can dictate repair pathway choice of G4-induced DSBs and identify a mutagenic homology-driven repair (HDR) mechanism that uses >4 base pair homology at the presumptive DSB ends and can bypass the requirement of polymerase Theta/POLQ-1 for G4-induced deletion formation. Deletion frequency analysis at endogenous G4 sites revealed that HDR can locally dominate over TMEJ and that some TMEJ substrates can be channeled into HDR, illustrating that both mechanisms can repair similar substrates. However, given the specific homology requirements of HDR, TMEJ remains the major repair route genome-wide. We propose that the key role of POLQ-1 polymerase is to create *de novo* homologous sequences at DSB ends, providing a stable double-stranded intermediate to extent 3′ DNA ends and seal replication-born DSBs.

Introduction

Impediments to DNA replication hamper the cell in copying its genome with high fidelity and therefore are a major threat to genome stability (Tourriere and Pasero 2007; Budzowska and Kanaar 2009; Preston *et al.* 2010). Damaged DNA templates, as well as unresolved DNA secondary structures, can stall replicative polymerases, preventing duplication of the DNA past the lesion. One well-studied DNA secondary structure that is very stable under physiological conditions and is a potent replication block *in vitro* is the G4 quadruplex (Howell *et al.* 1996; Han *et al.* 1999; Huppert 2010). Given that the human genome harbors more than 300,000 guanine rich motifs that can adopt G4 quadruplex configurations, G4 DNA poses a serious threat to replication fidelity. Several specialized DNA helicases such as FANCJ/DOG-1 can resolve G4 quadruplexes *in vitro* and loss of these helicases results in elevated levels of genomic rearrangements at G4 sites *in vivo* (Tarsounas and Tijsterman 2013; Murat and Balasubramanian 2014). Recent data indicate that G4 DNA can cause genetic and epigenetic alterations in various model organisms and G4 motifs have been associated with structural genomic variations in human cancers (Tarsounas and Tijsterman 2013; Murat and Balasubramanian 2014). The molecular mechanisms responsible for G4-induced genomic variations are, however, poorly understood.

In the current model, replication fork stalling at unresolved G4 structures causes DNA double strand breaks (DSBs) that can be repaired in an error-pone fashion, possibly leading to genomic rearrangements that drive malignant transformation (Koole *et al.* 2014; Murat and Balasubramanian 2014). In recent years, several alternative repair pathways have been identified that can repair DSBs parallel to the two major DSB repair pathways: non-homologous end joining (NHEJ) and homologous recombination (HR) (Fishman-Lobell *et al.* 1992; Ma *et al.* 2003; Chan *et al.* 2010; Deriano and Roth 2013; Roerink *et al.* 2014). While all DSB repair pathways have been shown to act in replicating cells, their relative contribution to DSB repair depends heavily on sequence context. For instance, NHEJ can seal DSBs independent of sequence context (0 nt), while HR requires extensive sequence homology from an undamaged template (>100nt) (San Filippo *et al.* 2008; Lieber 2010). The alternative DSB repair routes often require base pairing of complementary DNA to align and seal DSB ends, yet the extent of this DNA template dependence varies among the different pathways. In fact, DSB repair via polymerase Theta mediated end joining (TMEJ) hardly requires homology (≤1nt), while other homology driven repair (HDR) routes typically require longer stretches of complementary sequences to align and repair the break (>4nt) (Fishman-Lobell *et al.* 1992; Ma *et al.* 2003; Roerink *et al.* 2014). To date, the molecular characteristics and genetic requirements of mutagenic HDR are still ill defined and may encompass interconnected mechanisms that have previous been designated as alternative end joining (alt-EJ), micro-homology mediated end joining (MMEJ) or single strand annealing (SSA), all of which use

complementary DNA sequences to seal DSBs. Since the exact nature and genetic distinction of these individual pathways is still controversial, we here define HDR as a mutagenic DSB repair mode that uses >4nt homology.

We recently identified TMEJ as the major repair route responsible for mutagenic repair of replication-associated DSBs in *C. elegans* and found TMEJ to prevail over NHEJ and HR in the repair of G4-induced DSBs (Koole *et al.* 2014; Roerink *et al.* 2014). The highly conserved polymerase theta/POLQ-1 is at the heart of TMEJ and is also required for the frequent flank insertions associated with TMEJ, yet why such a polymerase is crucial for replication-associated DSB repair is still unclear.

Here we investigate alternative DSB repair mechanisms that may act on G4-induced substrates and found that HDR can also result in deletion formation. In fact, we found that deletion formation at endogenous G4 sites that are flanked by short stretches of homology can occur independent of POLQ-1 activity and can locally dominate over TMEJ when homology is readily present at the presumptive DSB ends. All G4 deletions smaller than 600 base pairs (bp) found in *polq-1*-deficient animals used flanking homology, representing an alternative repair product to the >10,000 bp deletion products reported in *polq-1* mutants at non-repetitive loci (Koole *et al.* 2014). In accordance with previous studies, we found G4 sites not flanked by apparent homology to depend entirely on POLQ-1 for deletion formation (<1kb). Deletion frequency analysis at endogenous G4 sites revealed that some TMEJ substrates can be channeled into HDR, yet the efficiency is limited and correlates with homology abundance.

All together these data argue that G4-induced DSBs can be repaired by TMEJ and HDR, yet given the specific homology requirements for HDR, TMEJ is the major repair route genome-wide. Nevertheless, the bypass of POLQ-1 requirement by the presence of flanking homology strongly suggests that the major role for POLQ-1 is to create minimal homology between both DSB ends, providing a stable double-stranded intermediate to extent 3′ DNA ends and seal replication born DSBs.

Results

Transgenic reporters reveal POLQ-1-independent deletion formation

The first indication that G4-induced DSBs could be repaired by other means than TMEJ came from the analysis of a transgenic reporter assay we had previously employed to identify genes required for G4 instability (Figure 1A). We previously screened randomly mutagenized animals carrying a multi-copy transgene of pRP1879, a LacZ-based reporter construct that reads out mutagenic repair of G4-induced DSBs and found only *dog-1*-deficient animals to express LacZ positive cells (Kruisselbrink *et al.* 2008). Given the established role of DOG-1 in suppression of G4 instability at endogenous G4 loci, this screen validated our transgenic reporter setup, however the nature of repair events underlying LacZ expression was unknown.

Deletions at endogenous G4 sites typically rely on TMEJ and are uni-directional, 50-300bp in size, use 0-1bp homology and start directly at the G4 motif (Koole *et al.* 2014). Consequently, G4-induced TMEJ events normally leave the sequence upstream of the G4 motif intact (Figure 1A, G4 motif in yellow). The pRP1879 transgene, however, expresses LacZ only when both stop codons flanking the G4 site are removed, which means that a part of the upstream sequence needs to be lost during the repair reaction (Figure 1A, white bars represent stop codon). In fact, HDR using the upstream homologous (230bp) LacZ repeat would result in exclusion of both stop codons and render the LacZ open reading frame (ORF) functional (Figure 1B). Since deletions at G4 sites typically rely on TMEJ, we wondered if these putative HDR events would also rely on POLQ-1. Strikingly, ORF correction of pRP1879 still occurred with high frequency in *polq-1*-deficient animals, arguing that G4-induced deletions can occur in a TMEJ-independent fashion (Figure 1C).

To study whether the position and length of flanking homology could influence *polq-1* dependency, we constructed a novel LacZ-based reporter transgene pLM20, in which we positioned a shorter (50bp) homologous sequence directly upstream (left) and 24bp downstream (right) of the G4 site, allowing both TMEJ and HDR to correct the reporter ORF (Figure 1D and 1E, homology depicted in red). Also here pLM20 transgene expression was specifically induced upon *dog-1* deficiency, suggesting that LacZ expression indeed reflects repair of G4-induced DSBs (Figure 1F). To test the relative contribution of TMEJ in pLM20 expression, we generated *dog-1; polq-1* double mutants and found LacZ expression to be significantly reduced, but not absent, compared to *dog-1* single mutants (Figure 1F). These results imply that most pLM20 ORF correction events depend on TMEJ, yet some level of TMEJ-independent repair is possible. Based on these observations we hypothesized that HDR of G4-induced DSBs is possible and, depending on the degree of flanking homology, may compete with TMEJ for repair.

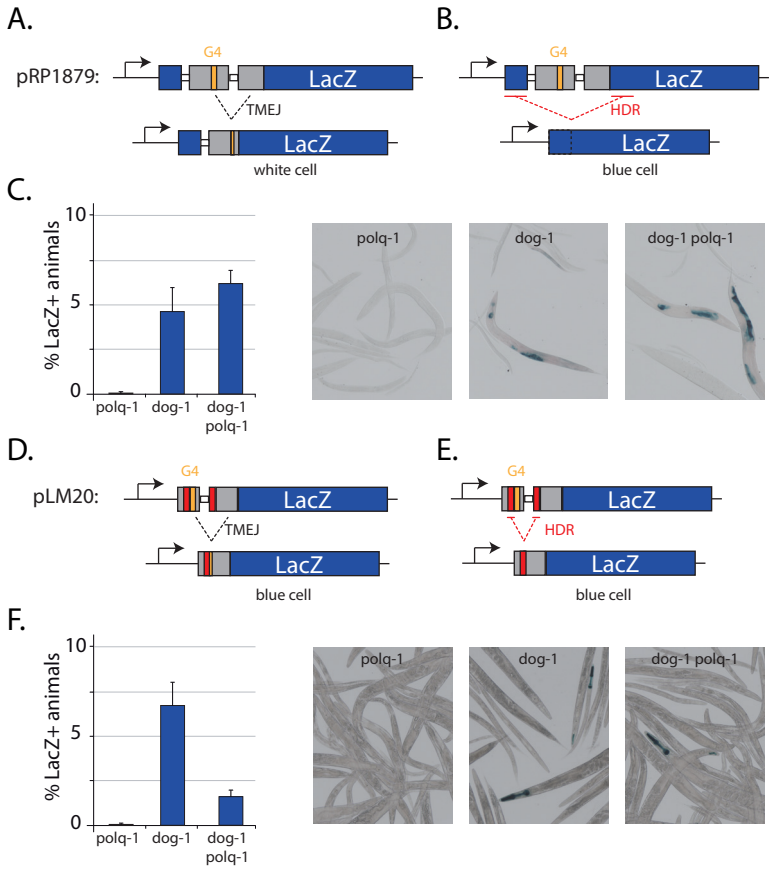

Figure 1. Transgenic reporters reveal POLQ-1-independent deletion formation of G4 sites
A. Schematic diagram of G4 instability reporter pRP1879 and repair outcome via TMEJ. pRP1879 is driven by a *hsp-16.41* promoter that allows expression in various somatic tissues. Deletion formation by TMEJ is not expected to remove the upstream stop codon (white blocks) and thus will not result in a blue cell. **B.** Schematic diagram of G4 instability reporter pRP1879 and repair outcome via HDR. HDR using the upstream repeats corrects the LacZ ORF and will result in a blue cell. **C.** Histogram shows quantification of stochastic pRP1879 ORF correction measured by the percentage of LacZ-positive animals of the indicated genotype. Average percentage of LacZ-positive animals of three independent experiments is depicted and error bars represent S.E.M. Representative pictures of the stochastic LacZ expression patterns are shown on the right. **D.** Schematic diagram of G4 instability reporter pLM20 and repair outcome via TMEJ. pLM20 is driven by a *myo-2* promoter that allows specific expression in pharyngeal muscle cells. Deletion formation by TMEJ is expected to remove the downstream stop codon (white blocks) irrespective of the homologous repeats (red) and can result an in-frame LacZ ORF and a blue cell. **E.** Schematic diagram of G4 instability reporter pLM20 and repair outcome via HDR using the 50bp repeats (red). HDR using the homologous repeats corrects the LacZ ORF and will result in a blue cell. **F.** Histogram shows quantification of stochastic pLM20 ORF correction measured by the percentage of LacZ-positive animals of the indicated genotype. Average percentage of LacZ-positive animals of three independent experiments is depicted and error bars represent S.E.M. Representative pictures of the stochastic LacZ expression patterns are shown on the right.

Flanking homology at endogenous G4 sites allows POLQ-1-independent deletion formation

In order to directly compare TMEJ and HDR events in a single-copy environment, we searched the *C. elegans* genome for endogenous G4 sites that had different degrees of flanking homology. We selected four loci that resided on chromosome I, II, III and IV, respectively: Qua213, Qua375, Qua915 and Qua1277. While Qua375 has no apparent flanking homology, Qua1277, Qua213 and Qua915 have increasing levels of flanking homology, respectively, and harbor short genomic repeats that potentially could support HDR (Figure 2A and S1 for entire sequence context). Especially Qua915 is located in a highly repetitive genomic context and is flanked by many different short repeats and three major repeats of 29bp (Figure 2A).

To analyze deletion formation at these repetitive loci and study TMEJ dependency, we performed nested PCR reactions on genomic DNA lysates of *polq-1*, *dog-1* and *dog-1; polq-1* double mutant animals using primers that flank the G4 motif as well as the surrounding repeat sequences (Figure 2B and S1). While *polq-1* single mutants did not display G4 instability at any of the loci tested, *dog-1*-deficient animals showed many differently sized deletions at all four loci, indicating that also at these loci the DOG-1 helicase is required to prevent the induction of G4-induced deletions. To test if these deletions depended on TMEJ, we analyzed deletion formation in *dog-1; polq-1* double mutants and found that indeed all small deletions at Qua375 depended on POLQ-1 (Figure 2B). In contrast, Qua1277, Qua213 and Qua915 still showed some small deletion in the absence of POLQ-1, indicating that these homology-rich loci can spawn deletions independent of TMEJ (Figure 2B). Interestingly, the residual deletions at Qua1277 or Qua213 were always of identical size, suggestive of a preferred repair outcome specific for each locus. Sequence analysis revealed that all TMEJ-independent deletion events at Qua1277 or Qua213 used HDR based on the two major repeats flanking the G4 sites (Figure 2A).

HDR footprints imply available 3′ overhangs at G4-induced DSBs

While these observations provided further evidence that TMEJ-independent repair mechanisms exist, they also provided clues regarding the molecular nature of the predicted G4-induced substrate: a replication-derived DSB (see Figure 3 for the current model). In TMEJ-proficient *dog-1* animals Qua375 and Qua1277 behaved very similarly: all deletions were uni-directional and started directly at the G4 motif (Figure 2C). The typical position of the upstream deletion breakpoint implies that the location of the G4 structure dictates the position of the resultant DSB end and the strong preservation of the sequences upstream the G4 motif suggests that the 3′ end of this DSB is quite stable during the repair process (Figure 2C and 2D).

Furthermore, the HDR footprints at Qua1277 in *dog-1; polq-1* animals imply that the upstream repeat was exposed and able to anneal to its homologous counterpart, suggesting that the upstream DSB end was not blunt ended but instead had >100bp 3′ overhangs (Figure

2C and 2D). This observation is supported by the data acquired using the pRP1879 transgene. Similar to the upstream repeat at Qua1277, the upstream LacZ repeat in pRP1879, positioned 270bp away from the G4 motif, needs to be available to allow HDR to occur and the LacZ reporter gene to be expressed (Figure 1A). Likewise, G4 deletions at Qua915 frequently involved annealing of repeats residing 15-80bp upstream of the G4 motif, even in the presence of POLQ-1, suggesting that the upstream DSB end may intrinsically have a 3′ overhang that could serve as a substrate for both HDR and TMEJ; a feature consistent with a model for replication-born DSBs (Figure 2C and 3).

No evidenced for NHEJ activity at G4-induced DSBs

The idea that G4-derived DSBs inherently may have substantial 3′ overhangs would be in line with the reported lack of NHEJ activity on these substrates (Youds *et al.* 2006; Koole *et al.* 2014). NHEJ can efficiently repair blunt-ended DSBs but not resected DSBs (Lieber 2010). Although both NHEJ and TMEJ should be able to repair DSBs in the absence of homologous sequences, TMEJ is the pathway of choice to repair G4-induced DSBs (Koole *et al.* 2014). Recently several well-conserved factors, including FANCD2/*fcd-2* and CtIP/*com-1,* have been identified that suppress NHEJ activity at endogenous DSBs by initiating DNA end resection (Adamo *et al.* 2010; Lemmens *et al.* 2013). To test if NHEJ would be able to repair G4-induced DSBs in the absence of these NHEJ-suppressors, we constructed *dog-1; polq-1; fcd-2* and *dog-1; polq-1; com-1* triple mutants and analyzed deletion formation at Qua375. Similar to the *dog-1; polq-1* double mutant controls, none of the triple mutant animals showed homology-independent deletions, suggesting that also in these genetic backgrounds NHEJ cannot act on G4-derived DSBs (Figure S2). In contrast, we observed many deletion products in the POLQ-1 proficient *dog-1* controls, indicating that TMEJ is the key pathway to repair G4-induced DSBs in the absence of flanking homology (Figure S2).

A limited number of TMEJ events can channel into HDR

To study the effects of TMEJ deficiency and address the relative contribution of TMEJ and HDR events, we examined deletion formation at Qua375, Qua213 and Qua915 in >360 *dog-1* and >360 *dog-1;polq-1* animals and determined the deletion frequencies at the different G4 loci in the same population (Figure 2E). While in all cases the deletion frequency dropped in *dog-1;polq-1* animals compared to *dog-1* single mutants, the extent of *polq-1* dependency differed substantially between loci. While the deletion frequency at the repetitive locus Qua915 was hardly affected by *polq-1* loss (85%), the deletion frequency at Qua213 dropped drastically in the absence of *polq-1* (6%) and deletions were even completely absent at Qua375 (0%), suggesting that the extent of flanking homology correlates directly to the potency of deletion formation in the absence of POLQ-1 (Figure 2E).

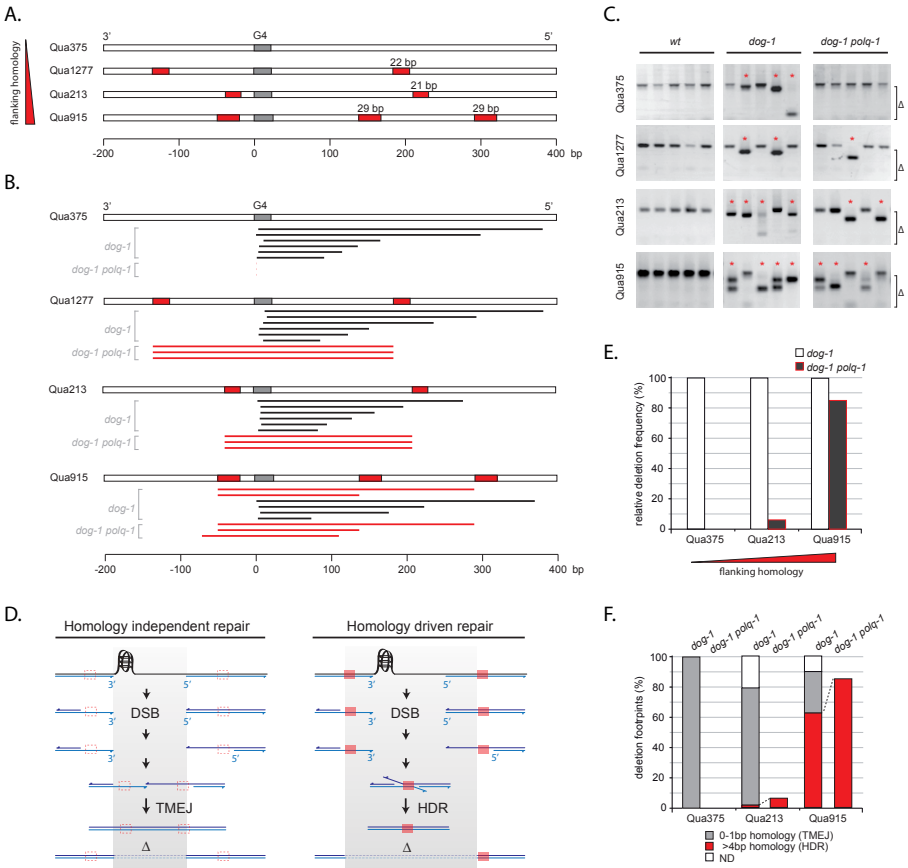

Figure 2. Flanking homology at endogenous G4 sites allows POLQ-1-independent deletion formation

A. Schematic diagram of four endogenous G4 loci with different degrees of flanking homology. G4 loci are aligned relative to the 5′ position of the G4 motif and the most prominent homologous repeats are indicated in red. **B.** Graphic illustration of G4 deletions profiles at three endogenous G4 loci. For each locus six typical G4 deletions in *dog-1* and three typical G4 deletions in *dog-1; polq-1* animals are depicted. Black bars represent homology-independent deletions; red bars represent homology-dependent events. **C.** Representative images of the different PCR-based assays used to identify G4-induced deletions at the indicated G4 loci. Per lane genomic DNA of three adult animals was PCR-amplified using primers flanking the G4 motif and homologous repeats. Asterisks indicate stochastic deletions, which manifest as shorter than wild-type products and Δ indicates the size-range of the PCR-amplified deletion products. **D.** Models for G4-induced deletions formation via TMEJ (left) and HDR (right). Filled red boxes indicate homologous sequences. Grey gradients illustrate the association between deletion size/position and the G4-induced ssDNA gap (in case of TMEJ) or the position of the homologous repeats (in case of HDR). **E.** Histogram depicts relative deletion frequencies at the indicated G4 loci as determined by the PCR-based assay on 1% single worm lysates of *dog-1* (white bars) and *dog-1; polq-1* animals (black bars). Depicted frequencies are relative to the deletion frequency in *dog-1* single mutants to allow comparison of loci expressing different stochastic G4 deletion rates (n>360, see methods section for details). **F.** Histogram depicts relative frequencies of deletion footprints with >4bp homology (red) and without homology (grey) as identified by the PCR-based assay at the indicated G4 loci (see methods section for details). Repair footprints were analyzed from PCR-amplified deletion products obtained from 1% single worm lysates of *dog-1* (left) and *dog-1; polq-1* animals (right).

We next extracted the deletion products at Qua375, Qua213 and Qua915 and determined the repair footprints. All residual deletions in *polq-1*-deficient animals used extensive homology (>4bp) and deleted sequences far upstream of the G4 motif, indicative of HDR events (Figure 2F). Importantly, POLQ-1-proficient *dog-1* animals also showed HDR footprints, revealing that TMEJ does not completely suppress HDR. When we directly compared the frequencies of TMEJ and HDR footprints among *dog-1* and *dog-1;polq-1* animals, we observed an increase in HDR events at the expense of TMEJ products in *polq-1* deficient animals, suggesting that some TMEJ substrates can be channeled into HDR (Figure 2F).

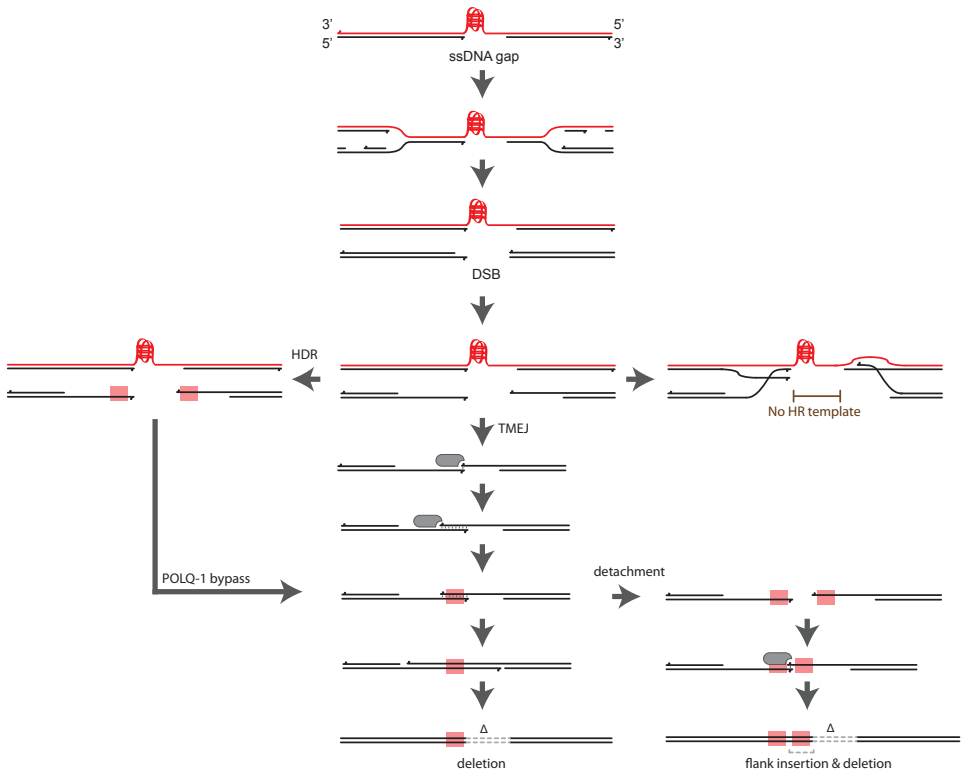

Figure 3. Model for G4-induced deletion formation
Model describes the origin of replication-born DSBs from G4-induced ssDNA gaps and subsequent DSB repair via HDR and TMEJ. The DNA strand bearing the persistent G4 quadruplex is depicted in red. Transparent red boxes indicate homologous sequences. Polymerase Theta/POLQ-1 is depicted in grey. See main text for further details.

HDR can locally dominate repair of G4-induced DSBs

The observation that the requirement for POLQ-1 in G4 deletion formation can be bypassed by the presence of homologous sequences lead us to question which repair mode was initiated first. To investigate how sequence context around G4 motifs controlled the choice between HDR and TMEJ, we plotted the distribution of all homology-independent deletions at Qua375, Qua213 and Qua915, and sorted the deletions based on their position relative to the G4 motif (illustrated by the black bars in Figure 4A). Subsequently all deletions were binned in 50bp windows to obtain a 5′ deletion junctions distribution relative to the G4 motif (4B). In accordance with previous studies on non-repetitive G4 loci (Koole *et al.* 2014), we found the vast majority of Qua375 and Qua213 deletions to be 50-300bp in size (>85%), with most 5′ deletion junctions residing 101-150bp downstream of the G4 motif (~30%) (Figure 4B, white and grey bars). The G4 deletions at Qua915 were also typically 50-300bp in size (>85%), however the distribution of 5′ deletion junctions was significantly different (Figure 4B, black bars). Strikingly, none of the homology-independent deletions at Qua915 had 5′ deletion junctions residing 101-150bp downstream of the G4 motif (0%), clearly contrasting the distribution found at other G4 sites (Figure 4B, highlighted in pink). Also no homology-independent Qua915 deletions were observed 251-300bp downstream of the G4, while these were observed at Qua375 and Qua213 (Figure 4B, highlighted in pink). The fact that the major homologous repeats flanking Qua915 are located exactly downstream of the regions devoid of homology-independent deletions strongly argues for a dominant role of these repeats in sequestering TMEJ substrates. These data imply that G4-derived DSBs that contain homologous repeats of sufficient size at both break ends are preferably repaired via HDR and not TMEJ (Figure 4C, middle panel). Such a dominant effect of homologous sequences also explains why HDR events are frequent at Qua915, even in the presence of functional POLQ-1 (Figure 2F).

We also noted that the dominant effect of the homologous sequences only suppressed the TMEJ events with 5′ deletion junctions upstream (left) of the repeat but not those with 5′ junctions directly downstream (right) of the repeat (Figure 4B, highlighted in pink and grey, respectively). In fact, the vast majority of the homology-independent deletions at Qua915 had 5′ deletion junctions residing 151-200bp downstream of the G4 motif (~45%), which is directly adjacent to the dominant repeat (Figure 4B, highlighted in grey). This directional effect of the homologous sequences is in perfect agreement with our model of G4-derived DSBs (Figure 3 and 4C). This model predicts that the 5′ deletion junction of a TMEJ event is determined by the size of the ssDNA gap caused by the replication-blocking G4 structure: replication of the G4-induced ssDNA gap results into a DSB that lacks the DNA sequence covered previously by the ssDNA gap (Figure 3 and 4C). Repair of these DSBs by TMEJ results in deletions with junctions corresponding directly to the position and size of the initial gap (Figure 2D and 3). In cases where the ssDNA gaps are small and reach just up to the homologous sequences,

the following DSB ends will contain flanking homology and HDR will be the preferred mode of repair (Figure 4C, middle panel): resulting in a lack of homology-independent Qua915 deletions with 5′ junctions upstream (left) of the repeat (Figure 4B, highlighted in pink). However, when the ssDNA gaps are larger and cover the homologous repeats, the DSB will not contain homologous sequences at both ends and TMEJ will be the preferred mode of repair (Figure 4C, right panel): indeed resulting in multiple homology-independent Qua915 deletions with 5′ junctions downstream (right) of the repeat (Figure 4B, highlighted in grey).

This model also predicts that repeats that are very close to the G4 site are poor substrates for HDR, even if they were larger than the 29bp repeats at Qua915, given that the ssDNA gaps often would cover the homologous sequences and the following DSBs would not have homologous ends (Figure 4C, right panel). Indeed, the vast majority of pLM20 ORF corrections was still *polq-1*-dependent and did not use the relatively large 50bp repeat positioned just 24bp downstream of the G4 site (Figure 1F and S3). All together these data support a model in which homologous sequences that flank G4 sites can mediate DSB repair but only when they are of sufficient size and located such that they are present in the subsequent DSB ends; in all other cases POLQ-1 activity is required for deletion formation (Figure 4C).

Figure 4. HDR can locally dominate repair of G4-induced DSBs ➔
A. Graphic illustration of G4 deletions profiles at Qua375 and Qua915 in *dog-1* deficient animals. Black bars represent homology-independent deletions. Genomic regions that display local dominance of HDR are highlighted in pink and reside directly left (5′) of the major repeats at Qua915 (red blocks). Genomic regions that reside directly right (3′) of the major repeats at Qua915 are highlighted in grey. **B.** Distribution of homology-independent deletions binned in 50bp windows based on the position of their 5′ junctions relative to the G4 motif. Genomic regions devoid of homology-independent events at Qua915 are highlighted in pink and reside directly left (5′) of the major repeats present at this locus. Genomic regions that reside directly right (3′) of the major repeats at Qua915 are highlighted in grey. Asterisk indicates significant difference between the local deletion frequency at Qua915 and the two other G4 loci that lack the downstream repeat ($p<0.01$ by Fisher's exact test, two tailed). **C.** Different models for G4-induced deletion formation depending on the presence of flanking homology. Left model: scenario at G4 sites lacking flanking homology, typically resulting in TMEJ products. Middle model: scenario at G4 sites with flanking repeats that are still present in the following DSB ends, resulting in HDR dominance. Right model: scenario at G4 sites with flanking repeats of which one is lost in the following DSB ends, again resulting in TMEJ products.

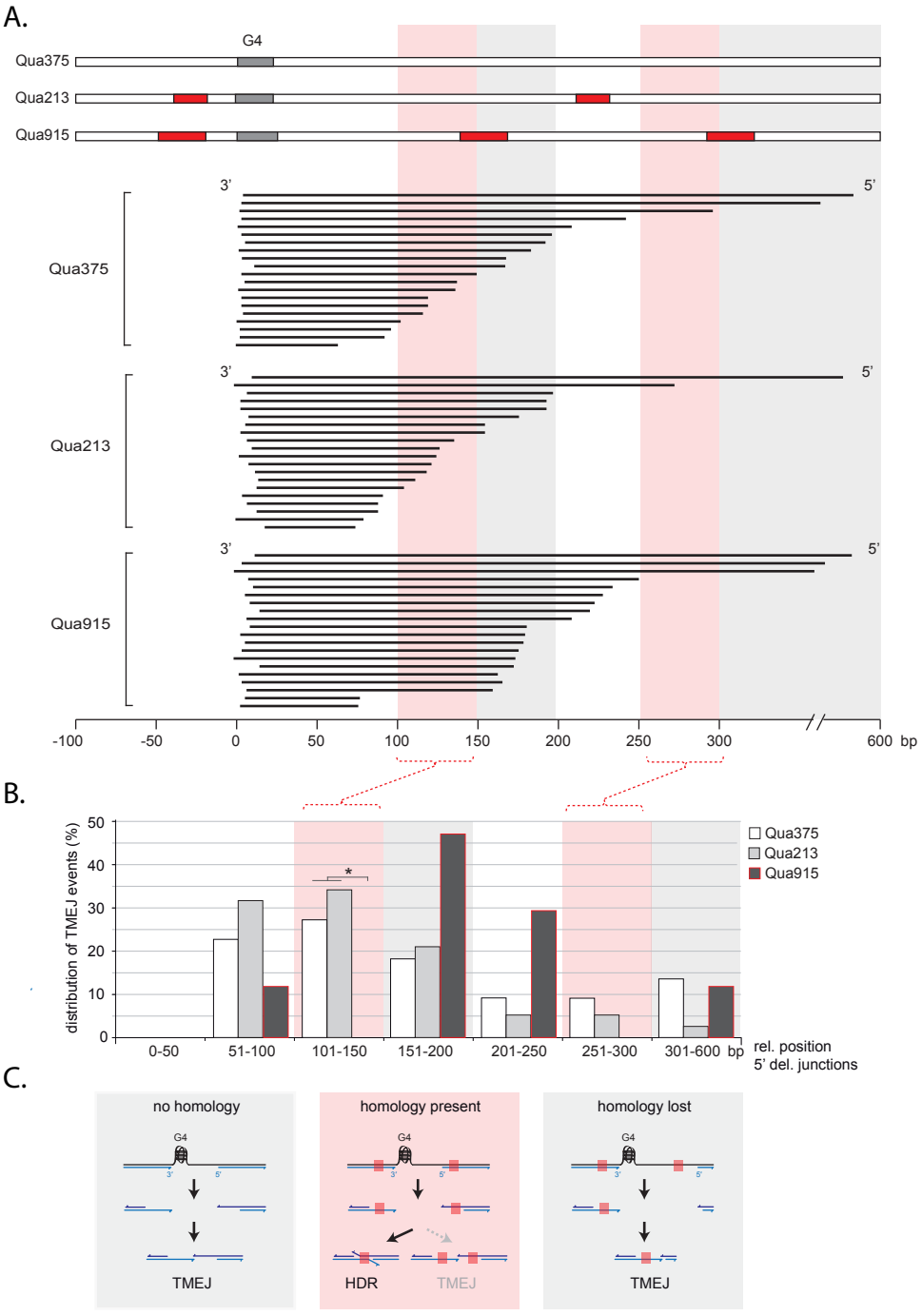
A.
G4
Qua375
Qua213
Qua915
3'
5'
-100
-50
0
50
100
150
200
250
300
600 bp
B.
distribution of TMEJ events (%)
Qua375
Qua213
Qua915
*
0-50
51-100
101-150
151-200
201-250
251-300
301-600 bp
rel. position
5' del. junctions
C.
no homology
homology present
homology lost
TMEJ
HDR
TMEJ
TMEJ

Discussion

Our genetic analysis revealed that homology-independent deletion events at G4 loci require TMEJ and that a subset of POLQ-1 substrates can be channeled into HDR provided that flanking homology is present. The local dominance of HDR at repetitive loci further illustrates the dynamic balance between TMEJ and HDR events and suggests that the presence of homologous repeats can direct repair pathway choice.

Based on these observations we propose a model in which unresolved G4 structures result in DSBs that can be repaired either via TMEJ or HDR depending on the sequence context (Figure 3 and 4C). The presence of homologous repeats at both DSB ends bypasses the need for POLQ-1 to create complementary 3′ DNA ends and allows immediate annealing of the DSB ends: paving the way for TMEJ-independent deletion formation.

When flanking homology is absent at the DSB and the sister-chromatid still harbors a persistent G4 structure, the cell relies on TMEJ to adequately repair G4-induced DSBs (Figure 3). We propose that stalled replication at persistent G4 structures leads to 50-300bp ssDNA gaps that in the next S-phase result in replication-born DSBs that are neither compatible for NHEJ (potentially due to long 3′ overhangs) nor have a suitable HR template (due to the persistent G4 structure) and thus require TMEJ or HDR for repair.

Replication-born DSBs are likely to be processed by DNA end resection nucleases in an attempt to initiate error-free HR repair via the sister-chromatid, given that such nucleases are activated during S-phase (Ferretti *et al.* 2013; Truong *et al.* 2013). Moreover, previous studies detected increased RAD-51 foci (a marker for resected DSBs) in genetic backgrounds with increased TMEJ products, including animals deficient for the G4-resolving helicase DOG-1 (Koole *et al.* 2014; Roerink *et al.* 2014). These studies also revealed that G4-induced DSBs lacking obvious flanking homology are processed extensively in TMEJ-deficient animals, ultimately resulting in elevated levels of RAD-51 foci, bi-directional deletions and extensive loss of genetic material (Koole *et al.* 2014; Roerink *et al.* 2014). Repair via TMEJ or HDR would prevent continuous DSB processing and putative deleterious signaling events, promoting proper animal development at the expense of small deletions. The notion that G4-induced DSBs can be repaired via TMEJ or HDR, but not NHEJ, implies that these DSBs contain substantial 3′ overhangs that allow annealing of homologous sequences but prevent binding of Ku (a dimeric protein complex that binds blunt DSB ends and initiates NHEJ). In the absence of repair via TMEJ, HDR or HR these 3′ overhangs could be a substrate for DNA end resection nucleases, resulting in persistent RAD-51 foci and bi-directional deletions (Koole *et al.* 2014).

We propose that the key role of polymerase Theta is to create *de novo* complementary sequences at 3′ DNA ends, allowing bridging of DSBs that lack flanking homology: a unique ability needed to repair DSBs genome-wide when canonical repair mechanisms such as HR and NHEJ are not feasible.

Material and Methods

Genetics

All strains were cultured according to standard *C. elegans* procedures (Brenner 1974). Alleles used in this study include: *LGI; dog-1(gk10), dog-1(pk2247), fnci-1(tm3081), LGIII: polq-1(tm2026), exo-1(tm1842), com-1(t1626) LGIV: fcd-2(tm1298), mre-11(ok179), LGX; pkIs2170 [pRP1879], LG unknown; lfIs55 [pLM20].*

LacZ-based transgenic reporter assay to visualize G4 deletions

Transgenic strains were obtained by microinjection of reporter construct pLM20 [myo-2::C23::stops::NLS::LacZ] and mCherry-based co-expression markers pGH8 pCFJ104 to generate *lfIs55* (Frokjaer-Jensen *et al.* 2008) or by microparticle bombardment of reporter construct pLM20 and *unc-119* expression marker to generate *pkIs2170.* To visualize stochastic G4 deletions, >4 clonal lines of *dog-1* deficient *lfIs55* or *pkIs2170* animals were stained for LacZ expression per experiment (Pothof *et al.* 2003).

PCR-based assays to identify G4 deletions at endogenous loci

Stochastic deletion formation at endogenous G4 DNA loci was assayed using a PCR-based approach. Genomic DNA was isolated either from single worms or pools of worms and subjected to nested rounds of PCRs with primers that flank the G4 motif and flanking repeats if present (see Figure S1 for detailed sequence context). To obtain stochastic deletions frequencies at Qua375, Qua213 and Qua915, we analyzed two independent PCR reactions on 1% lysate fractions of >190 *dog-1* proficient and >330 *dog-1* deficient animals. L4 stage animals were used (1 worm per 10ul lysis reaction) and ~0.1ul lysate (1%) was transferred into 15ul PCR reactions using a 384 pin replicator (Genetix X5050). Subsequently 0.2ul of PCR product was used for 15ul nested PCR reactions. PCR reactions were typically run for 35 cycles with 54°C primer annealing and 72°C extension for 120 seconds. Unique deletion products were discriminated based on size by gel-electrophoreses and repair footprints were analyzed by Sanger sequencing. Strictly deletions verified by both PCR reactions were analyzed and used to determine the deletion frequency.

Supplemental information

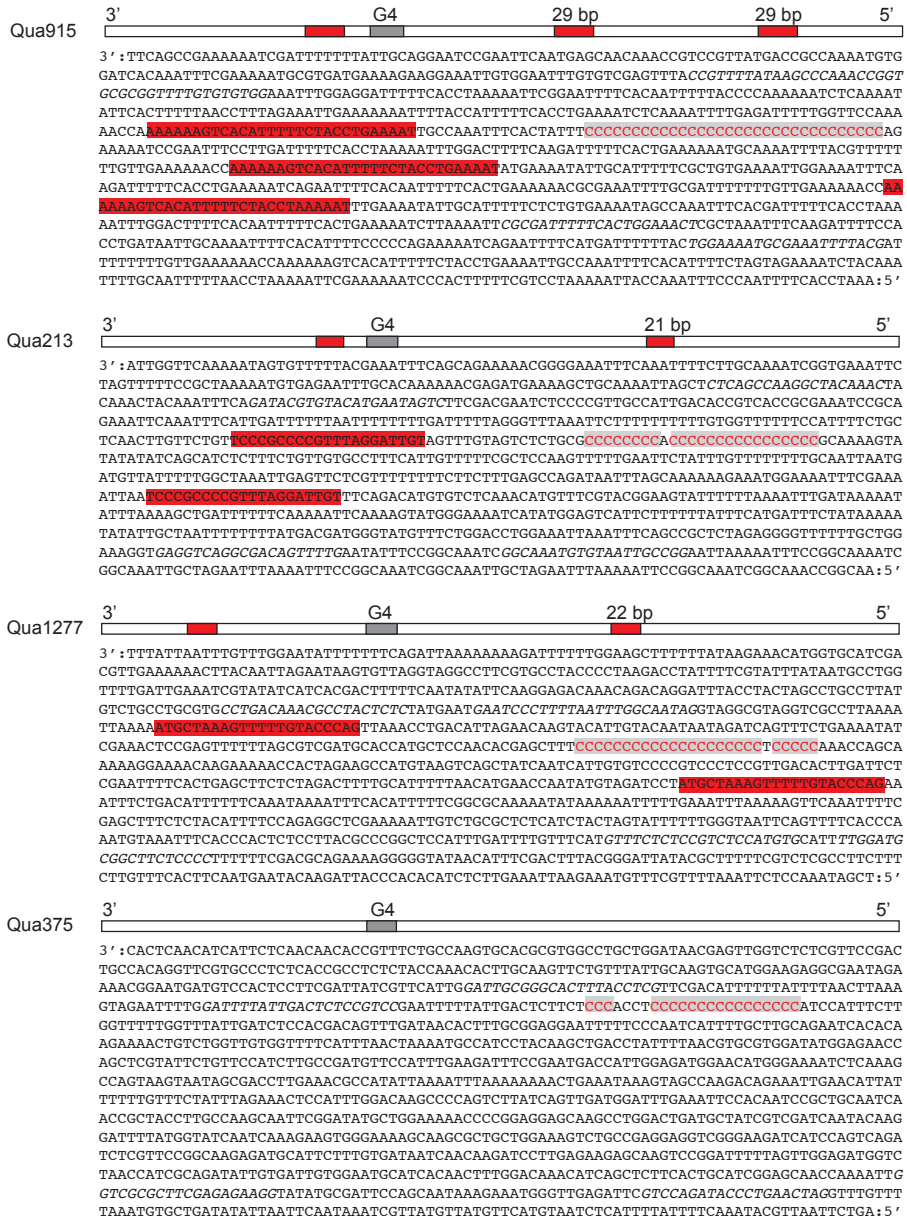

Figure S1. Sequence context of endogeous G4 sites tested for TMEJ/HDR events
Schematic diagrams and DNA sequence contexts of Qua915, Qua213, Qua1277 and Qua375. G4 motifs are highlighted in grey and prominent flanking repeats are highlighted in red. Primer sequences used for PCR amplification are italic.

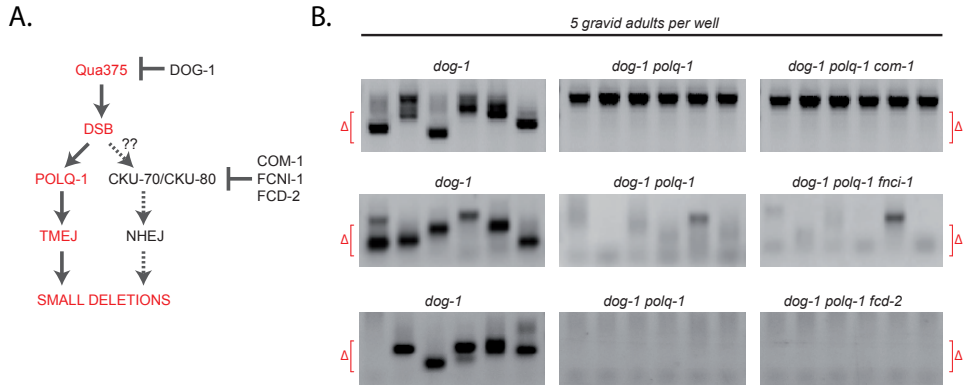

Figure S2. Stochastic G4 deletions at Qua375 depend on TMEJ even in absence of NHEJ suppressors

A. Model for G4-induced deletion formation and hypothetical suppression of NHEJ to act parallel to TMEJ

B. PCR analysis of G4 instability at endogenous G4 site Qua375; each well represents an independent PCR reaction on 10% lysate of five gravid adults of the indicated genotype; size-range of PCR-amplified deletions products is indicated by Δ. Upper panels: genomic lysates were obtained from first-generation *com-1* homozygous adults containing several embryo's to minimize the contribution of maternal COM-1. Middle and lower panels: PCR reactions were run with shorter extension times (1min) to hinder the formation of abundant wild-type products and enrich for G4 deletion products. In all cases, PCR conditions allowed efficient detection of multiple deletion events in *polq-1* proficient controls (left panels).

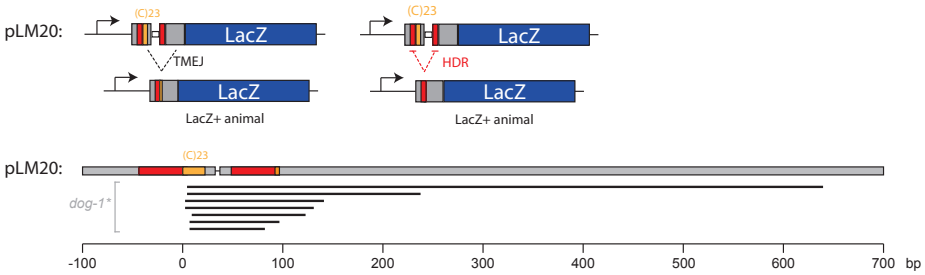

* Out of 2000 independent populations of dog-1 deficient pLM20 animals, 9 were identified that carried a germline LacZ ORF restoration event. Deletion footprint analysis revealed that 7 out of 7 tested populations contained non-homologous deletions resulting in an in-frame LacZ product. Although the sample size is small, these data suggest that only a minor fraction of repair events use the flanking repeat positioned very close to the G4 motif. This observation is in line with the substantial reduction in LacZ ORF correction events in TMEJ defecient pLM20 animals (Figure 1).

Figure S3. Frequent non-homologous germline G4 deletions (TMEJ events) at pLM20 reporter locus

Upper panels depict the pLM20 reporter construct and the anticipated TMEJ (left) and HDR (right) outcomes. Lower panel depicts germline G4 deletions profiles at the pLM20 reporter locus. *Out of 2000 independent populations of dog-1 deficient pLM20 animals, 9 were identified that carried a germline LacZ ORF restoration event. Deletion footprint analysis revealed that 7 out of 7 tested populations contained non-homologous deletions resulting in an in-frame LacZ product (black bars). Although the sample size is small, these data suggest that only a minor fraction of repair events use the flanking repeat positioned very close to the G4 motif. This observation is in line with the substantial reduction in LacZ ORF correction events in TMEJ defecient pLM20 animals (Figure 1).

Acknowledgments

The authors thank Shohei Mitani (National Bioresource Project, Japan) and the Caenorhabditis Genetics Center for strains; Jane van Heteren for technical support and valuable comments on the manuscript

References

Adamo, A., S. J. Collis, C. A. Adelman, N. Silva, Z. Horejsi *et al.*, 2010 Preventing nonhomologous end joining suppresses DNA repair defects of Fanconi anemia. Mol Cell 39**:** 25-35.

Brenner, S., 1974 The genetics of Caenorhabditis elegans. Genetics 77**:** 71-94.

Budzowska, M., and R. Kanaar, 2009 Mechanisms of dealing with DNA damage-induced replication problems. Cell Biochem Biophys 53**:** 17-31.

Chan, S. H., A. M. Yu and M. McVey, 2010 Dual roles for DNA polymerase theta in alternative end-joining repair of double-strand breaks in Drosophila. PLoS Genet 6**:** e1001005.

Deriano, L., and D. B. Roth, 2013 Modernizing the nonhomologous end-joining repertoire: alternative and classical NHEJ share the stage. Annu Rev Genet 47**:** 433-455.

Ferretti, L. P., L. Lafranchi and A. A. Sartori, 2013 Controlling DNA-end resection: a new task for CDKs. Front Genet 4**:** 99.

Fishman-Lobell, J., N. Rudin and J. E. Haber, 1992 Two alternative pathways of double-strand break repair that are kinetically separable and independently modulated. Mol Cell Biol 12**:** 1292-1303.

Frokjaer-Jensen, C., M. W. Davis, C. E. Hopkins, B. J. Newman, J. M. Thummel *et al.*, 2008 Single-copy insertion of transgenes in Caenorhabditis elegans. Nat Genet 40**:** 1375-1383.

Han, H., L. H. Hurley and M. Salazar, 1999 A DNA polymerase stop assay for G-quadruplex-interactive compounds. Nucleic Acids Res 27**:** 537-542.

Howell, R. M., K. J. Woodford, M. N. Weitzmann and K. Usdin, 1996 The chicken beta-globin gene promoter forms a novel “cinched” tetrahelical structure. J Biol Chem 271**:** 5208-5214.

Huppert, J. L., 2010 Structure, location and interactions of G-quadruplexes. FEBS J 277**:** 3452-3458.

Koole, W., R. van Schendel, A. E. Karambelas, J. T. van Heteren, K. L. Okihara *et al.*, 2014 A Polymerase Theta-dependent repair pathway suppresses extensive genomic instability at endogenous G4 DNA sites. Nat Commun 5**:** 3216.

Kruisselbrink, E., V. Guryev, K. Brouwer, D. B. Pontier, E. Cuppen *et al.*, 2008 Mutagenic capacity of endogenous G4 DNA underlies genome instability in FANCJ-defective C. elegans. Curr Biol 18**:** 900-905.

Lemmens, B. B., N. M. Johnson and M. Tijsterman, 2013 COM-1 promotes homologous recombination during Caenorhabditis elegans meiosis by antagonizing Ku-mediated non-homologous end joining. PLoS Genet 9**:** e1003276.

Lieber, M. R., 2010 The mechanism of double-strand DNA break repair by the nonhomologous DNA end-joining pathway. Annu Rev Biochem 79**:** 181-211.

Ma, J. L., E. M. Kim, J. E. Haber and S. E. Lee, 2003 Yeast Mre11 and Rad1 proteins define a Ku-independent mechanism to repair double-strand breaks lacking overlapping end sequences. Mol Cell Biol 23**:** 8820-8828.

Murat, P., and S. Balasubramanian, 2014 Existence and consequences of G-quadruplex structures in DNA. Curr Opin Genet Dev 25C**:** 22-29.

Pothof, J., G. van Haaften, K. Thijssen, R. S. Kamath, A. G. Fraser *et al.*, 2003 Identification of genes that protect the C. elegans genome against mutations by genome-wide RNAi. Genes Dev 17**:** 443-448.

Preston, B. D., T. M. Albertson and A. J. Herr, 2010 DNA replication fidelity and cancer. Semin Cancer Biol 20**:** 281-293.

Roerink, S. F., R. van Schendel and M. Tijsterman, 2014 Polymerase theta-mediated end joining of replication-associated DNA breaks in C. elegans. Genome Res 24**:** 954-962.

San Filippo, J., P. Sung and H. Klein, 2008 Mechanism of eukaryotic homologous recombination. Annu Rev Biochem 77**:** 229-257.

Tarsounas, M., and M. Tijsterman, 2013 Genomes and G-quadruplexes: for better or for worse. J Mol Biol 425**:** 4782-4789.

Tourriere, H., and P. Pasero, 2007 Maintenance of fork integrity at damaged DNA and natural pause sites. DNA Repair (Amst) 6**:** 900-913.

Truong, L. N., Y. Li, L. Z. Shi, P. Y. Hwang, J. He *et al.*, 2013 Microhomology-mediated End Joining and Homologous Recombination share the initial end resection step to repair DNA double-strand breaks in mammalian cells. Proc Natl Acad Sci U S A 110**:** 7720-7725.

Youds, J. L., N. J. O'Neil and A. M. Rose, 2006 Homologous recombination is required for genome stability in the absence of DOG-1 in Caenorhabditis elegans. Genetics 173**:** 697-708.

7

General discussion and future prospects

7

This dissertation discusses several aspects of DNA double strand break (DSB) repair and provides mechanistic insights in the occurrence and repair of DSBs during *C. elegans* development. DSB repair is crucial to ensure genome stability in developing animals, as unrepaired DSBs can result in extensive loss of genetic material and aneuploidy upon cell division. However, DSB repair is not error-free and can cause mutations and chromosome aberrations. In fact, mutagenic DSB repair can leave many genetic scars throughout development and ultimately promote malignant transformation (Aparicio *et al.* 2014). Eukaryotic cells possess many different DSB repair activities, some of which are intrinsically mutagenic (see Dutch summary, Figure 2). Cells need to tightly control the different DSB repair activities to limit the genetic consequences but also support efficient repair. Although the studies presented in this thesis provide further insight in the consequences of DSB repair pathway choice during animal development, still many questions remain to be addressed. Especially the temporal and spatial regulation of the different DSB repair pathways is poorly understood and will require future study. Furthermore, the molecular mechanisms that dictate repair template choice remain elusive. A selection of outstanding questions will be discussed in more detail below.

How to employ DSB repair in the right place and at the right time?

The consequences of mutagenic repair are mainly determined by the developmental context. For example, mutations in terminally differentiated somatic cells only affect the function of that particular cell, whereas mutations in germ stem cells may affect the fitness of the whole brood of the animal. It is thought that due to these different levels of evolutionary pressure, tissue-specific DSB repair modes could arise. In line with those concepts, *C. elegans* germ stem cells typically use error-free homologous recombination (HR) for DSB repair, while somatic cells rely on various error-prone DSB repair mechanisms (Clejan *et al.* 2006; Pontier and Tijsterman 2009). Interestingly, differential DSB repair activities are even present within the different germ line tissues. As described in Chapter 2, we found that certain germ cells depend heavily on COM-1 and EXO-1 for DNA end resection of DSBs, a crucial step in regulating DSB repair pathway choice. Interestingly, the requirement for these DNA end resection nucleases is regulated in a temporal and/or spatial fashion, given that certain germ cells at specific developmental stages were proficient in DNA end resection even in the absence of COM-1 and EXO-1. These specific germ cells are predicted to use the sister chromatid as a template for HR, whereas germ cells that require COM-1 and EXO-1 for DNA end resection use the homologous chromosome for repair (Hayashi *et al.* 2007). How early DSB processing factors are regulated during gametogenesis and how their activities are linked to chromosome organization and repair template availability is unknown to date. Similarly, we found LIN-61 to be required for HR in mitotic germ cells but not meiotic germ cells, again revealing tissue-specific DSB repair activities (Chapter 3). How these differential repair activities are controlled

and how malignant brain tumour domain proteins akin to LIN-61 regulate DSB repair on a mechanistic level requires further study.

How to choose between the good, the bad and the ugly?

The notion that DSB repair can have both benign and harmful consequences for animal development is well illustrated by the non-homologous end joining (NHEJ) pathway. As discussed in this thesis, NHEJ is vital to promote genome stability in somatic tissues (Chapter 4), but can also cause highly toxic repair products in germ cells (Chapter 2). Next to being toxic directly, NHEJ is also error-prone and thus creates mutations. A single DSB repair pathway can thus be "good", "bad" and "ugly" in light of genome maintenance.

The mutagenic attribute or the "ugly side" of DSB repair is adressed in more detail in Chapter 5 and 6, where we demonstrate that DSBs induced by unresolved replication barriers cause genomic deletions whose nature depends on sequence context and the mode of DSB repair. We have recently identified the major DSB repair pathway responsible for these deletions and named the pathway Theta-mediated end joining (TMEJ), as it required polymerase Theta/POLQ-1 (Koole *et al.* 2014; Roerink *et al.* 2014). In Chapter 5 we investigated the potential endogenous sources underlying TMEJ-mediated mutagenesis and found that a single unresolved DNA secondary structure, such as a G4-quadruplex, could serve as a continuous source of TMEJ substrates, ultimately leading to multiple deletions during *C. elegans* development. Subsequent in-depth analysis of repair footprints, revealed an alternative DSB repair mechanism that can compete with TMEJ for G4-induced deletion formation (Chapter 6). In contrast to TMEJ, this alternative homology driven repair (HDR) mechanism requires substantial sequence homology at both break ends. Because of these specific homology requirements, HDR is only feasible at highly repetitive loci. Nevertheless, the notion that TMEJ and HDR share the same substrates suggests an intimate connection between TMEJ and homology search mechanisms. Interestingly, genetic backgrounds that suffer from increased TMEJ-mediated deletions also show increased levels of HR intermediates (detected as RAD-51 foci), substantiating the idea that TMEJ and HR may act on similar substrates (Koole *et al.* 2014; Roerink *et al.* 2014). How cells decide between error-free repair via HR ("good") and mutagenic repair via TMEJ ("bad") is still an open question. As noted in Chapter 2, we identified a genetic factor, COM-1, that dictates the balance between HR ("good") and NHEJ ("bad") in germ cells. If COM-1 is also needed to prevent TMEJ to act on meiotic DSBs remains to be studied, but some level of genome instability remained in *com-1* animals that were deficient for NHEJ, suggesting that alternative end joining pathways may act on meiotic DSBs under these conditions (Chapter 2). Future genome-wide sequencing studies may reveal elevated level of TMEJ- and/or HDR-mediated mutagenesis in *com-1* deficient backgrounds.

What is the mechanism and biological significance of TMEJ and HDR?

In recent years several alternative DSB repair mechanisms have been described that in contrast to NHEJ use complementary DNA sequences to seal DSBs. These alternative DSB repair mechanisms have received different names including alternative end joining (alt-EJ), micro-homology mediated end joining (MMEJ) or single strand annealing (SSA). To date the molecular characteristics and genetic requirements of these pathways are still ill defined and may encompass common mechanisms that include single-strand DNA exposure, annealing of complementary sequences and removal of non-complementary flaps. Depending on the availability, length and position of the complementary sequences, these alternative DSB repair mechanisms may require genetic factors that support DNA resection, annealing or nicking, respectively. In Chapter 6, we describe two alternative DSB repair mechanisms that are distinct from NHEJ and can act on G4-induced DSBs: HDR, which requires >4bp sequence homology and TMEJ, which does not require extensive homology but needs polymerase Theta/POLQ-1. Further research is needed to elucidate to which extent the earlier described alternative DSB repair activities involve TMEJ and/or HDR mechanisms.

Because genetic studies often use a limited amount of model substrates to measure DSB repair outcomes, pathway definitions and extrapolation of genetic requirements to a genome-wide level has proven to be problematic. To this end, genome-wide sequencing approaches will become attractive tools to evaluate the impact of alternative DSB repair pathways on genome maintenance and study their role at numerous genomic locations.

Under which conditions are DSBs repaired via TMEJ?

In this thesis we focused on TMEJ in the context of G4-induced DSBs, which because of their fixed genomic location proved to be a powerful approach to study the genetic consequences of low-frequency replication barriers (Chapter 5 and 6). Recently our lab has identified additional roles for TMEJ on DSBs derived from other sources, including transposition (unpublished data). By comparing the different genetic interactions and repair outcomes of TMEJ events triggered by various sources of DSBs, one should be able to identify the genetic features that are intrinsic to TMEJ reactions (e.g. frequent flank insertions) and distinguish these features from those that are provoked by the substrate (e.g. deletion size).

How to find new components and potential regulators of TMEJ?

Similar to NHEJ, TMEJ could be harmful, as it is not error-free and in case of multiple DSBs could lead to translocations. This latter attribute may also have clinical implications given that up-regulation of polymerase Theta is associated with poor prognosis in human cancers (Higgins *et al.* 2010). On the other hand, the ability of TMEJ to seal DSBs without the need of extensive sequence homology makes it a valuable pathway to repair DSBs genome-wide. Although in-depth genetic analysis of repair outcomes, as described in chapters 5 and 6,

provided important clues on the mechanism of TMEJ, complementary approaches such as unbiased screens to identify additional genetic factors required for TMEJ could provide vital insights into the mechanism and regulation of this pathway. In addition, targeted proteomics approaches could reveal new players of TMEJ as well as novel post-translational modifications on polymerase Theta itself.

As described in Chapter 4, we performed unbiased forward genetics screens to identify new regulators of NHEJ and found several mRNA binding factors to be required for efficient NHEJ in somatic cells. Subsequent transcriptome analysis resulted in the identification of specific mRNA splicing defects in several newly identified mutants, revealing a potential novel link between mRNA splicing and DSB repair. The identification of canonical NHEJ factors (e.g. CKU-70 and CKU-80) and novel factors such as THOC-5 and PNN-1 validated the screen and demonstrated the power of such unbiased approaches. Still, one drawback of forward genetics screens is the typically need for the obtained alleles to be homozygous viable, which hinders the identification of essential genes. We obtained a point mutation in *thoc-2* that causes a NHEJ defect in *C. elegans* but did not completely block the essential function of THO, given that *thoc-2* null mutants are sterile (Castellano-Pozo *et al.* 2012). Thus forward genetics screens as performed here can reveal essential genes in DSB repair, but the identification of such alleles typically requires substantial screening depth.

We have established various transgenic reporter systems that can measure TMEJ activity at G4 sites, which can be used to screen for new factors required for TMEJ. Given that many TMEJ factors may be intrinsically connected to DNA replication and HR (which are both essential processes in *C. elegans*), careful design of future screens is needed to acquire many alleles and thus potential hypomorphic mutations. Conversely, identification of viable alleles of HR or DNA replication factors could open new research avenues as they provide new tools to study these important biological processes in other developmental contexts.

Concluding remarks

As discussed in this thesis, the efficacy and choice of DSB repair pathways can have tremendous influence on the toxicity and mutagenicity of DSBs. Future research to delineate the different DSB repair modes is vital to understand the genetic consequences of DSBs for animal development. Ultimately, new insights concerning the endogenous sources and consequences of genomic instability in developing tissues could provide important clues on the origin and possible treatment strategies of cancer.

References

Aparicio, T., R. Baer and J. Gautier, 2014 DNA double-strand break repair pathway choice and cancer. DNA Repair (Amst) 19**:** 169-175.

Castellano-Pozo, M., T. Garcia-Muse and A. Aguilera, 2012 R-loops cause replication impairment and genome instability during meiosis. EMBO Rep 13**:** 923-929.

Clejan, I., J. Boerckel and S. Ahmed, 2006 Developmental modulation of nonhomologous end joining in Caenorhabditis elegans. Genetics 173**:** 1301-1317.

Hayashi, M., G. M. Chin and A. M. Villeneuve, 2007 C. elegans germ cells switch between distinct modes of double-strand break repair during meiotic prophase progression. PLoS Genet 3**:** e191.

Higgins, G. S., A. L. Harris, R. Prevo, T. Helleday, W. G. McKenna *et al.*, 2010 Overexpression of POLQ confers a poor prognosis in early breast cancer patients. Oncotarget 1**:** 175-184.

Koole, W., R. van Schendel, A. E. Karambelas, J. T. van Heteren, K. L. Okihara *et al.*, 2014 A Polymerase Theta-dependent repair pathway suppresses extensive genomic instability at endogenous G4 DNA sites. Nat Commun 5**:** 3216.

Pontier, D. B., and M. Tijsterman, 2009 A robust network of double-strand break repair pathways governs genome integrity during C. elegans development. Curr Biol 19**:** 1384-1388.

Roerink, S. F., R. van Schendel and M. Tijsterman, 2014 Polymerase theta-mediated end joining of replication-associated DNA breaks in C. elegans. Genome Res 24**:** 954-962.

Addendum

Summary

Nederlandse samenvatting

Acknowledgements

Curriculum vitae

List of publications

S

Thesis summary

This thesis describes several studies conducted to examine how living organisms preserve their genetic material and how different DNA repair pathways influence genome stability. To study these questions the nematode *C. elegans* was used as a model organism, as it allows efficient genetic manipulation as well as in-depth genetic analysis of mutagenic processes. We exploited these unique attributes to i) convert these animals into *in vivo* sensors of DNA damage ii) identify factors not implicated in genome stability before, iii) unveil mechanisms that dictate DNA repair pathway choice, and iv) determine the biological consequences of endogenous barriers that impede DNA replication.

The genetic code of life is stored in DNA molecules that consist of two parallel strands of coupled nucleotides that form a DNA double helix. One of the most deleterious forms of DNA damage is a DNA double-strand break (DSB) in which both strands of the helix are broken. When not repaired adequately DSBs can lead to extensive loss of genetic information and/or genomic rearrangements, ultimately fueling genome instability, cellular dysfunction and malignant transformation. The high mutagenic and cytotoxic potential of DSBs poses a serious threat to human health, but also can be exploited to eradicate malignant cells. In fact, rapidly dividing cancer cells are often hypersensitive to DSB-inducing agents, including ionizing radiation (IR) and radiomimetic drugs. Surprisingly, certain cellular developmental programs actually depend on DSB formation, including the generation of gametes. Novel insights on the endogenous sources of DSBs as well as the mechanisms that deal with these toxic lesions should help us to better understand the complex processes underlying diseases such as cancer, as well as providing clues for treatment optimization. Furthermore, fundamental research on genome stability helps clarifying the driving forces of species evolution.

Chapter 1 summarizes the major contributions and recent progress in the *C. elegans* research field aimed to elucidate the complex networks involved in DSB repair. We describe the role of different DSB repair routes during nematode development and focus on two major DSB repair pathways: Non-Homologous End Joining (NHEJ) and Homologous Recombination (HR), the latter being widely studied due to its crucial role during gametogenesis.

Chapter 2 describes the identification of COM-1 (the ortholog of tumor suppressor CtIP) as a key factor dictating DSB repair pathway choice during gametogenesis. Germ cells lacking COM-1 suffer from unscheduled NHEJ activities that disturb programmed HR events during meiosis, ultimately resulting in chromosomal abnormalities and loss of progeny viability. Deleting the toxic NHEJ components in *com-1* deficient animals alleviated the meiotic defects and restored embryonic survival. Further genetic dissection revealed a redundant role for COM-1 and the nuclease EXO-1 in DNA end resection, a DSB processing step that enables HR.

Chapter 3 involves the characterization of the malignant brain tumour (MBT) domain protein LIN-61, which was identified in our lab to maintain genome stability in *C. elegans* germ cells. We combined various DNA repair assays and germline cytology techniques to reveal a role for LIN-61 in DSB repair via HR.

Chapter 4 entails our search for novel regulators of NHEJ, the major DSB repair pathway in somatic tissues. By generating a transgenic strain that allowed *in vivo* detection of NHEJ activity and performing unbiased forward genetics screens, a set of mutant animals was identified that had altered DSB repair efficacy. Interestingly, several mutants not only displayed defects in NHEJ and somatic IR-resistance, but also had common defects in mRNA splicing, revealing a new link between mRNA metabolism and NHEJ regulation.

In *chapter 5* we look into endogenous sources of DSBs and found an important role for DNA secondary structures in genome instability. Next to the canonical double helix, certain DNA sequences can fold into other inter- and intramolecular structures. One well-studied DNA secondary structure that is very stable under physiological conditions and is a potent replication block *in vitro* is the G4 quadruplex. Here evidence is presented for a model in which a single persistent G4 quadruplex can result in multiple genomic rearrangements during animal development, revealing the mutagenic potential of G4 DNA sequences and the biological significance of helicases that act on these DNA secondary structures.

Chapter 6 describes our efforts in resolving the repair mechanisms that act on G4-induced DSBs. Previously, our lab identified a novel DSB repair pathway, called polymerase Theta-Mediated End Joining (TMEJ) that acts on replication-born DSBs. Here we show that DNA sequence context can direct repair pathway choice at G4 sites: While G4-induced genomic rearrangements at non-repetitive DNA typically requires TMEJ, the presence of short DNA repeats flanking the G4 sequence bypasses this requirement and promotes homology-directed repair mechanisms.

All together these data indicate that animals possess a wide range of repair mechanisms to fix deleterious DSBs, which can arise from various sources, including IR, developmentally programmed nucleases and stochastic DNA replication impairments. Different repair routes can be used depending on cell type, protein expression, DSB nature, sequence context and repair substrate availability. Because each DSB repair route has unique consequences on repair outcome, the choice of repair can have tremendous influence on the genetic footprint a DSB leaves behind. This delicate balance has allowed DSBs to evolve as crucial substrates for developmental programs including gametogenesis, but also provides clues on how such lesions can change our genomes and promote serous diseases like cancer.

Nederlandse samenvatting

Dit proefschrift beschrijft een aantal studies die we hebben uitgevoerd om te onderzoeken hoe levende organismen hun genetisch materiaal op orde houden en hoe verschillende reparatiemechanismen hun sporen achter laten in het DNA van ontwikkelende dieren. De opeenstapeling van fouten in DNA kan leiden tot ernstige ontwikkelingsdefecten en veroudering, en ligt ten grondslag aan ziekten zoals kanker. Maar wat is DNA precies en waarom kunnen kleine foutjes in DNA zo'n grote gevolgen hebben? Om deze vraag te beantwoorden zal ik eerst het moleculairbiologisch kader schetsen waarin deze processen zich afspelen.

Een kijkje in de cel

Het menselijk lichaam bestaat uit vele miljarden cellen met elk hun taak en specialisatie. Fascinerend genoeg komt ieder mens voort uit één enkele cel, die na het samensmelten van de zaad- en eicel vele malen moet delen om alle weefsels en organen te kunnen vormen. Deze ene cel bevat alle informatie nodig om een compleet organisme te maken en is een mix van genetische eigenschappen van zowel vader als moeder.

Een cel vormt de kleinste bouweenheid van elk organisme, maar is tegelijkertijd ook een hele wereld op zich, of beter gezegd een stad (Figure 1). Zoals elke grote stad heeft iedere cel ook een stadsmuur (celmembraan), energie centrales (mitochondriën), fabrieken (ribosomen), transportbedrijven (golgi-systeem) en een bibliotheek (*celkern*). De bibliotheek is heel belangrijk, want hier is alle informatie opgeslagen die de stad nodig heeft om te kunnen functioneren. In deze bibliotheek liggen alle boeken, genaamd *chromosomen*, waar in staat hoe de cel de bouwstoffen en gereedschappen moet maken die nodig zijn om de stad te kunnen repareren indien nodig, maar ook hoe een stad/cel zich kan vermenigvuldigen. Elke keer dat een cel deelt moet deze hele bibliotheek dus ook netjes worden gekopieerd (*DNA replicatie*), zodat de dochtercellen ook toegang hebben tot alle genetische informatie.

DNA: het recept voor leven

Deze genetische informatie is opgeslagen in de vorm van *DNA*: twee complementaire kralensnoeren die een wenteltrap/helix vormen (Figuur 1 en 2A). De genetische informatie is gecodeerd in de volgorde van de kralen/traptreden, genaamd *basen* en er zijn vier verschillende DNA basen: guanine (G), cytosine (C), adenine (A) en thymine (T). Het feit dat G altijd paart met C in de DNA helix, en A altijd met T, zorgt er voor dat de twee strengen kunnen dienen als een backup voor elkaar wanneer één streng haar coderende informatie verliest (Figuur 2A). Deze structuur maakt DNA zo'n succesvolle en veilige drager van de genetische code.

Een stuk coderend DNA noemen we een *gen* en het hele genenpakket van een organisme noemen we het *genoom* (Figuur 1). Genen coderen vaak voor *eiwitten*, de bouwstenen en werkpaarden voor een cel. De eigenschappen van een cel worden bepaald door welke genen worden afgelezen (Figuur 1). Met andere woorden, alle cellen binnen een organisme bevatten dezelfde bibliotheek, maar niet alle boeken zijn op dezelfde pagina's opgeslagen. Een intact genoom is van cruciaal belang omdat beschadigde genen foute instructies kunnen geven, waardoor de cel kan sterven of juist ongeremd gaat delen. Dat laatste noemen we *kanker*.

Gezien de mogelijke desastreuse gevolgen van DNA schade worden de chromosomen beschermd van de buitenwereld en blijven deze 'boeken' uitsluitend in de celkern. Om de gen-instructies toch naar de eiwitfabrieken buiten de celkern te brengen wordt de genetisch code vertaald naar strengen 'messenger RNA' of *mRNA* (Figuur 1). De stabiliteit, vorm en lokalisatie van mRNA biedt de cel nog een extra laag van regulatie op eiwitproductie en daarmee ook op allerlei moleculaire processen.

DNA onderhoud: een millennia oude noodzaak

Een belangrijke set van genen is die van DNA reparatiegenen. De integriteit van ons genoom wordt continue bedreigd door agentia die DNA kunnen beschadigen, waaronder zonlicht, chemische stoffen uit bijvoorbeeld sigaretten, maar ook diverse bijproducten die intrinsiek gekoppeld zijn aan ons cellulair metabolisme. Processen die leiden tot veranderingen in het genoom noemen we *mutageen*. Zonder DNA reparatie-eiwitten accumuleert het genoom veel veranderingen (*mutaties*), waardoor in de loop der tijd cellen kunnen ontstaan die zich gaan misdragen. Personen die een mutatie dragen in het BRCA1 gen bijvoorbeeld, hebben een defect in het repareren van DNA breuken, en families met zo'n mutatie hebben een sterk verhoogde kans op kanker. Omdat defecten in DNA reparatiegenen vaak ten grondslag liggen aan verscheidende erfelijke vormen van kanker worden deze genen vaak ook *tumorsuppressors* genoemd.

Het belang van DNA reparatiegenen wordt nog eens verder benadrukt door het feit dat deze genen sterk geconserveerd zijn tijdens evolutie. Met andere woorden, de universele en essentiële rol van DNA heeft er toe geleid dat genen betrokken bij het kopiëren en repareren van DNA zijn behouden zelfs na miljoenen jaren selectie. Dit betekent ook dat DNA reparatiegenen in een fruitvlieg, worm, muis of mens veel met elkaar gemeen hebben en dat we de functies van deze factoren in modeldieren vaak kunnen extrapoleren naar die van de mens.

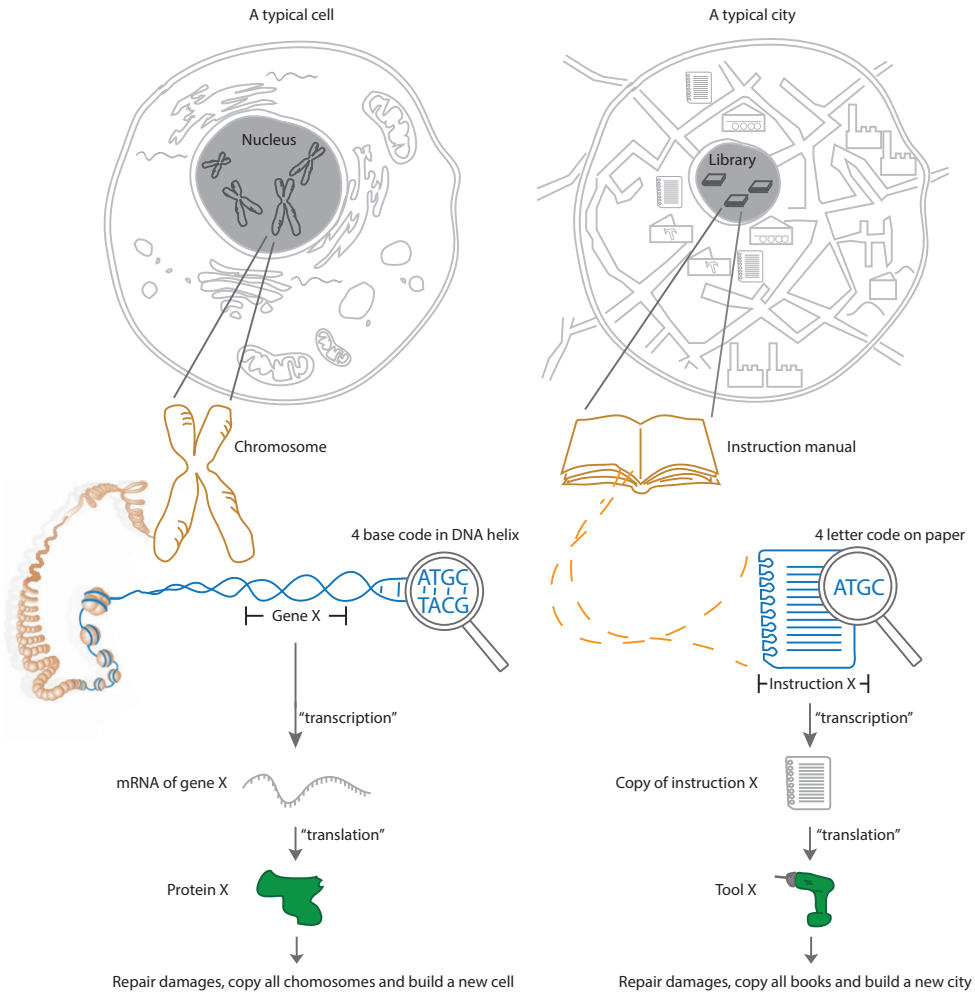

Figuur 1: Vergelijking tussen een menselijke cel en een stad
Schematisch weergave van een menselijke cel (links) en een stad (rechts). Menselijke cellen en steden hebben vergelijkbare structuren, zoals de celkern (nucleus) en de bibliotheek (library). De integriteit van informatiedragers, zoals het DNA in chromosomen (in de cel) of de tekst in boeken (in de stad) zijn van cruciaal belang voor het goed functioneren van de cel/stad. Zie Nederlandse samenvatting voor details.

DNA dubbelstrengs breuken

Dit proefschrift concerteert zich op het herstellen van zogenaamde *DNA dubbelstrengs breuken* (*DSBs*), dat wil zeggen, lesies waarbij beide strengen van de DNA helix zijn gebroken (Figuur 2B). DSBs zijn erg gevaarlijk omdat ze kunnen leiden tot het verlies van grote stukken genetische informatie en/of ongewenste chromosoomfusies, wat uiteindelijk weer kan leiden tot genoominstabiliteit, cellulaire dysfunctie en kanker. De mutagene en cytotoxische eigenschappen van DSBs vormen een ernstige bedreiging voor de volksgezondheid, maar

kunnen gelukkig ook worden benut om kwaadaardige cellen uit te roeien. Sneldelende kankercellen zijn namelijk overgevoelig voor DSB-inducerende middelen, zoals ioniserende straling en diverse chemotherapeutische geneesmiddelen. Daarnaast zijn bepaalde cellulaire ontwikkelingsprogramma's verrassend genoeg afhankelijk van DSB formatie. Zo ondergaat bijvoorbeeld elke geslachtscel tientallen geprogrammeerde DNA breuken tijdens haar ontwikkeling.

Nieuwe inzichten over de endogene bronnen van DSBs en de mechanismen die omgaan met deze gevaarlijke lesies kunnen helpen om complexe ziekten zoals kanker beter te begrijpen, alsmede aanwijzingen verschaffen die de behandeling van kanker kunnen optimaliseren. Bovendien kan fundamenteel onderzoek naar DSB reparatie helpen bij het blootleggen van de drijvende krachten achter evolutie en soortvorming.

***Caenorhabditis elegans* als diermodel**

Om DSB reparatie te bestuderen heb ik gebruik gemaakt van een nematodesoort genaamd *C. elegans.* Dit 1 millimeter lange wormpje dient als een eenvoudig diermodel voor complexe organismen zoals de mens en heeft al geleid tot vele belangrijke ontdekkingen waar onder meer verschillende Nobelprijzen voor zijn uitgereikt. *C. elegans* heeft een korte levenscyclus (2-3 dagen) en een relatief compact genoom (30 keer kleiner dan de mens). Daarnaast kunnen we haar genoom relatief makkelijk aanpassen, waardoor we de worm nieuwe eigenschappen kunnen geven (*genetische manipulatie*). Deze eigenschappen maken diepgaande genetische analyse van mutagene processen mogelijk en we hebben deze eigenschappen dan ook benut om i) deze dieren te veranderen in levende sensoren van DNA-schade ii) nieuwe factoren te vinden betrokken bij genoomstabiliteit, iii) mechanismen te onthullen die DNA-reparatie keuze dicteren, en iv) de biologische gevolgen te bepalen van DSBs die voortkomen uit DNA replicatie problemen.

DSB reparatieroutes

Er zijn verschillend reparatiemechanismen geëvolueerd die DSBs kunnen 'lijmen' (Figuur 2B). Welke DSB reparatieroute gebruikt wordt is onder meer afhankelijk van het celtype (en de reparatiefactoren die hierin tot expressie komen), de DNA sequentiecontext van de breuk en de aanwezigheid van 'reparatie-templates.'

De voornaamste DSB reparatieroute in menselijke cellen heet *non-homologous end joining* (*NHEJ*) en kan breuken repareren onafhankelijk van de DNA sequentie context (Figuur 2B). De eerste stap in NHEJ is het beschermen van de dubbelstrengs breukeinden door zogenaamde Ku eiwitten (*DSB end protection*). Vervolgens rekruteren de Ku eiwitten een eiwitcomplex dat de breukeinden bijeenhoud (*DSB end bridging*). Dit complex bevat ook een DNA ligase die de DNA uiteinden daadwerkelijk aaneen lijmt (*DNA ligation*). NHEJ is een snelle en effectieve manier van DSB herstel maar heeft één groot nadeel: de afwezigheid van

een DNA sequentie controle. Hierdoor kan NHEJ resulteren in kleine deleties of inserties en in het geval van meerdere DSBs leiden tot foutieve chromosoomfusies. Om deze redenen wordt NHEJ *'error-prone'* genoemd.

De overige DSB reparatieroutes beginnen in tegenstelling tot NHEJ met '*DNA end resection'*; een DSB verwerkingstap waarbij de dubbelstrengs breukeinden niet worden beschermd maar juist worden omgezet in enkelstrengs DNA staarten (Figuur 2B). Deze blootgelegde enkelstrengs DNA sequenties kunnen nu gaan paren met 'homologe' DNA sequenties waardoor de stabiele dubbelstrengs DNA helix wordt hersteld. Als beide breukeinden homologe/passende sequenties bevatten kunnen deze '*repeats'* paren om zo de breuk te overbruggen; afhankelijk van de lengte van de homologe sequenties spreekt men dan van *single strand annealing* (*SSA*) of *microhomology mediated end joining* (*MMEJ*) (Figuur 2B). SSA en MMEJ zijn per definitie mutageen omdat er van twee repeats één wordt gemaakt en er dus altijd genetische informatie verloren gaat.

Recentelijk heeft onze onderzoeksgroep een alternatieve DSB reparatieroute beschreven genaamd *polymerase Theta mediated end joining* (*TMEJ*). Deze route is belangrijk bij het herstellen van DSBs die ontstaan tijdens het kopiëren van het genoom en kan acteren in de afwezigheid van homologe repeats. In het opgestelde model herstelt TMEJ een DSB door één DNA base van beide breukeinden te laten paren en deze te laten verlengen door polymerase Theta, een eiwit dat DNA basen kan inbouwen (Figuur 2B). Hierdoor ontstaat weer een stabiele dubbelstrengs DNA helix en is de breuk overbrugd. Ook hier kunnen enkele basenparen verloren raken en soms bouwt polymerase Theta extra DNA basen in, hetgeen TMEJ mutageen maakt.

Er is echter één DSB reparatiemechanisme dat in principe geen mutaties achterlaat: *homologous recombination* (*HR*). Ook HR begint met 'DNA end resection', maar nu worden de enkelstrengs DNA staarten geladen met zogenaamde *recombinase* eiwitten (Figuur 2B). Zo'n DNA/recombinase complex kan nu op zoek gaan naar homologe DNA templates die niet beschadigd zijn, en vanuit daar de verloren informatie inkopiëren. In delende cellen kan bijvoorbeeld het recentelijk gemaakte kopie van het chromosoom (*zusterchromatide*) dienen als ideaal reparatie-template. Tijdens HR wordt zo'n intact homoloog template gebruikt om de enkelstrengs DNA eindjes te verlengen, zodat deze lang genoeg zijn om de breuk kunnen overbruggen (Figuur 2B). Zodra eventueel overgebleven gaatjes weer zijn gevuld en beide strengen zijn dichtgelijmd door DNA ligases is de DNA helix weer volledig hersteld en is er geen informatie verloren gegaan.

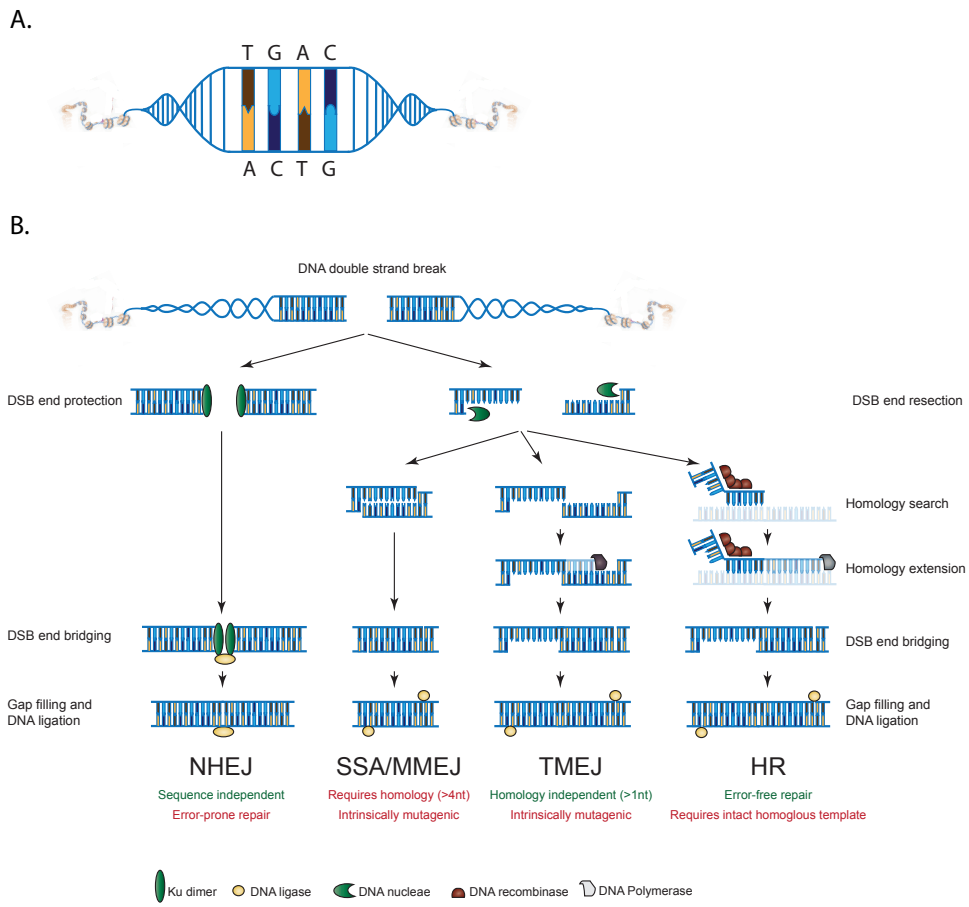

Figuur 2: Verschillende mechanismen om dubbelstrengs DNA breuken te repareren
A. Schematische weergave van de genetische code zoals opgeslagen in de base-volgorde van de DNA helix **B.** Overzicht van de verschillende DNA dubbelstrengs breuk reparatieroutes en hun voor- en nadelen. Bescherming van de breukeinden door Ku eiwitten (DSB end protection) initieert NHEJ, terwijl het exposeren van enkelstrengs breukeinden (DSB end resectie) kan resulteren in SSA, MMEJ, TMEJ en HR. Deze laatste reparatieroutes maken allen gebruik van DNA basenparing, maar de oorsprong en hoeveelheid van de benodigde homologe basen is verschillend. Legenda toont de kern-eiwitfuncties nodig voor DNA dubbelstrengs breuk herstel. Zie Nederlandse samenvatting voor details.

De wetenschappelijke bijdrage van dit proefschrift

Dit proefschrift beschrijft de experimenten die zijn uitgevoerd om de gevolgen en reparatiemogelijkheden van DSBs verder in kaart te brengen. Hoofdstuk 1 geeft een overzicht van de recente ontwikkelingen in het onderzoeksveld waarbij *C. elegans* is gebruikt om DSB reparatiemechanismen op te helderen. Hieruit blijkt dat veel onderzoek is gedaan naar DSB herstel via HR omdat dit de dominante reparatieroute is om de geprogrammeerde DNA breuken in geslachtscellen te herstellen.

In hoofdstuk 2 beschrijven we een nieuwe rol voor het eiwit COM-1 (de wormenvariant van de menselijke tumorsuppressor CtIP) tijdens de productie van geslachtscellen. We brengen een essentiële rol voor COM-1 aan het licht die gelegen is in het onderdrukken van NHEJ in geslachtcellen; in de afwezigheid van COM-1 worden de geprogrammeerde DSBs niet gerepareerd via HR maar gebonden door Ku eiwitten, met vele NHEJ-gemedieerde chromosoomfusies tot gevolg. Door Ku te verwijderen in COM-1 deficiënte dieren konden we deze chromosomale afwijkingen opheffen en de hoeveelheid levensvatbaar nageslacht drastisch verbeteren. Deze observaties geven een nieuwe kijk in de biologische functie van de tumorsuppressor CtIP alsmede de mogelijke toxische gevolgen van NHEJ.

In hoofdstuk 3 en hoofdstuk 4 beschrijven we de identificatie en karakterisatie van nieuwe factoren nodig voor efficiënte DSB reparatie. Zo beschrijven we een nieuwe rol voor het eiwit LIN-61 in HR en een verrassende rol van mRNA bindende eiwitten in het bevorderen van NHEJ in *C. elegans*. Om deze nieuwe factoren te kunnen vinden hebben we verschillende wormen geconstrueerd die groen fluorescerend licht geven wanneer ze een DSB hebben hersteld. Deze studies dragen bij aan het in kaart brengen van de cellulaire mechanismen die genoomstabiliteit bevorderen en bieden onderzoekers extra gereedschappen om DSB reparatie in levende dieren te meten.

Hoofdstukken 5 en 6 omvatten nieuwe bevindingen omtrent DNA replicatie blokkades en hun rol in het genereren van DSBs tijdens de ontwikkeling van dieren. DNA sequenties rijk aan de base guanine kunnen naast de DNA helix ook andere vormen aannemen, zogenaamde G4-quadruplex structuren. Dit zijn een soort knopen van enkelstrengs DNA waar de DNA polymerase die normaal het genoom kopieert op vast loopt. Deze 'DNA knopen' moeten daarom worden ontwonden door speciale *helicase* eiwitten zoals DOG-1 (de wormenvariant van tumorsuppressor FANCJ). In hoofdstuk 5 dragen we bevindingen aan die argumenteren dat in de afwezigheid van DOG-1 deze 'DNA knopen' in het genoom van de worm blijven zitten en leiden tot meerdere DSBs gedurende de ontwikkeling van het dier. Dit is de eerste keer dat het lot van één enkele secondaire DNA structuur is blootgelegd in levende dieren en benadrukt het belang van dit soort helicases voor genoomstabiliteit; ook gegeven het feit dat het menselijk genoom meer dan honderdduizend G-rijke sequenties bevat die mogelijk G4-quadruplexes kunnen vormen. In hoofdstuk 6 laten we zien dat deze G4-geïnduceerde DSBs veelal gerepareerd worden via TMEJ, maar dat de noodzaak van polymerase Theta wordt opgeheven als er flankerende DNA repeats aanwezig zijn. Deze laatste observatie geeft inzicht in het mechanisme van de nog redelijk onbekende TMEJ route en doet suggereren dat polymerase Theta vooral nodig is om homologe sequenties aan breukeinden te creëren om zo uiteindelijk de DSB te kunnen overbruggen (Figuur 2).

Conclusie

Dit proefschrift biedt verscheidende nieuwe inzichten in het ontstaan en repareren van DSBs en legt de mogelijke gevolgen bloot van mutagene reparatiemechanismen. Zo hebben we nieuwe regulators van NHEJ gevonden die belangrijk zijn voor DSB herstel in *C. elegans*, maar we tonen ook aan dat NHEJ erg gevaarlijk kan zijn tijdens de ontwikkeling van geslachtscellen. Strakke coördinatie is dus nodig om de verschillende reparatieroutes op elkaar af te stemmen zodat DNA breuken efficiënt maar ook accuraat worden hersteld.

Daarnaast dragen we additioneel bewijs aan dat specifieke DNA sequenties in het genoom een bedreiging kunnen vormen voor genoomstabiliteit omdat ze stabiele DNA structuren kunnen vormen die het nauwkeurig kopiëren van het genoom verhinderen. Secundaire DNA structuren die niet worden ontwonden vormen een aanhoudende bron van DSBs die na reparatie via TMEJ meerdere mutaties kunnen veroorzaken in ontwikkelde dieren.

Curriculum vitae

Bennie Lemmens was born on February 21, 1984 in Casteren, the Netherlands. He attended the Pius X College in Bladel from 1996 to 2002, where he specialized in the “Nature and Health” profile. After receiving his VWO diploma, he enrolled the study Biology at the Utrecht University and obtained his Bachelor’s degree in 2005. Later that year he enrolled the international prestige Master ‘Developmental Biology and Biomedical Genetics’ at the Utrecht University. As part of his Master’s program he performed his first internship at the laboratory of Dr. Rene Medema at the Utrecht Medical Centre, where he studied the role of Polo-like kinase 1 in DNA damage checkpoint signaling in human cancer cells. His second internship was performed at the laboratory of Dr. Ronald Plasterk at the Hubrecht Institute, where he used the model organism *C. elegans* to study microsatellite instability and screened for new DNA repair genes. In 2007 he wrote his Master thesis on the clinical applications of RNA interference at the lab of Dr. Rene Ketting and was awarded Master of Science. In October of the same year, Bennie started his PhD studies under the supervision of Dr. Marcel Tijsterman at the Hubrecht Institute in Utrecht. In 2009, the Tijsterman group moved to the city of Leiden where the research was continued in the department of Toxicogenetics at the Leiden University Medical Centre. The key results Bennie obtained during his PhD are described in this thesis and involve various aspects of genome instability during animal development. In 2014 he will continue his career as a postdoctoral fellow at the Karolinska Institute in Stockholm, Sweden, where he will use high-end microscopy to study DNA damage signaling and cell cycle regulation in the laboratory of Dr. Arne Lindqvist.

A

Acknowledgements

Jaren heb ik hier naar toegewerkt en trots ben ik op het resultaat: een boekje met allerlei wetenschappelijke bevindingen die voor de eerste keer zijn geobserveerd op deze aarde. Ik realiseer me ook dat er veel níet in staat. Mappen vol experimenten die het proefschrift helaas niet hebben gehaald omdat de technieken, tijd, of biologie niet wilden mee werken. Maar ook dát is wetenschap en ik hoop me nog jaren te kunnen verwonderen over de prachtige biologie die onze aarde rijk is. Maar wetenschappelijk onderzoek doe je niet alleen. Ik ben ontzettend dankbaar voor de steun, wijze lessen en fijne tijd die ik heb mogen ervaren tijdens mijn promotie. Super bedankt allemaal voor jullie bijdrage aan dit werk!

Op de eerste plaats Marcel; mijn promotor, baas, compagnon, sparringpartner en ideeën kanon. Je gaf me veel vrijheid en je deur stond altijd open: voor mij een ideale leer- en werkomgeving. We hebben naast ontelbare mailtjes met (te) gekke hypotheses, ook vele ideeën uitgewisseld over het bedrijven van wetenschap: van het runnen van gelen tot het runnen van een onderzoeksgroep. Ik heb veel respect voor je enthousiasme en je open doch scherpe blik op de wereld.

Leon bedankt voor het warme welkom in Leiden, je jarenlange inzet voor de afdeling en het feit dat je mijn interim-promotor wilde zijn.

Waar zou ik zijn zonder mijn directe collega's en oud-collega's van de Tijstermangroep: Daphne, Evelien, Karin, Kristy, Sophie, Wouter, Jennemiek, Nick, Marijn, Ron, Robin, Jane, Ivo, Evelina, Jordi, Maartje en Juliëtte. Stuk voor stuk toppers en een geweldig team door de jaren heen. Daphne, ik heb veel van je geleerd als student én collega en heb je boekje menigmaal opengeslagen. Ook een speciaal bedankje voor Jennemiek, Evelien, Ron en Jane; jullie buitengewone inzet heeft het onderzoek in hoofdstuk 3 en 6 vele malen versneld. Also thanks to my fellow 'mannex'-members, Nick, Marijn and Wouter; you all gave me support when I needed it very badly and brought a wide spectrum of music into my life, both of which I will never forget. Sophie en Ivo, jullie ideeën waren vaak om te smullen. Evelina, Maartje en Juliëtte, bedankt voor jullie frisse kijk op mijn experimenten en jullie hulp bij het zoeken naar end joining factoren. Jordi, thanks a lot for helping me out on my job search in Sweden.

Mijn studenten Claudia, Chantal, Cynthia en Renier bedankt voor jullie bijdrage aan mijn onderzoek. Verder wil ik ook alle overige collega's op het Hubrecht, UMC, UU, Erasmus MC en LUMC niet vergeten, omdat ze een vruchtbare omgeving hebben gevormd die mij als wetenschapper enorm hebben gesterkt. Zo wil ik graag het Medema lab bedanken voor mijn eerste lab-ervaringen en de wijze lessen op het gebied van kankerwetenschap, de Utrechtse 'worm club' voor leuke seminars, de Hubrecht crew voor fantastische borrels, Teije en Martin voor een onvergetelijke trip naar de International *C. elegans* meeting, alle TOXGEN collega's voor de hevige literatuurdiscussies, alle lotgenoten van MGC voor de fameuze PhD workshops en my fellow Lemmy's-fans (including Wouter W, Godelieve, Angela, Mark, Agata,

Erik, Thomas and Mona) for all the witty discussions about evolution and ethanol. Allemaal bedankt voor de geweldige tijd!

Promovendus zijn betekent soms hele dagen door de microscoop turen, duizenden wormen picken, avonden puzzelen op een observatie, dat manuscript toch nog maar eens doorlezen op bed en wakker liggen van negatieve resultaten. Afleiding is dan ook broodnodig om succesvol te kunnen zijn op je werk. Gelukkig kon ik bij veel vrienden terecht voor een lach, een tactische spelletje of gewoon een goed gesprek. Boven de rivieren, mijn jaarclub (Aike, Alban, Ayelt, Bas, Gijs, Hanno, Ido, Kawai, Mattijs, Menne, Paul en Youri), het BG en Club Funghi en onder de rivieren, vrienden van het eerste uur (Tijs, Gijs, Hans, Melvin, Ronnie en Olav) en alle gezellige aanhang natuurlijk.

Ik ben ook dankbaar dat de genetica mij nooit in de steek heeft gelaten en dan doel ik op mijn directe bloedverwanten, hun partners en kruisnageslacht. Als jongste broertje en ome Bennie heb ik zo veel geleerd van jullie: Doret, Johan, Timo, Isa, Jordi, Stijn, Heidi, Djoy, Juul, Frank, Susanne, Lynn, Ise, Jorn, Anton, Linda, Guusje en Ties. Aan de nieuwsgierigheid en open blik van een kind kan menig wetenschapper een voorbeeld nemen.

En natuurlijk mijn ouders; jullie hebben me gesteund in ieder aspect van mijn leertraject en me de kans gegeven om me te ontplooien tot wetenschapper. Pap, helaas heeft het niet zo mogen zijn dat je mijn verdediging mee hebt kunnen maken; ik had je graag de bloemen op de berg laten zien. Mam, je hebt altijd in me gelooft en ik kan altijd op je rekenen. Je bent een rots voor ons allemaal.

Dan rest me nog om mijn paranimfen te bedanken. Het is een luxe om twee slimmeriken van dit kaliber aan mijn zijde te hebben. Robin, je bent onmisbaar geweest voor dit werk; van wormeninjecties tot bio-informatisch abracadabra, geen verzoekje ging je te ver. Dimitris, you are a great scientist and as ‘wise as’ Solomon.

Last but not least, Ana. Your advice and moral support has made this thesis a better product and has led me to new scientific adventures. You give me direction and make me complete.

List of publications

Lemmens BB, Tijsterman M.
DNA double-strand break repair in *Caenorhabditis elegans*
Chromosoma. 2011

Lemmens BB, Johnson NM, Tijsterman M.
COM-1 promotes homologous recombination during *Caenorhabditis elegans* meiosis by antagonizing Ku-mediated non-homologous end joining
PLoS Genet. 2013

Lemmens BB, van Schendel R, Tijsterman M.
PNN-1 and UAF-1 link RNA splicing to DNA repair by Non-Homologous End Joining
Manuscript in preparation

Lemmens BB, van Schendel R, Tijsterman M.
A single unresolved G4 quadruplex structure spawns multiple genomic rearrangements during animal development
Manuscript in preparation

Johnson NM, **Lemmens BB**, Tijsterman M.
A role for the malignant brain tumour (MBT) domain protein LIN-61 in DNA double-strand break repair by homologous recombination
PLoS Genet. 2013

Waaijers S, Portegijs V, Kerver J, **Lemmens BB**, Tijsterman M, van den Heuvel S, Boxem M.
CRISPR/Cas9-Targeted Mutagenesis in *Caenorhabditis elegans*
Genetics. 2013